



Terms and Conditions of Use of Digitised Theses from Trinity College Library Dublin

Copyright statement

All material supplied by Trinity College Library is protected by copyright (under the Copyright and Related Rights Act, 2000 as amended) and other relevant Intellectual Property Rights. By accessing and using a Digitised Thesis from Trinity College Library you acknowledge that all Intellectual Property Rights in any Works supplied are the sole and exclusive property of the copyright and/or other IPR holder. Specific copyright holders may not be explicitly identified. Use of materials from other sources within a thesis should not be construed as a claim over them.

A non-exclusive, non-transferable licence is hereby granted to those using or reproducing, in whole or in part, the material for valid purposes, providing the copyright owners are acknowledged using the normal conventions. Where specific permission to use material is required, this is identified and such permission must be sought from the copyright holder or agency cited.

Liability statement

By using a Digitised Thesis, I accept that Trinity College Dublin bears no legal responsibility for the accuracy, legality or comprehensiveness of materials contained within the thesis, and that Trinity College Dublin accepts no liability for indirect, consequential, or incidental, damages or losses arising from use of the thesis for whatever reason. Information located in a thesis may be subject to specific use constraints, details of which may not be explicitly described. It is the responsibility of potential and actual users to be aware of such constraints and to abide by them. By making use of material from a digitised thesis, you accept these copyright and disclaimer provisions. Where it is brought to the attention of Trinity College Library that there may be a breach of copyright or other restraint, it is the policy to withdraw or take down access to a thesis while the issue is being resolved.

Access Agreement

By using a Digitised Thesis from Trinity College Library you are bound by the following Terms & Conditions. Please read them carefully.

I have read and I understand the following statement: All material supplied via a Digitised Thesis from Trinity College Library is protected by copyright and other intellectual property rights, and duplication or sale of all or part of any of a thesis is not permitted, except that material may be duplicated by you for your research use or for educational purposes in electronic or print form providing the copyright owners are acknowledged using the normal conventions. You must obtain permission for any other use. Electronic or print copies may not be offered, whether for sale or otherwise to anyone. This copy has been supplied on the understanding that it is copyright material and that no quotation from the thesis may be published without proper acknowledgement.

**An investigation of the specificity of interaction in
two-component systems using YycFG and PhoPR
of *Bacillus subtilis* as a model system**

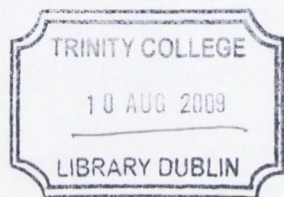
A Thesis submitted to the University of Dublin
for the Degree of Doctor of Philosophy

by

Inga Jende

Smurfit Institute of Genetics
School of Genetics and Microbiology
University of Dublin
Trinity College
Dublin 2

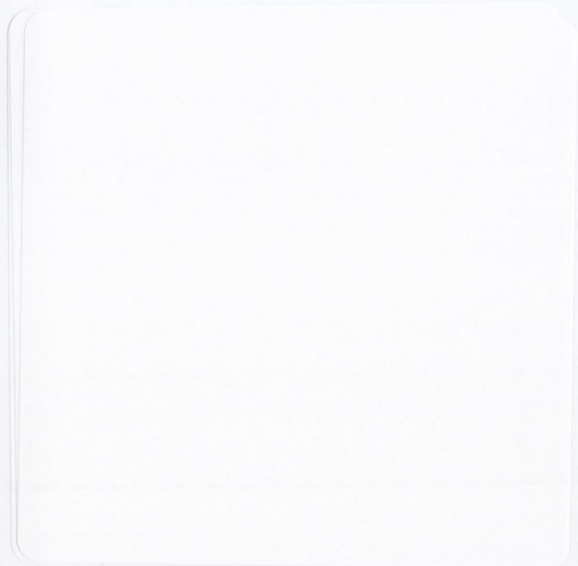
October 2008



THESIS
8822

Declaration

This thesis has not been previously submitted to this or any other university for examination for a higher degree. The work presented here is entirely my own except otherwise acknowledged. This thesis may be made available for consultation within the university library. It may be copied or lent to other libraries for purposes of consultation.



To my sister and brothers

Two roads diverged in a wood,
and I--
I took the one less traveled by,
And that has made all the
difference.

(Robert Frost – The Road Not Taken, 1915)

Acknowledgements

I am grateful to my supervisor Prof. Kevin Devine for taking me on in his lab and for helping me to become a truly independent researcher.

A sincere thank you to K.I. Varughese who was always open to discussions.

Special thanks to my colleagues Brian Jester and Efi Lioliou for not only generously opened their scientific expertise to me but also for becoming friends for life. I would love to work with you again. Thanks also to the other lab members and to Paul, Brenda, David and Sue.

I am enormously indebted to all my close friends who always been there for me and supported me in many ways on the journey to this PhD. This list includes but is certainly not limited to: Erin Gray, Anna-Sofie Gierlichs & family, Conor O'Kelly, Annika Beyer, Axel Litty, Jens Reimers and my German study mates: Sabine Graf, Volker Behrends, Oliver Arendt, Martin Osterholz... and the rest of Göttingen's Bio 1999.

A heartfelt thanks to the members of UCD Judo Club, especially my coach Paul and Shona, my friend & training partner, who not only gave me a welcomed change of environment but made sure I kept my head straight and my feet on the ground.

Thanks also go to: Gudrun and Peter Elsner for encouraging words when needed, Heidrun Korthals, my former biology teacher, for teaching me about genetics, plasmids and stuff thus starting a lasting fascination.

Above all, a very special thanks to my family: My granny Thea, my parents Siegfried and Sabine for supporting my in whatever I do and my siblings Lars, Jörg and Britta who I always can count on. Love you!

This work was supported by a Science Foundation Ireland Investigator Award (03/IN3/B409) and EU Sixth Framework grant BACELL Health (LSHC-CT-2004-503468)

awarded to Professor Kevin Devine and an award from the Arkansas Biosciences Institute to K.I. Varughese.

Table of Contents	I
List of Tables and Figures	IV
Summary	X
Abbreviations	XII

Table of Contents

Chapter 1

1. Introduction

1.1	<i>Bacillus subtilis</i> : a model system	1
1.2	Two-components systems	1
1.3	Histidine Kinases	4
1.4	Response regulators	7
1.5	Specificity of HK:RR interaction	8
1.6	Crosstalk	10
1.7	The two-component system YycFG	11
1.8	The two-component system PhoPR	13
1.9	Observations leading to this study	14
1.10	Objective of this study	15

Chapter 2

2. Materials and Methods

2.1	Bacterial strains	17
2.2	Sequence analysis	17
2.3	DNA manipulation	17
2.4	Immunoblot Analysis	18
2.5	β -galactosidase assays of promoter fusions	18
2.6	Protein Expression Plasmids	19
2.7	Purification of Proteins	19
2.8	<i>In vitro</i> protein phosphorylation assay	19
2.9	Quantitative <i>in vitro</i> phosphorylation assay	20
2.10	Growth of <i>B. subtilis</i> in microtiter plates	20
2.11	Plasmids and strain constructions	21

Results

Chapter 3 - Mutational analysis of the HK YycG

3.	Introduction – Structural comparison of YycG and PhoR	27
3.1	<i>In vivo</i> study of interaction between the HK YycG* and the RR PhoP	28
3.1.1	An <i>in vivo</i> system to investigate the specificity of interaction between YycG and PhoP	28
3.1.2	Expression of a second <i>yycG</i> gene at the <i>thrC</i> locus on the <i>B. subtilis</i> chromosome	30
3.1.3	Confirmation of correct genetic structure of strains	31
3.2	Qualitative evaluation of PhoP phosphorylation by YycG and mutated derivatives (YycG*) <i>in vivo</i>	33
3.2.1	Evaluation of PhoP phosphorylation by YycG* in IJW strains growing on LB agar	33
3.2.2	Evaluation of PhoP phosphorylation by YycG* in IJR strains growing on LB agar	33
3.2.3	$P_{phoA-lacZ}$ expression is PhoP~P dependent	34
3.2.4	Effects of YycG mutations on <i>yocH</i> expression not detectable <i>in vivo</i>	34
3.3	Quantitative analysis of PhoP phosphorylation by YycG* <i>in vivo</i> during growth in LB broth	36
3.3.1	Evaluation of β -galactosidase activity of strain set IJW <i>in vivo</i>	36
3.3.2	Evaluation of β -galactosidase activity of strain set IJR (Δ <i>phoR</i>) <i>in vivo</i>	36
3.3.3	<i>In vivo</i> evaluation of β -galactosidase activity of strain set IJPR (Δ <i>phoPR</i>)	37
3.4	YycG is expressed at a constant level throughout growth	38
3.5	Phosphorylation properties of mutant 'YycG* proteins <i>in vitro</i>	39
3.5.1	Purification of HKs and RRs	39
3.5.2	<i>In vitro</i> phosphorylation of cognate pairs YycFG and PhoPR	40
3.5.3	<i>In vitro</i> phosphorylation assay of mutant 'YycG*	41
3.6	Kinetic analysis of phosphotransfer from wild-type and mutant kinases	42
3.6.1	Determination of conditions for an <i>in vitro</i> kinetic analysis	42
3.6.2	Quantitative <i>in vitro</i> phosphorylation assay of mutant 'YycG*s	44
3.7	Phenotypical characterization of strains exhibiting PhoP phosphorylation by YycG*	48
3.7.1	Growth phenotype on LB agar	48
3.7.2	Growth phenotype in LB broth	48
3.8	Discussion	51

Chapter 4 - Mutational analysis of the RR PhoP

4.	Introduction	57
4.1	Computational determination of specificity amino acids on the PhoP surface	57
4.2.1	An <i>in vivo</i> system to investigate the specificity of interaction between YycG and PhoP	58
4.2.2	Confirmation of correct genetic structure of strains	59
4.2.3	Qualitative evaluation of interaction between YycG and PhoP* <i>in vivo</i>	60
4.2.4	Optimization of growth conditions in LB broth	62
4.2.5	Quantitation of phosphorylation of mutated PhoP* proteins by YycG <i>in vivo</i>	63
4.2.6	P _{phoA} - <i>laz</i> expression is P _{xyI} phoP* dependent	65
4.2.7	Growth phenotype of IJPR-PhoP* strains in LB broth	65
4.3	Analysis of the effect of amino acid changes in PhoP on phosphorylation <i>in vitro</i>	66
4.3.1	Purification of HKs and RRs	66
4.3.2	<i>In vitro</i> phosphorylation of cognate pairs YycFG and PhoPR	66
4.3.3	Analysis of phosphorylation of PhoP* proteins with amino acid changes by the non-cognate 'YycG kinase <i>in vitro</i> .	67
4.4	Discussion	79
Chapter 5		
5.	Conclusions	85
	Future Work	87
	References	91

List of Tables and Figures

Figures and Tables - Chapter 1

- Figure 1.1 Diagram of a classic two-component system
- Figure 1.2 Diagram of a phosphorelay
- Figure 1.3 Grouping of histidine kinases in *B.subtilis* according to Fabret *et al.*, 1999
- Figure 1.4 Grouping of histidine kinases in *B.subtilis* according to Mukhophyay and Varughese, 2000
- Figure 1.5 Domain structure of a histidine kinase
- Figure 1.6 The dimerization domain of a HK
- Figure 1.7 A model of the domain structure of a response regulator (RR)
- Figure 1.8 A model of the RR receiver domain
- Figure 1.9 Model of the HK interacting residues of the α 1-helix
- Figure 1.10 YycFG: operon organization, regulon and domain architecture
- Figure 1.11 Diagram of the operon, regulon and domain structure of PhoPR
- Figure 1.12 Model of phosphotransfer between YycFG and PhoPR

Figures and Tables - Chapter 2

- Table 2.1 Strains used in this study
- Table 2.2 Plasmids used in this study
- Table 2.3 Oligonucleotides used in this study
- Table 2.4 Amino acid changes introduced into YycG
- Table 2.5 Amino acid changes introduced into PhoP

Figures and Tables Chapter - 3

- Figure 3.1 Alignment of phosphorylation site of group IA HKs of *B.subtilis*
- Figure 3.2 Alignment of YycG and PhoR residues in the vicinity of the active histidine and mutated YycG*
- Table 3.1 Amino acid changes introduced into YycG
- Figure 3.3 Genetic structure of strain sets IJW and IJR
- Figure 3.4 Westernblot analysis showing cellular levels of YycG
- Figure 3.5 α -amylase assay of IJW99 putative transformants
- Figure 3.6 PCR mapping of IJW99 putative transformants to confirm integration of the P_{phoA} -*lacZ* fusion
- Figure 3.7 α -amylase assay of IJR99 putative transformants

- Figure 3.8 PCR mapping of IJR99 putative transformants
- Figure 3.9 Screening of putative transformants of the $P_{xyI}yycG$ integration at the *thrC* locus
- Figure 3.10 Evaluation of PhoP phosphorylation by mutant YycG* in IJW strains *in vivo*
- Figure 3.11 Evaluation of phosphotransfer between mutant YycG* and PhoP in IJR strains *in vivo*
- Figure 3.12 Genetic properties of strain set IJPR
- Figure 3.13 β -galactosidase activity of strains carrying YycG mutant protein is PhoP~P dependent
- Figure 3.14 Genetic structure of strain set IJPR121-131
- Figure 3.15 Expression of $P_{yocH-lacZ}$ fusion
- Figure 3.16 Growth and β -galactosidase profiles of IJW99 to IJW106
- Figure 3.17 Growth and β -galactosidase profiles of IJW107, IJW108, IJW112, IJW114 and IJW115
- Figure 3.18 Growth and β -galactosidase profiles of IJR99 to IJR106
- Figure 3.19 Growth and β -galactosidase profiles of IJR107, IJR108, IJR112, IJR114 and IJR115
- Figure 3.20 Growth and β -galactosidase profiles of IJPR strains
- Table 3.2 YycG*:PhoP interaction and PhoP~P mediated regulation of *phoA* expression in exponential growth
- Figure 3.21 Western Blot analysis of YycG protein levels in wild-type strain 168 and selected IJR strains
- Figure 3.22 Analysis of purified 'YycG and 'PhoR kinases and the response regulators YycF and PhoP by SDS-PAGE
- Figure 3.23 Autophosphorylation and phosphotransfer *in vitro* of TCS pairs YycFG and PhoPR
- Figure 3.24 Phosphorylation of YycF and PhoP by 'YycG105 *in vitro*
- Figure 3.25 Phosphorylation of YycF and PhoP by 'YycG112 *in vitro*
- Figure 3.26 Phosphorylation of YycF and PhoP by 'YycG114 *in vitro*
- Figure 3.27 Phosphorylation of YycF and PhoP by 'YycG107 *in vitro*
- Figure 3.28 Determination of optimal ATP levels for *in vitro* phosphorylation
- Figure 3.29 Test of different YycF concentrations for *in vitro* phosphorylation
- Figure 3.30 Test of different PhoP concentrations for *in vitro* phosphorylation
- Figure 3.31 Phosphorylation of the response regulator YycF by 'YycG and 'Yyc105

- in vitro*
- Figure 3.32 Phosphorylation of the response regulator PhoP by 'PhoR and 'Yyc105 *in vitro*
- Figure 3.33 Phosphorylation of the response regulator YycF by 'YycG and 'Yyc112 *in vitro*
- Figure 3.34 Phosphorylation of the response regulator PhoP by 'PhoR and 'Yyc112 *in vitro*
- Figure 3.35 Phosphorylation of the response regulator YycF by 'YycG and 'Yyc114 *in vitro*
- Figure 3.36 Phosphorylation of the response regulator PhoP by 'PhoR and 'Yyc114 *in vitro*
- Figure 3.37 Phosphorylation of the response regulator YycF by 'YycG and 'Yyc107 *in vitro*
- Figure 3.38 Phosphorylation of the response regulator PhoP by 'PhoR and 'Yyc107 *in vitro*
- Figure 3.39 Growth of strains IJR108, IJR105, IJR112, IJR114 and IJR107 on LB agar
- Figure 3.40 Growth of IJR strains in LB broth
- Figure 3.41 Growth of IJR strains in LB broth supplemented with 0.0025% xylose
- Figure 3.42 Growth of IJR strains in LB broth supplemented with 0.005% xylose
- Figure 3.43 Summary of qualitative phosphorylation of YycF and PhoP RRs by the 'YycG, 'YycG* and PhoR kinases
- Table 3.3 Summary of *in vivo* and *in vitro* assay results
- Figure 3.44 Alignment of the interacting residues of the YycG and PhoR α 1-helices

Figures and Tables - Chapter 4

- Figure 4.1 Alignment of the receiver domains of YycF, PhoP and Spo0F.
- Figure 4.2 Anchor, catalytic and variable amino acids of Spo0F, PhoP and YycF.
- Table 4.1 Amino acids changes introduced into PhoP
- Figure 4.3 Genetic structure of strain sets IJW140-155, IJR140-155 and IJPR140-155.
- Figure 4.4 Evaluation of PhoP* protein phosphorylation by YycG *in vivo*.
- Figure 4.5 Evaluation of β -galactosidase activity in strains IJR140-155 in the presence of 0.005% xylose *in vivo*.
- Figure 4.6 Evaluation of β -galactosidase activity of strains IJPR140-155 *in vivo*.

- Figure 4.7 *In vivo* β -galactosidase activity of strains IJPR140-155 in the presence of 0.0025% xylose.
- Figure 4.8 Evaluation of strains IJPR140-155 *in vivo* in the presence of 0.005% xylose supplementation.
- Table 4.2 β -galactosidase activity of PhoP containing a single amino acid change
- Table 4.3 β -galactosidase activity of PhoP containing two amino acid changes
- Table 4.4 β -galactosidase activity of PhoP containing three and four amino acid changes
- Figure 4.9 Growth and β -galactosidase profiles of IJPR140, IJPR143 and IJPR155.
- Figure 4.10 Growth of IJPR $P_{xyI}phoP^*$ strains in LB broth supplemented with 0.005% xylose.
- Figure 4.11 Growth of IJPR $P_{xyI}phoP^*$ strains in LB broth supplemented with 0.005% xylose.
- Figure 4.12 Growth of IJPR $P_{xyI}phoP^*$ strains in LB broth without addition of xylose.
- Figure 4.13 Growth of IJPR mutant strains in LB broth supplemented with 0.005% xylose.
- Figure 4.14 Analysis of purified mutated PhoP* protein by SDS PAGE.
- Figure 4.15 Phosphorylation of response regulators YycF and PhoP by 'YycG *in vitro*.
- Figure 4.16 Phosphorylation of response regulators PhoP and YycF by 'PhoR *in vitro*.
- Figure 4.17 Phosphorylation of response regulators YycF and PhoP141 by 'YycG *in vitro*.
- Figure 4.18 Phosphorylation of response regulators PhoP and PhoP141 by 'PhoR *in vitro*.
- Figure 4.19 Phosphorylation of response regulators YycF and PhoP142 by 'YycG *in vitro*.
- Figure 4.20 Phosphorylation of response regulators PhoP and PhoP142 by 'PhoR *in vitro*.
- Figure 4.21 Phosphorylation of response regulators YycF and PhoP143 by 'YycG *in vitro*.
- Figure 4.22 Phosphorylation of response regulators PhoP and PhoP143 by 'PhoR *in vitro*.
- Figure 4.23 Phosphorylation of response regulators YycF and PhoP144 by 'YycG

- in vitro.*
- Figure 4.24 Phosphorylation of response regulators PhoP and PhoP144 by 'PhoR
in vitro.
- Figure 4.25 Phosphorylation of response regulators YycF and PhoP145 by 'YycG
in vitro.
- Figure 4.26 Phosphorylation of response regulators PhoP and PhoP145 by 'PhoR
in vitro.
- Figure 4.27 Phosphorylation of response regulators YycF and PhoP146 by 'YycG
in vitro.
- Figure 4.28 Phosphorylation of response regulators PhoP and PhoP146 by 'PhoR
in vitro.
- Figure 4.29 Phosphorylation of response regulators YycF and PhoP147 by 'YycG
in vitro.
- Figure 4.30 Phosphorylation of response regulators PhoP and PhoP147 by 'PhoR
in vitro.
- Figure 4.31 Phosphorylation of response regulators YycF and PhoP148 by 'YycG
in vitro.
- Figure 4.32 Phosphorylation of response regulators PhoP and PhoP148 by 'PhoR
in vitro.
- Figure 4.33 Phosphorylation of response regulators YycF and PhoP149 by 'YycG
in vitro.
- Figure 4.34 Phosphorylation of response regulators PhoP and PhoP149 by 'PhoR
in vitro.
- Figure 4.35 Phosphorylation of response regulators YycF and PhoP150 by 'YycG
in vitro.
- Figure 4.36 Phosphorylation of response regulators PhoP and PhoP150 by 'PhoR
in vitro.
- Figure 4.37 Phosphorylation of response regulators YycF and PhoP151 by 'YycG
in vitro.
- Figure 4.38 Phosphorylation of response regulators PhoP and PhoP151 by 'PhoR
in vitro.
- Figure 4.39 Phosphorylation of response regulators YycF and PhoP152 by 'YycG
in vitro.
- Figure 4.40 Phosphorylation of response regulators PhoP and PhoP152 by 'PhoR
in vitro.

- Figure 4.41 Phosphorylation of response regulators YycF and PhoP153 by 'YycG
in vitro.
- Figure 4.42 Phosphorylation of response regulators PhoP and PhoP153 by 'PhoR
in vitro.
- Figure 4.43 Phosphorylation of response regulators YycF and PhoP154 by 'YycG
in vitro.
- Figure 4.44 Phosphorylation of response regulators PhoP and PhoP154 by 'PhoR
in vitro.
- Figure 4.45 Phosphorylation of response regulators YycF and PhoP155 by 'YycG
in vitro.
- Figure 4.46 Phosphorylation of response regulators PhoP and PhoP155 by 'PhoR
in vitro.
- Table 4.5 Summary of *in vivo* and *in vitro* assay results.
- Figure 4.47 Superimposed receiver domains of PhoP and YycF.
- Figure 4.48 Structures of Leucine and Isoleucine.

Summary

Presented in this thesis is a study of the specificity of interaction between histidine kinases and response regulators in two-component systems using YycFG and PhoPR as model system in *B. subtilis*.

Two-component regulatory systems (TCS) control a variety of cellular processes and are responsible for the adaptation of bacteria to environmental changes. In prokaryotes these TCSs allow the bacteria to adapt to changes in their surrounding environment by sensing a signal, transducing that signal into the cell and adjusting gene expression or direction of movement accordingly. These systems are highly adaptable phosphotransfer schemes that comprise two conserved components: a histidine protein kinase (HK) and a response regulator protein (RR). The cognate pairs HKs and RRs are commonly transcribed from the same operon. This ensures that they are expressed simultaneously at the same stage of growth and are up or down-regulated by the same stimuli. The HK consists of a variable signal detection domain and a conserved catalytic domain. Upon an input signal, monitored directly or indirectly through the sensing domain, HKs undergo an ATP-dependent autophosphorylation at a conserved histidine residue, thereby creating a high-energy phosphoryl group that is subsequently transferred to an aspartate residue on the response regulator (RR) (Silhavy and Hoch, 1995; Stock *et al.*, 2000). Upon phosphorylation, the RR, which usually functions as a transcription factor, undergoes conformational changes in order to interact with target gene promoters (Parkinson and Kofoid, 1992; Gao *et al.*, 2007).

YycFG and PhoPR are two examples of a TCS in *Bacillus subtilis* that encodes a total of 34 such systems. Like all histidine kinases YycG and PhoR interact with their cognate response regulators and activate the latter through the transfer of a phosphoryl group. This interaction between cognate partners is highly specific implying a high level of discrimination and specificity. The studies reported here were initiated to determine the properties necessary for discrimination between cognate and non-cognate partners. Usually a histidine kinase interacts with and consequently phosphorylates only its cognate response regulator. Despite there being 34 response regulators present in *Bacillus subtilis*. However atypically, unidirectional crosstalk has been shown between PhoR and YycF (Howell *et al.*, 2003, 2006).

By changing the interactions surface of YycG to that of PhoR the reciprocal reaction, crosstalk between YycG and PhoP was achieved in this study. Analysis

using *in vivo* transcriptional assays and *in vitro* phosphorylation reveal that five amino acids play major role in discrimination. Results show that: (i) changing all five amino acids enables the phosphorylation of PhoP by YycG *in vivo* and *in vitro*; (ii) positions +3, +8, +10, +11 and +12 are important to discriminate recognition of response regulators by YycG and PhoR; (iii) the size of amino acid side chains, *i.e.* steric hindrance, plays a role in discrimination between interaction partners; (iv) PhoR negatively influences the phosphorylation state of PhoP in cells grown under non-phosphate starvation conditions.

The interaction surface of the RR PhoP was also investigated. Sequence alignment of PhoP and YycF revealed that four amino acids differ between those proteins in the region thought to be relevant for recognition and subsequent phosphoryl acceptance from the cognate HK. *In vivo* and *in vitro* studies show that though these four amino acids are relevant for the interaction with the cognate HK, these amino acids contribute to a different extent to the specificity. Results show that: (i) changing all four amino acids allows the phosphorylation of PhoP by the non-cognate HK YycG (ii) amino acids positions on the alpha1-helix (13, 17 and 20) and the region of loop5 (107) are important to discriminate between PhoP and YycF in recognition of their cognate HKs PhoR and YycG and (iii) the structure of the amino acid side chains play a role in the selectivity for the cognate partners.

Abbreviations

aa	Amino acids
Amp	Ampicillin
Amp ^R	Ampicillin resistant
APase	Alkaline phosphatase
ATP	Adenosine triphosphate
BLAST	Basic Local Alignment Search Tool
bp	Base pairs
β-gal.	β-galactosidase
C-	Carboxy-
Cm	Chloamphenicol
Cm ^R	Chloramphenicol resistant
DNA	Deoxyribonucleic acid
DTT	Dithiothreitol
dNTP	Deoxynucleoside triphosphate
EDTA	Ethylenediaminetetraacetic acid
Erm	Erythromycin
Erm ^R	Erythromycin resistant
G+C	Guanosine + Cytidine
HAMP	Histidine kinase, Adenylyl cyclase, Methyl accepting chemotaxis protein, Phosphatase
HK	Histidine kinase
IPTG	Isopropyl β-D-1-thiogalactopyranoside
kb	Kilobase pair
LacZ/lacZ	β-galactosidase protein / structural gene
LB	Luria Bertani
N-	Amino-
Neo	Neomycin
Neo ^R	Neomycin resistant
MM	Minimal medium
OD	Optical density
ONPG	o-Nitrophenyl β-D-galactopyranosidase
PAS	Per-Arnt-Sim (subdomain)
PCR	Polymerase chain reaction
~P	Phosphorylated

RBS	Ribosome binding site
RNase	Ribonuclease
rpm	Revolutions per minute
RR	Response regulator
SDS	Sodium dodecyl sulfate
Spec	Spectinomycin
Spec ^R	Spectinomycin resistant
TCS	Two-component system
X-gal	5-bromo-4-chloro-3-indolyl- beta-D-galactopyranoside

Chapter 1
Introduction

1. Introduction

1.1 *Bacillus subtilis*: a model organism

Bacillus subtilis is a rod shaped Gram-positive bacterium commonly found in soil, water, and close to plants (Priest *et al.*, 1993). As *B.subtilis* is not pathogenic, it is used in industry for the production of proteases and amylases (Sonenshein *et al.*, 1993) as well as in food production *i.e.* fermentation of soybeans in the traditional Japanese dish called natto. *B.subtilis* has proven to be easy to manipulate genetically and has thus become widely adopted as a model organism for laboratory studies of related pathogenic Gram-positive bacteria such as *S.aureus*, *B.anthraxis* and *S.pneumoniae* (Sonenshein *et al.*, 2002).

In the natural environment of bacteria, nutrients are the limiting factor of growth. In order to bypass any shortages of nutrients, *B.subtilis* has a number of tactics to maintain growth. These include adjusting metabolic pathways to utilize alternative nutrient sources, inducing motility, releasing degradative enzymes or antibiotics, and taking up foreign DNA, a state known as competence. In the event that none of the former strategies support further vegetative growth, sporulation is initiated (Sonenshein *et al.*, 1993) This process forms a chemical-, irradiation- and heat-resistant endospore, protecting the cell from extreme environmental conditions (Kunst *et al.*, 1997; Stragier & Losick 1996). Moreover, each of these responses require a sophisticated system to detected and respond to the prevailing conditions in an appropriate manner.

1.2 Two component systems

A group of regulatory systems known as two-component systems (TCS) are the most widespread form of signal transduction, which originated in bacteria and spread by horizontal gene transfer to plants and fungi (Wolanin *et al.*, 2002; Mizuno, 2005; Loomis *et al.*, 1998). Even though TCSs are commonly utilized to promote microbial survival, these pathways have not been found in higher eukaryotes, *i.e.* humans and animals (Thomason and Kay, 2000). These pathways could thus serve as selective targets for the development of antimicrobial therapy (for review Stephenson and Hoch, 2002a, b, 2004; Matsushita and Janda, 2002).

In prokaryotes, the TCSs allow the bacterium to adapt to changes in its surrounding environment by first sensing a signal, transducing that signal into the cell, and then altering for example gene expression or direction of movement

accordingly. Underlying this mechanism are highly adaptable phosphotransfer schemes that comprise two conserved components: a histidine protein kinase (HK) and a response regulator protein (RR).

The cognate HKs and RRs pairs are commonly transcribed from the same operon. This ensures that they are expressed simultaneously at the same stage of growth and are up or down-regulated by the same stimuli.

The HK consists of a variable signal detection domain and conserved catalytic domain. Upon an input signal, monitored directly or indirectly through the sensing domain, HKs undergo an ATP-dependent autophosphorylation at a conserved histidine residue, thereby creating a high-energy phosphoryl group that is subsequently transferred to an aspartate residue on the response regulator (RR) (for review Silhavy and Hoch, 1995; Stock *et. al.*, 2000). Upon phosphorylation, the RR, which usually functions as a transcription factor, undergoes conformational changes in order to interact with target gene promoters (Parkinson and Kofoid, 1992; Gao *et al.*, 2007). The phosphotransfer reaction is shown in Figure 1.1.

In addition to the 'classic' TCS where a single phosphotransfer from a histidine to an aspartate residue occurs, there is the more complex phosphorelay that involves two additional phosphotransfer steps. In this phosphorelay, a phosphoryl group is transferred from the His residue of one or multiple kinases to the aspartate residue of an intermediate receiver, then to the His of a phosphotransferase domain and finally to the receiver domain of a RR (Figure 1.2), thus introducing two additional specific protein interactions. An example of a phosphorelay, first described by Burbulys *et al.* (1991), is a pathway controlling the initiation of sporulation in *Bacillus subtilis*. Sporulation is initiated through the activation of multiple kinases (KinA, KinB, KinC, KinD and KinE) which in turn phosphorylate a common single domain RR, namely Spo0F. From the intermediate receiver Spo0F, the phosphoryl group is transferred to the final acceptor Spo0A via the intermediate phosphotransferase protein Spo0B.

Similar to the phosphorelay, are the hybrid-type HKs that have an additional aspartate and histidine domain within the same protein. The phosphoryl group is transferred within the HK twice before finally reaching the receiver domain of the RR (Zhang and Shi, 2005).

These more complex phosphotransfer mechanisms allow for multiple levels of regulation when compared to classical TCSs by providing additional sites for potential interference and a broader range of input to a single output.

The number of TCSs present in bacteria varies considerably between species and ranges from 0 in *Mycoplasma* to around 80 in some cyanobacteria (Kiil *et al.*, 2005). The number of TCSs present within an organism appears to correlate positively with the degree of variation found in the inhabited environment rather than the complexity of the organism itself. In other words, the broader the spectrum of environmental variables encountered by a certain bacterium, the greater the number of TCSs found whereas bacteria adapted to thrive in less variable niches tend to have fewer TCSs (Kiil *et al.*, 2005; Mizuno *et al.*, 1996, Galperin, 2005; Rodrigue *et al.*, 2000).

There are 34 two-component systems encoded in the genome of *B.subtilis* which is one of many organisms for which the entire genome has been sequenced and annotated showing that it encodes over 4000 putative protein coding sequences (<http://genolist.mirror.edu.cn/Subtilist/>; Kunst *et al.*, 1997; Moszer 2002). Of the TCSs found among those proteins 30 HK-RR pairs reside in operons (Kunst *et al.*, 1997; Fabret *et al.*, 1999). Among these 34 TCSs, only the YycF-YycG system has been reported to be essential (Fabret *et al.*, 1998; Fukuchi *et al.*, 2000).

For more than 20 years, TCSs have been intensely studied from many perspectives including evolution, regulation of cellular processes, and as potential drug targets (for review see Alm *et al.*, 2006; Bekker *et al.*, 2006 and Stephenson and Hoch 2002). The approaches undertaken to investigate the role and physiological function of TCSs are thus very diverse, for example:

(i) Phylogenetic analysis: The construction of a phylogenetic tree points to an evolutionary relationship of two-component signal transduction in bacteria, archaea and eukaryotes (Koretke *et al.*, 2000).

(ii) Microarray analysis: DNA microarray work performed by Kobayashi *et al.* (2001) determined the target genes of 24 of 34 two-component systems found in *B.subtilis*. The approach was to overproduce the RR in the absence of the HK *in vivo*. This study gives insight into overlaps of TCS targets in addition to providing an extensive list of targets for future analysis.

(iii) *In vitro* analysis: Yamamoto *et al.* (2005) carried out an *in vitro* study on all TCSs found in *E.coli*, examining the specificity of interaction and transphosphorylation between purified HKs and RRs in all possible combinations. The results showed a substantial kinetic preference of HKs for their cognate RR where phosphotransfer reactions happen in less than 30 seconds. A few exceptions of non-cognate phosphotransfer were demonstrated, with a frequency of around 3% but this is more the exception than the rule.

(iv) Combined *in vivo* and *in vitro* analysis: Work from the lab of M. Laub rewired the specificity of the HK EnvZ of *E.coli* to change its interaction preference from the RR OmpR to RstA (Skerker *et al.*, 2008) showing that only a couple of amino acids within the $\alpha 1$ helix of EnvZ determine the specificity of the interaction.

(v) Structural analysis: A number of TCS proteins have been structurally characterized following the initial analysis of the RR CheY of *Escherichia coli* (Stock *et al.*, 1989). With every structure resolved, the preliminary theory of a common structural motif surrounding the active site becomes stronger.

1.3 Histidine kinases

Classifications of histidine kinases

Numerous attempts have been made to classify kinases based on various criteria. Prior to the wide dissemination of sequence data, HKs were grouped by domain homology (Parkinson and Kofoed, 1992). Another system to organize HKs was based on the homology surrounding the active histidine of the kinases. According to that criterion, five groups were determined, namely: Group I, Group II (NarL), Group IIIA (OmpR), Group IIIB and Group IV (Fabret *et al.*, 1999) which is shown in Figure 1.3. A comparative sequence analysis based on 348 kinases led to 11 different subfamilies categorized according to sequence clusters (Grebe and Stock, 1999). However, in order to perform a computational analysis of the interaction surface of HKs, Mukhopadhyay and Varughese (2005) regrouped 34 of 36 HKs found in *B.subtilis* into six main groups, namely IA, IAI, IC, II, III and IV where the kinase CheY-A forms a class of its own. The criteria for those classifications are a combination of phylogenetic analysis (Kim and Forst, 2001) and function as described previously (Silhavy and Hoch, 1995, Fabret *et al.*, 1999, for detail see Mukhopadhyay and Varughese, 2005) as shown in Figure 1.4. The classification of Mukhopadhyay and Varughese (2005) is here preferred over the others because it focused on the $\alpha 1$ -helix of the HK where the conserved site of phosphorylation is found and therefore includes variations of the interaction surface.

Structure and function of HKs

All histidine kinases are composed of similar domains with highly flexible interdomain sequences. However their organization varies, reflecting their specific localization, function and regulatory mechanism within the cell (Dutta *et al.*, 1999). Typical HKs are proteins comprised of two distinct modules: (i) an N-terminal

sensing domain and (ii) a C-terminal catalytic domain. The overall domain architecture is presented in figure 1.1 and 1.2.

The sensing domain is highly variable between HKs, resulting in the variety of kinases able to respond to a diverse range of signals. As many of those signals are linked to changes in the environment, the sensing domain is often anchored extracellularly to the membrane by two or more transmembrane domains (TMs). Although less common, cytoplasmic HKs that possess no TM exist too (for review Mascher *et al.*, 2006; Wolanin *et al.*, 2002). In those displaying the more commonly found membrane topology with two TMs, the sensing domain is separated from the catalytic domain by a TM and a linker domain (Figure 1.5).

The linker domain is thought to play a critical role in signal transduction (Mascher *et al.*, 2006; Stock *et al.*, 2000). It often contains a PAS domain and sometimes a HAMP domain as well. PAS domains are located in the cytosol and were first described in three proteins: the periodic circadian protein, the vertebrate aryl hydrocarbon receptor translocator, and the single minded protein (Ponting and Aravind, 1997).

Currently, thousands of PAS domains have been identified in sensory proteins across all kingdoms of life: archaea, prokaryotes and eukaryotes (Taylor and Zhulin, 1999). The spectrum of stimuli sensed by this domain is diverse, ranging from oxygen ligands and light over redox potential but is also involved in protein-protein interaction. Despite their structural similarity, PAS domains are often associated with cofactors that are likely to contribute to the variation of signaling (for review Taylor, 2007 and Taylor and Zhulin, 1999). In *Bacillus subtilis*, one of the kinases initiating sporulation, KinA, contains three PAS domains (A, B and C). The function of PAS-A appears to be very important for the enzymatic activity and the structural integrity of the C-terminal region that contains the catalytic region of the HK. PAS-B and PAS-C play a crucial role in dimerization (Wang *et al.*, 2001).

Adjacent to the PAS domain, there is often found a HAMP domain which is generally found in sensory proteins such as histidine kinases, adenylate cyclases, methyl-accepting chemotaxis proteins and phosphatases (Aravind and Ponting, 1999). The HAMP domain appears to consist of two α -helices separated by a linker presented as a conserved helix-turn-helix motif. To date it is unclear what the typical conformation is: (i) an extended helix or (ii) a parallel α -helical hairpin; the latter would allow the formation of a four helix bundle in the dimerized HK. The function of the HAMP domain is thought to involve the stabilization of the PAS fold and intramolecular transmission of the signal, likely through conformational changes.

Therefore it is likely that the HAMP domain plays a role not directly in signal sensing but in transmission. Taken together, the PAS and HAMP domains appear to work together as an input-output module within a HK thus ensuring the transduction of a signal throughout the length of the protein by providing the appropriate molecular conformation to enable downstream reactions producing the response (for review Taylor, 2007).

The catalytic domain is highly conserved in HKs, reflecting the common mechanism of signal transduction. The catalytic domain can be further divided into the dimerizing phosphotransferase domain that contains the conserved His residue and the catalytic ATP-binding domain. Within the catalytic domain there are highly conserved sequence motifs, namely the N, G1, F and G2 boxes, which form together the ATP-binding site (Grebe and Stock *et al.*, 1999).

Important insights on the structure and interaction of HKs and RRs were derived from the cocrystal structure of Spo0F: Spo0B, serving as a prototypical model of RRs and HKs respectively (Zapf *et al.*, 2000). The dimerization domain of a HK is formed by two helices that form a hairpin, helix $\alpha 1$ and helix $\alpha 2$ (Figure 1.6) and a C-terminal α/β fold. The conserved His protrudes from the middle of helix $\alpha 1$ and is the site of phosphorylation. In order to form an active kinase complex, two HK monomers associate to form a homodimer thus forming a four helix bundle (Varughese *et al.*, 1998). The ATP-dependent autophosphorylation within a homodimer is a bimolecular reaction. Upon activation through a signal the ATP-binding subunit of one monomer catalyzes the phosphotransfer of the γ -phosphoryl group of the bound ATP to the histidine residue of the other protomer through the association with the phosphotransferase domain (Varughese *et al.*, 2006; Stock *et al.*, 2000). To date it is unknown what triggers the conformational changes that initially bring the ATP-binding domain in close proximity to the active His residue and subsequently displaces it to allow space for the RR to bind. The histidine associated phosphoryl group is presented on a surface that facilitates the interaction with a response regulator molecule thus allowing phosphotransfer. The phosphotransfer between the HK and RR requires close contact between the two proteins and is facilitated by the alignment of hydrophobic patches provided by the interaction surfaces. The interaction surface of the HK is comprised of a four helix bundle provided largely by the $\alpha 1$ -helix. The residues in close vicinity to the site of phosphorylation on the $\alpha 1$ -helix are conserved within a group of HKs and are therefore likely to play a role in discrimination of non-group members. The $\alpha 2$ -helix also plays a role in discrimination as the lower part of the $\alpha 2$ -helix appears to interact

with the RR as shown in the Spo0F: Spo0B complex, possibly contributing to selectivity (Mukhopadhyay and Varughese, 2005).

In addition to the kinase activity, many HKs possess a phosphatase activity to dephosphorylate their cognate RRs. This provides a mechanism to regulate the activity of the TCS through the bidirectional control of the phosphorylation state of the downstream RR (Stock *et al.*, 2000). The RR can be dephosphorylated by other unrelated phosphatases and also by intramolecular catalyzed hydrolysis (Hess *et al.*, 1988; Perego 2001; Zhao *et al.*, 2002). Even though rarely reported, a reverse phosphor-transfer from the phosphorylated RR to the HK can occur (Shi *et al.*, 1999; Georgellis *et al.*, 1998; Dutta and Inouye, 1996).

1.4 Response regulators

Most RRs are comprised of two domains: a conserved N-terminal receiver domain and a variable C-terminal effector domain connected by a linker region (Figure 1.7). The receiver domain contains a conserved aspartate residue, known to be the site of phosphorylation. Significant insight has been gained from structural work on Spo0F that serves as a model for receiver domains of RRs (Tzeng and Hoch, 1997). Spo0F consists of a central β -sheet formed by five β -strands and is surrounded by five α -helices. Two of the α -helices are located on one side of the β -sheet and three on the other (Figure 1.8). The phosphoryl receiver residue is a conserved aspartate found at the C-terminal end of β 3 within a catalytic pocket. This pocket is formed by four additional conserved residues; two aspartates, a threonine and a lysine. Those catalytic residues are surrounded by the loops that connect the β -sheet with the α -helices (Varughese *et al.*, 2002). The structural features of the receiver domain appear to be highly conserved within RRs where the active site is always located at the carboxy-terminal end of the β -sheet (Volz, 1993). The phosphotransfer and phosphate hydrolysis require a divalent metal ion, usually Mg^{2+} or Mn^{2+} within the catalytic pocket which is held in place by acidic residues of the β 1- α 1 loop (see Gao *et al.*, 2007 for review; Birck *et al.*, 2003). The phosphoryl group is usually received from the cognate HK but small molecules such as acetyl phosphate can also serve as phosphodonors (Stock *et al.*, 1995; in Silhavy and Hoch; Stock *et al.*, 2000).

Alanine scanning mutagenesis of Spo0F revealed a number of residues, exposed and buried, that are involved in the interaction with SpoB and mapped on the same surface as the site of phosphorylation (Tzeng and Hoch, 1997; Jiang *et al.*, 1999). It was shown that buried residues in Spo0F have an influence on the

molecular recognition of the HK. Those residues are involved in conformation of the $\beta 4$ - $\alpha 4$ loop that is directed towards the HK (McLaughlin *et al.*, 2007).

A linker domain connects the receiver domain with the effector domain and is most likely involved in transmitting the signal throughout the protein by allowing conformational changes and therefore effecting the activation of the RR activity (Walthers *et al.*, 2003).

The C-terminal effector domain of RRs is highly variable and serves to interact with target molecules. Most RRs are transcriptional regulators and their effector domain is hence comprised of variations of helix-turn helix motifs that facilitate binding to DNA. Other functions of this domain include protein or RNA binding, enzymatic activity, and serving as a phosphorelay intermediate (see Gao *et al.*, 2007 for review).

Once phosphorylated at the N-terminal receiver domain, the RR becomes active, dimerizes and changes its conformation. This allows the C-terminal effector domain to engage in its mechanistic, enzymatic, or transcriptional regulating function. The result is a diverse range of output possibilities despite the common input domain structure and activation mechanism (see Gao *et al.*, 2007 for review; Dutta *et al.*, 1999).

The active state of the RR is regulated through multiple mechanisms. Many RRs can be inactivated by one or all of these mechanisms: autophosphatase activity, dephosphorylation by their cognate kinase, and also dephosphorylation by other unrelated phosphatases (Laub and Goulian, 2008; Cho *et al.*, 2001; Stock *et al.*, 2000; Perego and Hoch 1996). By employing these mechanisms to regulate the state of RR phosphorylation, the cell possesses yet another level of control and adjustment of the response to a certain signal.

1.5 Specificity of HK:RR interaction

Bacteria contain none to many TCSs depending on the complexity of their habitat. In order to respond specifically to a given environmental change the cell has to have defined signaling pathways. These pathways consist of HKs and RRs which each form a group of signaling proteins that display highly similar domain structures. Yet, each TCS controls a defined set of responses because a HK only phosphorylates its cognate RR. Therefore, there must be a specific recognition mechanism between the two components to interact only with their cognate partners. How the specific interaction between cognate HK:RR pairs is achieved despite the overall similarity of the domain structures is still not fully understood.

The high degree of specificity of HK/RR pair recognition lies within their interacting surfaces. To date, the only representative example of HK:RR interaction is the cocrystal structure of the Spo0F:Spo0B complex. Analysis of this complex has provided insight into the recognition of cognate TCS pairs (Zapf *et al.*, 2000). The proteins Spo0F and Spo0B are part of the sporulation initiation phosphorelay (see Figure 1.2). Spo0F belongs to the superfamily of RR proteins and Spo0B is a phosphotransferase bearing structural and functional similarities to the phosphohistidine domain of conventional HKs. The interaction surface of Spo0F consists of a hydrophobic patch that is formed by five residues: Leu15, Ile18, Pro105, Phe106 and Ile108 (Madhusudan *et al.*, 1996).

The phosphorylation site of Spo0B is surrounded by residues that form a similar hydrophobic patch and contains residues within the α 1-helix that are likely to contribute to specificity (Figure 1.9). During phosphotransfer, the active His of the HK and the active Asp of the RR must come into close proximity and this requires exact positioning of the residues. Through the alignment of the hydrophobic patches of both proteins, an ideal environment for phosphotransfer is provided. Surrounding the site of phosphorylation and hydrophobic patch are highly variable residues that also form part of the interaction surface and may be responsible for discrimination between cognate and non-cognate partners (Mukhopadhyay and Varughese 2005; Varughese, 2002).

The specificity of signal transduction in TCSs on a cellular and molecular level has been recently reviewed in detail by Laub and Goulian (2007). Briefly, on a cellular level, temporal control of TCS expression, substrate competition, and phosphatase activity decreases the possibility of phosphorylation of non-cognate RRs. To further decrease the possibility of phosphotransfer between non-cognate HKs and RRs, HKs exhibit a strong kinetic preference for their cognate partner *in vitro* to the exclusion of all other RRs. Therefore, the specificity of the phosphotransfer is likely to be found at the molecular level.

One step in that direction was reported recently in a covariance analysis identifying six clusters of amino acid positions within the facing surfaces of HKs and RRs. Clusters one to five are located on the α 1-helix of HKs and mainly on the α 1-helix of RRs that interact with each other. The sixth cluster contains amino acids that do not appear to be directly interacting with each other but have been shown to play a role in the phosphotransfer experimentally. The interactions of those amino acids provides the environment for phosphoryl transfer and are therefore likely to contribute to the specificity of interaction (Szurmant *et al.*, 2008a).

An experimental approach to identify the determinants for specificity of interaction between HKs and RRs was carried out by M. Laub's group (Skerker *et al.*, 2008). In this study, the HK EnvZ was systematically altered to enable the change of preference to phosphorylate its cognate RR OmpR to the non-cognate RstA. This was achieved by initially swapping the histidine phosphotransfer domain of heterologous HKs followed by narrowing the region of the $\alpha 1$ helix of EnvZ down to three amino acids conferring the specificity. By changing these three amino acids in position 7, 11 and 12 respectively to the site of phosphorylation from those of EnvZ to those found in RstB a 200-fold preference for the non-cognate RR RstA was achieved over the cognate RR OmpR. When these three residues were changed to those of other kinases, only a partial change of specificity was observed which was enhanced significantly by also swapping the adjacent loop connecting the $\alpha 1$ with $\alpha 2$ helix (Skerker *et al.*, 2008).

This study has significantly contributed to the understanding of the specificity of the interaction between a HK and RR showing experimentally the significance of individual amino acids within the interaction surface of a HK. However, it appears that there are additional determinants of specificity between TCS pairs that the other side of this protein:protein interaction, namely the interaction surface of the RR, has not been considered.

1.6 Crosstalk

Crosstalk is a term that has been coined to describe the phenomenon of phosphotransfer between non-cognate HKs and RRs which otherwise form an independent TCS. This interaction has been reported in *in vitro* studies, but the reaction occurs at a rate that is not comparable with those found in cognate pairs (Yamamoto *et al.*, 2005). Crosstalk *in vitro* and *in vivo* between the catalytic domain of a HK and the non-cognate RR from another organism has also been reported (Fisher *et al.*, 1995). They expressed the catalytic domain of the HK VanS of *Enterococcus faecium* BM4147 in *Escherichia coli* stripped of all potential phosphodonors for the RR PhoB. Activation of VanS could then be observed *in vivo* by PhoB~P activated *phoA* (alkaline phosphatase) expression showing that VanS is indeed able to phosphorylate PhoB. This result was supported by an *in vitro* analysis with purified proteins that clearly showed that PhoB phosphorylation is possible by VanS even though phosphotransfer from the cognate HK PhoR is about 100-fold more efficient. Crosstalk between other TCSs in *E.coli* has been experimentally investigated by Verhamme *et al.* (2002). This group focused on four TCSs (UhpBA,

PhoRB, NtrBC and ArcBA) in *E.coli* which play a major role in metabolism. Crosstalk between these four TCSs was monitored by *lacZ* fusions of a specific regulon gene of each TCS. Only one incidence of crosstalk could be observed, PhoR and UhpB could activate NtrC but only in a NtrB negative background. In fact, most reported observations of crosstalk *in vivo* seem to occur only when the cognate kinase was mutated, overexpressed, or absent (Kim *et al.*, 1996; Matsubara & Mizuno *et al.*, 1999; McCleary *et al.*, 1993; Ninfa *et al.*, 1988; Silva *et al.*, 1998). Taken together, these experiments neither elucidate the occurrence nor the significance of crosstalk *in vivo* within wild-type cells (Laub and Goulian, 2007; Wanner, 1992).

There are two different signal transduction pathways that differ from the straight forward phosphotransfer chain within a TCS or phosphorelay and could be mistaken for crosstalk. Firstly, there are phosphotransfer reactions involving two or more kinases that phosphorylate the same response regulator. An example for this is that the five Kin kinases (KinA, KinB, KinC, KinD and KinE) of *B.subtilis* all phosphorylate the single domain RR Spo0F (Jiang *et al.*, 2000). Secondly, a HK can phosphorylate more than one RR as it is reported in *E.coli* chemotaxis where CheA phosphorylates CheB and CheY (Stock *et al.*, 1988). Additionally, there are regulatory interactions between different TCS in order to form sensory transduction networks such as ResDE and PhoPR do (Birkey *et al.*, 1998). Other regulatory networks are formed by several TCSs that have overlapping target genes as has been shown in an extensive DNA microarray analysis of 24 TCS in *B.subtilis* (Kobayashi *et al.*, 2001). Their approach was to overexpress RRs in the absence of their cognate HK showing a remarkable overlap of target genes for RR belonging to the NarL family.

However, Howell *et al.*, (2006) reported unidirectional crosstalk between the kinase PhoR and the non cognate RR YycF which appears to occur in natural conditions.

1.7 The two-component system YycFG

In *B.subtilis*, the RR YycF and the HK YycG are transcribed from a multicistronic operon (Figure 1.10A) along with YycH, YycI, YycJ and the HtrA-like protease YyxA (Fabret and Hoch, 1998). Three different sized transcripts result from the *yycFG* operon: (i) a 7.4 kb transcript found in early vegetative growth phase (ii) at the same phase a 2.4 kb transcript is detectable and (iii) a *yyxA* probe detects a 1.4 kb transcript during the late phase of sporulation (Fukuchi *et al.*, 2000). YycH and

YycI are membrane bound proteins that regulate YycG activity. The function of YycJ and the regulation of the *yycFG* operon is unknown.

The YycF-YycG TCS is present in all low G+C Gram positive bacteria and is the only essential TCS in *B.subtilis* and *S.aureus* but only the RR YycF has been found to be essential in *S.pneumoniae* and *E. faecalis* (Fabret and Hoch 1998; Martin *et al.*, 1999; Ng *et al.*, 2003; Hancock and Perego, 2004). It has been recently reported that its essentiality appears to be polygenic in nature, as it controls genes critical for cell wall metabolism in *B.subtilis* and similarly in *S.aureus* and *S.pneumoniae* (Bisicchia *et al.*, 2007; Dubrac *et al.*, 2007; Ng *et al.*, 2005).

So far there have been 9 members of the YycFG regulon established in *B.subtilis* (Figure 1.10B) namely *yvcE*, *lytE*, *ydjM*, *yoeB* and *yjeA*, the *tagAB* and *tagDEF* operons, *yoch*, *ykvT* and *ftsAZ* (Bisicchia *et al.*, 2007; Howell *et al.*, 2003; Fukuchi *et al.*, 2000). The genes *yoch* and *ykvT*, encode putative autolysins that are directly regulated by YycFG (Howell *et al.*, 2003). Also regulated by YycFG is the *tag* operons which code for essential genes of teichoic acid biosynthesis. The *tag* regulation by YycFG appears to be indirect and restricted to repression of the divergent promoter during phosphate limitation (Howell *et al.*, 2006). The proteins encoded by *ftsAZ* are involved in cell division. YycFG overexpression leads directly to upregulation of *ftsAZ* but is not necessary to maintain basal levels of *ftsAZ* expression (Fukuchi *et al.*, 2000; Fukushima *et al.*, 2008). The latest identified members of the YycFG regulon as described in Bisicchia *et al* (2007) are also involved in cell wall metabolism. YvcE and LytE belong to the same family of autolysins as YocH and YkvT; YjeA is a peptidoglycan deacetylase, YdjM has no known function but shows features shown for other cell wall mutants and YoeB regulates autolysin activity (Salzberg and Hellmann 2007).

The domain architecture of the histidine kinase YycG and its cognate response regulator YycF are shown in Figure 1.10C. The HK YycG is a 611 amino acid protein expressed during exponential growth (Howell *et al.*, 2003). YycG is a membrane bound HK composed of an extracellular sensing domain, two transmembrane domains, and a cytoplasmic catalytic domain containing the site of phosphorylation at H386. C-terminal of the conserved His YycG has the additional features of PAS and HAMP linker domains. It has been recently reported that the kinase YycG is located at the division septum of growing cells and co-localizes with the FtsZ, its localization depending on the latter (Fukushima *et al.*, 2008). The cognate RR YycF is 235 amino acids in size, consisting of the classical receiver and effector domains. YycF acts as a DNA-binding transcriptional regulator upon

activation by YycG (Fabret and Hoch, 1998). YycF's location is associated with the nucleoid which is also dependent on FtsZ (Fukushima *et al.*, 2008).

YycH and YycI are shown to be membrane bound proteins that form a ternary complex with the YycG (Szurmant *et al.*, 2008b). It is thought that this direct interaction regulates the activity of the HK YycG and therefore might be involved in signal mediation because either deletion of YycH or YycI leads to a constitutive active state of YycG (Szurmant *et al.*, 2005; 2007). The transmembrane domains of YycH and YycI control YycG activity at the membrane level as a deletion study showed that their transmembrane domains are sufficient to repress YycG activation (Szurmant *et al.*, 2008b). A depletion study showed that an additional feature of YycG activation appears to be the division septum in growing cells because in the absence of FtsZ, YycG appears to have decreased kinase activity towards YycF (Fukushima *et al.*, 2008).

1.8 The two-component system PhoPR

The HK PhoR and its cognate RR are transcribed from a bicistronic operon (Figure 1.11A) with a complex regulatory region that contains at least six promoter start sites: P_{A6} , negatively controlled by CcpA (carbon catabolite protein A); P_5 , control element unknown; P_{A4} and P_{A3} , require $E\sigma^A$; P_{E2} $E\sigma^E$ and $P_{B1}E\sigma^B$. The presence of PhoP~P amplifies the expression from P_{E2} , P_{A4} and P_{A3} (Puri-Taneja *et al.*, 2005; Paul *et al.*, 2004).

The PhoPR TCS is activated upon phosphate starvation conditions. The PhoPR regulon and the integration of PhoPR in a regulatory network with both ResD/ResE and the Spo0A phosphorelay has been intensively studied (for more detail see Hulett, 1996; Birkey *et al.*, 1998; Pragai *et al.*, 2004 and Allenby *et al.*, 2005). The PhoPR regulon is comprised of 34 genes (Figure 1.11B). The members of the regulon include phosphate transporters, alkaline phosphatases, phosphodiesterases and genes encoding proteins of unknown function. Additionally, PhoPR plays a key role in regulating anionic cell wall polymer synthesis controlling the switch from teichoic acid to teichuronic acid synthesis during phosphate starvation (Qi and Hulett, 1998). Therefore, PhoPR is also involved in cell wall metabolism in phosphate limited conditions. The PhoPR operon is part of its regulon because it is partially self regulated. Phosphorylated PhoP (PhoP~P) regulates the *phoPR* operon through a positive feedback-loop and is required for the induction or repression of other members of the Pho regulon (for review see Hulett, 1996, Pragai *et al.*, 2004). One of the regulon members is the secreted alkaline phosphatase

PhoA that facilitates the recovery of inorganic phosphate from organic sources. The expression of PhoA is activated by its only known activator Pho~P (Allenby *et al.*, 2005, Liu *et al.*, 1998).

The domain architecture of PhoR and its cognate response regulator is shown in Figure 1.11C. The 579 amino acid HK PhoR autophosphorylates under phosphate limited conditions and transfers the phosphoryl group to its cognate RR PhoP (Hulett, 1996). PhoR is a typical HK that resides in the cytoplasmic membrane containing a periplasmic loop that is anchored in the membrane by two transmembrane domains. A linker region connects the second TM domain with the C-terminal catalytic domain. This linker region contains a predicted PAS domain of approximately 106 amino acids. Adjacent to the PAS is the dimerization domain that contains the conserved site of phosphorylation His360 and the ATP-binding domain. The activating signal for the Pho response has not been identified to date but a cysteine residue within the PAS domain (Cys303) appears to play an important role in the regulation of the level of phosphorylated PhoP probably by stabilizing the intermediate state of PhoR and PhoP during phosphotransfer (Eldakak and Hulett 2007). The response regulator PhoP consists of two domains, the receiver domain with the conserved phosphorylation site D53 that is connected to the effector domain through a long linker region. PhoP belongs to the OmpR superfamily based on sequence similarities of the N-terminal effector domain. The crystal structure of the receiver domain of PhoP was resolved in 2003 (Birck *et al.* 2003) and, despite the overall structural similarities to other members of the OmpR subfamily, the conformation of loop 4 and helix α 1 differ in position from the others.

1.9 Observations leading to the presented study

A computational study of HK four helix bundles in *B. subtilis* (Mukhopadhyay and Varughese, 2005) showed that the α -helix 1 consists of highly variable as well as conserved residues and displays a hydrophobic region. Those variable regions might hold the means of specificity of the interaction between a HK and a cognated RR. Several problems arise while studying the specific interaction of cognate partners *in vivo*: (i) HKs and RRs are highly conserved around their active sites. The similarities within the conserved regions are as high as 96%. (ii) In order to transfer a phosphoryl group, the proteins have to come in close proximity for interaction. (iii) Even *in vitro* HKs preferentially interact with their cognate partners (Yamamoto *et al.*, 2005).

Properties of YycFG and PhoPR enabling the current study

The two systems YycFG and PhoPR are phylogenetically closely related. They are expressed under different conditions (phosphate rich vs. phosphate depleted) as well as during different stages of the growth cycle (exponential vs. stationary phase). YycG is expressed and phosphorylates YycF during the exponential phase of growth in a nutrient rich medium (Howell *et al.*, 2003) whereas the PhoPR TCS is expressed and activated upon phosphate starvation in stationary phase (Hulet *et al.*, 1994). Under non-starvation conditions, PhoP is present but unphosphorylated at a low concentration (Hulet, 1996).

It is well established that the phosphotransfer occurs between cognate pairs and usually only between the cognate partners. One important exception is the unidirectional crosstalk between PhoR and YycF (Howell *et al.*, 2003 and 2006). This shows that YycF can be phosphorylated by the non-cognate PhoR during phosphate starvation, although the reciprocal phosphorylation of PhoP by YycG does not seem to occur (Figure 1.8 and Howell *et al.*, 2003, 2006). Thus these two TCSs, YycFG and PhoPR, are ideal to study how specificity is determined between cognate kinases and response regulators of the same family.

1.10 Objective of this study

This study aims at the elucidation of determinants of the specificity of the interaction in TCSs using YycFG and PhoPR of *B.subtilis* as a model system.

In an effort to understand the specificity of molecular recognition between a HK and an RR, a comprehensive analysis of YycG was undertaken by changing defined amino acids that are predicted to contribute to the specificity of the HK:RR interaction. The amino acids positioned C-terminal of the site of phosphorylation that comprises the region of interaction were changed individually and in combination to mimic those of PhoR. The consequences of such mutations were examined *in vivo* to determine the ability of YycG* to phosphorylate PhoP. Whether this PhoP~P is due to a direct interaction with the mutated YycG* was further investigated with purified proteins *in vitro*. This approach also allowed the observation of the loss of specificity for the cognate RR YycF. In addition, a kinetic analysis was carried out enabling direct comparison of the phosphotransfer reaction of wild type and mutant HKs.

Additionally, the interaction surface of the response regulator PhoP was altered by defined mutations, singly and in combination. The effect of those changes was

examined *in vivo* in order to establish the amino acids conferring on PhoP the ability to receive a phosphoryl group from the non cognate HK YycG. All mutated PhoP*s were purified and examined *in vitro* in an effort to establish the level of phosphor acceptance from the non cognate HK YycG and the loss of ability to receive a phosphoryl group from its cognate partner PhoR.

Chapter 2
Methods and Materials

2. Methods and Materials

2.1 Bacterial strains

The bacterial strains and plasmids used in this study are listed in Table 2.1. All strains were grown aerobically in Luria Bertani medium (LB; Miller, 1972) at 37°C with the addition of antibiotics as appropriate (for *Escherichia coli*, ampicillin at 100 µg/ml; for *Bacillus subtilis*, chloramphenicol at 3 µg/ml; neomycin at 7 µg/ml; spectinomycin at 100 µg/ml, erythromycin at 3 or 150 µg/ml). Minimal medium was supplemented with 1% (w/v) tryptophan, 1% (w/v) threonine as appropriate (Yoshida *et al.*, 2000). Xylose was added to the medium where necessary at concentrations specified in the text. X-gal was used at 100 µg/ml for LB agar. Integration at the *amyE* locus of the *B.subtilis* chromosome was screen for on LB agar plates supplemented with 0.2% starch. Putative transformants were grown overnight and an iodine solution was added leading to the discoloration of the plate showing a halo for colonies that remain *amyE* positive whereas correct transformants show no halo.

2.2 Sequence analysis

DNA sequencing reactions were performed by MWG Biotech and GATC (Germany). Sequences were confirmed by comparison to the *B. subtilis* genome using the BLASTn search program available on the SubtiList website (<http://www.genolist.mirror.edu.cn/SubtiList>). *B. subtilis* protein sequences were also obtained on SubtiList. Alignments were carried out with ClustalW (<http://www.ebi.ac.uk/clustalw/>).

2.3 DNA manipulation

Standard procedures were used for DNA manipulation (Sambrook *et al.*, 1989). Restriction enzymes were supplied by New England Biolabs (Beverly, Massachusetts) and T4 DNA ligase was obtained from Roche (Mannheim, Germany). To facilitate blunt end cloning DNA Polymerase I / Large Klenow Fragment (Klenow) (New England Biolabs, Beverly, Massachusetts), T4 Polynucleotide Kinase (Promega, Wisconsin USA) and Shrimp Alkaline Phosphatase by Roche (Mannheim, Germany) were used. Small scale plasmid DNA preparation was carried out using a boiling lysis technique modified from Sambrook *et al.*, (1989) followed by further purification using JET quick PCR product purification SpinKit (GenoMED, Löhne, Germany) according to the manufacturer's instructions. Chromosomal DNA was isolated from *Bacillus subtilis* strains as described (Harwood

and Cutting, 1990). Polymerase chain reaction (PCR) reactions were generally set up according to manufacturer's instructions with either Taq polymerase (Invitrogen, Paisley, UK) or the high fidelity polymerase Pfu turbo (Stratagen; Amsterdam, The Netherlands) and Phusion (Finnzymes, NEB, Beverly, Massachusetts).

2.4 Immunoblot Analysis

Cell lysates of exponential growth phase cultures (OD_{600} 1-1.5) were prepared as described in Howell *et al.*, (2006) and separated on 10% SDS-PAGE gels according to the method of Laemmli (1970). Protein quantification was performed using the Non-Interfering Protein Assay according to the manufacturer's instructions (Calbiochem-Novabiochem Corporation, USA) using BSA as the protein standard. YycG from *B.subtilis* was detected by Western blotting using a primary rabbit antibody (Howell *et al.*, 2006) and secondary antibody anti-rabbit IgG peroxidase conjugate developed in goat (Sigma, Missouri, USA). Chemiluminescent detection was carried out using the Supersignal West Dura HRP Detection Kit (Pierce, Perbio).

2.5 β -galactosidase assay of promoter fusion

β -galactosidase activity was measured as described previously (Miller, 1972). Strains containing promoter fusions were streaked onto LB plates containing appropriate antibiotics from frozen stocks and grown overnight. One colony was used to inoculate 10 ml of LB medium followed by aerobic growth at 37°C with shaking for 2.5 hours. An aliquot of these cultures was used to inoculate 100 ml LB at starting $OD_{600} = 0.01$. Cells of 10 ml culture were harvested by centrifugation every 15 min throughout exponential growth starting at a OD_{600} of approximately 0.2 by centrifugation at 4000 rpm for 6 min at 4°C. Pellets were resuspended in Z buffer (Miller, 1972) containing 0.1 μ g/ml of lysozyme, 0.01 μ g/ml DNase and 1mM dithiothreitol (DTT) then lysed in eppendorf tubes by incubation at 37°C for 25 min. The lysed samples were spun in a microfuge at 12,500 rpm for 5 min. The supernatant was transferred to a fresh eppendorf tube and was used for both the β -galactosidase assay and the determination of the protein level. Protein quantification was performed using the BCA assay (BioRad, Hercules, CA, USA) using IgG as the protein standard (Bradford, 1976). Aliquots of lysate were added to 100 μ l reaction mixtures, in a 96-well plate, containing o-nitrophenyl-D-galactopyranoside (ONPG) as a substrate. This plate was incubated at 28°C until being stopped by the addition

of 60 μ l 1M Na₂CO₃. The reaction time was recorded and the OD₄₂₀ of the reaction was read. The β -gal units were determined using the following formula:

$$\beta\text{-gal units: } \frac{(\text{OD}_{420})(3.3)}{(\text{mg/ml protein})(\text{ml sample})(\text{minutes of reaction})(0.00486)}$$

2.6 Protein Expression Plasmids

To construct plasmids for overproduction of the cytoplasmic region of each HK and the full length RRs, DNA fragments were generated by PCR using the corresponding plasmids from the IJ series as templates and a set of primer pairs P_{ycG5'} and P_{ycG3'}. After digestion with *NdeI/BamHI*, the PCR-amplified fragments were inserted between the same restriction site of vector pET21b (Novagen). All plasmids constructed were verified by DNA sequencing. Plasmids to express PhoP and mutated PhoP* were constructed as described in more detail in 2.11 Plasmid and Strain construction.

2.7 Purification of Proteins

The expression strain *E.coli* BL21[DE3] containing plasmids carrying the target proteins were grown in Luria-Bertani medium containing 75 μ g ampicillin ml⁻¹ at 37°C with shaking. When the cultures had reached an OD₆₀₀ of 0.6-0.8, the production of protein was induced by addition of 1mM isopropyl thio- β -D-galactoside (IPTG) and cultures were transferred to a growth temperature of 28°C. Cells were harvested by centrifugation 3 h post-induction, resuspended in ice-cold lysis buffer (500 mM NaH₂PO₄, 300 mM NaCl, 20 mM imidazole, 0.1% (v/v) Tween) and lysed by lysozyme treatment (1 mg ml⁻¹, 1% v/v protease inhibitor) and sonicated. To remove cell debris and unbroken cells, the lysate was centrifuged at 12,000 rpm for 30 min at 4°C. The supernatant was subjected to affinity chromatography on Ni²⁺-NTA His·Bind Resins (Novagen). Following sample application, the protein was allowed to bind for 2 h, followed by four washes with wash buffer (50 mM NaH₂PO₄, 300mM NaCl, 40 mM imidazole) containing 0.1% v/v Tween and four washes with wash buffer without Tween. The proteins were eluted in elution buffer (50 mM NaH₂PO₄, 300mM NaCl, 250 mM imidazole) and 1% (v/v) protease inhibitor was added. Elutes were dialyzed over night against 50% storage buffer (20 mM Tris-HCl pH 8.0, 300mM NaCl, 50% v/v glycerol) and stored at -20°C.

2.8 *In vitro* protein phosphorylation assay

All phosphorylation assays were carried out at room temperature in a final volume of 30 μ l composed of 12 μ g of the respective protein(s), phosphorylation buffer (100 mM Tris-HCl pH 8.0, 200 mM KCl, 4 mM MgCl₂, 0.5 mM DTT, 0.1 mM EDTA, 3.5% glycerol) and 10% (v/v) radiolabelled ATP mixture (0.96 μ M ATP, 5 μ Ci [γ -³²P]-ATP). The reactions were initiated by the addition of the radiolabelled ATP mixture and stopped at various times by adding 5 μ l reaction mixture to an equal volume of 2x SDS loading buffer and gentle heating to 37°C. The samples were analyzed by SDS-PAGE on 10% acrylamide gels. The gels were dried and analyzed by autoradiography.

2.9 Quantitative *in vitro* phosphorylation assay

The phosphorylation reactions were carried out as described above with the exception of protein and ATP concentrations. The HKs YycG and PhoR were present at a final concentration of 2.5 μ M each. Response regulators were added at 25 μ M when phosphotransfer from mutated YycG* was tested and at 2.5 μ M when incubated with the HK PhoR. However, RRs were added at a concentration of 25 μ M when incubated with the HK YycG. The phosphorylation buffer is described above. The radiolabelled ATP mixture (2mM ATP, 20 μ Ci [γ -³²P]-ATP) was added as 10% of the final reaction volume of 30 μ l. After the reactions were carried out and subjected to SDS gel analysis, the gels were dried and exposed to a phosphor screen and quantified by using the Fujifilm Phosphoimager (FLA-3000series) with MultiGauge Ver.2.0. The initial rates were determined by measuring the rate of RR phosphorylation between 10 and 300 sec of cognate HK:RR pairs and between 30 and 1200s of non-cognate pairs.

2.10 Growth of *B.subtilis* in microtiter plates

In order to carry out these growth experiments, strains were streaked fresh on LB agar with the appropriate antibiotic supplementation the night before the actual experiment. The following day, from a single colony cells were transferred to a well of a 96-well plate filled with 100 μ l LB and the appropriate antibiotic. This was carried out in triplicate for each strain. The outer wells remain uninoculated to prevent evaporation. The plate was incubated shaking at 37°C for 3-4 hours, then an OD₆₀₀ reading was taken. The cultures were diluted back to a starting OD₆₀₀ of 0.02 into a fresh plate. This plate was transferred into the BioTek Synergy 2 machine. The machine was programmed to incubate the plate at 37°C with shaking. OD₆₀₀

readings were taken every 10 minutes over a period of 10 hours. The media was supplemented with xylose as indicated in the text. The software used for controlling the machine and analyze the data was Gen5 from BioTek.

2.11 Plasmid and strain constructions

Construction of vector pIJ100

Based on the plasmid pXT, that allows placing expression of a gene of interest under inducible xylose control as well as integration via double crossover into the *thrC* locus of the chromosome of *B.subtilis*, plasmid pIJ100 was constructed to facilitate easy introduction of amino acid changes in the histidine kinase domain of *yycG*.

Therefore, the first ~1140 bp of the *yycG* gene, encoding the N-terminal start of the wild type *B.subtilis yycG* coding region was amplified by PCR. The forward primer PIJ100F includes a RBS, optimized for spacing and sequence with respect to the start codon ATG and the reverse primer PIJ100R. This fragment was cloned into a, with DNA Polymerase I Large (Klenow) blunt ended, *EcoRI* site of the vector pXT (Derre *et al.*, 2000) creating vector pIJ100. This plasmid was transformed into *E.coli* Tg1, selecting for Amp^R, isolated and sequenced.

pIJ101-pIJ108

The remaining 706 bp of the *yycG* gene encoding the C-terminal domain were amplified by PCR with the forward primers PIJ101-P108. Each primer encoded the desired amino acid changes listed in Table 2.4 and were designed to facilitate cloning into the naturally occurring *EcoRI* site of *yycG* within plasmid pIJ100 and reverse primers PIJ101R. These fragments were subcloned into vector pBluescript KS- utilizing the *EcoRI/SmaI* site. Upon digestion with *EcoRI/SphI* and subsequent gel elution, the fragments were individually cloned into the *EcoRI/SphI* site of vector pIJ100, resulting in plasmids pIJ101-pIJ108. All plasmid was transformed into *E.coli* Tg1, selecting for Amp^R, isolated and sequenced.

pIJ112 and pIJ114

Plasmids pIJ112 and pIJ114 where constructed to introduce two and four amino acid changes into the α 1-helix of YycG. Therefore, the 310 bp encoding the catalytic His domain of *yycG* were amplified by PCR with the forward primers PIJ112 & PIJ114, (containing amino acid changes listed in Table 2.4) and reverse primer

PIJ112-114 designed to facilitate cloning into the naturally occurring *EcoRI* and *BglII* site of *ycgG* within plasmid pIJ108. These fragments were subcloned into vector pBluescript KS- (pKS) utilizing the *SmaI* site. Upon digestion with *EcoRI* and *BglII* and subsequent gel elution, the fragments were individually cloned into the *EcoRI* and *BglII* site of vector pIJ108, resulting in plasmids pIJ112 and pIJ114.

pIJ115

In order to create a hybrid kinase of YycG' and PhoR that would display the perfect interaction surface to phosphorylate PhoP the regions encoding the N-terminal sensing domain of YycG and the C-terminal catalytic domain of PhoR was constructed by overlapping PCR. In the first reaction(s) basepairs 1-1113 of *ycgG*, corresponding to amino acids M1-E371, were amplified with the primer pair PIJ110F and PIJ111R using plasmid pIJ108 as template. Primers PIJ111F and PIJ110R were used to amplify *phoR* from base 1038 to 1737, corresponding to residues E346-A579 using DN1103 as a template. The obtained fragments were mixed in equal amounts and used as template for the second reaction that was carried out with the primers PIJ110F and PIJ110R. The fragment, encoding the hybrid gene *ycgG'*-*phoR*, was cloned into the *BamHI/HindIII* site of vector pXT resulting in plasmid pIJ115.

Plasmid pKS140

A small plasmid carrying the wild type *phoP* needed to be created to be used as template for PCR mutagenesis. Therefore, the 720bp gene *phoP* was amplified by PCR with the forward primer 115F that includes a RBS, optimized for spacing and sequence in respect to the start codon ATG and primer 115R. The resulting fragment was directionally cloned into the *BamHI* and *HindIII* sites of vector pbluescript II KS, creating vector pKS140. This vector was transformed into *E.coli* TG1, selected for Amp^R, isolated and sequenced.

Plasmid pKS141

A second template for site directed mutagenesis was created to facilitate the combinations of single amino acid changes in PhoP. The plasmid pKS141 was created by site-directed mutagenesis using wild type *phoP* containing plasmid pKS140 as template. The plasmid was amplified with primers 116F and 116R containing the amino acid change P107T. The PCR product was digested with *DpnI* and transformed into *E.coli* TG1, selected for Amp^R and isolated. The correct plasmid was identified by sequencing.

Plasmids pKS142-pKS148

The plasmids pKS142-pKS148 were created by site-directed mutagenesis introducing single and combinations of amino acid changes into PhoP. The wild type *phoP* containing plasmid pKS140 was used as template and amplified with the forwards primers 117F-123F paired with the respective reverse primers 117R-123R. The amino acid changes contained in these primers are listed in Table 1. The PCR generated plasmids were digested with *DpnI* and transformed into *E.coli* TG1, selected for Amp^R and isolated. The correct plasmid was identified by sequencing.

Plasmids pKS149-pKS155

The plasmids pKS149-pKS155 were created by site-directed mutagenesis in order to create the remaining amino acid changes in PhoP. The plasmid pKS141 containing the amino acid change P107T in the *phoP* gene was used as template and amplified with the forwards primers 117F-123F paired with the respective reverse primers 117R-123R. The amino acid changes contained in these primers are listed in Table 1. The PCR generated plasmids were digested with *DpnI* and transformed into *E.coli* TG1, selected for Amp^R and isolated. The correct plasmid was identified by sequencing.

Plasmids pIJ140-pIJ155

These vectors were created in order to integrate a mutated copy of *phoP* into the *thrC* locus of the *B.subtilis* chromosome. The plasmids pIJ140-pIJ155 were constructed by the digestion of the respective pKS140-155 plasmid with *Bam*HI/*Hind*III. The resulting fragments were subsequently individually cloned into the respective restriction site of vector pXT. The resulting plasmids were transformed into *E.coli* TG1 and selected for Amp^R. The correctness of the insert sequence was verified previously in the pKS plasmid through sequencing.

Plasmids for protein purification:

pETYycG, pET105, pET112, pET114, pET107

This set of plasmids was constructed in order to express and purify wild type and mutated YycG* protein. The 1181 bp encoding the truncated 'YycG protein excluding the sensing and transmembrane domains were amplified by PCR using the forward primer yycG5' and the reverse primer yycG3' and the corresponding pIJ plasmid as template (pIJ108, pIJ105, pIJ112, pIJ114 and pIJ107). The fragments

were directionally cloned into the *NdeI* and *BamHI* of the expression vector pET21b (Novagen) resulting in plasmids pETYycG, pET105, pET112, pET114 and pET107.

Plasmids pET140-155

These plasmids were constructed to express and purify wild type and mutated PhoP* protein. The plasmids were constructed by the digestion of plasmids p141-p155 with *NdeI* and *XhoI*. The inserts were then ligated into the respectively digested vector pET21b and transformed into *E.coli* TG1, selected for Amp^R and isolated. The correct plasmid was identified by restriction mapping and verified by sequencing.

Parental strains:

IJW99 [*trpC2 amyE::P_{phoA}-lacZ Cm^R*]

IJR99 [*trpC2 ΔphoR::neo amyE::P_{phoA}-lacZ Cm^R, Neo^R*]

To construct *phoA-lacZ* reporter strains, the genomic region coding for the putative *phoA* promoter (*B.subtilis* 168, nucleotides -159 to +266 relative to the initiation point of transcription) was amplified by PCR using the primers IJ99F and IJ99R and cloned into *EcoRI* and *BamHI* site of the vector pDG268 (Antoniewski *et al.*, 1990), creating plasmid pIJ99. This plasmid was transformed into strains *B.subtilis* strain 168 and strain AH057, thereby creating strains IJW99 and IJR99 which serve as parental strains for P_{xyr}-yycG constructs. The correct integration of the construct into the *amyE* locus of both strains IJW99 and IJR99 was screened for by selection for Cm^R, and Cm^R, Neo^R respectively and screening for amylase deficiency.

IJPR99 [*trpC2 ΔphoPR::erm amyE::P_{phoA}-lacZ Cm^R, Erm^R*]

To construct a *phoA-lacZ* reporter strain in *ΔphoPR* background, strain IJW99 was transformed with chromosomal DNA of AH024 resulting in strain IJPR99.

AH037 [*trpC2 amyE::P_{yoch}-lacZ Cm^R*]

IJR98 [*trpC2 ΔphoR::neo amyE::P_{yoch}-lacZ Cm^R, Neo^R*]

Strain IJR98 was constructed by transformation of AH037 [*trpC2 amyE::P_{yoch}-lacZ Cm^R*] with chromosomal DNA of AH024 [*trpC2 ΔphoR::neo Neo^R*] resulting in a transcriptional *yoch-lacZ* fusion at the *amyE* locus in a *ΔphoR* background.

Strain set IJW101 - IJ108

[*trpC2 amyE::P_{phoA}-lacZ thr::P_{xyf}-yycG Cm^R,Spec^R*]

To construct strains IJ101-108 the plasmids pIJ101-108 were linearized by digestion with *Sma*I and individually transformed into the parental strain *B.subtilis* IJW99. Colonies growing on Cm and Spec were further characterized.

Strain set IJR101 - IJR108

[*trpC2 ΔphoR::neo amyE::P_{phoA}-lacZ thr::P_{xyf}-yycG Cm^R,Neo^R,Spec^R*]

To construct strains IJR101 – IJR108 the plasmids pIJ101-108 were linearized by digestion with *Sma*I and individually transformed into the parental strain *B.subtilis* IJR99. Colonies growing on Cm, Neo and Spec were further characterized.

Strain set IJPR105 - IJPR114

[*trpC2 ΔphoPR::erm amyE::P_{phoA}-lacZ thr::P_{xyf}-yycG'-phoR Cm^R,Erm^R,Spec^R*]

To construct strains IJPR105 to IJPR114, the corresponding strain from the IJW set was transformed with chromosomal DNA of AH024. Colonies growing on Cm, Erm and Spec were further characterized.

Strain set IJW121 - IJW128

[*trpC2 amyE::P_{yocH}-lacZ thr::P_{xyf}-yycG Cm^R,Spec^R*]

To construct strains IJ101-108 the plasmids pIJ101-108 were linearized by digestion with *Sma*I and individually transformed into the parental strain *B.subtilis* AH037. Colonies growing on Cm and Spec were further characterized.

Strain set IJR121 - IJR128

[*trpC2 ΔphoR::neo amyE::P_{yocH}-lacZ thr::P_{xyf}-yycG Cm^R,Neo^R,Spec^R*]

To construct strains IJ101-108 the plasmids pIJ101-108 were linearized by digestion with *Sma*I and individually transformed into the parental strain *B.subtilis* IJ98. Colonies growing on Cm, Neo and Spec were further characterized.

Strain IJW115

[*trpC2 amyE::P_{phoA}-lacZ thr::P_{xyf}-yycG'-phoR Cm^R,Spec^R*]

To construct strain IJ115, the plasmid pIJ115 was linearized by digestion with *Sma*I and transformed into the parental strain IJ99. Colonies growing on Cm and Spec were further characterized.

Strain IJR115

[*trpC2 ΔphoR::neo amyE::P_{phoA}-lacZ thr::P_{xyr}-yycG'-phoR Cm^R,Neo^R,Spec^R*]

To construct strain IJR115, the plasmid pIJ115 was linearized by digestion with *Sma*I and transformed into the parental strain IJR99. Colonies growing on Cm, Neo and Spec were further characterized.

Strain IJRP115

[*trpC2 ΔphoPR::erm amyE::P_{phoA}-lacZ thr::P_{xyr}-yycG'-phoR Cm^R,Erm^R,Spec^R*]

To construct strain IJRP115, the plasmid pIJRP115 was linearized by digestion with *Sma*I and transformed into the parental strain IJRP99. Colonies growing on Cm, Erm and Spec were further characterized.

Strains IJW140-IJW155

To construct strain IJW140-IJW155, plasmids pIJ115 to pIJ123P were linearized by digestion with *Sma*I and transformed individually into parental strain IJ99. Colonies growing on Cm and Spec were further characterized.

Strains IJR140-IJR155

To construct strain IJW140-IJW155, plasmids pIJ115 to pIJ123P were linearized by digestion with *Sma*I and transformed individually into parental strain IJR98. Colonies growing on Cm and Spec were further characterized.

Strains IJPR140-IJR155

To construct strain IJW140-IJW155, plasmids pIJ115 to pIJ123P were linearized by digestion with *Sma*I and transformed individually into parental strain IJPR99. Colonies growing on Cm and Spec were further characterized.

Chapter 3
Mutational analysis of the HK YycG

Results

Chapter 3 - Mutational analysis of the HK YycG

Introduction

Two-component systems are ubiquitously found in bacteria, enabling the sensing of environmental changes and translating them into a cellular response. The prototypical two-component system is composed of a sensing histidine kinase and its cognate response regulator that usually is a transcription factor.

Three distinct reactions have been observed in HKs: (i) autophosphorylation of a conserved histidine residue (ii) phosphorylation of the cognate RR (iii) dephosphorylation of the cognate RR. The interaction between the HK and its cognate RR is very specific and involves the binding of two conserved domains for phosphotransfer. Thus neither the overall nor domain structure can account for that high level of specificity; therefore the cause of specificity has to lie at the molecular level. Insight into the nature of the interacting surfaces and how phosphotransfer is achieved has been established by crystallography and mutational analysis of many TCS. The model for this study is Spo0B and Spo0F which are a phosphotransferase and single receiver domain respectively, that represent the interaction surfaces of a HK and RR. The four helix bundle found in Spo0B is also found in HKs including YycG and PhoR. As described in Howell *et al.* (2006) and Skerker *et al.* (2008), the region C-terminal of the His active site residue is most likely to contribute to specificity.

Structural comparison of YycG and PhoR

Both HKs YycG and PhoR are, in location, topology and sequence very similar, and importantly the region flanking the phosphorylated histidine is highly conserved. In group IA, according to the classification by Mukhopadhyay and Varughese (2005), the residues found at position -4, -3, -1, +1, +3, +4, +7, +8, +10, +11 and +12 - relative to the active His (H0) - are the most interesting as they face towards the RR and comprise the interaction surface (Figure 1.9 and 3.1). Thus these eleven residues are predicted to contribute to the specificity of interaction. Comparing the $\alpha 1$ helices of PhoR and YycG, this interaction surface is strikingly similar, only differing in five of the eleven positions, namely +3, +8, +10, +11, and +12, and identical at the other six positions (Figure 3.1 and Figure 3.2A).

Positions +3 and +10 are containing an arginine (R) in YycG and lysine (K) in PhoR (Figure 3.1) It is noteworthy that position +10 is highly variable throughout the group IA of HKs, whereas position +3 always contains an R or K. Also, position +8 is hypervariable within this group, although the threonine (T) in YycG and the serine (S) in PhoR are very similar amino acids. Position +11 is always either a serine (S) as in YycG or a glycine (G) as in PhoR, where both amino acids differ significantly in the size of the side chain. In four out of six kinases in group IA, position +12 is occupied by a tyrosine (Y) with the exceptions of PhoR and YckK bearing a phenylalanine (F) or a leucine (L) respectively (Mukhopadhyay and Varughese, 2005). It has also been indicated that the side chains of amino acids in these positions are significantly bigger in YycG than in PhoR (Howell *et al.*, 2006). Therefore it has been postulated that size matters and spatial fit plays a role in the ability of a HK and a RR to interact.

This study aims at the elucidation of the specific residues contributing to the ability of a kinase to distinguish its cognate partner from all possible RR. Therefore the related two-component systems YycFG and PhoPR were chosen to conduct this study. Changing the amino acids in the HK YycG facing the RR YycF to those found at similar position in PhoR should allow for the molecular recognition of PhoP and the subsequent phosphotransfer (Figure 3.2 and Table 3.1). Two alternative approaches were adopted: Firstly an *in vivo* system was established to allow the manipulation of the essential YycG and to monitor the effect of mutations in YycG on the phosphorylation of PhoP. Secondly, *in vitro* phosphorylation assays were carried out to establish the increase of phosphorylation of PhoP by YycG but also to evaluate the loss of specificity for its cognate RR YycF.

3.1 *In vivo* study of interaction between the HK YycG* and the RR PhoP

3.1.1 An *in vivo* system to investigate the specificity of interaction between YycG and PhoP

Howell *et al* (2006) reports that the HK PhoR can phosphorylate both its cognate RR PhoP and the non-cognate RR YycF. To study the determinants of specific recognition between the HK YycG and the RR YycF and to gain insight into the unidirectional crosstalk between PhoR and the RRs PhoP and YycF, we established an *in vivo* system of analysis, outlined in Figure 3.2. The characteristic features of this system are (i) all strains carry the wild-type *yycFGHIJyyxA* locus since *yycFG* is essential and cannot be deleted (ii) an additional copy of the *yycG* gene under the control of a xylose inducible promoter (P_{xyI}): either wild-type, mutated

or hybrid-kinase *yycG* genes are inserted at the heterologous *thrC* locus (iii) a transcriptional P_{phoA} -*lacZ* fusion introduced in single copy at the *amyE* locus. Other mutations such as $\Delta phoR$ and $\Delta phoPR$ were introduced as appropriate. Expression of the P_{phoA} -*lacZ* fusion reflects the phosphorylation of PhoP, since Pho~P is the only known activator of this promoter. This promoter is inactive under conditions of growth in LB. To study the requirements of YycFG and PhoPR interactions, specific amino acids within the interacting surface of the $\alpha 1$ helix of the HK YycG were mutated to change its specificity of interaction from YycF to PhoP (Figure 3.2 and Table 3.1). The ability of mutated YycG* to phosphorylate PhoP is detectable by increased β -galactosidase expression.

In order to screen for the interaction between wild-type or mutated YycG* and PhoP, the above described system was established. Therefore a transcriptional reporter gene fusion (P_{phoA} -*lacZ*) was introduced in single copy at the *amyE* locus of *B. subtilis* strains 168 and strain AH057 ($\Delta phoR$), creating new strains designated IJ99 and IJR99. To study whether amino acid changes in the HK YycG alter its specificity for interaction and subsequent ability to phosphorylate the closely related non-cognate RR PhoP but not to interfere with the essential nature of the YycFG TCS, two sets of strains were constructed. Both sets carry an additional, in most incidences, mutated YycG* (as detailed in Table 3.1 and Figure 3.2) under the control of a xylose inducible promoter (P_{xyl} *yycG*) integrated via double crossover into the unessential threonine locus of strains IJW99 and IJR99 ($\Delta phoR$). The modifications introduced into YycG are detailed in Table 3.1. This gave rise to the strain sets IJW (wild-type PhoR) and IJR (deleted for PhoR), which allowed the study of modified *yycG* while leaving the wild-type YycG operon intact. This also facilitated the monitoring of PhoP phosphorylation through the activation of P_{phoA} -*lacZ* (Figure 3.3).

3.1.2 Expression of a second *yycG* gene at the *thrC* locus on the *B.subtilis* chromosome

To confirm that the additional copy of *yycG* under the control of a xylose promoter ($P_{xyI}yycG$) results in expressed YycG protein of correct M_r and can be induced to a sufficient level for further studies, western blot analysis was carried out on total cell lysate of strains 168, IJ99, IJR108, IJR107 and IJR105 using a YycG specific antibody. The results are shown in Figure 3.4.

The wild-type strain 168 displays a single band of correct molecular weight. Purified truncated YycG protein was loaded as positive control; it shows a single band that displays a smaller size as expected, demonstrating the specificity of this antibody. Strain IJW99, expressing the single wild-type copy of *yycG*, shows a single band of the same size as strain 168 at comparable levels displaying no difference between growth in LB with or without the addition of the inducer xylose as expected. The strains IJR108, IJR107 and IJR105 that are carrying $P_{xyI}yycG$ show a band of the same size as strains 168 and IJ99 at substantially elevated levels of YycG in non-induced growth conditions, *i.e.* the absence of xylose. Upon induction by addition of 0.5 % (v/w) xylose into the growth medium, YycG was overproduced in all three strains to a point where some protein appears to be degraded, displaying a second band of lower molecular weight. This analysis shows that wild-type and mutated YycG are expressed; that the expression of mutant YycG* is inducible; and that the mutant protein is expressed from the P_{xyI} promoter at levels that makes the induction with xylose unnecessary in further studies. This P_{xyI} promoter was previously reported to be leaky (Jester et al., 2003),

3.1.3 Confirmation of correct genetic structure of strains

The strains generated had alterations at two genetic loci: at the amylase locus (*amyE*:: P_{phoA} -*lacZ*) and at the threonine locus (*thrC*:: P_{xyI} *yycG*). To confirm that these loci had the predicted genetic structure, three tests were performed: (i) starch / iodine: integrants at the *amyE* locus produce amylase negative strains (ii) PCR with diagnostic primers and (iii) testing for threonine auxotrophy. The results for strains IJW99 and IJR are presented in Figure 3.5 to 3.8.

To monitor whether crosstalk occurs between mutated *YycG** and *PhoP* the *PhoP*~P dependent *phoA* promoter, 425 bp spanning the region -160 to +257, was cloned in front of the promoterless *lacZ* gene in pDG268. The resulting plasmid pIJ99 was sequenced, linearized and integrated at the *amyE* locus of *B.subtilis* 168 giving parental strain IJW99. This strain was tested for correct integration at the *amyE* locus by screening for the inability to metabolize starch (Figure 3.5). The map of the predicted plasmid integrations and the result of the diagnostic PCR with two different primer sets are shown in Figure 3.6. The PCR products were expected to be 4.3 kb and 3.1 kb. The PCR reactions were visualized on an agarose gel and the correct size confirmed. Therefore the plasmid IJW99 integration resulted in the correct structure.

In order to further investigate if phosphotransfer is occurring between mutant *YycG** and *PhoP* or whether *PhoR* dephosphorylates its cognate response regulator *PhoP*, a set of strains was constructed similar to those mentioned above. The *phoA-lacZ* fusion was therefore integrated into strain AH057 ($\Delta phoR$) giving rise to strain IJR99. This strain was tested for *amyE* deficiency as described above before (Figure 3.7 and 3.8). A putative from each strain, IJW99 and IJR99, that tested negative for amylase activity and positive for the integration of the correct insert was isolated and used for further manipulation.

In addition to the essential *yycG* gene, a second, in most incidences mutated *yycG** (Table 3.1), under the control of a xylose inducible promoter ($P_{xyl}yycG$) was integrated into the nonessential *thrC* locus of strain IJW99 giving the strain set IJW (Figure 3.2). The resulting putative strains were screened for tryptophan and threonine auxotrophy, erythromycin sensitivity and spectinomycin resistance to confirm integration of $P_{xyl}yycG$ via double crossover (Figure 3.9). Secondly, the same $P_{xyl}yycG$ constructs were transformed into the strain IJR99 giving strain set IJR (Figure 3.3). The resulting strains were tested for auxotrophy and spectinomycin resistance as shown in Figure 3.9 and screened for the maintenance of the *phoR* deletion on neomycin (data not shown). The correct transformants are expected to be threonine and tryptophan auxotrophs and therefore expected to show no growth on minimal medium (MM), MM supplemented with either threonine (Thr) or tryptophan (Tryp) but will grow on MM supplemented with both Thr and Tryp. To distinguish between insertions via a single- and double-crossover event of the $P_{xyl}yycG$ construct putative transformants were plated on high level erythromycin (150Erm) and spectinomycin (Spec). The desired mode of insertion was by double-crossover, therefore the right transformants were those growing on Spec and not on 150Erm. A LB agar plate without supplementation was used at the end of this streak series to confirm that no growth was due to the undesired property and not to the loss of cells.

This data shows that the genetic manipulations of each strain were successful and gave rise to the desired strains. Two sets of strains were created, IJW and IJR. Each strain set possesses a second, in most cases manipulated copy of $P_{xyl}yycG$ in addition to the reporter gene fusion $P_{phoA}-lacZ$ at the respective desired loci.

3.2 Qualitative evaluation of PhoP phosphorylation by YycG and mutated derivatives (YycG*) *in vivo*

3.2.1 Evaluation of PhoP phosphorylation by YycG* in IJW strains growing on LB agar

To qualitatively evaluate the ability of phosphotransfer between mutated YycG* and PhoP, all strains of the IJW ($P_{xyI}yycG$, $P_{phoA-lacZ}$) set were plated on solid LB medium supplemented with X-gal. When the $P_{phoA-lacZ}$ fusion is expressed as a consequence of the presence of PhoP~P, strains will show a blue color whereas strains lacking phosphorylated PhoP, the only known activator of *phoA*, will remain white. The results are shown in Figure 3.10. Strain IJ101 does not display any β -galactosidase activity as expected, the modification H0A in *yycG* gene renders the kinase to be inactive and the colonies remain white. The lack of β -galactosidase activity of strains IJ108, that carries a second wild-type copy of YycG shows that even elevated levels of the YycG protein do not activate PhoP as the colonies also remain white. In fact, all strains of the IJW set, those carrying single and those with multiple mutations in the *yycG* gene remain white, indicating that the Pho~P dependent P_{phoA} promoter is inactive (Figure 3.10). This analysis shows that under these conditions PhoP is not activated through phosphorylation by mutant YycG*.

No activation of PhoP was observed in the IJW set of strains. However, under these growth condition *i.e.* phosphate replete LB medium, the PhoPR TCS is not induced. In non-activated conditions HKs often display phosphatase activity on their cognate RRS, therefore it is possible that PhoR is in phosphatase mode dephosphorylating PhoP~P that is generated by phosphorylation by YycG*.

3.2.1 Evaluation of PhoP phosphorylation by YycG* in IJR strains on LB agar.

To investigate whether phosphorylation of PhoP through YycG and its mutated forms is occurring but the resulting PhoP~P is dephosphorylated by PhoR, the IJR set of strains was constructed where *phoR* is deleted. This set of strains with $\Delta phoR$ background (IJR) was plated on X-gal supplemented LB agar, testing for β -galactosidase activity. The results are shown in Figure 3.11. As expected, neither IJR101 [$P_{xyI}yycG$ (H0A)], bearing the inactive kinase, nor IJR108 [$P_{xyI}yycG^{WT}$], carrying the reconstituted wild-type, show β -galactosidase activity, demonstrating the inactivity of PhoP, *i.e.* PhoP is not

phosphorylated. It is notable that strains containing $P_{xyI}yycG$ with a single modified amino acid (i.e. IJPR102, 103, 104, 106) remain white. However strain IJR105 is an exception: strain IJR105 carries $P_{xyI}yycG$ with the single amino acid change of serine to glycine at position 11 (S11G), and displays a pale blue color.

Interestingly, when the single mutation of IJR105 (S11G, pale blue) and IJR106 (Y12F, white) are combined in strain IJR112 (S11G Y12F), it results in a dramatic increase of β -galactosidase activity that manifests in a deep blue color. Compared to the strains with single amino acid changes, all strains carrying multiple amino acid changes in YycG (IJR112, IJR114 and IJR107) developed a deep blue color. Interestingly, they do not differ in intensity when compared to each other or with the hybrid kinase IJR115 [YycG'-PhoR]. The hybrid kinase consists of the sensing region of YycG and the catalytic domain of PhoR this displaying the perfect interaction surface for PhoP phosphorylation. These results indicated that mutated YycG* is capable of interaction with the non cognate RR PhoP and results in its activation.

3.2.3 P_{phoA} -*lacZ* expression is PhoP~P dependent

As shown in the previous section, PhoP could be phosphorylated by mutated YycG* in five strains namely IJR105, IJR112, IJR114, IJR107 and IJR115.

To ensure that this activation of the P_{phoA} -*lacZ* fusion is indeed based on the presence of PhoP and its phosphorylated form PhoP~P, strains was generated deleted of both *phoP* and *phoR* (IJPR). Therefore, strains displaying blue colonies were transformed with chromosomal DNA of AH024 creating another strain set IJPR. Strains that showed no indication of PhoP activation by YycG* (101-104) were not further tested and not introduced into AH024 ($\Delta phoPR$). The genetic properties of those strains are presented in Figure 3.12. All of these strains were grown on X-gal supplemented LB agar plates. The results are shown in Figure 3.13. All strains of set IJPR remain white, indicating the inactivity of the P_{phoA} -*lacZ*. It is evident that β -galactosidase is expressed in the strains of set IJR but not in the IJPR strains, i.e. blue versus white colonies. These results confirm that the previously shown activation of expression of the P_{phoA} -*lacZ* fusion in IJR strains is PhoP dependent and is due to the presence of PhoP.

3.2.4 Effects of YycG mutations on *yoch* expression not detectable *in vivo*

In the strain sets IJW and IJR there are two types of YycG: the endogenous wild-type YycG encoded in the *yycFGHIJyyxA* operon and the mutated *yycG** encoded at the *thrC* locus. It has been shown that *yoch* is a member of the YycFG regulon and its

expression is activated by YycF~P (Howell *et al.*, 2003). The results of the previous section suggest that mutations in YycG* enables the phosphotransfer to PhoP. To establish whether these mutations in YycG have an effect on the phosphotransfer reaction to its cognate RR YycF, strains were constructed that carried a P_{yocH}-lacZ instead of a P_{phoA}-lacZ fusion in order to monitor *yocH* expression *in vivo*.

Therefore, all P_{xyr}-yycG constructs were integrated into strains AH037 (*phoPR*^{WT}) and IJR98 (Δ *phoR*), both carrying a P_{yocH}-lacZ transcriptional fusion at the *amyE* locus, giving rise to strain sets IJW121-131 and IJR121-131 respectively (Figure 3.14). These strain set were grown on LB supplemented with X-gal and the results are shown in Figure 3.15. Strains IJR98 and AH037, carrying only the P_{yocH}-lacZ fusion are both displaying blue colonies as expected since the wild-type TCS YycFG is intact and active in these conditions. The strains of sets IJW121-131 and IJR121-131, all carry the second P_{xyr}-yycG but neither modifications of this YycG nor the genetic background seems to have an influence on the expression of the P_{yocH}-lacZ fusion as all strains display blue colonies of the same intensity. The results show that these conditions do not allow detection of differential P_{yocH}-lacZ expression. Therefore, a statement about the loss of recognition between YycG* and YycF cannot be made.

3.3. Quantitative analysis of PhoP phosphorylation by YycG* *in vivo* during growth in LB broth

3.3.1 Evaluation of β -galactosidase activity of strain set IJW *in vivo*

In order to quantitatively evaluate the extent to which each amino acid change allowed phosphorylation of PhoP by YycG, the strains of sets IJW and IJR were examined in conditions where the YycFG TCS has been shown to be most active that is during the exponential phase of the growth cycle (Howell *et al.*, 2003).

All strains of set IJW (P_{phoA} -*lacZ*, P_{xyI} *YycG**) were grown in liquid culture, samples were taken throughout the exponential phase, and the accumulation of β -galactosidase activity was determined (Figure 3.16 and 3.17). Strain IJW99 carries only the P_{phoA} -*lacZ* fusion and displays a level of approximately 5 units of activity that is the background level. However, strains IJW108 and IJW101 show the same level of activity, as expected since neither the non-mutated YycG (IJW108) nor YycG* carrying the H0A mutation (IJW101) should be capable of phosphorylating PhoP. None of the remaining strains of set IJW, with single or with multiple mutations, exceeded this level of 5 units of activity significantly. These assays confirm the previous results obtained when strains were grown on LB agar, showing that even in exponential growth phase, where YycG is known to be active, no phosphorylation of PhoP can be detected in wild-type background.

3.3.2 *In vivo* evaluation of β -galactosidase activity of strain set IJR (Δ *phoR*)

When grown on LB agar plates containing X-gal (Figure 3.9), five members of strain set IJR display β -galactosidase activity namely: IJR105, IJR107, IJR112, IJR114 and IJR115. To quantitate this activity all IJR strains were grown exponentially in liquid culture and the β -galactosidase activity was determined (Figure 3.18 and 3.19). Strain IJR99 shows again only background level activity of about 5 activity units. Strains IJR108 and IJR101 also show only background activity levels as expected since they contain the (reconstituted) wild-type YycG and YycG with the H0A mutation respectively, confirming the results of the plate assay on LB containing x-gal. Consistent with the plate assay, all strains bearing single amino acid changes in P_{xyI} *YycG* display background level β -galactosidase activity. Interestingly, strain IJR105 does not show β -galactosidase activity above the background level of 5 units during exponential phase of growth but expression is induced upon entering stationary phase (Figure 3.18). Strain IJR105 displayed pale blue colonies on plate. Strain IJR112 appeared very blue when grown on plates. It also displays

only background levels of β -galactosidase activity during exponential phase of approximately 5 units but increases upon entry into stationary phase to ~600 units. Strains IJ114, IJR107 carrying YycG* with four and five amino acid replacements as well as strain IJR115, encoding a hybrid P_{xyI}yycG'-*phoP* kinase show elevated levels of β -galactosidase activity upon entry into stationary phase to levels of about 800 and 1200 units respectively (Figure 3.19). It is noteworthy that in these five strains the β -galactosidase activity continues to rise significantly after exponential phase and this was observed repeatedly.

In order to obtain representative value of β -galactosidase activity in exponential growing cultures, when YycG is active as a kinase, as opposed to a profile, strains IJR105, IJR112, IJR114, IJ107 and IJ115 were grown repeatedly under strictly equalized conditions to ensure that only exponentially growing cells were assayed. This experiment was carried out at least three times and the results of the expression from the transcriptional *phoA-lacZ* fusion are shown in Table 3.2.

Strain IJR108 served as control, carrying a second copy of the (reconstituted) wild-type YycG and it displayed a background β -gal activity of ~5 units. The same level of activity was determined for strain IJR106, carrying the single amino acid change Y12F, not exceeding the background level as shown previously. Interestingly, neither strain IJR105 (S11G) nor strain IJR112 (S11G and Y12F) significantly exceeds that background level, although a higher level was expected indicated by the blue color on plates. However IJR114 showed somewhat elevated levels of approximately 8 units. Notably, IJR107, that has five amino acid changed, exhibits a level of ~13 units of β -galactosidase activity during exponential phase, comparable with those of strain IJR115 that carries the hybrid kinase YycG'-PhoR and therefore bears the perfect surface for interaction with PhoP. These results are consistent with the idea that changing amino acids within the α 1-helix of YycG changes its specificity towards interaction with PhoP. However the activation of PhoP is most evident in stationary phase cells.

3.3.3 *In vivo* evaluation of β -galactosidase activity in strain set IJPR (Δ *phoPR*)

As previously shown on LB agar plates expression of the P_{phoA}-*lacZ* fusion is PhoP~P dependent. The phosphorylation of PhoP can be achieved through modified YycG* proteins with changes amino acid as described and is PhoP dependent. In order to test if expression is also PhoP dependent in liquid culture, strains IJPR (Δ *phoPR*) were grown in LB broth (Figure 3.20). As expected, neither IJPR99 (*yycG*^{WT}) nor IJPR108 (P_{xyI}yycG^{WT}) showed any significant elevation of β -galactosidase activity in neither

exponential nor stationary phase of growth. Nor does the strain IJPR106 containing amino acids change Y12F, that could be expected since this mutation in YycG did not lead to β -galactosidase activity on plates or in LB broth when combined with a Δ phoR background. In contrast, strains IJR105, IJR107, IJR 112, IJR114 IJR 112 and IJR115 did show increased levels of β -galactosidase activity in the presence of PhoP. In the *phoP* mutant background as in IJPR this β -galactosidase activity could not be observed. Thus showing that the β -galactosidase activity observed in IJR strains is indeed PhoP dependent.

3.4 YycG is expressed at a constant level throughout growth

As described in the previous section, strains that exhibit crosstalk between mutated YycG* and PhoP show elevated levels of β -galactosidase activity but only after the transition phase of growth. To test if these elevated levels of activity observed are due to elevated YycG expression or to 'bona fide' phosphorylation of PhoP by YycG*, a western blot analysis was carried out on selected strains with samples harvested from exponential and stationary phase of growth.

The results are shown in Figure 3.21. All strains were grown in LB without the addition of the inducer xylose. Strain 168 was used to show again the cellular level of wild type YycG. Of the strains carrying two copies of YycG one under the control of its natural promoter and the other under the control of the inducible xylose promoter, strain IJR108 was chosen because it contains two copies of YycG wild type. Strain IJR106 carries a second copy of YycG with a single amino acid mutation that did not lead to PhoP phosphorylation by YycG*. Strains IJR105, IJR107, IJR112 and IJR114 do carry amino acid changes in YycG that enabled phosphotransfer to PhoP. Strain IJR115 carries the wild-type copy of YycG and in addition a hybrid kinase consisting of the sensing region of YycG and the catalytic region of PhoR. For the western blot analysis, a sample of each strain was harvested at approximately OD₆₀₀0.5, in the exponential phase of growth and one sample in stationary phase, at an OD₆₀₀ of approximately 2. The results are shown in Figure 3.21. YycG is expressed and appears as a single band of correct M_r. It also shows that YycG is expressed at higher levels in strains that carry a second copy of *yycG* under a xylose controlled promoter even without the addition of xylose inducer. Finally, YycG is present not only in exponentially growing cells but also in stationary phase cells. Importantly, the level of YycG is the same in strains when no phosphorylation occurs (IJR108 and IJR106) as in strains where YycG does phosphorylate PhoP (IJR105, IJR107, IJR112, IJR114). From this it is concluded that the phosphorylation of PhoP by YycG is not

due to increased YycG levels in these strains. That IJR115 displays a lesser level of YycG may be due to the fact that the antibody was raised for the cytoplasmic part of YycG. In the hybrid kinase YycG115, the intracellular region mainly consists of PhoR.

3.5 Phosphorylation properties of mutant YycG* proteins *in vitro*

Results of the *in vivo* study indicate that amino acid modifications in the α 1-helix of YycG change its interaction surface and changes the specificity of interaction in a manner that allows the interaction with and phosphorylation of the non-cognate PhoP. In order to verify this putative phosphorylation of PhoP by YycG *in vitro* studies with purified proteins were performed. Such studies would allow not only to examine phosphorylation of PhoP by 'YycG, but also to examine a possible reduction in the ability of mutated 'YycG* proteins to phosphorylate the cognate YycF protein.

3.5.1 Purification of HKs and RRs

The genes encoding the cognate TCS pairs PhoP / PhoR and YycF / YycG, as well as the mutated YycG* kinases that showed activation of PhoP *in vivo* (YycG105, YycG112, YycG114 and YycG107), were cloned into the expression vector pET21b creating a translational fusion adding six histidine residues to the C-terminus and placing the gene under the control of an inducible T7 bacteriophage promoter. Constructs were verified by sequencing. The full-length coding sequences of the YycF and PhoP RRs could be expressed. However, proteins YycG and PhoR are membrane bound kinases each with two transmembrane domains. Therefore, in order to obtain purified enzymes for this study, truncated catalytic domains (*i.e.* lacking the TMs), of YycG (from residue M218 to 611) and PhoR (from amino acid S175 to 579) were constructed, expressed and purified from *E.coli*. SDS PAGE analysis was carried out to confirm the production of protein and its purity. The results are presented in Figure 3.22. The purified 'YycG proteins shows a single band that migrates slightly higher than the calculated 46 kDa an effect that might be due to the amount loaded. The single band of the truncated HK protein 'PhoR migrates approximately at its calculated M_r of 46.9 kDa. Both RR proteins, YycF and PhoP have a calculated molecular mass of 28 kDa and display a single band migrating slightly below the 32.5 kDa marker. This SDS-Page analysis revealed that all desired proteins are produced; they are produced at high concentration and are of sufficient purity for further experiments.

3.5.2. *In vitro* phosphorylation of cognate pairs YycFG and PhoPR

In order to ensure that the kinase activity for auto- and transphosphorylation was not impaired during protein purification procedures and to establish standardized conditions, *in vitro* phosphorylation of the cognate pairs YycFG and PhoPR were carried out. The results are shown in Figure 3.23. The autophosphorylation of the kinase 'YycG was rapid and to saturation level within a minute since this level does not increase over the course of 30 min (Figure 3.23 A). When the purified proteins 'YycG and YycF were incubated together, autophosphorylation of 'YycG and phosphotransfer from 'YycG to YycF could be observed, both reactions take place rapidly and efficiently in less than a minute (Figure 3.23A, left panel). However, when the proteins 'YycG and PhoP were incubated together, autophosphorylation of 'YycG could be observed but phosphotransfer between 'YycG and the non-cognate RR PhoP was not observed (Figure 3.23A, right panel). Autophosphorylation of the 'PhoR histidine kinase could also be shown, the reaction takes place in less than a minute to what appears to be saturation level (Figure 3.23B). The 'PhoR kinase phosphorylates its cognate RR PhoP with high efficiency in less than a minute (Figure 3.23B, left). In contrast, 'PhoR is also able to phosphorylate the non-cognate RR YycF but with lower efficiency, the phosphorylated YycF appears as a very faint band from 2 min increasing continuously in intensity over the 30 min time course as shown in Figure 3.23 B (right). It is noteworthy that this non-cognate phosphotransfer occurs at a significantly slower rate when compared to the transphosphorylation between cognate pairs.

These results demonstrate that both truncated HKs 'YycG and 'PhoR are active and capable of autophosphorylation as well as phosphorylation of their cognate partners YycF and PhoP respectively. The autophosphorylation of the kinases and the phosphotransfer reactions between cognate pairs is efficient. The results are in agreement with the demonstration of unidirectional crosstalk between the kinase PhoR and response regulator YycF as the inability of YycG to interact with PhoP as shown in Howell *et al.* (2003; 2006).

3.5.3 *In vitro* phosphorylation assay of mutant YycG*

Due to the essential nature of YycFG it was not possible to delete YycG and determine the effect of mutations on the interaction with the cognate RR YycF *in vivo*. Therefore, to investigate the effect of amino acid changes on the specific interaction with YycF and to verify that the interaction between mutant YycG and the non-cognate RR PhoP, as indicated by the *in vivo* data, is direct and results in phosphotransfer, the truncated mutant kinases 'YycG105, 'YycG112, 'YycG114 and 'YycG107 were tested *in vitro* for their autophosphorylation activities as well as their phosphotransfer activities with PhoP. A time course for each reaction was performed as detailed in methods and materials.

The purified kinase 'YycG105 that has the serine changed to glycine at position 11 (S11G) (with respect to the site of phosphorylation) is clearly capable of autophosphorylation (Figure 3.24). The phosphorylation of the cognate response regulator YycF also clearly occurs (Figure 3.24A) even though to a somewhat lesser extent than between the wild-type pair 'YycG and YycF (see Figure 3.23). However, 'YycG105, that differs in only one amino acid from 'YycG (S11G), also transfers its phosphoryl group to the non-cognate PhoP at a significant level, an effect consistent with results obtained *in vivo* but in stark contrast to that observed for 'YycG phosphorylating PhoP (Figure 3.23A).

The mutant protein 'YycG112 (S11G, Y12F), is catalytically active and shows rapid autophosphorylation (Figure 3.25). The phosphotransfer to YycF takes place within 1 min and increases over time. The phosphotransfer between 'YycG112 and PhoP is detectable within 1min although at a lower rate when compare to the cognate pair but at a higher level than between 'YycG105 and PhoP.

Four amino acids have been changed in 'YycG114 (R3K T8S S11G Y12F). It's ability to autophosphorylate is impaired (Figure 3.26). The reaction occurs at a slower rate compared to the wild-type kinase 'YycG (Figure 3.23). The rate of phosphotransfer of both response regulators YycF and PhoP to occurs at a similar rate.

Five amino acid changes have been made in 'YycG107 (R3K T8S R10K S11G Y12F) so that the RR interacting surface of the α 1-helix is very similar to that of PhoR. Results for the autophosphorylation of the mutant kinase 'YycG107, and its ability to phosphorylate the cognate RR YycF and the non-cognate PhoP are shown in Figure 3.27. The autophosphorylation reaction takes place rapidly initially but continues to increase in a gradual manner similar to what was observed for 'YycF114. The ability of 'YycG107 to phosphorylate YycF appears impaired because the level of phosphorylation increases over

time indicating a continuous reaction. The phosphotransfer between 'YycG107 and PhoP is comparable with that to YycF since both levels and rate appear to be the same.

The results of this *in vitro* study show that accumulation of mutations in YycG lead to (i) a decrease in specificity for phosphotransfer to its cognate response regulator YycF and (ii) increases in the ability to phosphorylate the non-cognate regulator PhoP despite the fact that autophosphorylation becomes impaired ('YycG114 and 'YycG107).

3.6 Kinetic analysis of phosphotransfer from wild-type and mutant kinases

3.6.1 Determination of conditions for an *in vitro* kinetic analysis

In the previous section it is clear that changes in 5 specific amino acids within the α 1-helix of 'YycG to those found at these positions of 'PhoR increases the ability of 'YycG to phosphorylate PhoP and decreases its ability to phosphorylate the cognate YycF response regulator. The reaction conditions chosen however did not allow further characterization of the kinetics involved so that the extent to which the specificity of interaction has been rewired could be determined. In order to establish and quantify the initial rate of phosphotransfer, a series of experiments was carried out to find the optimal concentration of ATP and the molar amounts of protein. The result is shown in Figures 3.28-3.30. Firstly, the appropriate concentration of ATP concentration was tested. In the set of experiments described previously (see also Methods and Material) a final concentration of 0.1 μ M ATP was used. It is possible that autophosphorylation and subsequent phosphotransfer are limited for substrate in these conditions. In contrast up to 500 μ M cold ATP were reportedly used for *in vitro* phosphorylation and published by other groups (Skerker *et al.*, 2008; Tzeng and Hoch 1997). To find the optimal ATP, the purified proteins 'PhoR and PhoP were used and set up in reactions containing 0.1 μ M, 1 μ M, 100 and 200 μ M cold ATP respectively. The reactions were allowed to continue for 2 and 20 minutes. The results are shown in Figure 3.28. The autophosphorylation and phosphotransfer are stronger in low levels of cold ATP but is also observable in reactions containing 200 μ M ATP. However, in the latter reactions (200 μ M ATP), the autophosphorylation is weaker and subsequently the phosphotransfer reaction is not as strong as in the reactions containing less ATP. Despite the weaker signal, the autophosphorylation and phosphotransfer observed with high levels of cold ATP (200 μ M) appeared sufficient to enable quantification of further experiments.

Having established the amount of ATP to be used in this set of experiments it was necessary to reevaluate the amount of protein used. Skerker *et al.* (2008) reports use of

equal amounts of 2.5 μM of HK and RR, whereas the group of James Hoch used an excess of phosphodonors over phosphoacceptor (Zapf *et al.*, 1998; Tzeng and Hoch 1997). To find the optimal ratio of HK to RR, 2.5 μM HK ('YycG and 'PhoR) were each incubated with a different amount (10 μM , 25 μM , 30 and 50 μM) of their respective RR, YycF and PhoP. The reactions were allowed to continue for 15 and 20 seconds. The phosphoimage results of 'YycG phosphorylation YycF and the respective quantification of the phosphoimage are shown in Figure 3.29 A and B. The autophosphorylation of 'YycG is equal in all reactions after 15 seconds. The phosphotransfer from 'YycG to YycF is very similar after 15 seconds independent of concentration (Figure 3.29A). To determine if the concentration of YycF indeed does not affect the signal obtained for YycF~P, the phosphoimage were quantified as described in Methods and Materials. At a reaction time of 15 seconds the concentration of YycF present in the reaction does not affect the level of YycF~P detected. The phosphoimager values determines for all reactions containing different concentrations of YycF are approximately 300 arbitrary units. After 30 seconds, the level of YycF phosphorylation observed is elevated for all concentrations (Figure 3.29B). The weakest signal was observed for the reaction containing 10 μM YycF. To determine if the concentration of YycF indeed doesn't affect the signal obtained for YycF~P, the phosphoimage was quantified (Methods and Materials). The level of YycF~P observed after a reaction time of 30 seconds is affected by the concentration of YycF present. The highest signal of YycF~P detected is in the presence of 25 μM YycF with a phosphoimager value of 800. This is followed by the value for 30 μM YycF with approximately 750 and 50 μM YycF with ~675. The lowest YycF concentration of 10 μM also shows the lowest phosphorylation with phosphoimager value of <500. Concluding from this analysis, the optimal amount of YycF for further *in vitro* phosphorylation experiments is 25 μM .

The amount of PhoP to use for *in vitro* phosphorylation was also tested. The resulting phosphoimages and the quantification of both images are shown in Figure 3.30A and B. The autophosphorylation of 'PhoR appears to be at the same level in both reactions, that continued for 15 and 30 seconds. The level of PhoP~P detectable after 15 seconds reaction time appears strongest in the presence of 10 μM PhoP. In the presence of 20, 30 and 50 μM PhoP the levels of Pho~P seem very similar. The quantification of the phosphoimage (as described in Methods and Materials) showed that the highest level of PhoP~P was detectable with the reaction that contained 10 μM PhoP giving a phosphoimager value of ~700 and the lowest level of PhoP~P with the reaction containing

50 μM PhoP with a phosphoimager value of ~ 400 (Figure 3.30A). After a reaction time of 30 seconds the levels of PhoP~P are overall elevated but does not seem to be affected by the concentration of PhoP displaying similar levels of phosphorylation (Figure 3.30B). After 30 seconds of reaction time the level of PhoP~P is the lowest in the presence of 50 μM PhoP with a phosphoimager value of ~ 1000 . In contrast PhoP at 10, 25 and 30 μM give a similar level of PhoP~P after 30 seconds with values of approximately 1200. The largest change in PhoP phosphorylation over the 15 seconds can be observed in the presence of 25 and 30 μM PhoP. Therefore, it was decided that a concentration of 25 μM RR protein would be used for further experiments.

3.6.2 Quantitative *in vitro* phosphorylation assays of mutant 'YycG*s

The above described experiments were carried out in order to establish the optimal amount of protein and ATP for quantitative *in vitro* phosphorylation assays. These assays serve the purpose to determine quantitatively the loss of specificity of 'YycG* to phosphorylate its cognate RR YycF and the gain of ability to phosphorylate the non-cognate PhoP. In order to achieve this, all the following reactions were set up using 2.5 μM of HK and 25 μM RR. The resulting gels were exposed to phosphoimager screens for the time indicated and quantified as described in Methods and Materials. The results are shown in Figures 3.31 to 3.38.

The signal amino acid change S11G was first investigated by *in vitro* phosphorylation (Figure 3.31). Purified HKs 'YycG and 'YycG105 were incubated with the RR YycF to assess if this amino acid change in 'YycG105 decreases the ability to phosphorylate its cognate RR. A steady increase of phosphorylated YycF can be observed when incubated with 'YycG over a time course of 5 minutes. In the first sample, taken after only 10 seconds YycF phosphorylation is visible. The mutant 'YycG105 also shows an increasing phosphotransfer to YycF over a time course of 20 min, the first sample was taken after 30 seconds reaction time. To compare the phosphotransfer reactions from both HKs, YycF~P phosphorylated by 'YycG and 'YycG105 was quantified and normalized to the highest phosphoimager value obtained for YycF~P and plotted versus time (Figure 3.31B). It is noticeable that the phosphotransfer from 'YycG is faster over time than that from 'YycG105. The latter reaction is slowing down after 1 minute, the second time point. In order to determine the initial rate of the phosphorylation of YycF, the initial time points, where the reaction appears to be linear, were normalized to the phosphoimager value obtained for YycF~P after incubation with 'YycG for 1 minute. The resulting values were

fitted with a trendline and the slope determined (Figure 3.31C). The slope for YycF~P phosphorylated by 'YycG is 1.67 compared to 0.807 when phosphorylated by 'YycG105. These results indicate that the single amino acids change from a serine to glycine (S11G) in YycG leads to an approximate 48% decrease in the efficiency for phosphorylating its cognate RR YycF.

The gain of the ability of 'YycG105 to phosphorylate the non-cognate RR PhoP was examined and compared to the phosphotransfer from the cognate HK PhoR as described above. The results are shown in Figure 3.32. For this PhoP was incubated with 'PhoR over a period of 5 minutes and with 'YycG105 for a period of 20 min and samples were taken at the indicated times (Figure 3.32A). An efficient phosphotransfer from PhoR to PhoP could be observed that increased steadily over the 5 minutes. The phosphotransfer from 'YycG105 to PhoP could not be observed until 20 minutes of reaction and even at that timepoint the band of PhoP~P was weak. The phosphoimage was quantified (Figure 3.32B) and the initial rate of PhoP~P phosphorylation evaluated as described above (Figure 3.32C). PhoP is rapidly and efficiently phosphorylated by PhoR. The phosphotransfer from 'YycG105 in contrast is not detectable within 5 minutes of reaction time. When evaluating the initial rate it is also clear that PhoP phosphorylation by 'YycG105 is only 0.2% as efficient as the phosphotransfer between 'PhoR and PhoP.

The analysis of the loss of specificity of 'YycG112 (S11G Y12F) for YycF is shown in Figure 3.33. The phosphoimage again shows phosphotransfer for wild-type pairs 'YycG and YycF and in addition phosphotransfer between 'YycG112 and YycF. The phosphoimage and the quantification of the phosphorylation of YycF by 'YycG and 'YycG112 indicate a substantial loss of phosphotransfer from 'YycG112 (Figure 3.33A and B). The comparison of the initial rates of YycF phosphorylation revealed that two amino acid changes in YycG ('YycG112) decreases the ability to phosphorylate YycF to 27% of that of wild type YycG.

The gain of ability of 'YycG112 to phosphorylate the non-cognate RR PhoP is shown in Figure 3.34. PhoR appears to phosphorylate PhoP efficiently and rapidly but phosphotransfer from 'YycG112 was very low (Figure 3.34A and B). The assessment of the initial rates of PhoP~P phosphorylation also show no ability of 'YycG112 to phosphorylate PhoP 0.2% (Figure 3.34C).

The four amino acid changes R3K T8S S11G Y12F was also investigated by *in vitro* phosphorylation (Figure 3.35). Purified HKs 'YycG and 'YycG114 were incubated with the RR YycF to assess if these amino acid changes in 'YycG114 decreases the ability to

phosphorylate its cognate RR YycF. An efficient and steady increase of phosphorylated YycF could be observed when incubated with 'YycG. The mutant 'YycG114 showed a drastic decrease in the ability to phosphorylate YycF over a time course of 20 min. To compare the phosphotransfer reactions from both HKs, YycF~P phosphorylated by 'YycG and 'YycG114 was quantified (Figure 3.35B). It is noticeable that the phosphotransfer from 'YycG is significantly faster over time than that from 'YycG114. The latter reaction appeared to start to take place after 2 minute, the third time point. In order to determine the initial rate of YycF phosphorylation after incubation with 'YycG and 'YycG114, the slope of a trendline fitted to the linear reaction was determined. The slope for YycF~P phosphorylated by 'YycG is 1.47 compared to 0.07 when phosphorylated by 'YycG114. These results indicate that the four amino acids changes (R3K T8S S11G Y12F) introduced into the α 1-helix of YycG leads to a decrease in efficiency for phosphorylating its cognate RR YycF to 0.5%.

The gain of the ability of 'YycG114 to phosphorylate the non-cognate RR PhoP was examined and compared to the phosphotransfer from the cognate HK PhoR as described above. The results are shown in Figure 3.36. For this analysis, PhoP was incubated with PhoR and with 'YycG114 with samples taken at the indicated times (Figure 3.36A). A strong efficient phosphotransfer from PhoR to PhoP could be observed that increased steadily over the 5 minutes reaction time. The phosphotransfer from 'YycG114 to PhoP could not be observed until 5 minutes of reaction and even at the 20 minute timepoint the band of PhoP~P appeared weak. The phosphoimage was quantified (Figure 3.36B) and the initial rate of PhoP~P phosphorylation evaluated as described above (Figure 3.36C). PhoP is rapid and efficiently phosphorylated by PhoR. The phosphotransfer from 'YycG114 in contrast is not detectable up to 5 minutes into the reaction. When evaluating the initial rate it is also clear that PhoP phosphorylation by PhoR is stronger than from 'YycG114 which is only 0.6% of that in wild-type pairs (Figure 3.36C).

Finally, the kinase 'YycG107 carrying five amino acid changes in the α 1-helix to match those found in PhoR (R3K T8S R10K S11G Y12F) was assessed (Figure 3.37 and 3.38). Purified HKs 'YycG and 'YycG107 were incubated with the RR YycF in order to evaluate if the ability to phosphorylate its cognate RR YycF is impaired. An efficient and steady increase phosphotransfer between wild-type pairs YycG and YycF could be observed over the five minutes reaction time (Figure 3.37A). The mutant 'YycG107 however, did not phosphorylate YycF detectably up to five minutes. To compare the

phosphotransfer reactions from both HKs, YycF~P phosphorylated by 'YycG and 'YycG107 was quantified (Figure 3.37B). It is noticeable that the phosphotransfer from 'YycG is significantly faster over time than that from 'YycG107. The latter reaction appeared to occur only slowly during the 20 minutes incubation time. The initial rate of YycF phosphorylation after incubation with 'YycG and 'YycG107 was determined (Figure 3.37C). A trendline was fitted to the linear reaction and the slope calculated. The slope of the phosphotransfer from 'YycG to YycF is 1.67 compared to 0.07 when phosphorylated by 'YycG107. These results indicate that the changes of five amino acids decrease the ability of 'YycG107 to phosphorylate YycF to 4%.

The gain of the ability of 'YycG107 to phosphorylate the non-cognate RR PhoP was examined and compared to the phosphotransfer from the cognate HK PhoR as described above. The results are shown in Figure 3.38. For this analysis, PhoP was incubated with PhoR and with 'YycG107 (Figure 3.38A). The phosphotransfer observed from PhoR to PhoP was efficient, increasing steadily over the 5 minutes reaction time. The phosphotransfer from 'YycG107 to PhoP, even though weak, was observed at 2 minutes of reaction. The signal became stronger until the 20 minute timepoint. The phosphoimage was quantified (Figure 3.38B) and the initial rate of PhoP~P phosphorylation evaluated (Figure 3.38C). The phosphotransfer from PhoR to PhoP is rapid and efficient. The phosphotransfer from 'YycG107 in contrast is detectable not until the second timepoint (120 sec) into the reaction. When evaluating the initial rate it is also clear that PhoP phosphorylation by PhoR is initially stronger than by 'YycG107 which is only 0.5% of that by the wild-type kinase 'PhoR (Figure 3.38C).

Taken together, this kinetic analysis of mutant 'YycG* kinases shows an increasing loss of specificity for its cognate RR YycF with increasing introductions of mutations into the YycG α 1-helix. However, the rate of phosphotransfer from mutant 'YycG to the non-cognate PhoP does not reach levels of that from 'PhoR. Additionally, these results show that the phosphotransfer is over 100-fold less than from the wild-type HK PhoR. Some of this may be due to the impaired autophosphorylation mutant YycG*.

3.7 Phenotypical characterization of strains exhibiting PhoP phosphorylation by YycG*

The strains in which mutated YycG* protein can phosphorylate PhoP show a number of interesting characteristics. In this section these phenotypes were investigated.

3.7.1. Growth phenotype on LB agar

While working with strains of the IJR series containing mutated YycG* that showed significant levels of PhoP dependent P_{phoA} -*lacZ* expression (IJR105, IJR112, IJR114 and IJR107) it was observed that these strains became translucent on plates that were left for a few days. The level to which they became translucent differs among the strains. In order to investigate this phenotype, strains IJR105, IJR112, IJR114, IJR107 containing YycG with one, two, four and five amino acid changes respectively were plated on LB agar. Strain IJR108 (wild-type YycG) was used as a control. This plate was monitored during a week; the results are shown in Figure 3.39. It appears that strain IJR107 lyses the quickest followed by strains IJR114 whereas IJR112 and IJR105 seem to take longer to show a phenotype. Additionally, in cell lysis displayed by strain IJR114, strains containing suppressor mutations arise. Strain IJR108 that carries a second copy of wild-type *yycG* displays colony morphology comparable to wild-type strain 168, as expected. These results indicate a graduation of lysis that occurs only in strains where YycG* can phosphorylate PhoP.

3.7.2 Growth phenotype in LB broth

In order to test whether these phenotypes were observed during growth in liquid culture and may influence the results obtained in the *in vivo* study, all strains were grown in LB broth and monitored over ten hours. All strains of the IJR series and wild-type strain 168 were streaked from frozen stock freshly on LB agar plates supplemented with the appropriate antibiotics and incubated overnight at 37°C. These are the exact conditions used to obtain the *in vivo lacZ* data. The following day, strains were grown in microtiter plates as described in Methods and Materials. The growth of strains was carried out in triplicate. The microtiter plate was placed into a Biotek machine that was programmed to allow growth at 37°C while shaking and taking OD₆₀₀ readings every 10 minutes without disrupting the growth over a period of 10 hours. The results are shown in Figure 3.40. The data shown for each strain is an average of three identical growth experiments. All strains, including those that show a growth phenotype on LB agar, show a very similar growth profile to wild type strain 168 in LB broth with the exception of strains IJR114 (four amino acid changes in YycG) and IJR107 (five amino acid changes in YycG). These two strains show a drop of OD after six hours into stationary phase. This suggests that the growth phenotype observed on plates did not compromise the *lacZ* data collected and described in the earlier section as the data was obtained no later than two hours into stationary

phase. The lytic phenotype observed on LB agar might be due to the elevated levels of mutated YycG* that results from the leakiness of the xylose promoter and only materializes over an extended period of time. In order to test if indeed the elevated levels of YycG* is responsible for the observed phenotype, the experiment described above was carried out in the presence of different levels of xylose to further increase YycG* levels.

The results are shown in Figure 3.41 and 3.42. Strains grown in the presence of 0.0025% xylose show a noticeable difference to those grown without xylose (Figure 3.41). None of the strains carrying a second copy of YycG appears to reach the same OD₆₀₀ as wild-type strain 168. The strains containing multiple amino acids changes, IJR107, IJR114 and IJR112 are dropping in OD₆₀₀ more rapid in late stationary phase than when grown without xylose. When strains were grown in LB broth supplemented with 0.005% of the inducer xylose, a decrease in culture density is monitored for all strains carrying a second copy of YycG whereas strains that showed activation of PhoP are more affected than strains that did not exhibit PhoP phosphorylation by YycG (Figure 3.42). For example, strain IJR107 grew at a similar rate as wild type strain 168 in the presence of 0.005% xylose but the OD₆₀₀ for strain IJR107 dropped continuously after approximately 1 hour into stationary phase whereas the OD₆₀₀ of strain 168 just plateaus upon entry into stationary phase. The OD₆₀₀ of strains IJR114 112 115 shows a similar profile to strain IJR107, the OD₆₀₀ of the other strains plateau similar to strain 168. The strains that show a drop in OD₆₀₀ in stationary phase are those that also showed PhoP phosphorylation by YycG* *in vivo*.

Conclusion

These observations indicate that overexpression of YycG* proteins containing amino acid changes that allow phosphorylation of PhoP results in cell lysis upon extended growth in LB. Strains that do not activate PhoP show growth on LB agar and in LB broth comparable to wild type strain 168 and the growth defect is observed only in where PhoP can be phosphorylated by YycG*. Thus, the activation of the phosphate starvation regulon during non-phosphate starved conditions or activation of both TCS YycFG and PhoPR at the same time is not compatible with viability. Finally, this set of experiments show that the conditions under which the *in vivo* study of mutated YycG* was carried out were not compromised.

3.8 Discussion

Two-component systems of prokaryotes function in signal-transduction, regulation of gene expression and adaptation to changing environments. TCSs are composed of four modules usually organized into two proteins: a HK consisting of a signal detection domain and a catalytic domain and a RR composed of a receiver domain linked to an effector domain (see Figure 1.7). Amongst all the signal detection domain is highly diverse, sensing a wide variety of signals. The output domain usually belongs to one of many classes of DNA-binding domains and binds to a specific DNA sequence. The domains involved in specificity of phosphotransfer are the catalytic and receiver domains. These domains are highly conserved amongst TCSs since each transmitter domain generally interacts only with its cognate receiver domain. These interactions must be extraordinarily specific. The objective of these studies was to determine the nature of this specificity.

K.I. Varughese proposed a model for the interaction surface of YycG based on the Spo0B:Spo0F interaction (Howell *et al.*, 2006). This model suggests that the determining residues for specificity are mainly located on the α 1-helix. To test this model of molecular discrimination in this interaction, two related TCSs were chosen namely YycFG and PhoPR. These were used to conduct this study for the following reasons: (i) The HKs YycG and PhoR are closely related phylogenetically. (ii) Few residues differ between the interaction surface of the YycG α 1-helices and PhoR that make YycG specific for interaction with YycF but not with PhoP. (iii) In wild-type cells growing in LB YycG is expressed and phosphorylates YycF. (iv) PhoP/R is only constitutively expressed at very low levels and PhoP is not phosphorylated during growth in LB (Pragai *et al.*, 2004). (v) YycG does not phosphorylate PhoP. (vi) Phosphorylated PhoP (Pho~P) is the only transcription factor known to activate *phoA* expression.

The in vivo system

In this study a system was established that allows the modification of the essential histidine kinase YycG and examination of its capability to phosphorylate PhoP *in vivo*. The effects of amino acid changes in YycG on the interaction with PhoP can be monitored through the expression of a transcriptional *phoA-lacZ* fusion. In wild-type cells growing in LB broth PhoR is inactive. However, some histidine kinases have two opposing activities: (i) a kinase activity, that is predominantly found in activated HKs and (ii) a phosphatase activity that predominates when the HK is not activated (for review see Stock *et al.*, 2000).. The signal activating the HK YycG is unknown but YycG is known to be active in

exponentially growing cells. However, the activation of PhoR occurs in response to phosphate limitation. Therefore, during growth in LB, YycG is activated whereas PhoR is not. Under these conditions the $P_{phoA-lacZ}$ fusion is not expressed. In addition it is important to note that under these conditions PhoR is in predominantly phosphatase mode, thus dephosphorylating any PhoP that should become phosphorylated.

In wild-type cells, the TCSs PhoPR and YycFG are transcribed from their operons and each kinase transfers, after autophosphorylation upon their specific signal a phosphoryl group to its cognate RR. The phosphorylated RR in turn becomes active and binds its target gene promoter, expression of *phoA* is dependent on PhoP~P and *yoch* on YycF~P respectively. Phosphotransfer between these two systems only occurs (and at very low level) from PhoR to YycF but not from YycG to PhoP (Howell *et al.*, 2006). In this study strains were constructed in which the HK PhoR is deleted and an additional copy of YycG is inserted, leaving the latter as the only possible phosphor donor for PhoP. This second copy of YycG can be wild-type or with specific amino acid changes. The *phoA-lacZ* reporter construct was used to monitor the activation of PhoP through mutated YycG*, based on the fact that the only way *phoA* expression can be activated is through phosphorylated PhoP. PhoP usually receives its phosphoryl group from its cognate kinase PhoR. Using this *in vivo* approach no phosphorylation of PhoP could be detected in wild-type background. However, phosphotransfer from mutated YycG* towards PhoP was observed in a background in which PhoR had been deleted. This indicates that the presence of the cognate kinase PhoR plays a role in preventing or reversing the phosphorylation reaction between mutated YycG* and PhoP. In phosphate limitation conditions PhoR acts as a kinase and phosphorylates PhoP whereas here strains are grown and maintained in phosphate rich LB medium. Therefore, growth conditions chosen here are not limiting for phosphate - meaning the PhoPR TCS is not active. In these conditions PhoR is predicted to exist predominantly in phosphatase mode, thereby dephosphorylating any PhoP~P generated. Since PhoP~ could only be generated when PhoR was absent, this supports the model that during growth in LB, PhoR dephosphorylating any PhoP~P generated.

A very unusual $P_{phoA-lacZ}$ expression profile could be observed in strains where PhoP is phosphorylated by YycG*. Little β -galactosidase activity was observed in exponentially growing cells but there was an induction at around transition phase, a phenomenon that has been observed repeatedly.

This profile might be due to the complicated regulation of the PhoPR regulon, having not only one but so far six characterized promoter regions involving amongst others autoinduction and repression of a CcpA promoter (Puri-Taneja *et al.*, 2004). A transition state regulator may repress expression from either the *phoPR* promoter or from the *phoA* promoter in cells growing exponentially. The unusual expression profile could also be the reason for the somewhat surprising discrepancy in results observed on the X-gal plate assay and those seen in liquid culture, *i.e.* dark blue colonies versus low level activity.

An unexpected result was obtained from the hybrid kinase in strain IJR115. This hybrid was created by fusing the sensing domain of YycG with the catalytic domain of PhoR, thus creating a novel histidine kinase that activates the Pho response upon the YycG stimulus. That the kinase is active is apparent from the *in vivo* assays although the low level of the *phoA-lacZ* induction in exponential phase is surprising as the hybrid kinase bears the perfect interaction surface for PhoP phosphorylation. This might be due to the YycG PAS domain that is different from that of PhoR. A cysteine residue was found in the PAS domain of PhoR at position 303 that has been reported to be crucial for phosphotransfer reaction in the PhoPR two-component system in *B. subtilis* (Eldakak and Hulett, 2006). That study of changing the Cys₃₀₃ from Cys to Ala indicated that this residue in the PAS domain of PhoR is required for the full activation of the Pho-system *in vivo*. This mutation did not seem to interfere with autophosphorylation of the kinase dimer but with the activity of the HK. The efficiency of phosphotransfer of PhoR* to its cognate response regulator is diminished, resulting in decreased Pho~P concentrations. In YycG this cysteine residue is not present at this position; in fact, there is no cysteine within the PAS domain. Since all mutant YycG* constructs, including the YycG'-PhoR hybrid kinase, possess the PAS domain of YycG, this may also contribute the low induction of the Pho response *in vivo*.

These strains that show a lytic phenotype carry a mutated YycG* that allows crosstalk with PhoP while grown on rich medium that is not phosphate depleted. Under these circumstances YycG is usually active as a kinase whereas PhoR is active as a phosphatase so that no phosphorylated PhoP is present. By introducing mutations into the second copy of YycG, PhoP does become phosphorylated in addition to the presence of phosphorylated YycF. In consequence, that means this both TCS are active at the same time. Both TCS are involved in cell wall metabolism with overlapping function but also regulating genes that are opposing: YycFG for example incorporates phosphate in the cell wall whereas PhoPR, when activated, up regulates the *tua* genes building cell wall without

phosphate (Howell *et al.*, 2006; Qi and Hulett, 1998). Having both systems on appears not to be compatible with viability over a prolonged period of time.

Five amino acids at position 3, 8, 10, 11 and 12 within the α 1-helix of YycG were changed to those found in PhoR at similar positions (R3K T8S R10K S11G Y12F). To determine whether these changes enabled phosphorylation of PhoP and to which extent each amino acid contributes to that, the described *in vivo* system was used that allowed to monitor PhoP phosphorylation with amino acid changes: (i) qualitatively on LB agar plated and (ii) quantitatively by growth in LB broth. In addition the mutated YycG proteins were investigated *in vitro*. The results are summarized in Figure 3.43 and Table 3.3.

The strains containing YycG with single amino acid changes IJR102 (R3K), IJR103 (T8S), IJR104 (R10K) and IJR106 (Y12F) showed very low β -galactosidase activity *in vivo* (white on LB agar plates and ~5 units). In contrast, strain IJR105 with the single amino acid change S11G showed a moderate phosphorylation of PhoP *in vivo* (pale blue and ~215 units). The 'YycG105 protein was purified and the ability to phosphorylate the non-cognate RR PhoP tested in the qualitative approach phosphotransfer from 'YycG105 to PhoP could be observed after 2 minutes. However, the initial rate of phosphotransfer to PhoP from 'YycG105 is only 0.2% of that from 'PhoR. The ability of 'YycG105 to phosphorylate its cognate RR YycF was decrease to 48% of that of 'YycG.

The strain IJR112 contains YycG with two amino acid changes (S11G Y12F) which resulted in high β -galactosidase activity *in vivo*; deep blue color on LB agar plates and 570 units when growth in LB broth. The qualitative *in vitro* assay showed that 'YycG112 is able to phosphorylate PhoP but the initial rate of 'YycG112 to phosphorylate PhoP *in vitro* was not increased and is only 0.2% of that from 'PhoR. The ability of 'YycG112 to phosphorylate its cognate RR YycF was decrease to 27% of that of 'YycG.

Strain IJR114 contains YycG with four amino acid changes (R3K T8S S11G Y12F) and showed an increased β -galactosidase activity that resulted in a deep blue color on LB agar plates and 800 units in liquid culture. Qualitatively 'YycG114 is able to transfer a phosphoryl group to PhoP *in vitro*. This indicated a drastic increase in the ability of 'YycG114 to phosphorylate the non-cognate RR PhoP but this could not be confirmed quantitatively. The ability to phosphorylate PhoP is only 0.6% than that of 'PhoR. Interestingly, the ability of 'YycG114 to phosphorylate its cognate YycF is drastically decreased to 0.5% of that of wild-type 'YycG.

All five amino acids of YycG are changed in strain IJR107 (R3K T8S R10K S11G Y12F) that lead to high levels of β -galactosidase activity *in vivo* (deep blue color on plates

and 450 units). The qualitative *in vitro* assay showed a strong phosphotransfer from 'YycG107 to PhoP supporting the results obtained *in vivo*. However, the quantitative analysis of the phosphotransfer from 'YycG107 to PhoP showed that the initial rate is only 0.5% of that from 'PhoR to PhoP. The ability of 'YycG107 to phosphorylate its cognate RR YycF was reduced to 4% of that from the wild-type 'YycG.

Taken together, the *in vivo* and *in vitro* data show that the amino acids changes introduced into the α 1-helix C-terminal of the active site do change the interaction between YycG* and YycF in terms of loss of phosphotransfer. The single amino acid change S11G drastically reduced the ability of YycG* to phosphorylate YycF by 50% and four amino acid changes (R3K T8S S11G Y12F) almost abolished phosphotransfer to YycF.

On the other hand, a gain of phosphotransfer from YycG* to the non-cognate PhoP is achieved. The *in vivo* results indicated a major increase in ability of YycG* to phosphorylate PhoP and the qualitative *in vitro* assessment of phosphotransfer between 'YycG* and PhoP was consistent with the *in vivo* results. However, somewhat disappointingly, the initial rate of phosphotransfer between 'YycG* and the non-cognate PhoP does not match that between 'PhoR and PhoP. However, the evaluation of phosphorylated PhoP is influenced by the impaired autophosphorylation of some of the mutated YycG* (see 'YycG114 and 'YycG107 in Figure 3.43).

Taken together, the amino acid change at position 11 had a major effect on the phosphotransfer between YycG and PhoP emphasizing the importance of amino acids at that position. Changing a serine to a glycine has an additional effect, glycine residues are known to introduce flexibility to the peptide chain. In Howell *et al.* (2006) it was postulated that the size difference between residues within the interaction surfaces of YycG and PhoR prevent YycG to interact with and phosphorylate PhoP (Figure 3.42). When these large amino acids were replaced by the smaller residues found in PhoR, a phosphotransfer was observed. Therefore, steric hindrance may play a role in specificity.

A very similar study has very recently been published in Cell (Skerker *et al.*, 2008). It reported the rewiring of the HK EnvZ to change specificity from its cognate RR OmpR to RstA. To achieve this, three amino acids in position 7, 11 and 12 respective to the site of phosphorylation were changed from those found in EnvZ to those found in RstB. The mutant YycG112 is identical in position 7 to PhoR and positions 11 and 12 where change to those found in PhoR. However, the almost complete switch in specificity of interaction reported by Skerker *et al.*, (2008) could not be observed. The mutant HK YycG107 that is even more similar to PhoR in the interaction surface also didn't show such a drastic

change in specificity. The ability to swap the specificity from EnvZ to RstB may be a special case as the group reports that changing the specificity amino acids of the α 1-helix was not sufficient to achieve phosphorylation of other non-cognate RRs. Taken together, the specificity of interaction between HKs and RRs has not been fully resolved but these two studies have taken it a step further in the right direction.

Chapter 4
Mutational analysis of the RR PhoP

Chapter 4 - Mutational analysis of the RR PhoP

Introduction

The source of specificity of interaction in two-component systems is found at the molecular interface formed by the HK and RR during phosphotransfer (Varughese, 1998). In the previous chapter the surface provided by the HK has been described and the role of particular amino acids in the specificity has been elucidated. This was achieved by changing those found in the HK YycG to those found in PhoR to enable phosphotransfer to the non cognate RR PhoP *in vivo* and *in vitro*.

Spo0F a single receiver domain, serves as a model for a RR and therefore gives insight into the nature of its interacting surface. How phosphotransfer is achieved has been established by crystallography and mutational analysis of a number of TCS (Zapf *et al.*, 2000; Tzeng and Hoch 1997) . The structure of the Spo0F, five β -strands surrounded by five α -helices, is commonly found in RRs of TCSs that usually also have output domains. As described in Mukhopadhyay and Varughese (2005) the variable region surrounding the catalytic aspartate residue is most likely to contribute to specificity. This region is also involved in forming the hydrophobic patch for the alignment with the HK interacting surface.

This study aims to elucidate the specific amino acids that contribute to the ability of the RR to distinguish its cognate partner from all other HKs. Therefore the previously introduced two-component system YycFG and PhoPR where used to conduct this study. Changing the amino acids in the RR PhoP to those found in YycF at similar positions should allow for its molecular recognition by YycG and subsequent phosphotransfer. Two alternative approaches were adopted: firstly the *in vivo* system described in the previous Chapter (3) was utilized to allow the easy mutation of PhoP whilst keeping the essential YycG intact and to monitor the effect of mutations in PhoP on the phosphorylation by YycG; secondly, quantitative *in vitro* phosphorylation assays were carried out to establish the increase of phosphorylation of mutated PhoP by wild-type YycG and measure loss of specificity for its cognate HK PhoR.

4.1 Computational determination of specificity amino acids on the PhoP surface

The specificity of recognition between HKs and RRs is determined by their interaction surfaces. The interaction surface of the HK is composed of the four helix bundle and the amino acids contributing substantially to the specificity of interaction with the RR were described in detail in the previous Chapter (3). Here, the interaction surface of the

response regulator (RR) will be investigated. The RR interaction surface is comprised of a hydrophobic patch formed by anchor amino acids surrounding four conserved catalytic amino acids that build a pocket for the site of phosphorylation, the aspartate amino acid. The anchor amino acids are also relatively conserved within a family. Additional to those two groups, there are amino acids found on the outer region of the hydrophobic patch that are variable and thought to contribute substantially to specificity in the recognition of the four helix bundle (Varughese, 2002; Mukhopadhyay and Varughese 2005). The three groups of amino acids of the hydrophobic patch and variable residues surrounding the catalytic region of Spo0F, PhoP and YycF are detailed in Figure 4.2.

In order to determine the interaction surfaces of PhoP and YycF, an alignment of their receiver domains with Spo0F was carried out (Figure 4.1). The catalytic amino acids are easy to identify due to their conserved nature (indicated in red in Figure 4.2). With the help of the known regions of Spo0F the anchor and variable amino acids of PhoP and YycF were located and compared (Figure 4.2). Within the groups of anchor and variable amino acids, only four residues differ between PhoP and YycF. One is found among the anchor amino acids at position 17, where PhoP has a leucine (L17) and YycF an isoleucine (I17). Three distinctive residues are observed within the group of variable amino acids at positions 13, 20 and 107: PhoP has a serine (S13), tyrosine (Y20) and proline (P107); YycF has a proline (13P), phenylalanine (20F) and a threonine (107T) in those positions respectively. It is very likely therefore that those four residues play a significant role in the discrimination of cognate and non cognate HKs. In this study, these four amino acids were changed from those found in PhoP to those found in YycF. All combinations of these four amino acids were generated to test whether mutated PhoP* is able to interact with YycG and to determine the extent to which each amino acid plays a role in specificity (Table 4.1).

4.2.1 An *in vivo* system to investigate the specificity of interaction between YycG and PhoP

Howell *et al.* 2006 reported that the kinase PhoR can phosphorylate both its cognate RR PhoP and the non cognate RR YycF, whereas the reciprocal reaction, the phosphorylation of PhoP by YycG, does not occur. In order to study the factors that contribute to the specificity of interaction between the RR and the HK, the *in vivo* system previously described in Chapter 3.1.1 was used. It has the following characteristic features: (i) all strains must carry the wild-type *yycFGHIJyyxA* locus due its essentiality (ii)

a heterologous copy of the *phoP* gene under a xylose inducible promoter (P_{xyI}): either the wild-type or mutated *phoP* genes are inserted at the *thrC* locus and (iii) a transcriptional P_{phoA} -*lacZ* fusion introduced at the *amyE* locus. Other mutations such as deletion of *phoR* ($\Delta phoR$) and deletion of *phoPR* ($\Delta phoPR$) were introduced into strains as appropriate. Expression of the P_{phoA} -*lacZ* fusion is a measure of the extent to which PhoP is phosphorylated (PhoP~P). To study the requirements of the interacting surface of PhoP, specific amino acids within the $\alpha 1$ helix and loop 5 region of the RR PhoP were mutated to change its specificity of interaction from PhoR to YycG (Table 4.1). Therefore an increased ability of YycG to phosphorylate mutated PhoP* is detectable by β -galactosidase expression.

Phosphorylated PhoP is the only known activator of *phoA*. Therefore the strains IJ99, IJR99 and IJPR99 carrying the transcriptional reported gene fusion (P_{phoA} -*lacZ*) in the wild-type, $\Delta phoR$ and $\Delta phoPR$ background were used.

Genes encoding wild-type *phoP* and mutated *phoP** were inserted into the chromosome of these strains in single copy at the threonine locus and their expression is under the control of the xylose inducible promoter (P_{xyI}). Therefore all mutated PhoP* proteins were expressed in wild-type background (strain set IJW140-155), in a $\Delta phoR$ mutants background (IJR140-155) and in a $\Delta phoPR$ mutant background (IJPR140-155). The ability of each PhoP* mutant to be phosphorylated by YycG was monitored by measuring β -galactosidase activity (Figure 4.3)

4.2.2 Confirmation of correct genetic structure of strains

The chromosomal arrangement of genes at the *yycFGHIJyyxA*, *thrC*, *amyE* and *phoPR* locus is shown in Figure 4.3. The *yycFGHIJyyxA* locus is intact in all strains since it is essential. Insertion of P_{phoA} -*lacZ* into *amyE* should result in chloramphenicol resistance and an amylase negative phenotype. Insertion of the P_{xyI} *phoP* at the nonessential *thrC* locus should result in threonine auxotrophy and resistance for spectinomycin while such series of strains were mutated for *phoR* / *phoPR* was neomycin or erythromycin resistant respectively. Putative strains of set IJW140-155 were tryptophan and threonine auxotroph as well as spectinomycin resistant. Putative strains IJR140-155 were tryptophan and threonine auxotroph and spectinomycin and neomycin resistant. Putative strains IJPR140-155 were screened for tryptophan and threonine auxotrophy and spectinomycin and erythromycin resistance. Therefore all strains showed the correct auxotrophy and drug resistance (Figure 4.3).

4.2.3 Qualitative evaluation of interaction between YycG and PhoP*

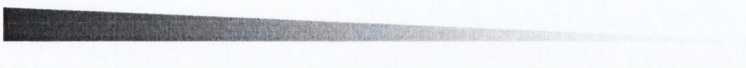
To qualitatively evaluate the ability of phosphotransfer between YycG and mutated PhoP* protein, all strains of set IJR ($\Delta phoR$, $P_{xyI}phoP^*$, $P_{phoA-lacZ}$) and set IJPR ($\Delta phoPR$, $P_{xyI}phoP$, $P_{phoA-lacZ}$) were plated on LB agar supplemented with X-gal. When the $P_{phoA-lacZ}$ fusion is expressed as a consequence of the phosphorylation of PhoP to generate PhoP~P, strains will show a blue color whereas strains lacking phosphorylated PhoP will remain white. The results are shown in Figure 4.4 and 4.6. None of the IJR or IJPR strains displays β -galactosidase activity, which was not expected.

To test whether the lack of β -galactosidase activity was due to the insufficient expression of PhoP, the strains were plated onto solid LB medium supplemented with X-gal and 1% xylose (data not shown). In this instance all the strains were blue colored as evidence of β -galactosidase activity. Therefore, this system works in principal. The conclusion was made that the level of induction of PhoP by xylose inducer would have to be optimized at > 0% (x/v) xylose and less than 1% (w/v) xylose. Since 0% (w/v) xylose (the P_{xyI} promoter is leaky) gives no β -galactosidase activity (*i.e.* no PhoP~P) and 1% xylose gives activity in all strains, the strains were plated onto a series of LB agar plates supplemented with different xylose concentrations in order to optimize the conditions, aiming for the minimal level of xylose that gave differential expression of β -galactosidase. The results are shown in Figure 4.5, 4.7 and 4.8. On plates containing 0.005% xylose, strains IJR140 (wild-type PhoP) and IJPR140 (wild-type PhoP) show a light blue color. At this level of xylose the other strains show differences in blueness (β -galactosidase activity) (Figure 4.5 and 4.8). At a level of 0.0025% xylose the strain carrying the wild-type *phoP* IJPR140 remains white whereas other strain containing mutated *phoP** show different levels of blueness (Figure 4.7). These results indicate that some mutations and combinations of mutations result in a higher level of β -galactosidase activity than others. Therefore we choose to use strain set IJPR with 0.0025% (w/v) xylose for further experiments.

Strains IJPR that carrying single amino acids changes in PhoP were examined. Results are shown in Table 4.2. Of those strains, IJPR 143 (L17I) seems to show the strongest β -galactosidase activation of the $P_{phoA-lacZ}$ construct with a deep blue color (active). Two strains IJPR144 (Y20F) and IJ141 (P107T) are light blue and pale blue. Interestingly, strain IJPR142 (S13P) appears very white, almost whiter than the wild type *phoP* carrying strain IJPR140. This indicated that amino acids change L17I has a strong effect on PhoP phosphorylation whereas changes Y20F and P107T may have a minor


effect. The amino acid change S13P appears to have an adverse effect on PhoP phosphorylation.

Table 4.2 β -galactosidase activity of PhoP containing a single amino acid change

Blue				White
IJPR 143	IJPR144	IJ141	IJ142	
L17I	Y20F	P107T	S13P	

The strains with two amino acid changes were examined. The results are shown in Table 4.3. Of those strains, strain IJPR 145 (S13P L17I) appeared very blue followed by strains IJPR150 (L17I P107T) and IJPR147 (L17I Y20F). Two strains showed only a hint of β -galactosidase activity resulting in a pale blue color blue, namely IJPR149 (S13P P107T) and IJPR146 (S13P Y20F). Strain IJPR151 with the amino acid changes Y20F P107T remains white, which is interesting because the combined single mutations Y20F and P107T by themselves showed a light blue color.

Table 4.3 β -galactosidase activity of PhoP containing two amino acid changes

Blue					White
IJPR145	IJPR150	IJPR147	IJPR149	IJPR146	IJPR151
S13P L17I	L17I P107T	L17I Y20F	S13P P107T	S13P Y20F	Y20F P107T

Examination of strains with three and four amino acid changes in PhoP lead to the following β -galactosidase activity: IJPR152 (S13P L17I P107T) displayed a very blue color followed by strains IJPR155 (S13P L17I Y20F P107T), IJPR148 (S13P L17I Y20F) and IJPR154 (L17I Y20F P107T) that all display lesser blue color. In contrast strain IJPR153 (S13P Y20F P107T) appears white.

Table 4.4 β -galactosidase activity of PhoP containing three and four amino acid changes

Blue				White
IJPR152	IJPR155	IJPR148	IJPR154	IJPR153
S13P	S13P	S13P	L17I	S13P
L17I	L17I	L17I	Y20F	Y20F
P107T	Y20F	Y20F	P107T	P107T
	P107T			

Noteworthy is that strains carrying the L17I amino acid change in PhoP always appear bluer than strain without this mutation, indicating that this amino acid change allows is a major contributor to phosphorylation of PhoP by YycG. These results indicate that some amino acid changes, especially L17I, contribute more to the ability of PhoP* to bind and receive a phosphoryl group from YycG than others, whereas the amino acid change S13P may have an inhibitory role.

In both strains sets IJR and IJPR (carrying a chromosomal copy of PhoP^{WT} and a mutated PhoP copy at the *thrC* locus) a differential level of *phoA-lacZ* expression is detectable. However, since PhoP functions as a dimer (Birck *et al.*, 2003), there is a possibility of heterodimer formation by wild-type PhoP and mutant PhoP*. It was therefore decided to continue only with strain set IJPR ($\Delta phoPR$).

4.2.4 Optimization of growth conditions in LB broth

The level of xylose inducer necessary to observe β -galactosidase activation in IJPR P_{xyr}-*phoP* strains needed to be established for growth in LB broth. The appropriate level of xylose inducer should allow differentiation of the effects of different amino acid changes in PhoP by differences in β -galactosidase activity. Therefore, strains IJPR140 (wild-type), IJPR143 (L17I) and IJPR155 (S13P L17I Y20F P107T) were selected and grown in LB broth supplemented with 0%, 0.0025% and 0.005% xylose. The results are shown in Figure 4.9.

Strains IJPR140, IJPR143 and IJPR155 were grown as previously described in LB broth supplemented with the appropriate antibiotics and samples were harvested at the appropriate time. Two observations could be made: Firstly, low levels of expression are observed in exponential growth with induction of expression observed during postexponential growth. Secondly, different levels of β -galactosidase activity are observed for the three strains but the difference increases with higher levels of added xylose. When

grown without xylose, a difference of β -galactosidase activity is detectable despite the white appearance of colonies of all three strains on LB agar plates. The level of β -galactosidase activity of strain IJPR140 is ~18 units that of strain IJPR143 are ~ 31 units and strain IJPR155 about 50 units. These levels of differential expression were not suitable to clearly distinguish the expression changes caused by different amino acid changes in PhoP. When grown in the presence of 0.0025% xylose, the levels of β -galactosidase activity in all strains increased. This rise in β -galactosidase activity also revealed the differences in LacZ expression between strains IJPR143 (L17I) and IJPR155 (S13P L17I Y20F P107T). The difference increased substantially when the strains were grown in the presence of 0.005% xylose. Strains IJPR143 and IJPR155, that both showed blue color on LB agar plates, can now be clearly distinguished by their in β -galactosidase activity: 262 and 436 units of lacZ activity respectively. Under these conditions the wild-type PhoP carrying strain IJPR140 now shows 43 units of β -galactosidase activity. Since a clear difference is observed between the β -galactosidase levels of strains IJPR140 (wild-type) and IJPR143 (L17I) and IJPR155 (S13P L17I Y20F P107T) when grown in the presence of 0.005% xylose, these conditions were used for all further experiments.

4.2.5 Quantitation of phosphorylation of mutated PhoP* proteins by YycG *in vivo*

In order to quantitatively evaluate the extent to which each amino acid change contributes to ability of PhoP to accept a phosphoryl group from YycG, strain set IJPR140-155 was grown in LB medium supplemented with 0.005% xylose as established in the previous section. This set of strains carrying deletion of both the *phoP* and *phoR* genes was chosen because PhoR displays phosphatase activity towards its cognate RR PhoP in phosphate replete conditions. Additionally in the absence of the wild-type PhoP the formation of heterodimers is prevented.

All strains of set IJPR140-155 ($P_{xyI}phoP P_{phoA-lacZ} \Delta phoPR$) were grown in LB broth as described in methods and material. The medium was supplemented with 0.005% xylose. The accumulation of β -galactosidase activity was determined and results are shown in Figure 4.10 and 4.11.

Strain IJPR140 contains the wild type PhoP and the β -galactosidase activity is very low as expected in exponential phase, and rises only slightly upon entry into stationary phase (Figure 4.10). Strains IJPR141 and IJPR144 carrying single amino acids changes P107T and Y20F in PhoP respectively, show very similar levels of β -galactosidase expression as IJPR140 (wild-type). Strain IJPR142 (S13P) that appeared very white on LB

agar plates shows a lower level of β -galactosidase activity than does strain IJPR140 when grown in LB broth. Strain IJPR143 that contains a single amino acid change at position 17, replacing leucine with an isoleucine (L17I), shows about 10-fold higher β -galactosidase expression than IJPR140 in stationary phase (Figure 4.10).

The β -galactosidase profiles of the six strains containing two amino acid changes in PhoP were examined. All six strains shown low β -galactosidase activity in exponential growth phase. The β -galactosidase activity of strains IJPR146 (S13P Y20F) and IJPR147 (L17I Y20F) rises slightly upon entry into stationary phase but only to levels below approximately 100 β -galactosidase unity. Of particular note is the β -galactosidase activity of strain IJPR145 (S13P L17I) that is induced strongly reaching levels of more than 1500 units of β -galactosidase units (Figure 4.10). In Figure 4.11 the remaining strains carrying double PhoP mutants IJPR49 (S13P P107T), IJPR150 (L17I P107T) and IJPR151 (Y20F P107T) are shown. Two strains, IJPR149 and IJPR151, show low β -galactosidase activity levels below 100 units in contrast strain IJPR150 shows increasing levels of β -galactosidase up to 600 units.

The strains carrying three and four amino acid changes in PhoP, IJPR148 (S13P L17I Y20F), IJPR152 (S13P L17I P107T), IJPR153 (S13P Y20F P107T) and IJPR154 (L17I Y20F P107T) were investigated. Results are shown in Figure 4.11. All four strains show an increase of β -galactosidase activity in stationary phase. The levels of β -galactosidase activity of strains IJPR148, IJPR152 and IJPR154 are at levels of ~500 units, ~1200 and ~250 units. Noteworthy is the β -galactosidase expression level of strain IJPR152 (S13P Y20F P107T) (<100 units) the only triple PhoP mutant strain without the L17I change.

Expression of β -galactosidase in the strain containing all four amino acid changes in PhoP, strain IJPR155 (S13P L17I Y20F P107T), was also determined (Figure 4.11). Low levels of activity were observed in exponential phase of growth that increased drastically upon transition phase reaching ~500 units of β -gal activity two hours into stationary phase.

These results show that (i) mutations in PhoP allow PhoP phosphorylation (ii) different amino acids and their combinations have different effects on phosphotransfer (iii) the amino acid at position 17 (Leu/Ile) appears to play a crucial role in the specificity of phosphotransfer from the YycG histidine kinase.

4.2.6 P_{phoA} *laz* expression is P_{xyI} *phoP** dependent

In the previous section describes β -galactosidase activity profiles that arise from possible phosphotransfer between wild-type YycG and mutated PhoP*. Expression of the mutated PhoP is under the control of an inducible xylose promoter and as shown in Section 4.2.3 and 4.2.4 *phoP* expression depends on the presence of the inducer xylose during growth on LB agar plates. To test whether xylose dependency of *phoP* expression is true also when strains are grown in LB broth, and to determine if the observed β -galactosidase activity is indeed depending on expression of the P_{xyI} *phoP**, each strain expressing β -galactosidase was grown in LB broth without xylose.

Strains IJPR140, IJPR143, IJPR145, IJPR148, IJPR150, IJPR152 and IJPR155 were grown in LB broth. The results are shown in Figure 4.12. As expected strain IJPR140 shows no β -galactosidase activity. This strain carries the wild-type copy of *phoP*: PhoP has been shown not to be phosphorylated by YycG (Howell *et al*, 2003; 2006) and the cognate HK PhoR is absent. All other strains also show no β -galactosidase activity (Figure 4.12).

These results show that (i) leaky expression from the xylose promoter is not sufficient to provide PhoP* for phosphorylation by YycG (ii) the observed β -galactosidase activity is dependent on PhoP, expressed from the P_{xyI} *phoP* locus.

4.2.7 Growth phenotype of IJPR-PhoP* strains in LB broth

In order to test whether a growth phenotype can be observed during growth in LB broth supplemented with 0.005% xylose that may influence the results obtained in the *in vivo* study, all strains were grown in LB broth and monitored over ten hours (Figure 4.13). The results of growth in microtiter plates are shown in Figure 4.13. The data shown for each strain is an average of three identical growth experiments. All strains show a very similar growth profile to wild type strain 168 in LB broth supplemented with 0.005% xylose. This observation indicates that expression of mutated PhoP* from the xylose promoter has no major effect on growth under these conditions. Thus, the level of phosphorylated PhoP and the subsequent activation of the phosphate starvation regulon during non-phosphate starved condition is not high enough to elicit a phenotype. Therefore, the conditions under which the *in vivo* study of mutated PhoP* was carried out were chosen correctly.

4.3. Analysis of the effect of amino acid changes in PhoP* on phosphorylation *in vitro*

The *in vivo* study indicates that the amino acid modifications in the interaction surface of PhoP that is predicted to be involved in the interaction with its cognate PhoR kinase changes the specificity of interaction, enabling PhoP to receive a phosphoryl group from the non-cognate HK YycG. The results of the *in vivo* study indicate that each amino acid change contributes differentially, some appear to enhance phosphorylation by YycG but others appear to have a negative effect. In order to verify this putative phosphorylation of PhoP* by YycG, *in vitro* studies with purified proteins were performed. Such studies would allow not only the examination of phosphorylation of PhoP* by 'YycG, but also to examine a possible reduction in the ability of mutated PhoP* proteins to be phosphorylated by the cognate 'PhoR protein.

4.3.1. Purification of HKs and RRs

All *phoP* genes encoding the appropriate amino acid changes (*phoP*140-155), were cloned into the expression vector pET21b to create an inducible His-tagged translation fusion of the full-length mutated PhoP* for expression and purification. The HKs 'YycG and 'PhoR were also purified at the same time to ensure consistency. The isolated proteins were analyzed by SDS PAGE to confirm of production of a protein of appropriate M_r and protein purity. The SDS PAGE analysis showed a purified mutant PhoP* proteins run as a single band with 35 kDa slightly bigger than the calculated M_r of 28.7 kDa (Figure 4.14). This has also been reported to be observed for the RR YycF (Howell *et al.*, 2003). This analysis revealed that all proteins are produced, are of expected M_r and of suitable purity for further experiments.

4.3.2 *In vitro* phosphorylation of cognate pairs YycFG and PhoPR

The conditions for the *in vitro* phosphorylation were previously established (Chapter 3) and the assays were carried out using this procedure changing only the response regulator concentrations. When the *in vitro* reactions contained the 'YycG/ YycF or 'YycG/PhoP* protein pairs, the YycF and PhoP* proteins were used at a concentration of 25 μ M. In contrast, when the *in vitro* reactions contained 'PhoR/PhoP or 'PhoR /PhoP*, then the PhoP and PhoP* proteins were used at a concentration of 2.5 μ M. The concentration of 'YycG and 'PhoR was 2.5 μ M in all reactions.

The results of the phosphorylation of YycF and PhoP by γ -YycG is shown in Figure 4.15. Over a time course of 300 seconds, an increasing and robust phosphotransfer from γ -YycG to YycF could be observed. In contrast, a phosphotransfer from γ -YycG to PhoP was not detectable (Figure 4.15A). The phosphoimage was quantified as describe in methods and materials. The resulting graph is shown in Figure 4.15B. The rate of YycF phosphorylation is linear up to one minute and begins to plateau from thereon (Figure 4.15B). The linear part of the reaction allows the determination of the initial rate of YycF phosphorylation and comparison to the rate with which PhoP is phosphorylated by YycG (Figure 4.15C). Therefore, the linear part of the response regulator phosphorylation was fitted with a trendline and the slope determined which expresses the rate of phosphorylation. The slope for YycF~P is 1.567 whereas that fro PhoP~P is 0. This result agrees with results shown in this study and in Howell *et al.*, (2006), showing that YycG phosphorylate its cognate RR YycF but not the non-cognate RR PhoP. The phosphotransfer from γ -PhoR to RRs PhoP and YycF was also tested. For this, the purified proteins were incubated with each other over a time course of 300 seconds. The resulting phosphoimage is shown in Figure 4.16A. During the reaction time course an increasing robust phosphorylation of PhoP is detectable, but no phosphorylation of YycF is observed. The phosphoimage was quantified (Figure 4.16B). A linear reaction was observed for PhoP phosphorylation up to 60 seconds before starting to plateau. Determination of the initial rate of PhoP by PhoR phosphorylation gave a value of 1.247 while the initial rate for YycF phosphorylation by PhoR was 0 (Figure 4.16C).

4.3.3 Analysis of phosphorylation of PhoP* proteins with changed amino acids by the non-cognated γ -YycG kinase *in vitro*

Described in this section is an assessment of the gain of mutant PhoP to accept a phosphoryl group from the non-cognate HK YycG by *in vitro* phosphorylation assays. Additionally, the loss of specificity to be phosphorylated by its cognate partner PhoR was tested. Protein concentrations were uses as follows: both HKs, YycG and PhoR were used at 2.5 μ M; the RRs, YycF, PhoP and PhoP* were used at 25 μ M when incubated with YycG and at 2.5 μ M when incubated with PhoR. In every single experiment phosphorylation of YycG-YycF or PhoR-PhoP cognate pairs, was included to be used as a control which allowed direct comparison of phosphotransfer between wild-type γ -YycG and PhoP proteins with amino acid changes.

Phosphorylation of PhoP141 with the single amino acid change P107T was first investigated by *in vitro* phosphorylation (Figure 4.17). The purified HK 'YycG was incubated with the RR YycF and PhoP141 to assess if this amino acid change in the latter affects the ability to accept a phosphoryl group from the non-cognate 'YycG HK. A steady increase of phosphorylated YycF can be observed when incubated with 'YycG over a time course of 5 minutes. In the first sample, taken after only 10 seconds YycF phosphorylation is visible. The mutant PhoP141 in contrast does not appear to become phosphorylated by YycG (Figure 4.17A). To compare the phosphotransfer reactions to both RRs, YycF~P and PhoP141~P phosphorylated by 'YycG were quantified and normalized to the highest phosphoimage value obtained for YycF~P and plotted versus time (Figure 4.17B). It is noticeable that the phosphotransfer from 'YycG to YycF is fast and linear over the first three time points (60 seconds) before slowing down. The plateau usually following the linear part of the reaction could not be observed within the five minute reaction time. In order to determine the initial rate of the phosphorylation of YycF and PhoP141, the initial time points, were plotted. The resulting values were fitted with a trendline and the slope determined (Figure 4.17C). The slope for YycF~P phosphorylated by 'YycG is 0.408, termed 100%, compared to 0% phosphorylation of PhoP141. This result indicates that the single amino acids change from a proline to a threonine (P107T) in PhoP does not enable detectable phosphorylation by 'YycG.

The loss of the ability of PhoP141 to be phosphorylated by the cognate 'PhoR HK was examined and compared to the phosphotransfer between 'PhoR and wild-type PhoP. The results are shown in Figure 4.18. 'PhoR was incubated with PhoP over a period of 5 minutes and with PhoP141 for a period of 20 min with samples taken at the indicated times (Figure 4.18A). A strong efficient phosphotransfer from PhoR to PhoP and PhoP141 could be observed. The phosphoimage was quantified (Figure 4.18B) Phosphorylation of PhoP141 increased steadily over 2 minutes dropping slightly at the 5 minute time point. The phosphotransfer from PhoR to PhoP141 showed the same steady increase of PhoP141~P up to two minute and plateau from thereon but not reaching the same level of phosphorylation. The initial rate of PhoP~P phosphorylation was evaluated as described above (Figure 4.18C). PhoP is rapid and efficiently phosphorylated by 'PhoR. The rate of phosphotransfer from 'PhoR to PhoP141 in contrast is approximately 63% of that observed with wild-type proteins (Figure 4.18C).

The analysis of the gain of ability of PhoP142 (S13P) to be phosphorylated by 'YycG is shown in Figure 4.19. The phosphoimage shows wild-type pairs 'YycG and YycF

and in addition phosphotransfer between 'YycG and PhoP142. The phosphoimage and the quantification of the phosphorylation of YycF are shown in Figure 4.19A and B. Change of this amino acid results in a low level of phosphotransfer between 'YycG and PhoP142. The comparison of the initial rates of YycF and Pho142 phosphorylation revealed that the amino acid change S13P has only a small effect on the ability of PhoP142 to accept a phosphoryl group from 'YycG of about 3% phosphorylation (Figure 4.19C).

The loss of the ability of PhoP142 to be phosphorylated by the cognate HK 'PhoR is shown in Figure 4.20. PhoR phosphorylates PhoP efficiently and rapidly but phosphotransfer to PhoP142 is lowered (Figure 4.20A and B). The assessment of the initial rates of PhoP and PhoP142 phosphorylation reveal that the rate of phosphorylation of PhoP142 is approximately 36% of that of PhoP (Figure 4.20C).

The single amino acid change L17I was investigated by *in vitro* phosphorylation (Figure 4.21). Purified HK 'YycG was incubated with the RRs YycF and PhoP143 to assess if these amino acid changes in PhoP increase the ability to be phosphorylated by the non-cognate HK 'YycG. An efficient and steady increase of phosphorylated YycF could be observed when incubated with 'YycG whereas PhoP142 phosphorylation only became visible after several minutes. The HK 'YycG showed efficient phosphorylation of YycF but only low ability to phosphorylate PhoP143 (Figure 4.21A). To compare the phosphotransfer reactions to both RRs, YycF~P and PhoP143 were quantified (Figure 4.21B). It is noticeable that the phosphotransfer to YycF is significantly faster over time than that to PhoP143. The latter reaction appeared to take place only slowly after 2 minutes (the third time point). In order to determine the initial rate of YycF and PhoP143 phosphorylation the slope of a trendline fitted to the linear reaction was determined. The slope for YycF phosphorylation is 0.434 compared to 0.021 for PhoP143~P. These results indicate that the amino acid change L17I by itself has only a small effect on the gain of specificity of PhoP143 for 'YycG that is about 5% (Figure 4.21C).

The loss of the ability of PhoP143 to be phosphorylated by 'PhoR was examined and compared to the phosphotransfer to the cognate RR PhoP as described above. The results are shown in Figure 4.22. A strong and efficient phosphotransfer from 'PhoR to PhoP could be observed that increased steadily over the 5 minutes reaction time. The phosphotransfer from 'PhoR to PhoP143 could also be observed even though it was substantially weaker. The phosphoimage (Figure 4.22B) was quantified and the initial rate of PhoP and PhoP143 phosphorylation by 'PhoR was evaluated as described above (Figure 4.22C). PhoP is rapidly and efficiently phosphorylated by PhoR. The

phosphotransfer to PhoP143 in contrast is not as fast and efficient. When evaluating the initial rate it is also clear that PhoP143 phosphorylation by 'PhoR reaches only 11.5% of that of PhoP (Figure 4.22C).

The RR PhoP144 (Y20F) was assessed next (Figure 4.23 and 4.24). Purified RR YycF and PhoP were incubated with the HK YycG in order to evaluate the ability of PhoP144 to be phosphorylated by 'YycG. An efficient and steady increasing phosphotransfer between wild-type pairs 'YycG and YycF could be observed over the five minute reaction time. The mutant Phop144 however did not become detectably phosphorylated by 'YycG up to five minutes (Figure 4.23A). This is also shown by the quantification of the phosphoimage (Figure 4.23B and C).

The phosphotransfer from 'PhoR to PhoP and PhoP144 (Y20F) was investigated and the results shown in Figure 4.24. The phosphoimage showed little visible difference between PhoP and PhoP144 phosphorylation (4.24A). The quantitative evaluation of the phosphoimage also showed a very similar phosphorylation profile for both RRs (Figure 4.24B) as does the initial rate (Figure 4.24C). Comparison of initial rates showed phosphorylation of PhoP144 by 'PhoR to be ~70% of that observed between PhoP and 'PhoR.

Phosphorylation of PhoP 145 (S13P L17I) by 'YycG was examined and the results are shown in Figure 4.25. It is clear that 'YycG can phosphorylate PhoP145, although to a lesser extent than phosphorylation of YycF (Figure 4.25A). Quantification of the level of phosphorylation is shown in Figure 4.25B and C. The initial rate of phosphorylation of PhoP145 by 'YycG is slower than that observed for YycF and estimated (Figure 4.25C) at approximately 16% of wild-type level.

The loss of the ability of PhoP145 to accept a phosphoryl group from 'PhoR was examined and compared to the phosphotransfer to the cognate RR PhoP as described above. The results are shown in Figure 4.26. The phosphotransfer observed from 'PhoR to PhoP was strong and efficient, increasing steadily over the first minute of reaction and a plateau was reached after 2 minutes. The phosphotransfer from 'PhoR to PhoP145, even though weaker, was observed after 30 seconds of reaction. The signal became stronger until the 5 minute timepoint. The phosphoimage was quantified (Figure 4.26B) and the initial rate of PhoP and PhoP145 phosphorylation evaluated (Figure 4.26C). The phosphotransfer from 'PhoR to PhoP is rapid and efficient. In contrast, the phosphotransfer from 'PhoR to PhoP145 in contrast is a lot less efficient and does not reach similar levels of phosphorylation as YycG. When evaluating the initial rate it is also

clear that PhoP145 phosphorylation by ϕ PhoR is only 13% of that observed for wild-type PhoP (Figure 4.26C).

Phosphorylation of PhoP146 containing two amino acid changes (S13P Y20F) by ϕ YycG was investigated. The results are shown in Figure 4.27. A steady increase of phosphorylated YycF can be observed when incubated with ϕ YycG over a time course of 5 minutes. In the first sample, taken after only 10 seconds YycF phosphorylation is visible. The mutant PhoP146 in contrast does not appear to become phosphorylated by ϕ YycG throughout the experiment. To compare the phosphotransfer reactions to both RRs YycF and PhoP146 from ϕ YycG, YycF~P and PhoP146~P were quantified (Figure 4.27B). It is noticeable that the phosphotransfer from ϕ YycG to YycF is fast and linear over the first three time points (60 seconds) before slowing down. The initial rate of the phosphorylation of YycF and PhoP146 was determined (Figure 4.27C). The slope for YycF~P phosphorylated by ϕ YycG is 0.506 compared to 0.005 phosphorylation of PhoP146. Therefore the amino acid changes in PhoP146 (S13P Y20F) do not enable it to be phosphorylated by ϕ YycG.

The loss of the ability of PhoP146 (S13P Y20F) to be phosphorylated by the cognate RR ϕ PhoR was examined and compared to the phosphotransfer between PhoR and wild-type PhoP. The results are shown in Figure 4.28. A strong efficient phosphotransfer from ϕ PhoR to PhoP and a somewhat weaker phosphorylation of PhoP146 could be observed (Figure 4.28A). The phosphoimage was quantified (Figure 4.28B) Phosphorylation of PhoP146 increased steadily over 2 minutes dropping slightly at the 20 minute time point. The phosphotransfer from ϕ PhoR to PhoP146 showed the same steady increase as seen in PhoP146~P for up to two minutes and plateaued from thereafter. However it did not quite reach the same level of phosphorylation. The initial rate of PhoP~P phosphorylation was evaluated (Figure 4.28C). PhoP is rapidly and efficiently phosphorylated by ϕ PhoR. The phosphotransfer from ϕ PhoR to PhoP146 in contrast appears similar and is ~63% as efficient as the phosphotransfer with wild-type PhoP (Figure 4.28C).

Phosphorylation of PhoP147 containing two amino acid changes (L17I Y20F) by ϕ YycG was investigated. The results are shown in Figure 4.29. A steady increase of phosphorylated YycF can be observed when incubated with ϕ YycG over a time course of 5 minutes. In the first sample, taken after only 10 seconds YycF phosphorylation is visible. The mutant PhoP147 in contrast does not appear to become phosphorylated by ϕ YycG until the 20 minute timepoint. To compare the phosphotransfer reactions to both RRs YycF

and PhoP147 from 'YycG, YycF~P and PhoP147~P were quantified (Figure 4.29B). It is noticeable that the phosphotransfer from 'YycG to YycF is fast and linear over the first three time points (60 seconds) before slowing down. The initial rate of the phosphorylation of YycF and PhoP147 was determined (Figure 4.29C). The slope for YycF~P phosphorylated by 'YycG is 0.772 compared to 0.015 phosphorylation of PhoP147. Therefore the amino acid changes in PhoP147 (L17I Y20F) have only a small effect ~2% on the ability to be phosphorylated by 'YycG.

The loss of the ability of PhoP147 (L17I Y20F) to accept a phosphoryl group from 'PhoR was examined and compared to the phosphotransfer to the cognate RR PhoP as described above. The results are shown in Figure 4.30. The phosphotransfer observed from 'PhoR to PhoP was strong and efficient, increasing steadily over the first minute of reaction and a plateau was reached after 2 minutes. The phosphotransfer from 'PhoR to PhoP147, even though weaker, was observed after 5 minutes of reaction. The signal became stronger until the 20 minute timepoint. The phosphoimage was quantified (Figure 4.30B) and the initial rate of PhoP and PhoP147 phosphorylation evaluated (Figure 4.30C). The phosphotransfer from 'PhoR to PhoP is rapid and efficient. In contrast, the phosphotransfer from 'PhoR to PhoP147 in contrast is a lot less efficient and does not reach similar levels of phosphorylation as YycG. When evaluating the initial rate it is also clear that PhoP147 phosphorylation by 'PhoR is only 3% of that observed for wild-type PhoP (Figure 4.30C).

Phosphorylation of PhoP148 containing two amino acid changes (S13P L17I Y20F) by 'YycG was investigated. The results are shown in Figure 4.31. A steady increase of phosphorylated YycF can be observed when incubated with 'YycG over a time course of 5 minutes. In the first sample, taken after only 10 seconds YycF phosphorylation is visible. The mutant PhoP148 in contrast does not appear to become phosphorylated by 'YycG until the 20 minute timepoint. To compare the phosphotransfer reactions to both RRs YycF and PhoP148 from 'YycG, YycF~P and PhoP148~P were quantified (Figure 4.31B). It is noticeable that the phosphotransfer from 'YycG to YycF is fast and linear over the first three time points (60 seconds) before slowing down. The initial rate of the phosphorylation of YycF and PhoP148 was determined (Figure 4.31C). The slope for YycF~P phosphorylated by 'YycG is 0.574 compared to a slope of 0.012 for the phosphorylation of PhoP148. Therefore the amino acid changes in PhoP148 (S13P L17I Y20F) have only a small effect ~2% on the ability to be phosphorylated by 'YycG.

The loss of the ability of PhoP148 (S13P L17I Y20F) to accept a phosphoryl group from 'PhoR was examined and compared to the phosphotransfer to the cognate RR PhoP as described above. The results are shown in Figure 4.32. The phosphotransfer observed from 'PhoR to PhoP was strong and efficient, increasing steadily over the first minute of reaction and a drop was observed after 2 minutes. The phosphotransfer from 'PhoR to PhoP148, even though weaker, was observed after 5 minutes of reaction. The signal became stronger until the 20 minute timepoint. The phosphoimage was quantified (Figure 4.32B) and the initial rate of PhoP and PhoP148 phosphorylation evaluated (Figure 4.32C). The phosphotransfer from 'PhoR to PhoP is rapid and efficient. In contrast, the phosphotransfer from 'PhoR to PhoP148 in contrast is a lot less efficient and does not reach similar levels of phosphorylation as YycG. When evaluating the initial rate it is also clear that PhoP148 phosphorylation by 'PhoR is only 7% of that observed for wild-type PhoP (Figure 4.32C).

Phosphorylation of PhoP149 containing two amino acid changes (S13P P107T) by 'YycG was investigated. The results are shown in Figure 4.33. A steady increase of phosphorylated YycF can be observed when incubated with 'YycG over a time course of 5 minutes. In the first sample, taken after only 10 seconds YycF phosphorylation is visible. The mutant PhoP149 in contrast does not appear to become phosphorylated by 'YycG until the 20 minute timepoint. To compare the phosphotransfer reactions to both RRs YycF and PhoP149 from 'YycG, YycF~P and PhoP149~P were quantified (Figure 4.33B). It is noticeable that the phosphotransfer from 'YycG to YycF is fast and linear over the first three time points (60 seconds) before slowing down. The initial rate of the phosphorylation of YycF and PhoP149 was determined (Figure 4.33C). The slope for YycF~P phosphorylated by 'YycG is 0.495 compared to 0.046 phosphorylation of PhoP149. Therefore the amino acid changes in PhoP149 (S13P P107T) allow PhoP149 phosphorylation by 'YycG at a level of ~9% as efficient as phosphorylation of YycF by 'YycG.

The loss of the ability of PhoP149 (S13P P107T) to accept a phosphoryl group from 'PhoR was examined and compared to the phosphotransfer to the cognate RR PhoP as described above. The results are shown in Figure 4.34. The phosphotransfer observed from 'PhoR to PhoP was strong and efficient, increasing steadily over the first minute of reaction and a plateau was reached after 2 minutes. The phosphotransfer from 'PhoR to PhoP149, even though a lot weaker was observed after 5 minutes of reaction. The signal did not become stronger until the 20 minute timepoint. The phosphoimage was quantified

(Figure 4.34B) and the initial rate of PhoP and PhoP149 phosphorylation evaluated (Figure 4.34C). The phosphotransfer from 'PhoR to PhoP is rapid and efficient. In contrast, the phosphotransfer from 'PhoR to PhoP149 is a lot less efficient and does not reach similar levels of phosphorylation as PhoP~P. Evaluation of the initial rates show that PhoP149 is phosphorylated by 'PhoR to a level of only 24% of that observed when PhoP is phosphorylated by 'PhoR (Figure 4.34C).

Phosphorylation of PhoP150 containing two amino acid changes (L17I P107T) by 'YycG was investigated. The results are shown in Figure 4.35. A steady increase of phosphorylated YycF can be observed when incubated with 'YycG over a time course of 5 minutes. In the first sample, taken after only 10 seconds YycF phosphorylation is visible. The mutant PhoP150 in contrast does not appear to become phosphorylated by 'YycG until the 5 minute timepoint. To compare the phosphotransfer reactions to both RRs YycF and PhoP150 from 'YycG, YycF~P and PhoP150~P were quantified (Figure 4.35B). It is noticeable that the phosphotransfer from 'YycG to YycF is fast and linear over the first three time points (60 seconds) before slowing down. The initial rate of the phosphorylation of YycF and PhoP150 was determined (Figure 4.35C). The slope for YycF~P phosphorylated by 'YycG is 0.440 compared to a slope of 0.153 for PhoP150. Therefore the amino acid changes in PhoP150 (L117I P107T) allow PhoP150 phosphorylation by 'YycG of ~35% as efficient as phosphorylation of YycF by 'YycG.

The loss of the ability of PhoP150 (L17I P107T) to accept a phosphoryl group from 'PhoR was examined and compared to the phosphotransfer to the cognate RR PhoP as described above. The results are shown in Figure 4.36. The phosphotransfer observed from 'PhoR to PhoP was strong and efficient, increasing steadily over the first minute of reaction and a drop was observed after 2 minutes. The phosphotransfer from 'PhoR to PhoP150, even though a lot weaker was observed after 5 minutes of reaction. The signal did not become stronger until the 20 minute timepoint. The phosphoimage was quantified (Figure 4.36B) and the initial rate of PhoP and PhoP150 phosphorylation evaluated (Figure 4.36C). The phosphotransfer from 'PhoR to PhoP is rapid and efficient. In contrast, the phosphotransfer from 'PhoR to PhoP150 is a lot less efficient and does not reach similar levels of phosphorylation as PhoP~P. Evaluations of the initial rates show that PhoP150 is phosphorylated by 'PhoR at a rate that is only ~6% of that observed when PhoP is phosphorylated by 'PhoR (Figure 4.36C).

Phosphorylation of PhoP151 containing two amino acid changes (Y20F P107T) by 'YycG was investigated. The results are shown in Figure 4.37. A steady increase of

phosphorylated YycF can be observed when incubated with γ -YycG over a time course of 5 minutes. In the first sample, taken after only 10 seconds YycF phosphorylation is visible. The mutant PhoP151 in contrast does not appear to become phosphorylated by γ -YycG. To compare the phosphotransfer reactions to both RRs YycF and PhoP151 from γ -YycG, YycF~P and PhoP151~P were quantified (Figure 4.37B). It is noticeable that the phosphotransfer from γ -YycG to YycF is fast and linear over the first three time points (60 seconds) before slowing down. The initial rate of the phosphorylation of YycF and PhoP151 was determined (Figure 4.37C). The slope for YycF~P phosphorylated by γ -YycG is 0.486 compared to 0 phosphorylation of PhoP151. Therefore the amino acid changes in PhoP151 (L171 P107T) did not allow phosphorylation by γ -YycG.

The loss of the ability of PhoP151 (Y20F P107T) to accept a phosphoryl group from γ -PhoR was examined and compared to the phosphotransfer to the cognate RR PhoP as described above. The results are shown in Figure 4.38. The phosphotransfer observed from γ -PhoR to PhoP was strong and efficient, increasing steadily over the first minute of reaction and a drop was observed after 2 minutes. The phosphotransfer from γ -PhoR to PhoP151, could not be observed even after 20 minutes of reaction. The phosphoimage was quantified (Figure 4.38B) and the initial rate of PhoP and PhoP151 phosphorylation evaluated (Figure 4.38C). The phosphotransfer from γ -PhoR to PhoP is rapid and efficient. In contrast, the phosphotransfer from γ -PhoR to PhoP151 is a lot less efficient and does not reach similar levels of phosphorylation as PhoP~P. Evaluation of the initial rates show that PhoP151 is phosphorylated by γ -PhoR at a rate that is only ~5% of that observed when PhoP is phosphorylated by γ -PhoR (Figure 4.38C).

Phosphorylation of PhoP152 containing three amino acid changes (S13P L171 P107T) by γ -YycG was investigated. The results are shown in Figure 4.39. A steady increase of phosphorylated YycF can be observed when incubated with γ -YycG over a time course of 5 minutes. In the first sample, taken after only 10 seconds YycF phosphorylation is visible. The mutant PhoP152 also shows an increasing phosphorylation signal over a time course of 20 minutes (Figure 4.39A). To compare the phosphotransfer reactions to both RRs YycF and PhoP151 from γ -YycG, YycF~P and PhoP151~P were quantified (Figure 4.39B). The phosphotransfer from γ -YycG to YycF is fast and linear over the first three time points (60 seconds) before slowing down. The phosphotransfer from γ -YycG to PhoP152 is also fast and linear over the first three time points even though it does not reach the same levels at wild-type. The initial rate of the phosphorylation of YycF and PhoP152 was determined (Figure 4.39C). The slope for YycF~P phosphorylated by γ -YycG

is 0.647 compared to 0.128 phosphorylation of PhoP151. Therefore the amino acid changes in PhoP152 (S13P L17I P107T) did allow PhoP151 to be phosphorylated by 'YycG to a levels of approximately 20% efficiency of that of phosphotransfer between cognate pairs.

The loss of the ability of PhoP152 (S13P L17I P107T) to accept a phosphoryl group from 'PhoR was examined and compared to the phosphotransfer to the cognate RR PhoP as described above. The results are shown in Figure 4.40. The phosphotransfer observed from 'PhoR to PhoP was strong and efficient, increasing steadily over the first minute of reaction and a drop was observed after 2 minutes. The phosphotransfer from 'PhoR to PhoP152 was observed after 1 minute of reaction. The phosphoimage was quantified (Figure 4.40B) and the initial rate of PhoP and PhoP152 phosphorylation evaluated (Figure 4.40C). The phosphotransfer from 'PhoR to PhoP is rapid and efficient. In contrast, the phosphotransfer from 'PhoR to PhoP152 is a lot less efficient and does not reach similar levels of phosphorylation as PhoP~P. Evaluation of the initial rates show that PhoP152 is phosphorylated by 'PhoR at a rate that is ~53% of that observed when PhoP is phosphorylated by 'PhoR (Figure 4.40C).

Phosphorylation of PhoP153 containing three amino acid changes (S13P Y20F P107T) by 'YycG was investigated. The results are shown in Figure 4.41. A steady increase of phosphorylated YycF can be observed when incubated with 'YycG over a time course of 5 minutes. In the first sample, taken after only 10 seconds YycF phosphorylation is visible. The mutant PhoP153 however shows no significant phosphorylation signal; a signal being visible after 20 minutes (Figure 4.41A). To compare the phosphotransfer reactions to both RRs YycF and PhoP153 from 'YycG, YycF~P and PhoP153~P were quantified (Figure 4.41B). The phosphotransfer from 'YycG to YycF is fast and linear over the first three time points (60 seconds) before slowing down. The phosphotransfer from 'YycG to PhoP153 is. The initial rate of the phosphorylation of YycF and PhoP152 was determined (Figure 4.41C). The slope for YycF~P phosphorylated by 'YycG is 0.612 compared to 0.012 phosphorylation of PhoP153. Therefore the amino acid changes in PhoP153 (S13P Y20F P107T) have only a small effect with ~2% phosphorylation by 'YycG.

The loss of the ability of PhoP153 (S13P Y20F P107T) to accept a phosphoryl group from 'PhoR was examined and compared to the phosphotransfer to the cognate RR PhoP. The results are shown in Figure 4.42. The phosphotransfer observed from 'PhoR to PhoP was strong and efficient, increasing steadily over the first minute of reaction and a

plateau was reached after 2 minutes. The phosphotransfer from 'PhoR to PhoP153 was observed after 1 minute of reaction. The phosphoimage was quantified (Figure 4.42B) and the initial rate of PhoP and PhoP153 phosphorylation evaluated (Figure 4.42C). The phosphotransfer from 'PhoR to PhoP is rapid and efficient. In contrast, the phosphotransfer from 'PhoR to PhoP153 is a lot efficient and does not reach similar levels of phosphorylation as PhoP~P. Evaluation of the initial rates show that PhoP153 is phosphorylated by 'PhoR to ~34% of that observed when PhoP is phosphorylated by 'PhoR (Figure 4.42C).

Phosphorylation of PhoP154 containing three amino acid changes (L17I Y20F P107T) by 'YycG was investigated. The results are shown in Figure 4.43. A steady increase of phosphorylated YycF can be observed when incubated with 'YycG over a time course of 5 minutes. In the first sample, taken after only 10 seconds YycF phosphorylation is visible. The mutant PhoP154 however shows a phosphorylation signal after 5 minutes (Figure 4.43A). To compare the phosphotransfer reactions to both RRs YycF and PhoP154 from 'YycG, YycF~P and PhoP154~P were quantified (Figure 4.43B). The phosphotransfer from 'YycG to YycF is fast and linear over the first three time points (60 seconds) before slowing down. The initial rate of the phosphorylation of YycF and PhoP154 was determined (Figure 4.43C). The rate for YycF~P phosphorylated by 'YycG is 0.844 compared to 0.032 phosphorylation of PhoP154. Therefore the amino acid changes in PhoP154 (L17I Y20F P107T) have only a small effect with ~4% phosphorylation by 'YycG.

The loss of the ability of PhoP154 (L17I Y20F P107T) to accept a phosphoryl group from 'PhoR was examined and compared to the phosphotransfer to the cognate RR PhoP. The results are shown in Figure 4.44. The phosphotransfer observed from 'PhoR to PhoP was strong and efficient, increasing steadily over the first minute of reaction and a drop was observed after 2 minutes. The phosphotransfer from 'PhoR to PhoP15 was observed after 2 minutes of reaction. The phosphoimage was quantified (Figure 4.44B) and the initial rate of PhoP and PhoP154 phosphorylation evaluated (Figure 4.44C). The phosphotransfer from 'PhoR to PhoP is rapid and efficient. In contrast, the phosphotransfer from 'PhoR to PhoP154 is a lot less efficient and does not reach similar levels of phosphorylation as PhoP~P. Evaluation of the initial rates show that PhoP154 is phosphorylated by 'PhoR to ~2% of that observed when PhoP is phosphorylated by 'PhoR (Figure 4.44C).

The PhoP155 protein with all four amino acid changes (S13P L17I Y20F P107T) was tested for the ability to be phosphorylated by 'YycG. The results are shown in (Figure 4.45). An efficient and steady increasing phosphotransfer between wild-type pairs 'YycG and YycF could be observed over the five minutes reaction time. The mutant PhoP155 also became phosphorylated by 'YycG which was detectable after 1 minute (Figure 4.45A). This is also shown by the quantification of the phosphoimage (Figure 4.44B) and the evaluation of the initial rate of phosphorylation (Figure 4.45C). Therefore, PhoP155 is able to receive a phosphorylate group from 'YycG at about 7% of the efficiency of YycF phosphorylation by 'YycG.

The loss of ability of PhoP155 to be phosphorylated by 'PhoR was evaluated and the results are shown in Figure 4.46. The phosphoimage revealed a significant difference between PhoP and PhoP155 phosphorylation (4.46A). PhoP became efficiently phosphorylated by 'PhoR whereas PhoP155 phosphorylation by 'PhoR could not be detected. The quantitative evaluation of the phosphoimage and determination of the initial rate also showed that PhoP155 does not appear to receive a phosphoryl group from 'PhoR (Figure 4.46B and C). This indicates that the four amino acid changes in PhoP155 (S13P L17I Y20F P107T) play a role in phosphotransfer from the cognate HK 'PhoR and at the same time allowing to accept a phosphoryl group from 'YycG.

4.4 Discussion

Phosphotransfer in cognate pairs between a HK and a RR occurs by aligning hydrophobic patches of the HK and RR in order to bring the sites of phosphorylation the histidine of the HK and the aspartate of the RR in close proximity (Varughese 2002). The residues surrounding the active site are also thought to confer specificity of interaction between a HK and a RR (Mukhopadhyay and Varughese, 2005). In the previous chapter, the interaction surface of the HK YycG was investigated in an attempt to change its specificity from its cognate RR YycF to the non-cognate RR PhoP. The studies of this chapter were initiated to investigate the other side of specificity, the interaction surface provided by the receiver domains of an RR, in this case PhoP. The structure of this highly conserved receiver domain is very similar in all RRs. Therefore, there must be distinct residues that confer specificity of interaction among cognate pairs of HKs and RRs. In this study the contribution of amino acids that vary between YycF and PhoP were evaluated for their roles in these specific interactions.

Varughese (2002) detailed three different types of amino acids on the Spo0F (model of a receiver domain) surface involved in interaction with Spo0B (model of the four helix bundle of HK proteins) and the specificity of phosphotransfer. These three groups are (i) the conserved catalytic amino acids surrounded by (ii) anchor amino acids and (iii) variable amino acids. Here, these three groups of residues were compared between YycF and PhoP. There are only four amino acids that differ in these groups. These four amino acids were changed in PhoP to match those found in YycF. One is an anchor amino acid found in the α 1-helic at position 17 where it is a leucine in PhoP and an isoleucine in YycF. Two additional residues of the α 1-helix that belong to the group of variable amino acids at position 13 and 20. At these positions PhoP has a serine (13) and a tyrosine (17) whereas YycF carries at these positions a proline (13) and a threonine (17). The fourth residue that differs between PhoP and YycF is also a variable amino acid that is a proline in PhoP at position 107 and a threonine in YycF. The amino acids at these four positions in PhoP were changed to the corresponding amino acids found at these positions in YycF to evaluate their roles in specificity and this showed that these amino acids play a role in the ability of PhoP to receive a phosphoryl group.

Mutant PhoP with all 15 combinations of these 4 amino acids was generated. The effects of these amino acid changes were investigated in three ways: *in vivo* using the system previously described to evaluate the effects (i) qualitatively and (ii) quantitatively and (iii) *in vitro* using purified proteins.

In order to avoid dephosphorylation of PhoP resulting from crosstalk with YycG and the formation of heterodimers the study was carried out in $\Delta phoPR$ strains. The *in vivo* data strongly indicates phosphorylation of some of the mutant PhoP* by 'YycG. In seven strains of the IJPR set, phosphorylation of mutant PhoP* through YycG could be observed *in vivo*, namely IJPR143, IJPR145, IJPR148, IJPR150, IJPR152, IJPR154 and IJPR155 (Results are summarized in Table 4.5). It is evident in the profiles of β -galactosidase activity in strains displaying $P_{phoA}/lacZ$ activation that the specific activity increases significantly at transition from exponential to stationary growth phase, a phenomenon that has been observed repeatedly and has also been described in Chapter 3.

In vitro phosphorylation assays were carried out with purified proteins to test (i) whether the phosphotransfer between 'YycG and PhoP* is direct and (ii) to evaluate gains in the ability of PhoP* to accept a phosphoryl group from 'YycG as well as (iii) to evaluate the reduced ability of PhoP* to be phosphorylated by the cognate 'PhoR (Results are summarized in Table 4.5).

Single amino acid changes in PhoP

Strains IJPR141 and IJPR142 containing PhoP with a single amino acid change, P107T and S13P respectively, showed very low levels of β -galactosidase activity *in vivo* (white on LB agar plates and ~20-40 units in LB broth). These amino acid changes had also a moderate effect on the increase of ability of PhoP* to be phosphorylated by 'YycG (0.007 and 2.88% respectively). At the same time, the ability of PhoP* to be phosphorylated by 'PhoR decreased to 45% and 35%. The strain IJPR144 containing PhoP with the single amino acid change Y20F led to a small increase in β -galactosidase activity *in vivo* (light blue, 90 units). However, *in vitro* little ability of PhoP144 to be phosphorylated by YycG and a modest effect on phosphorylation by the cognate PhoR was observed. Strain IJPR143 (L17I) showed a strong increase in β -galactosidase *in vivo* (deep blue on plates, 400 units in LB broth). There is an acquired ability of PhoP144 to be phosphorylated by 'YycG to a $1/20$ of the level of 'PhoR while there a concomitant decrease in recognition of PhoP144 by 'PhoR. These results show that there is a phosphotransfer from 'YycG to mutated PhoP*. They also show that some amino acid changes in PhoP lead to gains of ability to be phosphorylated by 'YycG and at the same time to a loss of ability to accept a phosphoryl group from PhoR. However, there appears to be no correlation between the gain and the loss of preference for the phosphodonor.

Two amino acid changes in PhoP

Three strains containing two amino acid changes in PhoP each, PhoP146 (S13P Y20F), PhoP147 (L17I Y20F) and PhoP151 (Y20F P107T), showed low levels of β -galactosidase activity *in vivo* (white on LB agar plates, < 100 units in LB broth). A moderate increase in the ability of PhoP* to accept a phosphoryl group from 'YycG *in vitro* was observed (0.79%, 1.95% and 0% respectively). The loss of ability to be phosphorylated by its cognate 'PhoR kinase was only mildly effect in PhoP146 but was drastically decreased for PhoP151 and PhoP147.

Strain IJPR145 contains the amino acid changes S13P and L17I and showed very high levels of β -galactosidase activity *in vivo* (very blue on plates, 1700 units in LB broth). This gain of ability to be phosphorylated by 'YycG was confirmed *in vitro* since PhoP145 reaches phosphorylation levels of ~16% of that of YycF. The loss of specificity for its cognate HK PhoR is decrease to ~13%.

Strain IJPR149 containing two amino acid changes in PhoP (S13P P107T) was white on plates and showed ~30 units of β -galactosidase activity in LB broth. In contrast, an increase of ability to be phosphorylated by 'YycG was observed *in vitro* of 9% of that of the wild-type YycF while there is a tree quarter decease in recognition by the cognate 'PhoR.

The combination of amino acid changes L17I P107T in PhoP of strain IJPR150 lead to an even higher gain of specificity for 'YycG *in vivo* (very blue on plates, 600 units in LB broth). A major increase of the ability of PhoP150 to be phosphorylated by 'YycG was observed *in vitro* with 34% of the level of YycF phosphorylation while the ability of recognition of PhoP150 by 'PhoR dropped to 5%.

Three amino acid changes in PhoP

The combinations of three amino acids changes in PhoP lead to four mutated PhoP*s, PhoP148 (S13P L17I Y20F), PhoP152 (S13P L17I P107F), PhoP153 (S13P Y20F P107F) and PhoP154 (L17I Y20F P107F).

Strains IJPR148 (S13P L17I Y20F) and PhoP154 (L17I Y20F P107F) showed blue color on LB agar plates and 460 and 245 units of β -galactosidase activity *in vivo*. However the gain of ability to be phosphorylated by 'YycG *in vitro* is 0.69% and 3.83% respectively of that of YycF. However, the loss of recognition by its cognate 'PhoR decreased to only 7% and 3% respectively.

The three amino acid changes in PhoP153 (S13P Y20F P107F) resulted in low levels of β -galactosidase activity *in vivo* (white on plates and 45 units in LB broth) and a small gain in phosphorylation by 'YycG *in vitro* (1.94%). The ability to be phosphorylated by the cognate 'PhoR dropped drastically to approximately 2% of that of wild-type of PhoP.

Very high levels of β -galactosidase activity could be observed for PhoP152 (S13P L17I P107F) *in vivo* that showed a deep blue color on plates and 1200 units of activity in LB broth. These amino acid changes allowed phosphotransfer from 'YycG at levels of ~20% phosphorylation. However, the recognition by its cognate PhoR is decreased by half.

Four amino acid changes in PhoP

The four amino acid changes in PhoP154 (S13P L17I Y20F P107F) lead to high levels of β -galactosidase activity *in vivo* (very blue on plates, 500 units in LB broth). An increase in the ability to accept a phosphoryl group from 'YycG *in vitro* of 6.55% could be observed. In contrast, the ability to be phosphorylated by its cognate HK 'PhoR is drastically decreased to 0.29%.

Interestingly, the loss of preference for PhoR and gain of ability to interact with YycG do not correlate. For example the four amino acid changes in PhoP155 lead to a greater loss of ability to accept a phosphoryl group from its cognate 'PhoR than a gain to accept the phosphorylate group from the non cognate 'YycG.

Taken together, the amino acid change leucine to isoleucine at position 17 must play a very significant role in specificity while the amino acids at the other positions play a lesser role. Nevertheless, the initial rates of phosphorylation of any mutated PhoP* does not match the rate of phosphorylation of YycF by 'YycG. This means that even though the amino acids in position 13, 17, and 107 of the receiver domain do play a role in discrimination between a cognate and non-cognate HK, these are not the only determinants. An alanine scanning analysis of Spo0F has shown that buried residues within the receiver domain subtly affect the surface structure which may explain the incomplete switch in preference (Tzeng and Hoch 1997).

When the residues investigated here are superimposed as shown in Figure 4.47 a size difference between those found in PhoP and in YycF can not be readily detected. The amino acid at position 17 is a leucine in PhoP but an isoleucine in YycF. These two amino acids are very similar with the difference of the position of a CH₃ (Figure 4.48) Therefore, it may not only size that matters but also the shape of amino acid side chains.

Taken together, the specificity of interaction between HKs and RRs has not been fully resolved but the study reported here is the first to attempt experimentally to resolve the specificity of interaction determined by the receiver domain of a RR.

Chapter 5
Conclusions

Chapter 5

Conclusions

The work presented here was initiated to assess the determinants of specificity of interaction between a HK and a RR using YycFG and PhoPR of *B.subtilis* as a model system. By changing specific amino acids within the α 1-helix of YycG and changing amino acids within the interaction surface of PhoP a change in preference was achieved for the non-cognate phosphorylation partner, resulting in phosphorylation between YycG and PhoP.

From the *in vivo* and *in vitro* data it can be concluded that the five amino acids located C-terminal of the site of phosphorylation on the α 1 helix of the HK YycG at position +3, +8, +10, +11 and +12 play a crucial role in the specificity of interaction of HK and RR. Replacing five residues in the α 1-helix of YycG with those of PhoR allowed it to interact with PhoP for phosphotransfer and subsequent activation. The side chains of these five amino acids are overall substantially bigger in YycG than in PhoR (Figure 3.) which may indicate that steric hindrance plays a role in discrimination between cognate and non-cognate partners. By replacing the larger residues in YycG with the smaller ones of PhoR, YycG may be enabled to bring the active histidine into closer proximity to the phosphoryl group accepting aspartate of PhoP. Similar to a key and lock type mechanism where the key's teeth have to have just the right size to be able to turn in the lock.

That the amino acids of the α 1-helix of the HK surrounding the phosphorylation site have a major contribution to the specificity of interaction has long been suspected. That the α 1-helix appears to be in contact with a surface provided by the RR was first indicated by docking modeling of Spo0B and Spo0F (Varughese *et al.*, 1998). This was later confirmed by co-crystallization that also implicated a common mechanism of binding of the two proteins by making contact through hydrophobic patches. These patches are formed by residues on the α 1-helix of the HK, C-terminal of the phosphorylation site and relatively conserved residues surrounding the active site of the RR (Zapf *et al.*, 2000; Hoch and Varughese, 2001; Varughese 2002; Mukhopadhyay and Varughese, 2005). Computational predictions methods have since been carried out in order to obtain information on determinants of protein-protein interaction especially with regard to specificity in TCS (White *et al.*, 2007, Surmant *et al.*, 2008). These studies detected residue clusters coupling HKs with RR on their interaction surface predicting that five of the six clusters, that localized mainly C-terminal of the α 1-helix of the HK and an the α 1 helix of the RR,

provide the docking mechanism. The sixth cluster, found N-terminal of the histidine residue on the HK and on the α 4 helix and the connecting loop with β 4 of the RR contributed further to specificity.

The study of Skerker *et al.* (2008) and the study reported here are the first attempts to validate these predictions experimentally. Both studies confirm the crucial role of the C-terminal region of the α 1-helix of a histidine kinase (EnvZ and YycG respectively) but these do not appear to be the only determinants for specificity. Changing the amino acids localized on the C-terminal region of EnvZ changed specificity from OmpR to RstA but not to other RRs. To achieve that further mutation of the α 1- α 2 helix connecting loop of the HK was also necessary. Five amino acid changes in YycG to match those found in PhoR also only partially changed preference for the non-cognate RR PhoP. The amino acid with the most dramatic effect was the single amino acid change S11G replacing the amino acid side chain CH_2OH with H whereas the other single amino acid changes had little effect on their own. This indicates that (i) spatial fit might play a role in the alignment of the kinase with its response regulator and (ii) the specificity of interaction is possible due to a combination of amino acids on the α 1-helix interaction surface - comparable with a key and lock type mechanism.

Additionally reported in this thesis are the amino acids of a RR, that are thought to play a role in specificity of interaction with a cognate kinase. Changes were made in PhoP to match YycF. Variable amino acid residues of the α 1-helix in position 13, 17 and 20 were exchanged, residues at position 13 (S13P) and 17 (L17I) are variable and so is the residue at loop 5 P107T. The fourth change was Y20F which is thought to be involved in anchoring the RR to the HK (Figure 4.2). The *in vivo* and *in vitro* results of the investigation of these four changes in PhoP singly and in combination complement each other. Amino acid changes that resulted *in vivo* in low $P_{\text{phoA-lacZ}}$ expression (*i.e.* low PhoP~P) also did not lead to a gain of phosphoryl acceptance from the non-cognate kinase YycG. In contrast, changes leading to high β -galactosidase levels *in vivo* also resulted in gain of ability to accept a phosphoryl group from YycG and loss of ability to be phosphorylated by the cognate PhoR *in vitro*. Again a single amino acid change (L17I) had a major contribution: mutant PhoP containing the L17L mutation changed specificity more significantly than the other three amino acids.

Future work

Of course, questions arise from this study that need to be further investigated. The results of the *in vitro* work indicated that YycG loses its affinity for its cognate partner but how does this effect manifest itself *in vivo*? In the course of this study two sets of strains (IJW121-131 and IJR121-131) have been established. When grown on LB agar, supplemented with X-gal, an indication of loss-of-specificity would have been a reduction in *lacZ* expression from the YycF~P-dependent *yocH* promoter and therefore a decrease of blueness of colonies (Figure 3.12). The β -galactosidase expression could not be discerned using the described *in vivo* system because the essential YycG could not be deleted to investigate the effect of the mutated YycG. Further characterization of these strains using an alternative system might help to elucidate the effects of mutated YycG* on this interaction *in vivo*.

An interesting observation was made when strains showing phosphotransfer between YycG and PhoP were grown in LB broth and P_{phoA} -*lacZ* expression was monitored. The observed β -galactosidase activity was very much induced upon entry into stationary phase. It was expected to see elevated β -galactosidase levels in exponential phase, the growth period where YycG and YycG* are active as a kinase and therefore phosphorylating the available phosphor acceptors mutant PhoP* and PhoP respectively. This indicates that P_{phoA} -*lacZ* expression is somehow suppressed in the exponential phase of growth and this is relieved during transition phase. It seems not entirely clear whether the Pho response is purely due to phosphate starvation or also to other regulatory mechanisms upon in transition phase. Nonetheless, the observed P_{phoA} -*lacZ* expression profile may be due to a transition state regulator of which AbrB appears to be a good candidate which may act on the *phoA* or *phoPR* promoter. In order to investigate the role of AbrB, strains have been developed that carry a P_{phoA} -*lacZ* or P_{phoPR} -*lacZ* fusion in a *phoPR abrB* double mutants. In a next step, the P_{xyI} YycG constructs can be introduced into these strains. If AbrB is indeed the reason for the low level of P_{phoA} -*lacZ* expression during exponential phase then this suppression should be relieved. This may result in non-viability as strains carrying cross-talking YycG constructs (e.g. in strains IJR105, IJR112, IJR114, IJR115 and IJR107) show a lytic phenotype. But strain IJR105 showed a low level of β -galactosidase activity and did lyse slower than strains like IJPR114 or IJPR107 and may be a good candidate to test for the involvement of AbrB on *phoA-lacZ* or *phoPR-lacZ*

expression during exponential growth. Additional possible regulators that may control this unusual expression profile could be also searched for with this approach.

The western blot analysis showed a substantially elevated level of YycG in strains that carry P_{xyI} -*yycG* when compared to the wild-type strain 168. It appears that the level of cellular YycG is increased by a factor of approximately 3, suggesting that there is more mutated than wild-type YycG present making the induction of the xylose promoter unnecessary. It is noteworthy that there should be a mixed population of histidine kinase dimers in the cell: (i) an excess of mutated YycG* homodimers, (ii) a few wild-type YycG homodimers and (iii) some heterodimers made of one wild-type and one mutated protomer. Whether these heterodimers are functional and what contribution they make needs to be further investigated.

During work with mutant YycG*s *in vitro*, it was notable that the autophosphorylation in these mutants was impaired. A quantification of this impairment is planned. This analysis will also give insights into the extent to which this decreased autophosphorylation influences the phosphotransfer to the non-cognate RR PhoP.

An *in vitro* analysis of the phosphatase activity of YycG might give interesting insight to its phosphatase properties and how this is affected by mutations in the catalytic domain.

Finally, new tools also emerged from this study that may be useful in further investigation of YycG essentiality and function. Firstly, a second copy of YycG has been placed under xylose control into the *B. subtilis* chromosome to allow manipulation of this gene without interfering with its essentiality. Here, it has been shown that P_{xyI} -*yycG* is expressed throughout growth leading to elevated YycG levels in the cell. Therefore it may now be possible to first mutate the *yycG* gene that is under the control of the xylose promoter and then to delete the wild-type *yycG* in order to investigate its function and essentiality. Secondly, a second copy of YycG with introduced mutations did give a signal of activity by activation P_{phoA} -*lacZ* expression. This could be used to screen for the unknown activation signal and the actual sensing region of the YycG kinase. This is because YycG* is likely to be localized at the septum as the wild-type YycG and therefore subjected to the same signals (Fukushima *et al.*, 2008). Any changes introduced either by manipulation of the sensing signal of the sensing region of the kinase could be detected by the loss of P_{phoA} -*lacZ* expression in both cases.

In summary, the specificity of interaction between a HK with a RR that allow distinction between cognate and non-cognate partners has not been fully resolved. This experimental study and that reported by Skerker *et al.*, (2008) has contributed to the understanding of the computational predictions. A complete switch in preference of a HK for a non cognate RR or the reverse, the switch of ability of a RR to accept a phosphorylate group from a non cognate HK was not achieved here. But amino acids C-terminal of the α 1-helix of HKs played a crucial role in the specificity of interaction. The loop connecting the α 1 to the α 2 helix of the HK further contributes to the specificity (Skerker *et al.*, 2008). Additionally, in RRs the interaction surface of the receiver domain that is largely provided by the α 1-helix and loop regions 4 and 5 also play a major role in discrimination of cognate and non cognate as showed here using PhoP. The remaining determinants contributing to the specificity of interaction between a HK and an RR remain to be elucidated.

References

References

- Allenby N.E., O'Connor N., Pragai Z., Ward A.C., Wipat A., Harwood C.R. (2005) Genome-wide transcriptional analysis of the phosphate starvation stimulon of *Bacillus subtilis*. *Journal of Bacteriology* **187**:8063-80
- Alm E., Huang K., Arkin A. (2006) The evolution of two-component systems in bacteria reveals different strategies for niche adaptation. *PLoS Comput Biology* **2**:e143.
- Aravin L. and Ponting C.P. (1999) The cytoplasmic helical linker domain of receptor histidine kinase and methyl-accepting proteins is common to many prokaryotic signaling proteins. *FEMS Microbiology Letters* **176**:111-116
- Birck C. Chen Y., Hulett F.M., Samama J.-P. (2003) The crystal structure of the phosphorylation domain in PhoP reveals a functional tandem association mediated by an asymmetric interface. *Journal of Bacteriology* **185**:254-261
- Birkey S.M., Liu W., Zhang X., Duggan M.F., Hulett F.M. (1998) Pho signal transduction network reveals direct transcriptional regulation of one two-component system by another two-component regulator: *Bacillus subtilis* PhoP directly regulates production of ResD. *Molecular Microbiology* **30**:943-53
- Bisicchia P., Noone D., Lioliou E., Howell A., Quigley S., Jensen T., Jarmer H., Devine K.M. (2007) The essential YycFG two-component system controls cell wall metabolism in *Bacillus subtilis*. *Molecular Microbiology* **65**:180-200.
- Bekker M., Teixeira de Mattos M.J., Hellingwerf K.J. (2006) The role of two-component regulation systems in the physiology of the bacterial cell. *Science Progress* **89**:213-42
- Birck C., Chen Y., Hulett F.M., Samama J.P. (2003) The crystal structure of the phosphorylation domain in PhoP reveals a functional tandem association mediated by an asymmetric interface. *Journal of Bacteriology* **185**:254-61.:
- Burbulys D., Trach K.A., Hoch J.A. (1991) Initiation of sporulation in *B. subtilis* is controlled by a multicomponent phosphorelay. *Cell* **64**:545-52
- Cai S.J., Inouye M. (2002) EnvZ-OmpR interaction and osmoregulation in *Escherichia coli*. *Journal of Biological Chemistry* **277**:4155-24161
- Cho H.S., Pelton J.G., Yan D., Kustu S., Wemmer D.E. (2001) Phosphoaspartates in bacterial signal transduction. *Current Opinion in Structural Biology* **11**:679-84
- Dubrac S., Boneca I.G., Poupel O., Msadek T. (2007) New insights into the WalK/WalR (YycG/YycF) essential signal transduction pathway reveal a major role in controlling cell wall metabolism and biofilm formation in *Staphylococcus aureus*. *Journal Bacteriology* **189**:8257-69
- Dutta R., Inouye M. (1996) Reverse phosphotransfer from OmpR to EnvZ in a Kinase⁻/Phosphatase⁺ Mutants of EnvZ (EnvZ-N347D), a bifunctional signal transducer of *Escherichia coli*. *Journal of Biological Chemistry* **271**: 1424-1429

- Dutta R., Qin L., Inouye M. (1999) Histidine kinases: diversity of domain organization. *Molecular Microbiology* **34**:633-40
- Eldakak A., Hulett F.M. (2007) Cys303 in the histidine kinase PhoR is crucial for the phosphotransfer reaction in the PhoPR two-component system in *Bacillus subtilis*. *Journal of Bacteriology* **189**:410-421
- Fabret C., Hoch J.A. (1998) A two-component signal transduction system essential for growth of *Bacillus subtilis*: implications for anti-infective therapy. *Journal of Bacteriology* **180**:6375-83
- Fabret C., Feher V.A., Hoch J.A. (1999) Two-component signal transduction in *Bacillus subtilis*: how one organism sees its world. *Journal of Bacteriology* **181**:1975-83
- Fisher SL, Jiang W, Wanner BL, Walsh CT. (1995) Cross-talk between the histidine protein kinase VanS and the response regulator PhoB. Characterization and identification of a VanS domain that inhibits activation of PhoB. *Journal of Biological Chemistry* **270**:23143-9
- Fukuchi K., Kasahara Y., Asai K., Kobayashi K., Moriya S., Ogasawara N. (2000) The essential two-component regulatory system encoded by *yycF* and *yycG* modulates expression of the *ftsAZ* operon in *Bacillus subtilis*. *Microbiology* **146**:1573-83.
- Fukushima T., Szurmant H., Kim E.J., Perego M., Hoch JA. (2008) A sensor histidine kinase co-ordinates cell wall architecture with cell division in *Bacillus subtilis*. *Molecular Microbiology* **69**:621-32
- Galperin M.Y. (2004) Bacterial signal transduction network in a genomic perspective. *Environmental Microbiology* 2004 **6**:552-67
- Galperin M.Y. (2005) A census of membrane-bound and intracellular signal transduction proteins in bacteria: bacterial IQ, extroverts and introverts. *BMC Microbiology* **5**:35
- Gao R., Mack T.R., Stock A.M. (2007) Bacterial response regulators: versatile regulatory strategies from common domains. *Trends in Biochemical Sciences* **32**: 225-34
- Georgellis D., Kwon O., De Wulf P., Lin E.C. (1998) Signal decay through a reverse phosphorelay in the Arc two-components signal transduction system. *Journal of Biological Chemistry* **273**:32864-32869
- Grebe T.W., Stock J.B. (1999) The histidine protein kinase superfamily. *Advances in Microbial Physiology* **41**:139-227
- Hancock L.E., Perego M. (2004) Systematic inactivation and phenotypic characterization of two-component signal transduction systems of *Enterococcus faecalis* V583. *Journal of Bacteriology* **186**:7951-8
- Harwood C.R., Cutting S.M. (1990) *Molecular Biological Methods for Bacillus*. NY: Wiley.

- Hess J.F., Bourret R.B., Oosawa K., Matsumura P., Simon M.I. (1988) Protein phosphorylation and bacterial chemotaxis. *Cold Spring Harbor Symposium Quantitative Biology* **53**:41-48
- Hoch J.A., Varughese K.I. (2001) Keeping signals straight in phosphorelay signal transduction. *Journal of Bacteriology* **183**:4941-4949
- Howell A., Dubrac S., Andersen K.K., Noone D., Fert J., Msadek T., Devine K. (2003) Genes controlled by the essential YycG/YycF two-component system of *Bacillus subtilis* revealed through a novel hybrid regulator approach. *Molecular Microbiology* **49**:1639-55.
- Howell A., Dubrac S., Noone D., Varughese K.I., Devine K. (2006) Interactions between the YycFG and PhoPR two-component systems in *Bacillus subtilis*: the PhoR kinase phosphorylates the non-cognate YycF response regulator upon phosphate limitation. *Molecular Microbiology* **59**:1199-215
- Hulett F.M., Lee J., Shi L., Sun G., Chesnut R., Sharkova E., Duggan M.F., Kapp N. (1994) Sequential action of two-component genetic switches regulates the PHO regulon in *Bacillus subtilis*. *Journal of Bacteriology* **176**:1348-58.
- Hulett F.M. (1996) The signal-transduction network for Pho regulation in *Bacillus subtilis*. *Molecular Microbiology* **19**:933-9
- Jiang M., Tzeng Y.L., Feher V.A., Perego M., Hoch J.A. (1999) Alanine mutants of the Spo0F response regulator modifying specificity for sensor kinases in sporulation initiation. *Molecular Microbiology* **33**:389-95.
- Jiang M., Weilan S., Perego M., Hoch J.A. (2000) Multiple histidine kinases regulate entry into stationary phase and sporulation in *Bacillus subtilis*. *Molecular Microbiology* **30**:535-542
- Kiil K., Ferchaud J.B., David C., Binnewies T.T., Wu H., Sicheritz-Pontén T., Willenbrock H., Ussery D.W. (2005) Genome update: distribution of two-component transduction systems in 250 bacterial genomes. *Microbiology* **151**:3447-52.
- Kim S.K., Wilmes-Riesenberg M.R., Wanner B.L. (1996) Involvement of the sensor kinase EnvZ in the in vivo activation of the response-regulator PhoB by acetyl phosphate. *Molecular Microbiology* **22**:135-47.
- Kim D., Forst S. (2001) Genomic analysis of the histidine kinase family in bacteria and archaea. *Microbiology* **147**:1197-212.
- Kobayashi K, Ogura M, Yamaguchi H, Yoshida K, Ogasawara N, Tanaka T, Fujita Y. (2001) Comprehensive DNA microarray analysis of *Bacillus subtilis* two-component regulatory systems. *Journal of Bacteriology* **83**:7365-70.
- Koretke K.K., Lupas A.N., Warren P.V., Rosenberg M., Brown J.R. (2000) Evolution of Two-Component Signal Transduction. *Molecular Biology & Evolution* **17**:1959-1970

- Kunst F., Ogasawara N., Moszer I., Albertini A.M., Alloni G., Azevedo V., Bertero M.G., Bessières P., Bolotin A., Borchert S., Borriss R., Boursier L., Brans A., Braun M., Brignell S.C., Bron S., Brouillet S., Bruschi C.V., Caldwell B., Capuano V., Carter N.M., Choi S.K., Codani J.J., Connerton I.F., Danchin A., *et al.* (1997) The complete genome sequence of the gram-positive bacterium *Bacillus subtilis*. *Nature* **390**: 249-56.
- Laemmli, U.K. (1970) Cleavage of structural proteins during the assembly of the head of bacteriophage T4. *Nature* **227**:680-685
- Laub M.T., Goulian M. (2007) Specificity in two-component signal transduction pathways. *Annual Review of Genetics* **41**:121-45.
- Liu W., Qi Y., Hulett F.M. (1998) Sites internal to the coding regions of *phoA* and *pstS* bind PhoP and are required for full promoter activity. *Molecular Microbiology* **28**:119-30.
- Loomis W.F., Kuspa A., Shaulsky G. (1998) Two-component signal transduction systems in eukaryotic microorganisms. *Current Opinion in Microbiology* **1**:643-8
- Madhusudan , Zapf J., Whiteley J.M., Hoch J.A., Xuong N.H., Varughese K.I. (1996) Crystal structure of a phosphatase-resistant mutant of sporulation response regulator Spo0F from *Bacillus subtilis*. *Structure* **15**:679-90
- Martin P.K., Li T., Sun D., Biek D.P., Schmid M.B. (1999) Role in cell permeability of an essential two-component system in *Staphylococcus aureus*. *Journal of Bacteriology* **181**:3666-73.
- Mascher T., Helmann J.D., Uden G. (2006) Stimulus perception in bacterial signal-transducing histidine kinases. *Microbiology and Molecular Biology Reviews* **70**:910-38
- Matsubara M., Mizuno T. (1999) EnvZ-independent phosphotransfer signaling pathway of the OmpR-mediated osmoregulatory expression of OmpC and OmpF in *Escherichia coli*. *Bioscience Biotechnol Biochem.* **63**:408-14.
- Matsushita M., Janda K.D. (2002) Histidine kinases as targets for new antimicrobial agents. *Bioorganic & Medicinal Chemistry* **10**:855-67
- McCleary W.R., Stock J.B., Ninfa A.J. (1993) Is acetyl phosphate a global signal in *Escherichia coli*? *Journal of Bacteriology* **175**:2793-8. Review.
- McLaughlin P.D., Bobay B.G., Regel E.J., Thompson R.J., Hoch J.A., Cavanagh J. (2007) Predominantly buried residues in the response regulator Spo0F influence specific sensor kinase recognition. *FEBS Letters* **581**:1425-9
- Miller J.H. (1972) *Experiments in molecular genetics*. Cold Spring Harbor, N.Y.: Cold Spring Harbor Laboratory
- Mizuno T., Kaneko T., Tabata S. (1996) Compilation of all genes encoding bacterial two-component signal transducers in the genome of the cyanobacterium, *Synechocystis* sp. strain PCC 6803. *DNA Research* **3**:407-14

- Mizuno T. (2005) Two-component phosphorelay signal transduction systems in plants: from hormone responses to circadian rhythms. *Biosci Biotechnol Biochem.* **69**:2263-76
- Moszer I., Jones L.M., Moreira S., Fabry C., Danchin A. (2002) SubtiList: the reference database for the *Bacillus subtilis* genome. *Nucleic Acids Research* **30**:62-5
- Mukhopadhyay D., Varughese K.I. (2005) A computational analysis on the specificity of interactions between histidine kinases and response regulators. *Journal of Biomolecular Structure & Dynamics* **22**:555-62
- Ng W.L., Robertson G.T., Kazmierczak K.M., Zhao J., Gilmour R., Winkler M.E. (2003) Constitutive expression of PcsB suppresses the requirement for the essential VicR (YycF) response regulator in *Streptococcus pneumoniae* R6. *Molecular Microbiology* **50**:1647-63
- Ng W.L., Tsui H.C., Winkler M.E. (2005) Regulation of the *pspA* virulence factor and essential *pcsB* murein biosynthetic genes by the phosphorylated VicR (YycF) response regulator in *Streptococcus pneumoniae*. *Journal of Bacteriology* **187**:7444-59
- Ninfa A.J., Ninfa E.G., Lupas A.N., Stock A., Magasanik B., Stock J. (1988) Crosstalk between bacterial chemotaxis signal transduction proteins and regulators of transcription of the Ntr regulon: evidence that nitrogen assimilation and chemotaxis are controlled by a common phosphotransfer mechanism. *Proceedings of the National Academy of Science of the United States of America* **85**:5492-6
- Parkinson J.S., Kofoed E.C. (1992) Communication modules in bacterial signaling proteins. *Annual Review of Genetics* **26**: 71-112
- Paul S., Birkey S., Liu W., Hulett F.M. (2004) Autoinduction of *Bacillus subtilis* *phoPR* operon transcription results from enhanced transcription from σ^A - and σ^E -responsive promoters by phosphorylated PhoP. *Journal of Bacteriology* **186**:4262-75
- Perego M. (2001) A new family of aspartyl phosphate phosphatases targeting the sporulation transcription factor Spo0A of *Bacillus subtilis*. *Molecular Microbiology* **42**:133-143
- Perego M., Hoch J.A. (1996) Protein aspartate phosphatases control the output of two-component signal transduction systems. *Trends in Genetics* **12**:97-101
- Ponting C.P. and Aravind L. (1997) PAS: a multifunctional domain family comes to light. *Current Biology* **7**:R674-R678
- Pragai Z., Allenby N.E., O'Connor N., Dubrac S., Rapoport G., Msadek T., Harwood C.R. (2004) Transcriptional regulation of the *phoPR* operon in *Bacillus subtilis*. *Journal of Bacteriology* **186**:1182-90
- Priest F.G. (1993) Systematics and Ecology of *Bacillus*. In *Bacillus subtilis and Other Gram -Positive Bacteri*. Sonsheim, A.L., Hoch, J.A., Losick, R. (ed) Washington, D.C.: American Society for Microbiology, pp. 3-16

- Puri-Taneja A., Paul S., Chen Y., Hulett F.M. (2006) CcpA causes repression of the *phoPR* promoter through a novel transcription start site, P(A6). *Journal of Bacteriology* **188**:1266-78
- Qi Y., Hulett F.M. (1998) Role of Pho-P in transcriptional regulation of genes involved in cell wall anionic polymer biosynthesis in *Bacillus subtilis*. *Journal of Bacteriology* **180**:4007-10
- Rodrigue A., Quentin Y., Lazdunski A., Méjean V., Foglino M. (2000) Two-component systems in *Pseudomonas aeruginosa*: why so many? *Trends in Microbiology* **8**:498-504
- Salzberg L.I., Helmann J.D. (2007) An antibiotic-inducible cell wall-associated protein that protects *Bacillus subtilis* from autolysis. *Journal of Bacteriology* **189**:4671-80
- Sambrook J., Fritsch E.F., Maniatis T. (1989) *Molecular Cloning: A Laboratory Manual*. Plainview, NY: Cold Spring Harbor Lab. Press
- Shi L., Wei L., Hulett F.M. (1999) Decay of activated *Bacillus subtilis* Pho response regulator, PhoP~P, involves the PhoR~P intermediate. *Biochemistry* **38**:10119-10125
- Silhavy J.S., Hoch J.A. (ed) (1995) *Two-Component Signal Transduction*. Washington, D.C.: American Society for Microbiology
- Silva J.C., Haldimann A., Prahalad M.K., Walsh C.T., Wanner B.L. (1998) In vivo characterization of the type A and B vancomycin-resistant enterococci (VRE) VanRS two-component systems in *Escherichia coli*: a nonpathogenic model for studying the VRE signal transduction pathways. *Proceedings of the National Academy of Sciences of the United States of America* **95**:11951-6.
- Skerker J.M., Perchuk B.S., Siryaporn A., Lubin E.A., Ashenberg O., Goulian M., Laub M.T. (2008) Rewiring the specificity of two-component signal transduction systems. *Cell* **133**:1043-54.
- Sonenshein A.L., Hoch J.A., Losick R. (ed) (1993) *Bacillus subtilis and other Gram-positive bacteria*. Washington, D.C.: ASM Press
- Sonenshein A.L., Hoch J.A., Losick R. (ed) (2002) *Bacillus subtilis and its closest relatives*. Washington, D.C.: ASM Press
- Stephenson K., Hoch J.A. (2002a) Virulence- and antibiotic resistance-associated two-component signal transduction systems of Gram-positive pathogenic bacteria as targets for antimicrobial therapy. *Pharmacology & Therapeutics* **93**:293-305. Review.
- Stephenson K., Hoch J.A. (2002b) Histidine kinase-mediated signal transduction systems of pathogenic microorganisms as targets for therapeutic intervention. *Current Drug Targets Infect Disord* **2**:235-46
- Stephenson K., Hoch J.A. (2004) Developing inhibitors to selectively target two-component and phosphorelay signal transduction systems of pathogenic microorganisms. *Current Medical Chemistry*. **11**:765-73

Stock A., Chen T., Welsh D., Stock J. (1988) CheA protein, a central regulator of bacterial chemotaxis, belongs to a family of proteins that control gene expression in response to changing environmental conditions. *Proceedings of the National Academy of Sciences of the United States of America* **85**:1403-1407

Stock A.M., Mottonen J.M., Stock J.B., Schutt C.E. (1989) Three-dimensional structure of CheY, the response regulator of bacterial chemotaxis. *Nature* **337**: 745-749

Stock A.M., Robinson V.L., Goudreau P.N. (2000) Two-component signal transduction. *Annual Review of Biochemistry* **69**:183-215

Stragier P., Losick R. (1996) Molecular genetics of sporulation in *Bacillus subtilis*. *Annual Review of Genetics* **30**:297-41. Review.

Szurmant H., Nelson K., Kim E.J., Perego M., Hoch J.A. (2005) YycH regulates the activity of the essential YycFG two-component system in *Bacillus subtilis*. *Journal of Bacteriology* **187**:5419-26

Szurmant H., Mohan M.A., Imus P.M., Hoch J.A. (2007) YycH and Yycl interact to regulate the essential YycFG two-component system in *Bacillus subtilis*. *Journal of Bacteriology* **189**:3280-9

Szurmant H., Bobay G.B., White R.A., Sullivan D.M., Thompson R.J., Hwa R., Hoch J.A., Cavanagh J. (2008a) Co-evolving motions at protein-protein interfaces of two-component signaling systems identified by covariance analysis. *Biochemistry* **47**:7782-7784

Szurmant H., Bu L., Brooks C.L. 3rd, Hoch J.A. (2008b) An essential sensor histidine kinase controlled by transmembrane helix interactions with its auxiliary proteins. *Proceedings of the National Academy of Sciences of the United States of America* **105**:5891-6

Taylor B.L. (2007) Aer on the inside looking out: paradigm for a PAS-HAMP role in sensing oxygen, redox and energy. *Molecular Microbiology*. **65**:1415-24

Taylor B.L., Zhulin I.B. (1999) PAS domains: internal sensors of oxygen, redox potential, and light. *Microbiology & Molecular Biology Reviews* **63**:479-506

Thomason P., Kay R. (2000) Eukaryotic signal transduction via histidine-aspartate phosphorelay. *Journal of Cell Science* **113**:3141-3150

Tzeng Y.L., Hoch J.A. (1997) Molecular recognition in signal transduction: the interaction surfaces of the Spo0F response regulator with its cognate phosphorelay proteins revealed by alanine scanning mutagenesis. *Journal of Molecular Biology* **272**:200-12

Varughese K.I., Madhusudan, Zhou X.Z., Whiteley J.M., Hoch J.A. (1998) Formation of a novel four-helix bundle and molecular recognition sites by dimerization of a response regulator phosphotransferase. *Molecular Cell* **2**:485-93.

Varughese K.I. (2002) Molecular recognition of bacterial phosphorelay proteins. *Current Opinion in Microbiology* **5**:142-8

- Varughese K.I., Tsigelny I., Zhao H. (2006) The crystal structure of beryllofluoride Spo0F in complex with the phosphotransferase Spo0B represents a phosphotransfer pretransition state. *Journal of Bacteriology* **188**:4970-7
- Verhamme D.T., Arents J.C., Postma P.W., Crielaard W., Hellingwerf K.J. (2002) Investigation of in vivo cross-talk between key two-component systems of *Escherichia coli*. *Microbiology* **148**:69-78
- Volz K. (1993) Structural conservation in the CheY superfamily. *Biochemistry* **32**:11741-53
- Walthers D., Tran V.K., Kenney L.J. (2003) Interdomain linkers of homologous response regulators determine their mechanism of action. *Journal of Bacteriology*. **185**:317-24
- Wang L., Fabret C., Kanamaru K., Stephenson K., Dartois V., Perego M., Hoch J.A. (2001) Dissection of the functional and structural domains of phosphorelay histidine kinase A of *Bacillus subtilis*. *Journal of Bacteriology* **183**:2795-802
- Wanner B.L. (1992) Is cross regulation by phosphorylation of two-component response regulator proteins important in bacteria? *Journal of Bacteriology* **174**:2053-8
- White R.A., Szurmant H., Hoch J.A. Hwa T. (2007) Features of protein-protein interactions in two-component signaling deduced from genomic libraries. *Methods in Enzymology* **422**: 75-101. (Chapter 4)
- Wolanin P.M, Thomason P.A., Stock J.B. (2002) Histidine protein kinases: key signal transducers outside the animal kingdom. *Genome Biology* **25**: 3(10): reviews3013.1–reviews3013.8.
- Yamamoto K., Hirao K., Oshima T., Aiba H., Utsumi R., Ishihama A. (2005) Functional characterization in vitro of all two-component signal transduction systems from *Escherichia coli*. *Journal of Biological Chemistry* **280**:1448-56
- Yoshida K., Ishio I., Nagakawa I.E., Yamamoto Y., Yamamoto M., Fujita Y. (2000) Systematic study of gene expression and transcription organization in the gntZ-ywaA region of the *Bacillus subtilis* genome. *Microbiology* **146**:573-579
- Zapf J., Madhusudan, Grimshaw C.E., Hoch J.A., Varughese K.I., Whitley J.M (1998) A source of response regulator autophosphatase activity: the critical role of a residue adjacent to the Spo0F autophosphorylation active site. *Biochemistry* **37**:7725-7732
- Zapf J., Sen U., Madhusudan, Hoch J.A., Varughese K.I. (2000) A transient interaction between two phosphorelay proteins trapped in a crystal lattice reveals the mechanism of molecular recognition and phosphotransfer in signal transduction. *Structure* **15**:851-62
- Zhang W., Shi L. (2005) Distribution and evolution of multiple-step phosphorelay in prokaryotes: lateral domain recruitment involved in the formation of hybrid-type histidine kinases. *Microbiology* **151**:2159-73
- Zhao R., Collins E.J., Bourret R.B., Silversmith R.E. (2002) Structure and catalytic mechanism of the *E.coli* chemotaxis phosphatase CheZ. *Nature Structural Biology* **9**:570-575

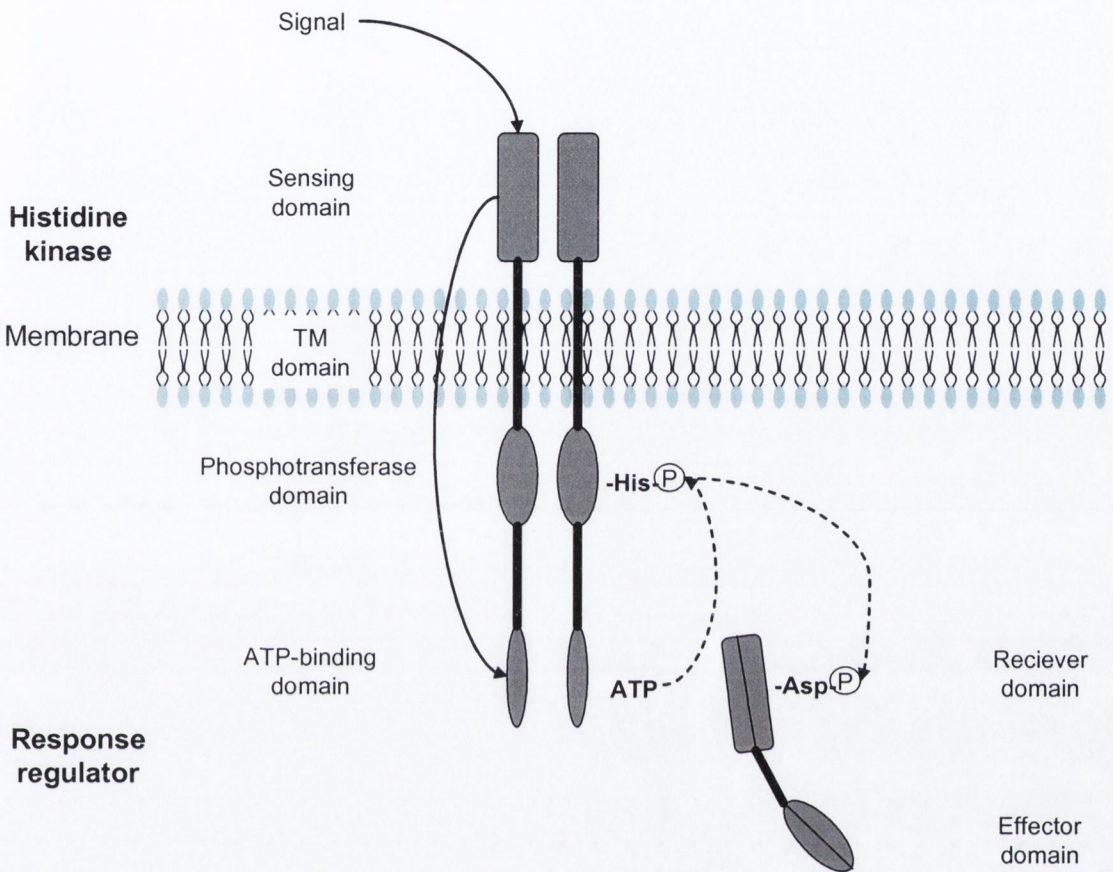


Figure 1.1 Diagram of a classic two-component system. The histidine kinase dimer is often anchored in the membrane, the domains are indicated. The signal is received by the sensing domain and mediated through the domains to the ATP-binding domain (solid arrows) inducing autophosphorylation at the conserved histidine residue. The phosphotransfer reactions are shown with broken arrows. The phosphoryl group is subsequently transferred to the conserved aspartate within the receiver domain of the response regulator (see text for details).

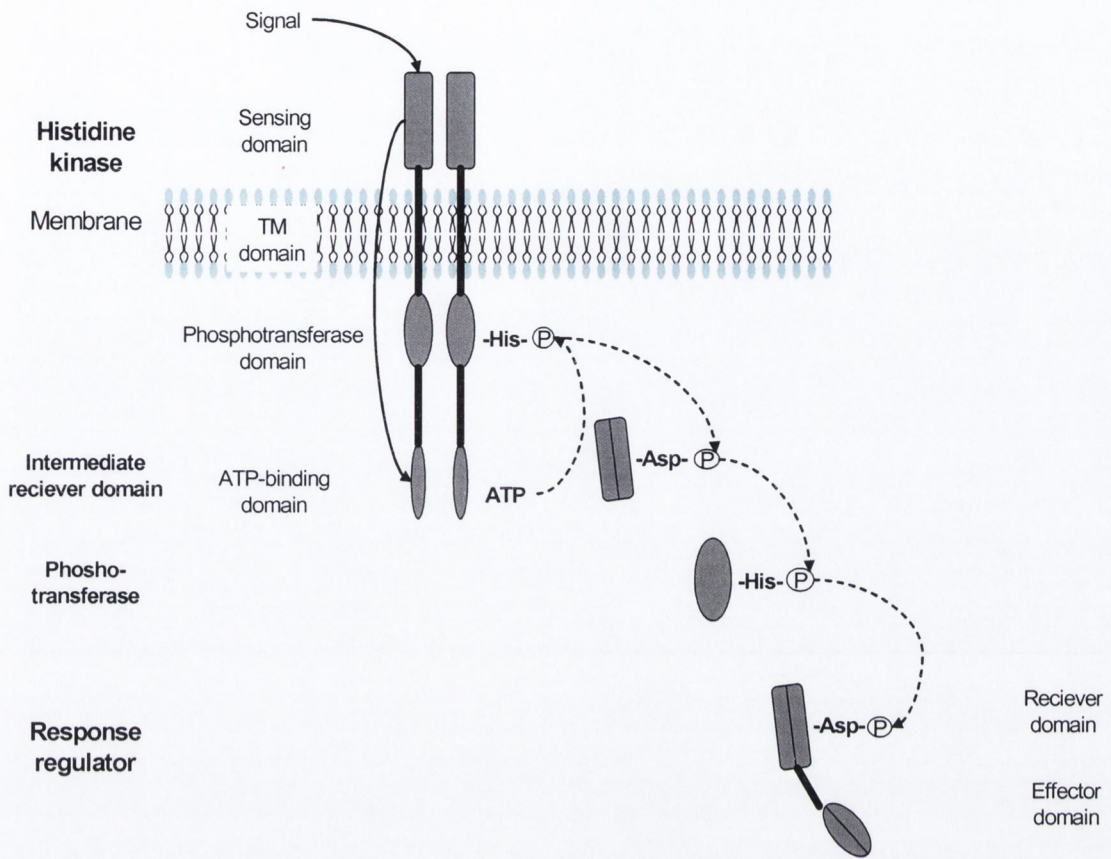


Figure 1.2 Diagram of a phosphorelay. The histidine kinase dimer is often anchored in the membrane, the domains are indicated. The signal is received by the sensing domain and mediated through the domains to the ATP-binding domain (solid arrows) inducing autophosphorylation at the conserved histidine residue. The phosphotransfer reactions are shown with broken arrows. The phosphoryl group is subsequently transferred to the conserved aspartate of the intermediate receiver, then to a histidine residue of a phosphotransferase and is finally transferred to the conserved aspartate of the receiver domain of the response regulator (see text for details).

Group I

LytS LQAQVNP~~H~~FLFNAIN~~T~~I
YesM LQAQINP~~H~~FLYNTLES~~I~~
YwpD LQSQIKP~~H~~FLYNVLNT~~I~~

} Others B

Group II

YvfT R..IARDLHDTLGH~~T~~LSL
YocF R..IARDLHDTLGQ~~K~~LSL
YxjM R..IARDIHDSIGHE~~L~~TS
YfiJ R..MAREIHDTVGH~~K~~MTA
YhcY R..LAQELHDSVNQ~~M~~LFS
YvqE R..LARDLHDAVSQ~~Q~~LFA
DegS R..VSREIH~~D~~GPAQMLAN
ComP RSG~~L~~ARDLHDSVLQ~~D~~LIS
YdfH R..MARDLHDTLAQ~~G~~LVS

} NarL

Group IV

Yf1R DLRAQTHE~~F~~SNKLYAI
YufL ALRAQSHE~~F~~MNKLHVI
YdbF ALRVQNHE~~H~~MNKLHTI
YcbA LYEETVHLK~~K~~TLKTTE

} Others A

Group IIIA

YxdK YMNQWV~~H~~QVKTPLS
YvcQ FTNQWV~~H~~HMKTPVS
YtsB ELMAWI~~H~~EVKTPLT
PhoR FVANVS~~H~~ELKTPIT
ResE FIANVS~~H~~ELRTPIS
YycG FVANVS~~H~~ELRTPLT
YclK FIADVS~~H~~ELKTPLT
YkoH FVQDAS~~H~~ELKTPLT
YvrG WIAGLS~~H~~DLKTPLS
YcbM MLTNMS~~H~~DLKTPLT
YvqB LLQNIS~~H~~DLKTPVM
YbdK LLQKLR~~H~~DINTPLT
YrkQ LVTEM~~S~~HDMRTPLT
YccG DVRSRN~~H~~DTMKHIT

} OmpR

Group IIIB

KinA LAAGIA~~H~~EIRNPLT
KinC LAAGIA~~H~~EVNRNPLT
YkrQ LAAGIA~~H~~EIRNPMT
YkvD LAASTA~~H~~EIRNPLT
KinB LAASVA~~H~~EVNRNPLT

Figure 1.3 Grouping of histidine kinases in *B.subtilis* according to Fabret et al., (1999).

The histidine kinases are sorted into five groups based on the homology of amino acid residues surrounding conserved histidine, the site of phosphorylation (H; grey).

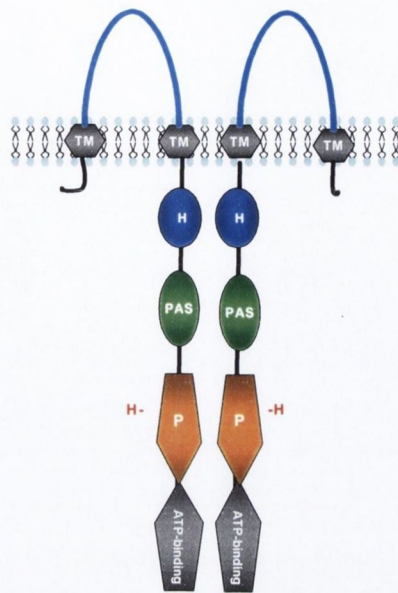


Figure 1.5 Domain structure of a histidine kinase. A histidine kinase functions as a dimer. The extracellular signal sensing domain (bright blue) is anchored by two transmembrane domains TM; grey). A linker domain often containing a HAMP (H; blue) and a PAS (PAS; green) domain. The catalytic domain is divided into a phosphotransferase (P; orange) and ATP-binding domain (ATP-binding; grey). The conserved His (H; red) is the site of phosphorylation and is found within the phosphotransferase domain.

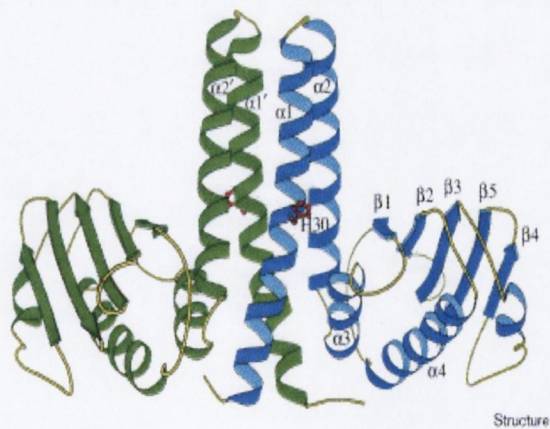


Figure 1.6 The dimerization domain of a HK. The structure of the Spo0B dimer serves as prototype of the four helix bundle formation. The N-terminal hairpin structures formed by the $\alpha 1$ and $\alpha 2$ helices of two monomers (green and blue) create the four helix bundle. The site of phosphorylation (His30) protrudes from the middle of the $\alpha 1$ helix. The C-terminal domain consists of a five stranded β -sheet and two helices $\alpha 3$ and $\alpha 4$. (from Zapf *et al.*, 2000).

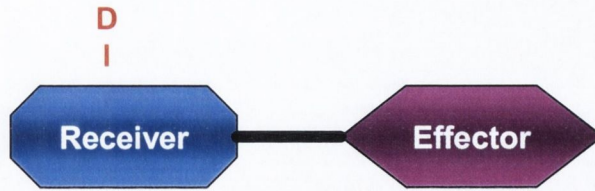


Figure 1.7 A model of the domain structure of a response regulator (RR). The receiver domain (blue) contains the conserved aspartate (D, red) which is the site of phosphorylation. A linker region (black) connects the receiver with the effector domain (purple) allows for conformational changes upon phosphorylation and therefore effects the activation state of the RR.

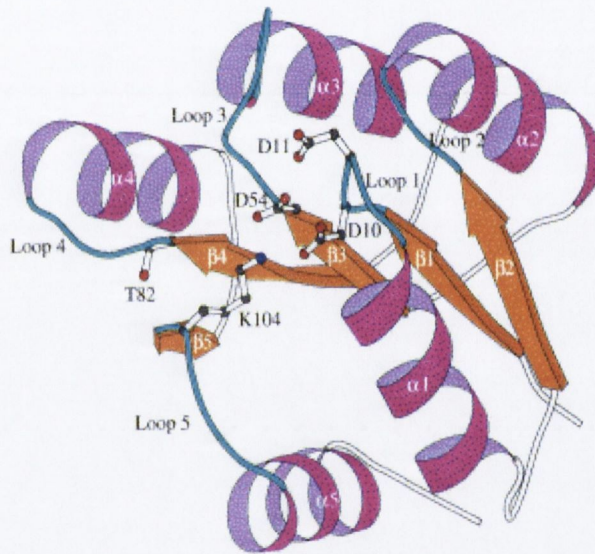


Figure 1.8 A model of the RR receiver domain. Shown here is the structure of Spo0F that serves as a model for the receiver domain of response regulators. The central β -sheet (orange) consisting of five parallel β -strands $\beta 2$, $\beta 1$, $\beta 3$, $\beta 4$, and $\beta 5$ between five α -helices (pink). Three helices ($\alpha 4$, $\alpha 3$ and $\alpha 2$) are located above and two ($\alpha 1$ and $\alpha 5$) below the β -sheet. The α -helices and β -sheets are connected by loops 1-5 (cyan). The conserved residues Asp10, Asp11, Thr82 and Lys104 that form a pocket for the active site Asp54 are indicated (from Zapf *et al.*, 2000).

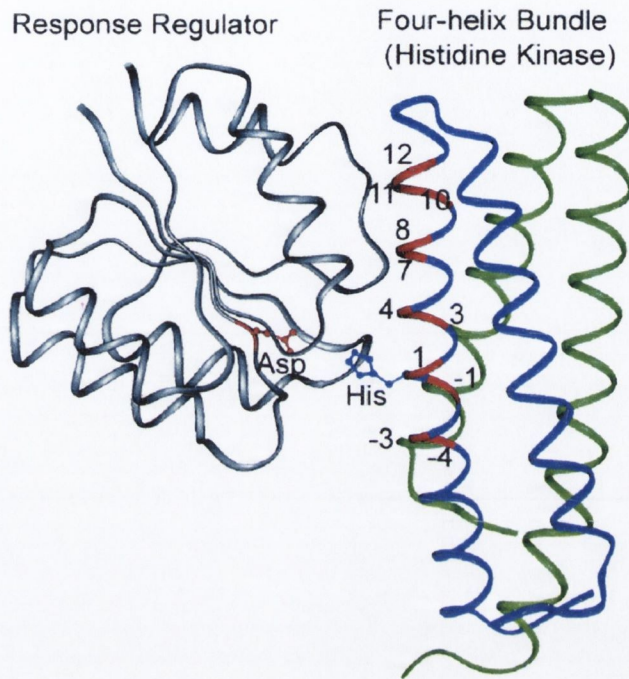


Figure 1.9 Model of the HK interacting residues of the $\alpha 1$ helix. Spo0F served as a model for the RR and its phosphorylation sites (Asp) which are shown in black. The four helix bundle which is based on the structure of Spo0B represents the HK shown in green and blue with its site of phosphorylation (His) indicated. Shown here is the interaction surface (red) of only one monomer (blue). The positions of residues involved in interaction with the RR are numbered relative to the site of phosphorylation (from Howell *et al.*, 2006).

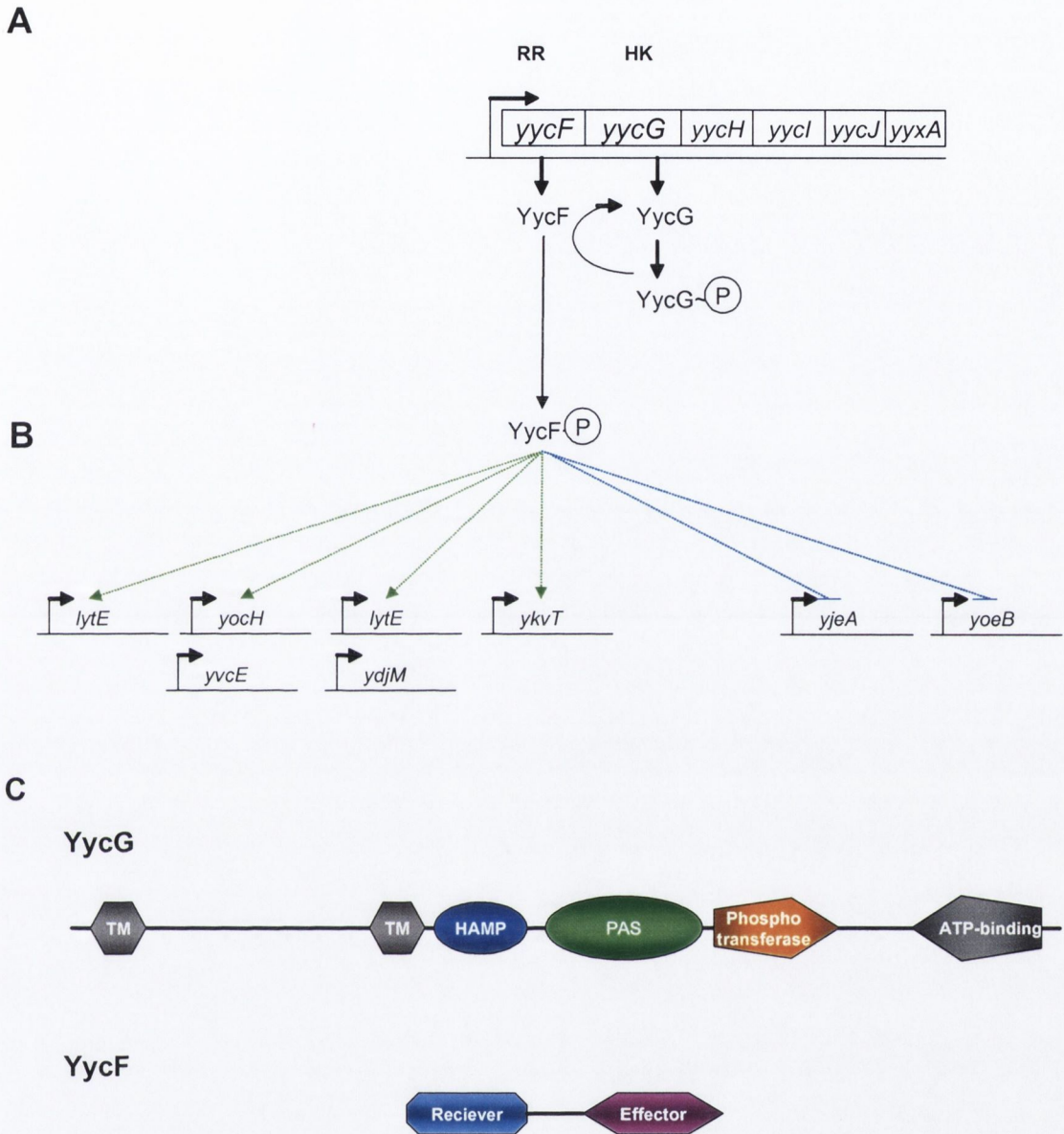


Figure 1.10 YycFG: operon organization , regulon and domain architecture.

A) Represented is the *yycFG* operon expressing the RR YycF and the HK YycG. The RR YycF is phosphorylated by the HK YycG.

B) Phosphorylated YycF~P regulates the expression of the regulon, positively (green arrows) and negatively (blue blunt lines). The arrows represent promoters.

C) Architecture of the HK YycG (top) and RR YycF (bottom), the details of each domain are described in the text (TM=transmembrane domain).

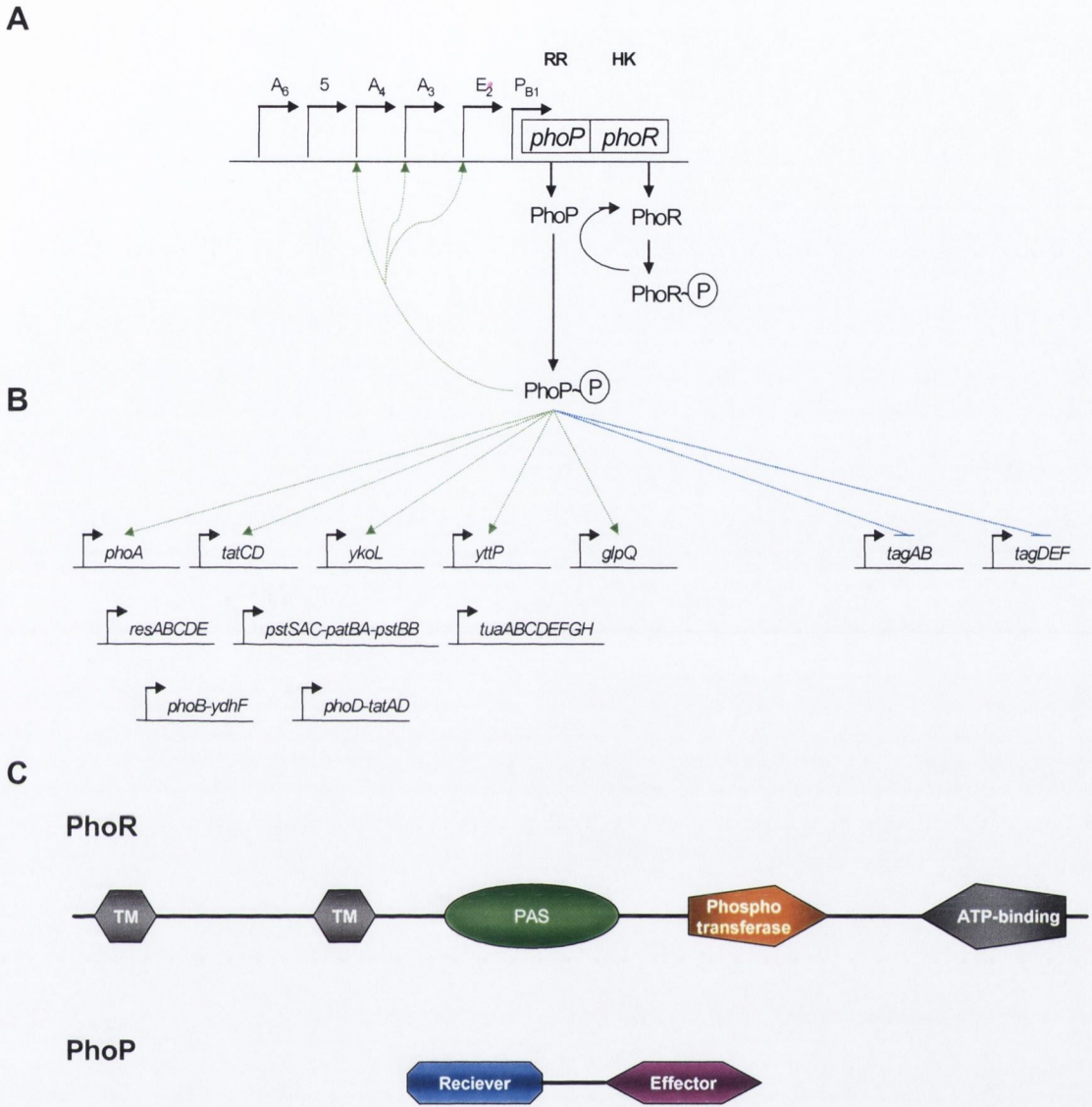


Figure 1.11 Diagram of the operon, regulon and domain structure of PhoPR.

A) Represented is the *phoPR* operon. The RR PhoP is phosphorylated by the HK PhoR.

B) Phosphorylated PhoP~P regulates the expression of the regulon, positively (green arrows) and negatively (blue blunt lines). Bent arrows represent promoters.

C) Architecture of the HK PhoR (top) and PhoP (bottom), the details are described in the text.

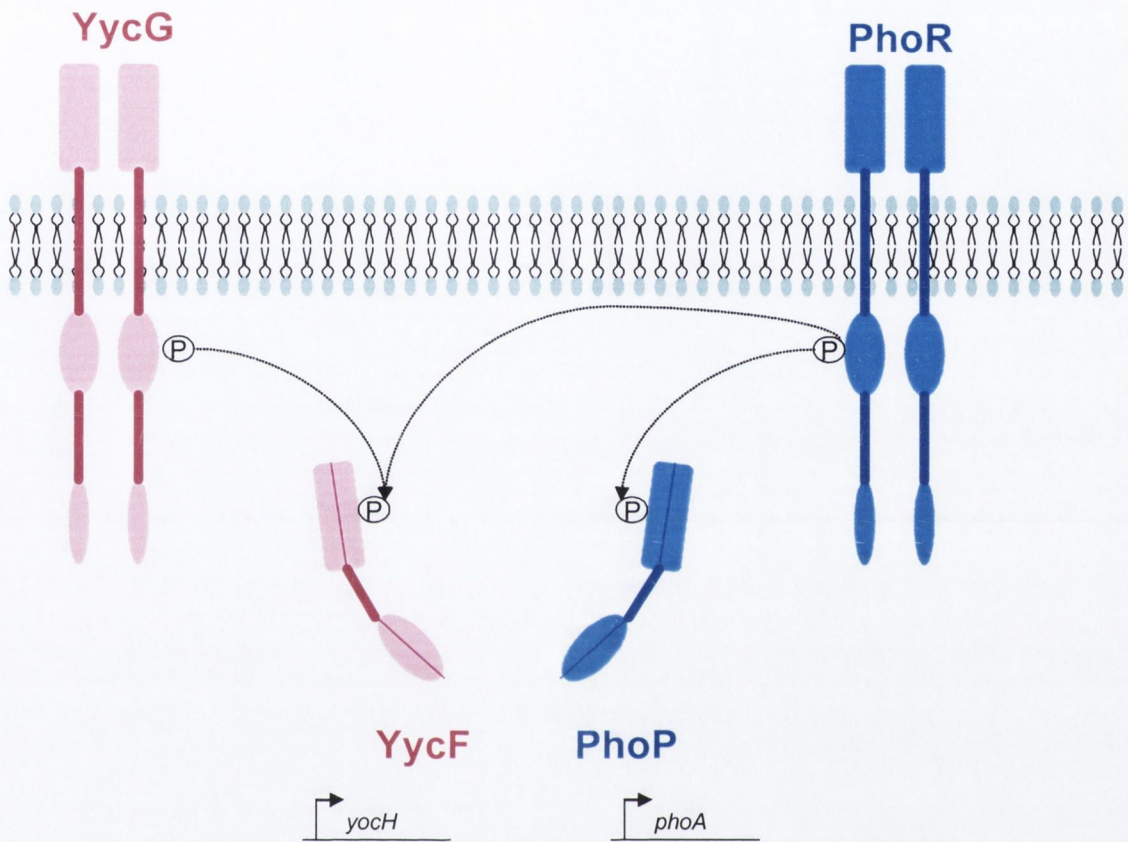


Figure 1.12 Model of phosphotransfer between YycFG and PhoPR. The two-component systems YycFG (pink) and PhoPR (blue) are shown here. Phosphotransfer (solid arrows) takes place from the HKs to their cognate RRs, i.e. from YycG to YycF and from PhoR to PhoP. Noticeably, there is also phosphotransfer between PhoR and the non-cognate RR YycF as reported in Howell *et al.*, (2003). Also shown is an example of a regulon member of each TCS: *yocH* and *phoA* which are positively regulated by phosphorylated YycF~P and PhoP~P respectively. Their expression can be used as reporters for the presence of the respective phosphorylated RR.

Table 2.1 Strains used in this study

<i>E. coli</i>		
TG1	<i>supE hsdΔ5 thi Δ(lac-proAB) F'(traD36 proAB⁺ lacI^q lacZΔ M15)</i>	Gibson (1984)
BL21(DE3)	<i>F ompT hsdS_B(r_Bm_B) gal dcm (DE3)</i>	Novagen
<i>B. subtilis</i>		
168	<i>trpC</i>	Laboratory stock
Parental strains		
AH024	<i>trpC2 ΔphoPR::erm Erm^R</i>	Howell <i>et al.</i> 2003
AH057	<i>trpC2 ΔphoR::neo Neo^R</i>	Howell <i>et al.</i> 2006
AH037	<i>trpC2 amyE::P_{yocH}-lacZ Cm^R</i>	A. Howell (unpubl. data)
IJR98	<i>trpC2 ΔphoR::neo amyE::P_{yocH}-lacZ Neo^R, Cm^R</i>	This work
IJW99	<i>trpC2 amyE::P_{phoA}-lacZ Cm^R</i>	This work
IJR99	<i>trpC2 ΔphoR::neo amyE::P_{phoA}-lacZ Cm^R, Neo^R</i>	This work
IJPR99	<i>trpC2 ΔphoPR::erm amyE::P_{phoA}-lacZ Cm^R, Erm^R</i>	This work
ΔphoR background & phoA-lacZ fusion		
IJR101	<i>trpC2 ΔphoR::neo amyE::P_{phoA}-lacZ thrC::P_{xyΓ}-yycG [H0A] Cm^R, Neo^R, Spec^R</i>	pIJ101->IJR99
IJR102	<i>trpC2 ΔphoR::neo amyE::P_{phoA}-lacZ thrC::P_{xyΓ}-yycG [R3K] Cm^R, Neo^R, Spec^R</i>	pIJ102->IJR99
IJR103	<i>trpC2 ΔphoR::neo amyE::P_{phoA}-lacZ thrC::P_{xyΓ}-yycG [T8S] Cm^R, Neo^R, Spec^R</i>	pIJ103->IJR99
IJR104	<i>trpC2 ΔphoR::neo amyE::P_{phoA}-lacZ thrC::P_{xyΓ}-yycG [R10K] Cm^R, Neo^R, Spec^R</i>	pIJ104->IJR99
IJR105	<i>trpC2 ΔphoR::neo amyE::P_{phoA}-lacZ thrC::P_{xyΓ}-yycG [S11G] Cm^R, Neo^R, Spec^R</i>	pIJ105->IJR99
IJR106	<i>trpC2 ΔphoR::neo amyE::P_{phoA}-lacZ thrC::P_{xyΓ}-yycG [Y12F] Cm^R, Neo^R, Spec^R</i>	pIJ106->IJR99
IJR107	<i>trpC2 ΔphoR::neo amyE::P_{phoA}-lacZ thrC::P_{xyΓ}-yycG [R3K T8S R10K S11G Y12F] Cm^R, Neo^R, Spec^R</i>	pIJ107->IJR99
IJR108	<i>trpC2 ΔphoR::neo amyE::P_{phoA}-lacZ thrC::P_{xyΓ}-yycG Cm^R, Neo^R, Spec^R</i>	pIJ108->IJR99
IJR112	<i>trpC2 ΔphoR::neo amyE::P_{phoA}-lacZ thrC::P_{xyΓ}-yycG [S11G Y12F] Cm^R, Neo^R, Spec^R</i>	pIJ112->IJR99
IJR114	<i>trpC2 ΔphoR::neo amyE::P_{phoA}-lacZ thrC::P_{xyΓ}-yycG [R3K T8S S11G Y12F] Cm^R, Neo^R, Spec^R</i>	pIJ114->IJR99
IJR115	<i>trpC2 ΔphoR::neo amyE::P_{phoA}-lacZ thrC::P_{xyΓ}-yycG'-phoR Cm^R, Neo^R, Spec^R</i>	pIJ115->IJR99

wildtype background & *phoA-lacZ* fusion

IJW101	<i>trpC2 amyE::P_{phoA}-lacZ thrC::P_{xyr}-yycG [H0A] Cm^R,Spec^R</i>	plJ101->IJW99
IJW102	<i>trpC2 amyE::P_{phoA}-lacZ thrC::P_{xyr}-yycG [R3K] Cm^R,Spec^R</i>	plJ102->IJW99
IJW103	<i>trpC2 amyE::P_{phoA}-lacZ thrC::P_{xyr}-yycG [T8S] Cm^R,Spec^R</i>	plJ103->IJW99
IJW104	<i>trpC2 amyE::P_{phoA}-lacZ thrC::P_{xyr}-yycG [R10K] Cm^R,Spec^R</i>	plJ104->IJW99
IJW105	<i>trpC2 amyE::P_{phoA}-lacZ thrC::P_{xyr}-yycG [S11G] Cm^R,Spec^R</i>	plJ105->IJW99
IJW106	<i>trpC2 amyE::P_{phoA}-lacZ thrC::P_{xyr}-yycG [Y12F] Cm^R,Spec^R</i>	plJ106->IJW99
IJW107	<i>trpC2 amyE::P_{phoA}-lacZ thrC::P_{xyr}-yycG [R3K T8S R10K S11G Y12F] Cm^R,Spec^R</i>	plJ107->IJW99
IJW108	<i>trpC2 amyE::P_{phoA}-lacZ thrC::P_{xyr}-yycG Cm^R,Spec^R</i>	plJ108->IJW99
IJW112	<i>trpC2 amyE::P_{phoA}-lacZ thrC::P_{xyr}-yycG [S11G Y12F] Cm^R,Spec^R</i>	plJ112->IJW99
IJW114	<i>trpC2 amyE::P_{phoA}-lacZ thrC::P_{xyr}-yycG [R3K T8S S11G Y12F] Cm^R,Spec^R</i>	plJ114->IJW99
IJW115	<i>trpC2 amyE::P_{phoA}-lacZ thrC::P_{xyr}-yycG'-<i>phoR</i> Cm^R,Spec^R</i>	plJ115->IJW99

 Δ *phoR* background & *yoch-lacZ* fusion

IJR121	<i>trpC2 ΔphoR::neo amyE::P_{yoch}-lacZ thrC::P_{xyr}-yycG [H0A] Cm^R,Neo^R,Spec^R</i>	plJ101->IJR98
IJR122	<i>trpC2 ΔphoR::neo amyE::P_{yoch}-lacZ thrC::P_{xyr}-yycG [R3K] Cm^R,Neo^R,Spec^R</i>	plJ102->IJR98
IJR123	<i>trpC2 ΔphoR::neo amyE::P_{yoch}-lacZ thrC::P_{xyr}-yycG [T8S] Cm^R,Neo^R,Spec^R</i>	plJ103->IJR98
IJR124	<i>trpC2 ΔphoR::neo amyE::P_{yoch}-lacZ thrC::P_{xyr}-yycG [R10K] Cm^R,Neo^R,Spec^R</i>	plJ104->IJR98
IJR125	<i>trpC2 ΔphoR::neo amyE::P_{yoch}-lacZ thrC::P_{xyr}-yycG [S11G] Cm^R,Neo^R,Spec^R</i>	plJ105->IJR98
IJR126	<i>trpC2 ΔphoR::neo amyE::P_{yoch}-lacZ thrC::P_{xyr}-yycG [Y12F] Cm^R,Neo^R,Spec^R</i>	plJ106->IJR98
IJR127	<i>trpC2 ΔphoR::neo amyE::P_{yoch}-lacZ thrC::P_{xyr}-yycG [R3K T8S R10K S11G Y12F] Cm^R,Neo^R,Spec^R</i>	plJ107->IJR98
IJR128	<i>trpC2 ΔphoR::neo amyE::P_{yoch}-lacZ thrC::P_{xyr}-yycG Cm^R,Neo^R,Spec^R</i>	plJ108->IJR98
IJR129	<i>trpC2 ΔphoR::neo amyE::P_{yoch}-lacZ thrC::P_{xyr}-yycG [S11G Y12F] Cm^R,Neo^R,Spec^R</i>	plJ112->IJR98
IJR131	<i>trpC2 ΔphoR::neo amyE::P_{yoch}-lacZ thrC::P_{xyr}-yycG [R3K T8S S11G Y12F] Cm^R,Neo^R,Spec^R</i>	plJ114->IJR98

wildtype background & *yoch-lacZ* fusion

IJW121	<i>trpC2 amyE::P_{yoch}-lacZ thrC::P_{xyr}-yycG [H0A] Cm^R,Spec^R</i>	plJ101->AH037
IJW122	<i>trpC2 amyE::P_{yoch}-lacZ thrC::P_{xyr}-yycG [R3K] Cm^R,Spec^R</i>	plJ102->AH037
IJW123	<i>trpC2 amyE::P_{yoch}-lacZ thrC::P_{xyr}-yycG [T8S] Cm^R,Spec^R</i>	plJ103->AH037
IJW124	<i>trpC2 amyE::P_{yoch}-lacZ thrC::P_{xyr}-yycG [R10K] Cm^R,Spec^R</i>	plJ104->AH037
IJW125	<i>trpC2 amyE::P_{yoch}-lacZ thrC::P_{xyr}-yycG [S11G] Cm^R,Spec^R</i>	plJ105->AH037

IJW126	<i>trpC2 amyE::P_{yochF}-lacZ thrC::P_{xyf}-yycG [Y12F] Cm^R,Spec^R</i>	pIJ106->AH037
IJW127	<i>trpC2 amyE::P_{yochF}-lacZ thrC::P_{xyf}-yycG [R3K T8S R10K S11G Y12F] Cm^R,Spec^R</i>	pIJ107->AH037
IJW128	<i>trpC2 amyE::P_{yochF}-lacZ thrC::P_{xyf}-yycG Cm^R,Spec^R</i>	pIJ108->AH037
IJW129	<i>trpC2 amyE::P_{yochF}-lacZ thrC::P_{xyf}-yycG [S11G Y12F] Cm^R,Spec^R</i>	pIJ112->AH037
IJW131	<i>trpC2 amyE::P_{yochF}-lacZ thrC::P_{xyf}-yycG [R3K T8S S11G Y12F] Cm^R,Spec^R</i>	pIJ114->AH037

ΔphoPR background & phoA-lacZ fusion

IJPR105	<i>trpC2 ΔphoPR::erm amyE::P_{phoA}-lacZ thrC::P_{xyf}-yycG [S11G] Cm^R,Erm^R,Spec^R</i>	AH024->IJ105
IJPR106	<i>trpC2 ΔphoPR::erm amyE::P_{phoA}-lacZ thrC::P_{xyf}-yycG [Y12F] Cm^R,Erm^R,Spec^R</i>	AH024->IJ106
IJPR107	<i>trpC2 ΔphoPR::erm amyE::P_{phoA}-lacZ thrC::P_{xyf}-yycG [R3K T8S R10K S11G Y12F] Cm^R,Erm^R,Spec^R</i>	AH024->IJ107
IJPR108	<i>trpC2 ΔphoPR::erm amyE::P_{phoA}-lacZ thrC::P_{xyf}-yycG Cm^R,Erm^R,Spec^R</i>	AH024->IJ108
IJPR112	<i>trpC2 ΔphoPR::erm amyE::P_{phoA}-lacZ thrC::P_{xyf}-yycG [S11G Y12F] Cm^R,Erm^R,Spec^R</i>	AH024->IJ112
IJPR114	<i>trpC2 ΔphoPR::erm amyE::P_{phoA}-lacZ thrC::P_{xyf}-yycG [R3K T8S S11G Y12F] Cm^R,Erm^R,Spec^R</i>	AH024->IJ114
IJPR115	<i>trpC2 ΔphoPR::erm amyE::P_{phoA}-lacZ thrC::P_{xyf}-yycG'-phoR Cm^R,Erm^R,Spec^R</i>	pIJ115->IJPR99

PhoP mutants

wild type background & phoA-lacZ fusion

IJW140	<i>trpC2 amyE::P_{phoA}-lacZ thrC::P_{xyf}-phoP Cm^R,Spec^R</i>	pIJP-> IJW99
IJW141	<i>trpC2 amyE::P_{phoA}-lacZ thrC::P_{xyf}-phoP [P107T] Cm^R,Spec^R</i>	pIJ116 -> IJW99
IJW142	<i>trpC2 amyE::P_{phoA}-lacZ thrC::P_{xyf}-phoP [S13P] Cm^R,Spec^R</i>	pIJ117 -> IJW99
IJW143	<i>trpC2 amyE::P_{phoA}-lacZ thrC::P_{xyf}-phoP [L17I] Cm^R,Spec^R</i>	pIJ118 -> IJW99
IJW144	<i>trpC2 amyE::P_{phoA}-lacZ thrC::P_{xyf}-phoP [Y20F] Cm^R,Spec^R</i>	pIJ119 -> IJW99
IJW145	<i>trpC2 amyE::P_{phoA}-lacZ thrC::P_{xyf}-phoP [S13P L17I] Cm^R,Spec^R</i>	pIJ120 -> IJW99
IJW146	<i>trpC2 amyE::P_{phoA}-lacZ thrC::P_{xyf}-phoP [S13P Y20F] Cm^R,Spec^R</i>	pIJ121 -> IJW99
IJW147	<i>trpC2 amyE::P_{phoA}-lacZ thrC::P_{xyf}-phoP [L17I Y20F] Cm^R,Spec^R</i>	pIJ122 -> IJW99
IJW148	<i>trpC2 amyE::P_{phoA}-lacZ thrC::P_{xyf}-phoP [S13P L17I Y20F] Cm^R,Spec^R</i>	pIJ123 -> IJW99
IJW149	<i>trpC2 amyE::P_{phoA}-lacZ thrC::P_{xyf}-phoP [S13P P107T] Cm^R,Spec^R</i>	pIJ117P -> IJW99
IJW150	<i>trpC2 amyE::P_{phoA}-lacZ thrC::P_{xyf}-phoP [L17I P107T] Cm^R,Spec^R</i>	pIJ118P-> IJW99
IJW151	<i>trpC2 amyE::P_{phoA}-lacZ thrC::P_{xyf}-phoP [Y20F P107T] Cm^R,Spec^R</i>	pIJ119P -> IJW99
IJW152	<i>trpC2 amyE::P_{phoA}-lacZ thrC::P_{xyf}-phoP [S13P L17I P107T] Cm^R,Spec^R</i>	pIJ120P -> IJW99

IJW153	<i>trpC2 amyE::P_{phoA}-lacZ thrC::P_{xyΓ}-phoP</i> [S13P Y20F P107T] Cm ^R ,Spec ^R	pIJ121P -> IJW99
IJW154	<i>trpC2 amyE::P_{phoA}-lacZ thrC::P_{xyΓ}-phoP</i> [L17I Y20F P107T] Cm ^R ,Spec ^R	pIJ122P -> IJW99
IJW155	<i>trpC2 amyE::P_{phoA}-lacZ thrC::P_{xyΓ}-phoP</i> [S13P L17I Y20F P107T] Cm ^R ,Spec ^R	pIJ123P -> IJW99
Δ<i>phoR</i> background & <i>phoA-lacZ</i> fusion		
IJR140	<i>trpC2 ΔphoR::neo amyE::P_{phoA}-lacZ thrC::P_{xyΓ}-phoP</i> Neo ^R ,Cm ^R ,Spec ^R	pIJP -> IJR99
IJR141	<i>trpC2 ΔphoR::neo amyE::P_{phoA}-lacZ thrC::P_{xyΓ}-phoP</i> [P107T] Neo ^R ,Cm ^R ,Spec ^R	pIJ116 -> IJR99
IJR142	<i>trpC2 ΔphoR::neo amyE::P_{phoA}-lacZ thrC::P_{xyΓ}-phoP</i> [S13P] Neo ^R ,Cm ^R ,Spec ^R	pIJ117 -> IJR99
IJR143	<i>trpC2 ΔphoR::neo amyE::P_{phoA}-lacZ thrC::P_{xyΓ}-phoP</i> [L17I] Neo ^R ,Cm ^R ,Spec ^R	pIJ118 -> IJR99
IJR144	<i>trpC2 ΔphoR::neo amyE::P_{phoA}-lacZ thrC::P_{xyΓ}-phoP</i> [Y20F] Neo ^R ,Cm ^R ,Spec ^R	pIJ119 -> IJR99
IJR145	<i>trpC2 ΔphoR::neo amyE::P_{phoA}-lacZ thrC::P_{xyΓ}-phoP</i> [S13P L17I] Neo ^R ,Cm ^R ,Spec ^R	pIJ120 -> IJR99
IJR146	<i>trpC2 ΔphoR::neo amyE::P_{phoA}-lacZ thrC::P_{xyΓ}-phoP</i> [S13P Y20F] Neo ^R ,Cm ^R ,Spec ^R	pIJ121 -> IJR99
IJR147	<i>trpC2 ΔphoR::neo amyE::P_{phoA}-lacZ thrC::P_{xyΓ}-phoP</i> [L17I Y20F] Neo ^R ,Cm ^R ,Spec ^R	pIJ122 -> IJR99
IJR148	<i>trpC2 ΔphoR::neo amyE::P_{phoA}-lacZ thrC::P_{xyΓ}-phoP</i> [S13P L17I Y20F] Neo ^R ,Cm ^R ,Spec ^R	pIJ123 -> IJR99
IJR149	<i>trpC2 ΔphoR::neo amyE::P_{phoA}-lacZ thrC::P_{xyΓ}-phoP</i> [S13P P107T] Neo ^R ,Cm ^R ,Spec ^R	pIJ117P -> IJR99
IJR150	<i>trpC2 ΔphoR::neo amyE::P_{phoA}-lacZ thrC::P_{xyΓ}-phoP</i> [L17I P107T] Neo ^R ,Cm ^R ,Spec ^R	pIJ118P -> IJR99
IJR151	<i>trpC2 ΔphoR::neo amyE::P_{phoA}-lacZ thrC::P_{xyΓ}-phoP</i> [Y20F P107T] Neo ^R ,Cm ^R ,Spec ^R	pIJ119P -> IJR99
IJR152	<i>trpC2 ΔphoR::neo amyE::P_{phoA}-lacZ thrC::P_{xyΓ}-phoP</i> [S13P L17I P107T] Neo ^R ,Cm ^R ,Spec ^R	pIJ120P -> IJR99
IJR153	<i>trpC2 ΔphoR::neo amyE::P_{phoA}-lacZ thrC::P_{xyΓ}-phoP</i> [S13P Y20F P107T] Neo ^R ,Cm ^R ,Spec ^R	pIJ121P -> IJR99
IJR154	<i>trpC2 ΔphoR::neo amyE::P_{phoA}-lacZ thrC::P_{xyΓ}-phoP</i> [L17I Y20F P107T] Neo ^R ,Cm ^R ,Spec ^R	pIJ122P -> IJR99
IJR155	<i>trpC2 ΔphoR::neo amyE::P_{phoA}-lacZ thrC::P_{xyΓ}-phoP</i> [S13P L17I Y20F P107T] Neo ^R ,Cm ^R ,Spec ^R	pIJ123P -> IJR99
Δ<i>phoPR</i> background & <i>phoA-lacZ</i> fusion		
IJPR140	<i>trpC2 ΔphoPR::erm amyE::P_{phoA}-lacZ thrC::P_{xyΓ}-phoP</i> Erm ^R ,Cm ^R ,Spec ^R	pIJP -> IJPR99
IJPR141	<i>trpC2 ΔphoPR::erm amyE::P_{phoA}-lacZ thrC::P_{xyΓ}-phoP</i> [P107T] Erm ^R ,Cm ^R ,Spec ^R	pIJ116 -> IJPR99
IJPR142	<i>trpC2 ΔphoPR::erm amyE::P_{phoA}-lacZ thrC::P_{xyΓ}-phoP</i> [S13P] Erm ^R ,Cm ^R ,Spec ^R	pIJ117 -> IJPR99
IJPR143	<i>trpC2 ΔphoPR::erm amyE::P_{phoA}-lacZ thrC::P_{xyΓ}-phoP</i> [L17I] Erm ^R ,Cm ^R ,Spec ^R	pIJ118 -> IJPR99
IJPR144	<i>trpC2 ΔphoPR::erm amyE::P_{phoA}-lacZ thrC::P_{xyΓ}-phoP</i> [Y20F] Erm ^R ,Cm ^R ,Spec ^R	pIJ119 -> IJPR99
IJPR145	<i>trpC2 ΔphoPR::erm amyE::P_{phoA}-lacZ thrC::P_{xyΓ}-phoP</i> [S13P L17I] Erm ^R ,Cm ^R ,Spec ^R	pIJ120 -> IJPR99
IJPR146	<i>trpC2 ΔphoPR::erm amyE::P_{phoA}-lacZ thrC::P_{xyΓ}-phoP</i> [S13P Y20F] Erm ^R ,Cm ^R ,Spec ^R	pIJ121 -> IJPR99
IJPR147	<i>trpC2 ΔphoPR::erm amyE::P_{phoA}-lacZ thrC::P_{xyΓ}-phoP</i> [L17I Y20F] Erm ^R ,Cm ^R ,Spec ^R	pIJ122 -> IJPR99

IJPR148	<i>trpC2</i> Δ <i>phoPR</i> ::erm <i>amyE</i> ::P _{phoA} - <i>lacZ</i> <i>thrC</i> ::P _{xyI} - <i>phoP</i> [S13P L17I Y20F] Erm ^R ,Cm ^R ,Spec ^R	pIJ123 -> IJPR99
IJPR149	<i>trpC2</i> Δ <i>phoPR</i> ::erm <i>amyE</i> ::P _{phoA} - <i>lacZ</i> <i>thrC</i> ::P _{xyI} - <i>phoP</i> [S13P P107T] Erm ^R ,Cm ^R ,Spec ^R	pIJ117P -> IJPR99
IJPR150	<i>trpC2</i> Δ <i>phoPR</i> ::erm <i>amyE</i> ::P _{phoA} - <i>lacZ</i> <i>thrC</i> ::P _{xyI} - <i>phoP</i> [L17I P107T] Erm ^R ,Cm ^R ,Spec ^R	pIJ118P -> IJPR99
IJPR151	<i>trpC2</i> Δ <i>phoPR</i> ::erm <i>amyE</i> ::P _{phoA} - <i>lacZ</i> <i>thrC</i> ::P _{xyI} - <i>phoP</i> [Y20F P107T] Erm ^R ,Cm ^R ,Spec ^R	pIJ119P -> IJPR99
IJPR152	<i>trpC2</i> Δ <i>phoPR</i> ::erm <i>amyE</i> ::P _{phoA} - <i>lacZ</i> <i>thrC</i> ::P _{xyI} - <i>phoP</i> [S13P L17I P107T] Erm ^R ,Cm ^R ,Spec ^R	pIJ120P -> IJPR99
IJPR153	<i>trpC2</i> Δ <i>phoPR</i> ::erm <i>amyE</i> ::P _{phoA} - <i>lacZ</i> <i>thrC</i> ::P _{xyI} - <i>phoP</i> [S13P Y20F P107T] Erm ^R ,Cm ^R ,Spec ^R	pIJ121P -> IJPR99
IJPR154	<i>trpC2</i> Δ <i>phoPR</i> ::erm <i>amyE</i> ::P _{phoA} - <i>lacZ</i> <i>thrC</i> ::P _{xyI} - <i>phoP</i> [L17I Y20F P107T] Erm ^R ,Cm ^R ,Spec ^R	pIJ122P -> IJPR99
IJPR155	<i>trpC2</i> Δ <i>phoPR</i> ::erm <i>amyE</i> ::P _{phoA} - <i>lacZ</i> <i>thrC</i> ::P _{xyI} - <i>phoP</i> [S13P L17I Y20F P107T] Erm ^R ,Cm ^R ,Spec ^R	pIJ123P -> IJPR99

Table 2.2 Plasmids used in this study

pXT	Vector enabling single copy gene expression under inducible control of the <i>B.subtilis xylA</i> promoter and integration at the <i>thrC</i> locus, Spec ^R , Erm ^R	Derre <i>et al.</i> (2000)
pDG268	Vector for insertion of transcriptional <i>lacZ</i> -fusions into the <i>B.subtilis amyE</i> locus Cm ^R , Amp ^R	Antoniewski <i>et al.</i> 1990
pET21b	Vector for overexpressing His-tagged proteins using a T7 bacteriophage promoter in <i>E.coli</i> , Amp ^R	Novagen
pET21d	Vector for overexpressing His-tagged proteins using a T7 bacteriophage promoter in <i>E.coli</i> , Amp ^R	Novagen
pbluescriptII KS-	Cloning vector allowing blue/white screening, Amp ^R	Stratagene
pIJ99	Vector for insertion of transcriptional <i>phoA-lacZ</i> -fusions into the <i>B.subtilis amyE</i> locus Cm ^R , Amp ^R phoA (425 bp) -160 to +248 inserted on EcoRI / BamHI	This work
pIJ100	Based on pXT, insert of <i>yycG</i> (1140 bp) into blunt ended EcoRI	This work
pKSWT	Based on pKS, insert of <i>yycG</i> (706 bp) inserted on EcoRI / SphI	This work
pKSHis	Based on pKS, insert of <i>yycG</i> (706 bp; H0A) inserted on EcoRI / SphI	This work
pKS1	Based on pKS, insert of <i>yycG</i> (706 bp; R3K) inserted on EcoRI / SphI	This work
pKS2	Based on pKS, insert of <i>yycG</i> (706 bp; T8S) inserted on EcoRI / SphI	This work
pKS3	Based on pKS, insert of <i>yycG</i> (706 bp; R10K) inserted on EcoRI / SphI	This work
pKS4	Based on pKS, insert of <i>yycG</i> (706 bp; S11G) inserted on EcoRI / SphI	This work
pKS5	Based on pKS, insert of <i>yycG</i> (706 bp; Y12F) inserted on EcoRI / SphI	This work
pKS5x	Based on pKS, insert of <i>yycG</i> (706 bp; R3k, T8S, R10K, S11G, Y12F) inserted on EcoRI / SphI	This work
pIJ101	pIJ100 with insert of <i>yycG</i> fragment recovered from pKSHis on EcoRI / SphI; Spec ^R , Erm ^R	This work
pIJ102	pIJ100 with insert of <i>yycG</i> fragment recovered from pKS1 on EcoRI / SphI; Spec ^R , Erm ^R	This work
pIJ103	pIJ100 with insert of <i>yycG</i> fragment recovered from pKS2 on EcoRI / SphI; Spec ^R , Erm ^R	This work
pIJ104	pIJ100 with insert of <i>yycG</i> fragment recovered from pKS3 on EcoRI / SphI; Spec ^R , Erm ^R	This work
pIJ105	pIJ100 with insert of <i>yycG</i> fragment recovered from pKS4 on EcoRI / SphI; Spec ^R , Erm ^R	This work
pIJ106	pIJ100 with insert of <i>yycG</i> fragment recovered from pKS5 on EcoRI / SphI; Spec ^R , Erm ^R	This work
pIJ107	pIJ100 with insert of <i>yycG</i> fragment recovered from pKS5x on EcoRI / SphI; Spec ^R , Erm ^R	This work
pIJ108	pIJ100 with insert of <i>yycG</i> fragment recovered from pKSWT on EcoRI / SphI; Spec ^R , Erm ^R	This work
pIJ112	pIJ108 with 310 bps fragment exchanged between EcoRI/BglIII; Spec ^R , Erm ^R	This work
pIJ114	pIJ108 with 310 bps fragment exchanged between EcoRI/BglIII, Spec ^R , Erm ^R	This work
pIJ115	Based on pXT, containing the hybrid insert of <i>yycG</i> '-phoR [(M1-E71)(E346-A579) kinase gene, Spec ^R , Erm ^R	This work
pKSP	pKS ⁻ with insert of <i>phoP</i> including upstream restriction sites BamHI/NdeI and downstream XhoI/HindIII	This work
pKS116	PCR generated from pKSP with the amino acid change in PhoP [P107T]	This work

pKS117	PCR generated from pKSP with the amino acid change in PhoP [S13P]	This work
pKS118	PCR generated from pKSP with the amino acid change in PhoP [L17I]	This work
pKS119	PCR generated from pKSP with the amino acid change in PhoP [Y20F]	This work
pKS120	PCR generated from pKSP with the amino acid change in PhoP [S13P L17I]	This work
pKS121	PCR generated from pKSP with the amino acid change in PhoP [S13P Y20F]	This work
pKS122	PCR generated from pKSP with the amino acid change in PhoP [L17I Y20F]	This work
pKS123	PCR generated from pKSP with the amino acid change in PhoP [S13P L17I Y20F]	This work
pKS117P	PCR generated from pKS116 with the amino acid change in PhoP [S13P]	This work
pKS118P	PCR generated from pKS116 with the amino acid change in PhoP [L17I]	This work
pKS119P	PCR generated from pK116 with the amino acid change in PhoP [Y20F]	This work
pKS120P	PCR generated from pK116 with the amino acid change in PhoP [S13P L17I]	This work
pKS121P	PCR generated from pK116 with the amino acid change in PhoP [S13P Y20F]	This work
pKS122P	PCR generated from pKS116 with the amino acid change in PhoP [L17I Y20F]	This work
pKS123P	PCR generated from pKS116 with the amino acid change in PhoP [S13P L17I Y20F]	This work
pIJ116	pXT with PhoP recovered from pJJKS116 [P107T] on BamHI/HindIII	This work
pIJ117	pXT with PhoP recovered from pJJKS117 [S13P] on BamHI/HindIII	This work
pIJ118	pXT with PhoP recovered from pJJKS118 [L17I] on BamHI/HindIII	This work
pIJ119	pXT with PhoP recovered from pJJKS119 [Y20F] on BamHI/HindIII	This work
pIJ120	pXT with PhoP recovered from pJJKS120 [S13P L17I] on BamHI/HindIII	This work
pIJ121	pXT with PhoP recovered from pJJKS121 [S13P Y20F] on BamHI/HindIII	This work
pIJ122	pXT with PhoP recovered from pJJKS122 [L17I Y20F] on BamHI/HindIII	This work
pIJ123	pXT with PhoP recovered from pJJKS123 [S13P L17I Y20F] on BamHI/HindIII	This work
pIJ117P	pXT with PhoP recovered from pJJKS117P [S13P P107T] on BamHI/HindIII	This work
pIJ118P	pXT with PhoP recovered from pJJKS118P [L17I P107T] on BamHI/HindIII	This work
pIJ119P	pXT with PhoP recovered from pJJKS119P [Y20F P107T] on BamHI/HindIII	This work
pIJ120P	pXT with PhoP recovered from pJJKS120P [S13P L17I P107T] on BamHI/HindIII	This work
pIJ121P	pXT with PhoP recovered from pJJKS121P [S13P Y20F P107T] on BamHI/HindIII	This work
pIJ122P	pXT with PhoP recovered from pJJKS122P [L17I Y20F P107T] on BamHI/HindIII	This work
pIJ123P	pXT with PhoP recovered from pJJKS123P [S13P L17I Y20F P107T] on BamHI/HindIII	This work
pET116	pET21b with PhoP recovered from pJJKS116 [P107T] on NdeI/XhoI	This work
pET117	pET21b with PhoP recovered from pJJKS117 [S13P] on NdeI/XhoI	This work
pET118	pET21b with PhoP recovered from pJJKS118 [L17I] on NdeI/XhoI	This work
pET119	pET21b with PhoP recovered from pJJKS119 [Y20F] on NdeI/XhoI	This work
pET120	pET21b with PhoP recovered from pJJKS120 [S13P L17I] on NdeI/XhoI	This work
pET121	pET21b with PhoP recovered from pJJKS121 [S13P Y20F] on NdeI/XhoI	This work

pET122	pET21b with PhoP recovered from pLJKS122 [L17I Y20F] on NdeI/XhoI	This work
pET123	pET21b with PhoP recovered from pLJKS123 [S13P L17I Y20F] on NdeI/XhoI	This work
pET117P	pET21b with PhoP recovered from pLJKS117P [S13F P107T] on NdeI/XhoI	This work
pET118P	pET21b with PhoP recovered from pLJKS118P [L17I P107T] on NdeI/XhoI	This work
pET119P	pET21b with PhoP recovered from pLJKS119P [Y20F P107T] on NdeI/XhoI	This work
pET120P	pET21b with PhoP recovered from pLJKS120P [S13P L17I P107T] on NdeI/XhoI	This work
pET121P	pET21b with PhoP recovered from pLJKS121P [S13P Y20F P107T] on NdeI/XhoI	This work
pET122P	pET21b with PhoP recovered from pLJKS122P [L17I Y20F P107T] on NdeI/XhoI	This work
pET123P	pET21b with PhoP recovered from pLJKS123P [S13P L17I Y20F P107T] on NdeI/XhoI	This work
pETYycG	pET21b derivative for overproduction of 'YycG	This work
pET105	pET21b derivative for overproduction of 'YycG105	This work
pET112	pET21b derivative for overproduction of 'YycG112	This work
pET114	pET21b derivative for overproduction of 'YycG114	This work
pET107	pET21b derivative for overproduction of 'YycG107	This work
pETDN1100	pET21b derivative for overproduction of YycF	Howell <i>et al.</i> (2006)
pETDN1103	pET21d derivative for overproduction of 'PhoR	D.Noon (unpubl. data)

Table 2.3 Oligonucleotides used in this study

PIJ99F-(EcoRI)-CGGAATTCATGCAAAAGACAGAGAGG	
PIJ99R-(BamHI)-CGGGATCCAACCTCGGGTATTCCGG	
PIJ100F-(Sall)-ACGGCTCGACAAAGAGGTAAATCAAAATGAATAAGGTTGGTTTTTTTTTCGGTCCG	
PIJ100R-(SphI/EcoRI)-ACATGCATGCATGTCGGGAATTCCTCGCTCCTGATCC	
PIJ101F-(EcoRI)-CAGAGAAATTCGTTGCCAATGTATCAGCTGAGCTGCCG	
PIJ102F-(EcoRI)-CAGAGAAATTCGTTGCCAATGTATCAGCTGAGCTGAAAACGCCCGC	
PIJ103F-(EcoRI)-CAGAGAAATTCGTTGCCAATGTATCAGCTGAGCTGCGGACGCCCGCTTACGTCTATGCCGACG	
PIJ104F-(EcoRI)-CAGAGAAATTCGTTGCCAATGTATCAGCTGAGCTGCGGACGCCCGCTTACGACAATGAAAAGCTATTTAGAAAGCG	
PIJ105F-(EcoRI)-CAGAGAAATTCGTTGCCAATGTATCAGCTGAGCTGCGGACGCCCGCTTACGACAATGCGCGGTTATTTAGAAAGCG	
PIJ106F-(EcoRI)-CAGAGAAATTCGTTGCCAATGTATCAGCTGAGCTGCGGACGCCCGCTTACGACAATGCGCAGCTTCTTTAGAAAGCG	
PIJ107F-(EcoRI)-CAGAGAAATTCGTTGCCAATGTATCAGCTGAGCTGAGCTGAAAACGCCCGCTTACGTCTATGAAAAGGTTTTCTTTAGAAAGCG	
PIJ108F-(EcoRI)-CAGAGAAATTCGTTGCCAATGTATCAGCTGAGCTGAGCTGAAAACGCCCGCTTACGTCTATGAAAAGGTTTTCTTTAGAAAGCG	
PIJ101R-(SphI)-ACATGCATGCTCACGCTTCATCCCAATCATCC	
PIJ112F-(EcoRI)-CAGAGAAATTCGTTGCCAATGTATCAGCTGAGCTGCGGACGCCCGCTTACGACAATGCGCGGTTTTCTTTAGAAAGCG	
PIJ113F-(EcoRI)-CAGAGAAATTCGTTGCCAATGTATCAGCTGAGCTGAAAACGCCCGCTTACGACAATGCGCGGTTTTCTTTAGAAAGCG	
PIJ114F-(EcoRI)-CAGAGAAATTCGTTGCCAATGTATCAGCTGAGCTGAAAACGCCCGCTTACGTCTATGCGCGGTTTTCTTTAGAAAGCG	
PIJ112R-(BglII)-GAAGATCTCTGTCCGGCAGATTGCGGATAAAC	
P1 amy1-GCTCGGGGCTGTATGACTGG	
P2 amy2-CGTATCATGCGGACTCTACCC	
Sequencing primers	
(forward)	
PIJ100.I-CGTTGTCCGGAGTATGG	
PIJ100.II-GAAGATTTAGTGGAACACGC	
PIJ100.III-CAGCATGTGGAGTTTATCC	
(reverse)	
PIJ100.IV-GCAACACCCGGTCGACGGG	
PIJ100.IV Re-CGTTGTGGCCAGCTGCC	
PIJ100.V Re-GCTTTGAAGAACCAGCCAC	
pXT primers	
pXT seq-TTGCCCTTGTCAACTCAGTC	
pXTL-CAACAAACTAATAGGTGATG	
pXTR-CCAGTCACGTTACGTTATTAG	

Table 2.4 Amino acid changes introduced into YycG

Strain	Amino acid change	Mutation Number	Positions on the α 1 helix
IJ101	His->Ala	Histidine	H0A
IJ102	Arg->Lys	Single	R3K
IJ103	Thr->Ser	Single	T8S
IJ104	Arg->Lys	Single	R10K
IJ105	Ser->Gly	Single	S11G
IJ106	Tyr->Phe	Single	Y12F
IJ107	Arg->Lys Thr->Ser Arg->Lys Ser->Gly Tyr->Phe	Quintuple	R3K T8S R10K S11G Y12F
IJ108		Reconstituted wt	
IJ112	Ser->Gly Tyr->Phe	Double	S11G Y12F
IJ114	Arg->Lys Thr->Ser Ser->Gly Tyr->Phe	Quadruple	R3K T8S S11G Y12F
IJ115	YycG'-PhoR	Hybrid kinase	PhoR catalytic domain

Table 2.5 Amino acid changes introduced into PhoP

Strain	Amino acid change	Mutation Number	Positions on the RR surface
IJ140		wild type	
IJ141	Pro->Thr	Single	107
IJ142	Ser->Pro	Single	13
IJ143	Leu->Ile	Single	17
IJ144	Tyr->Phe	Single	20
IJ145	Ser->Pro / Leu->Ile	Double	13/17
IJ146	Ser->Pro / Tyr->Phe	Double	13/20
IJ147	Leu->Ile / Tyr->Phe	Double	17/20
IJ148	Ser->Phe / Leu->Ile / Tyr->Phe	Triple	13/17/20
IJ149	Ser->Pro / Pro->Thr	Double	13/107
IJ150	Leu->Ile / Pro->Thr	Double	17/107
IJ151	Tyr->Phe / Pro->Thr	Double	20/107
IJ152	Ser->Pro / Leu->Ile / Pro->Thr	Triple	13/17/107
IJ153	Ser->Pro / Tyr->Phe / Pro->Thr	Triple	13/20/107
IJ154	Leu->Ile / Tyr->Phe / Pro->Thr	Triple	17/20/107
IJ155	Ser->Pro / Leu->Ile / Tyr->Phe / Pro->Thr	Quadruple	13/17/20/107

```

                                111111111
                                12345678901234567
YycG  VANVSHELRTPLTTMRSYLEALA
PhoR  VANVSHELKTPITSIKGFTETLL
ResE  IANVSHELRTPISMLQGYSEAIV
YkoH  VQDASHELKTPLTIIESYSSLMK
Yc1K  IADVSHELKTPLTTINGLVEGLN
YvrG  IAGLSHDLKTPLSSIYGYSMMLE

```

Figure 3.1 Alignment of phosphorylation site of group IA HKs of *B.subtilis*. (adapted from Mukhopadhyay and Varughese 2005, see for more details). The numbers indicate the position relative to the active histidine (red) that is assigned 0. Indicated in grey are five positions that differ between YycG and PhoR and are predicted to be involved in HK-RR interaction.

A

111
0123456789012
YycG VANV**S**HELRTPLTTMRSYLEALA
PhoR VANV**S**HELKTPITSIKGFTE~~LL~~

B

YycG108 VANV**S**HELRTPLTTMRSYLEALA
YycG101 VANV**S**AELRTPLTTMRSYLEALA
YycG102 VANV**S**HEL**K**TPLTTMRSYLEALA
YycG103 VANV**S**HELRTPLT**S**MRSYLEALA
YycG104 VANV**S**HELRTPLTTM**K**SYLEALA
YycG105 VANV**S**HELRTPLTTMR**G**YLEALA
YycG106 VANV**S**HELRTPLTTMRS**F**LEALA
YycG107 VANV**S**HEL**K**TPLT**S**M**KGF**LEALA
YycG112 VANV**S**HELRTPLTTMR**G**FLEALA
YycG114 VANV**S**HEL**K**TPLT**S**MR**G**FLEALA

Figure 3.2 Alignment of YycG and PhoR residues in the vicinity of the active histidine and mutated YycG*.

A) Alignment of YycG and PhoR α 1-helices. The numbers above indicate the position relative to the active histidine (bold) assigned 0. Amino acids that face the response regulator and differ between YycG and PhoR are shaded gray.

B) Alignment of mutated YycG α 1-helices. The site of phosphorylation is indicated in bold, the amino acids investigated are shaded grey and introduced mutations are shown in red.

Table 3.1 Amino acid changes introduced into YycG

Strain	Amino acid change	Mutation Number	Positions on the α 1 helix
IJ101	His->Ala	Histidine	H0A
IJ102	Arg->Lys	Single	R3K
IJ103	Thr->Ser	Single	T8S
IJ104	Arg->Lys	Single	R10K
IJ105	Ser->Gly	Single	S11G
IJ106	Tyr->Phe	Single	Y12F
IJ107	Arg->Lys Thr->Ser Arg->Lys Ser->Gly Tyr->Phe	Quintuple	R3K T8S R10K S11G Y12F
IJ108		Reconstituted wt	
IJ112	Ser->Gly Tyr->Phe	Double	S11G Y12F
IJ114	Arg->Lys Thr->Ser Ser->Gly Tyr->Phe	Quadruple	R3K T8S S11G Y12F
IJ115	YycG'-PhoR	Hybrid kinase	YycG sensing domain' 'PhoR catalytic domain

***B.subtilis* 168**

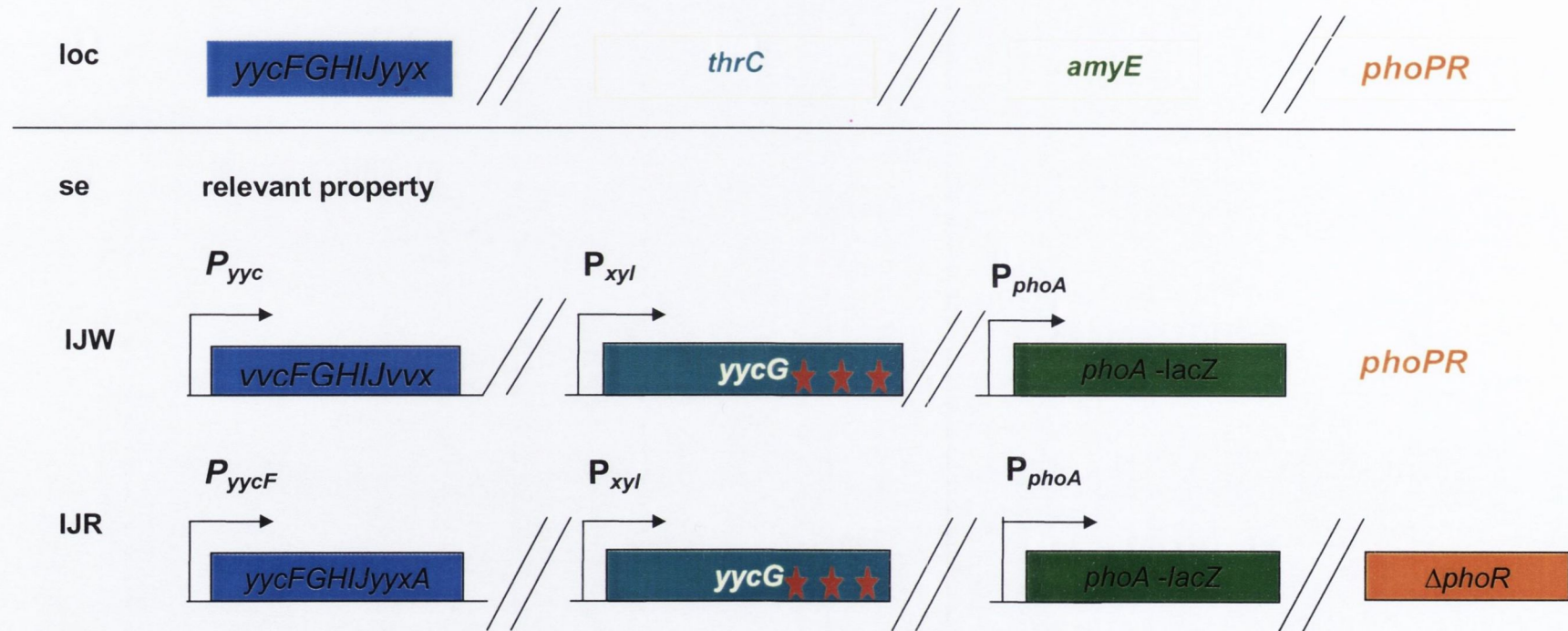


Figure 3.3 Genetic structure of strain sets IJW and IJR. The relevant chromosomal loci are indicated at the top and separated by //. The set name indicates the genetic background (W: wild-type and R: $\Delta phoR$). The bent arrow stands for a promoter and the red stars indicate modifications in *yycG* as outlined in Table 3.2.

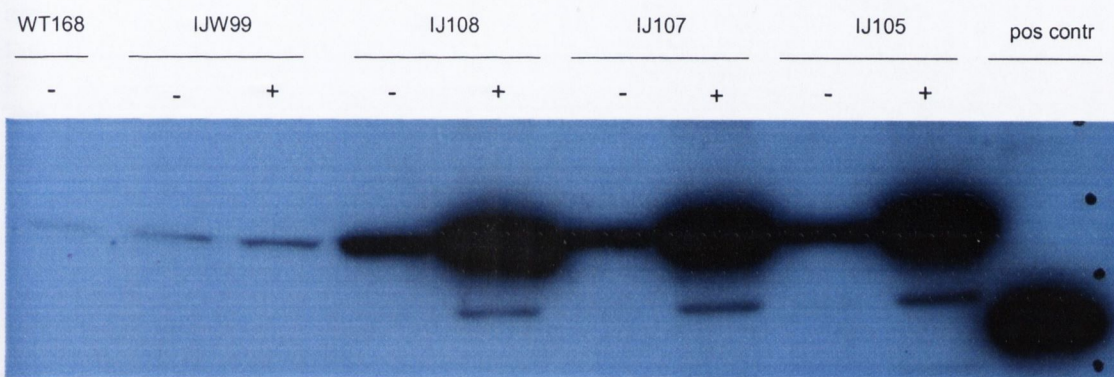


Figure 3.4 Western blot analysis showing cellular levels of YycG.

Cells of strains indicated above: 168 (wild-type strain), IJW99 (P_{phoA} -*lacZ*), IJR108 (P_{phoA} -*lacZ*, P_{xy} -*yycG* [wild-type], $\Delta phoR$), IJR107 (P_{phoA} -*lacZ*, P_{xy} -*yycG* [R3K T8S R10K S11G Y12F], $\Delta phoR$), IJR105 (P_{phoA} -*lacZ*, P_{xy} -*yycG* [S11G], $\Delta phoR$) were harvested in the presence (+) and absence (-) of 0.5% xylose at an OD_{600} of 1. 10 μ g of total protein was loaded per lane. Positive control is purified 'YycG (truncated) protein.

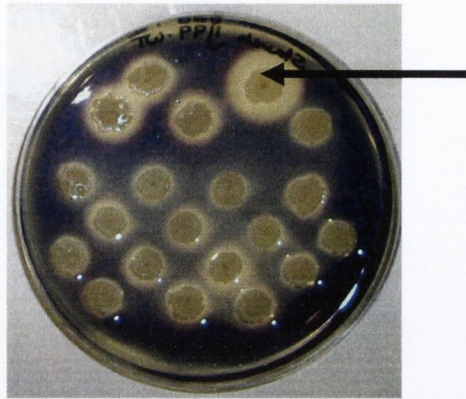


Figure 3.5 α -amylase assay of IJW99 putative transformants. Putative transformants of strain IJW99 were grown on LB agar containing 0.2% starch (w/v). The arrow indicates a colony that displays amylase activity in the form of a bright halo. The desired transformants display no halo after the addition of iodine solution as an effect of the interruption of the *amyE* locus.

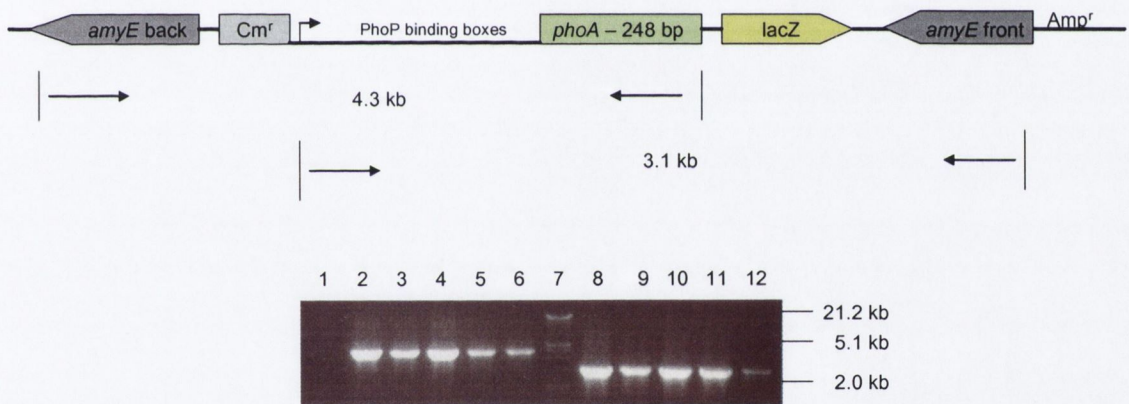


Figure 3.6 PCR mapping of IJW99 putative transformants to confirm integration of the P_{phoA} -*lacZ* fusion. Map of IJW99 [*trpC2 amyE::P_{phoA}-lacZ*] *amyE* locus and expected PCR products. Primer locations are indicated by arrows, the *phoA* promoter region is indicated after the bent arrow. Agarose gel of PCR products show bands of 4.3 kb and a 3.1 bp confirming the integration of P_{phoA} -*lacZ* via double crossover into the chromosome. Samples loaded: (1) chromosomal DNA negative control; (2-6 & 8-12) five IJW99 putatives with two different primer sets; (7) marker.

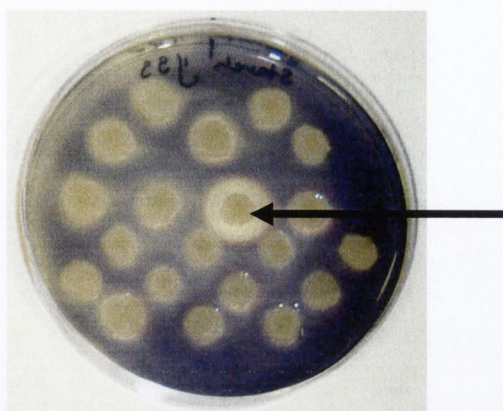


Figure 3.7 α -amylase assay on IJR99 putative transformants. Putative transformants of strain IJR99 were grown on LB agar containing 0.2% (w/v) starch. The arrow indicates a colony that displays amylase activity in the form of a bright halo. The desired transformants display no halo after addition of iodine solution as an effect of the interruption of *amyE* locus.

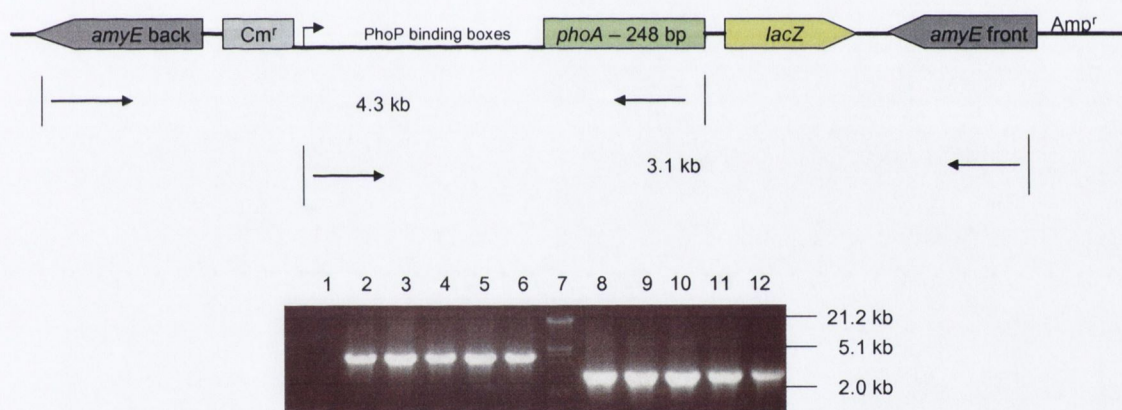


Figure 3.8 PCR mapping of IJR99 putative transformants. Map of IJR99 [*trpC2 amyE::P_{phoA}-lacZ*] *amyE* locus and expected PCR products. Primer locations are indicated by arrows, the *phoA* promoter region is indicated after the bent arrow. Agarose gel of PCR products show bands of 4.3 kb and a 3.1 bp confirming the integration of *P_{phoA}-lacZ* via double crossover into the chromosome. Samples loaded: (1) chromosomal DNA negative control; (2-6 & 8-12) five IJR99 putatives with two different primer sets; (7) marker.

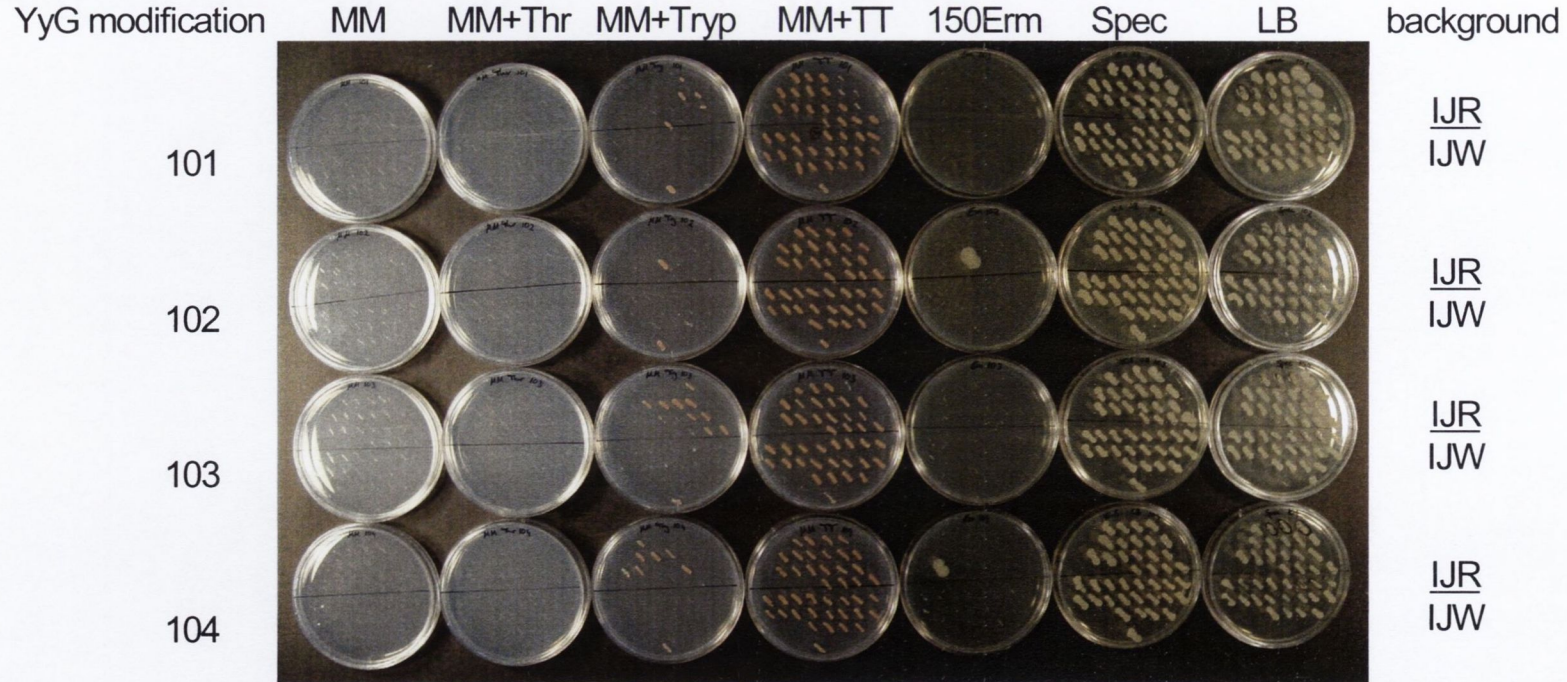


Figure 3.9 Screening of putative transformants for the $P_{xyI}yycG$ integration at the *thrC* locus. The putative transformants were grown on minimal medium (MM), MM supplemented with tryptophan (Tryp) or threonine (Thr), or both (MM+TT) as well as on LB supplemented with erythromycin (Erm) or spectinomycin (Spec). The correct transformants only grow on MM+TT and are Erm sensitive and Spec resistant. The modifications of $P_{xyI}yycG$ are indicated on the left (see Table 3.1 for details). As indicated on the right, the top half of each plate was used for strains with $\Delta phoR$ background the bottom half for wild-type background (wt). The picture is a representative for all $P_{xyI}yycG$ carrying strains of this study.



Figure 3.10 Evaluation of PhoP phosphorylation by mutant YycG* in IJW strains *in vivo*. β -galactosidase activity of strains carrying YycG* mutated protein in *phoPR*⁺ strains (IJW) grown on LB agar supplemented with X-gal. The strain names and amino acid changes in YycG are indicated on the right.

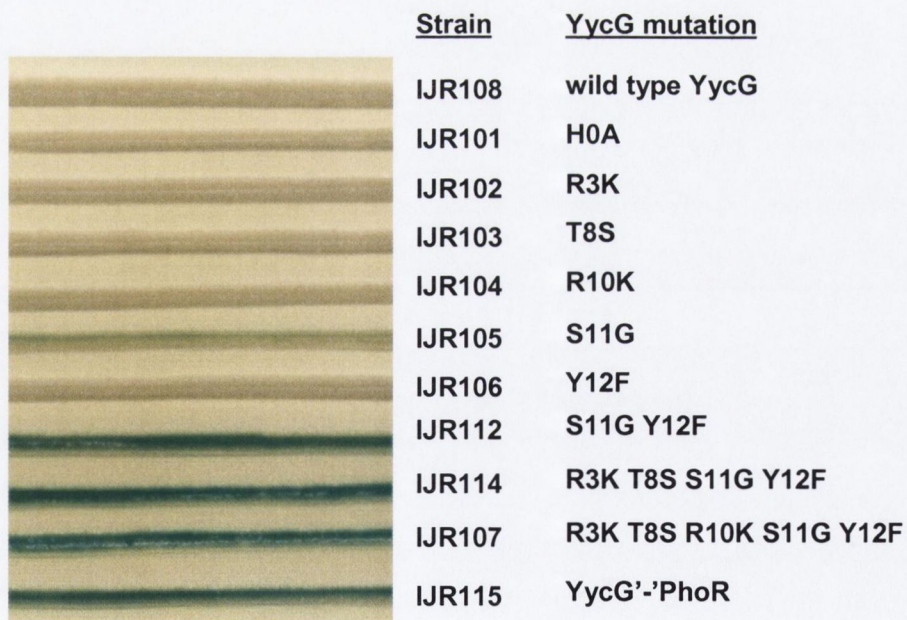


Figure 3.11 Evaluation of phosphotransfer between mutant YycG* protein and PhoP in IJR strains *in vivo*. β -galactosidase activity of strains carrying YycG* mutated protein in Δ *phoR* strains (IJR) on LB agar supplemented with X-gal. The strain names and amino acid changes in YycG are indicated on the right.

B. subtilis 168 chromosome

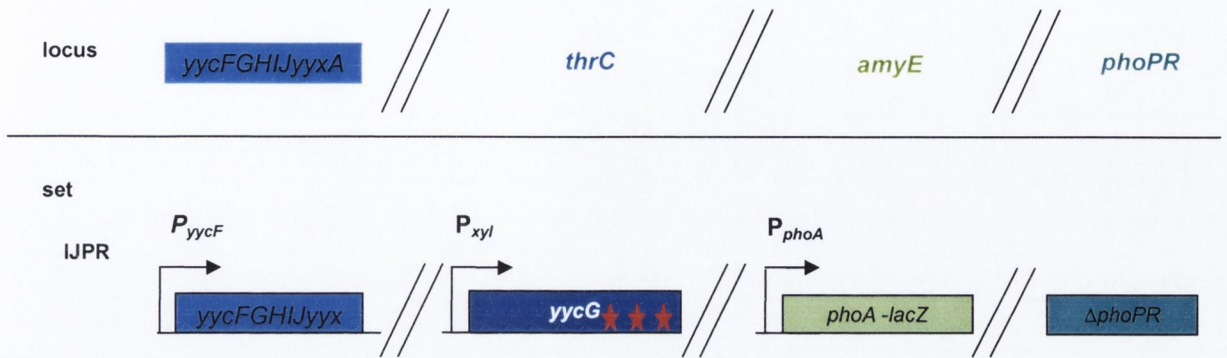


Figure 3.12 Genetic properties of strain set IJPR. The relevant loci are indicated at the top and are separated by //. The set name indicates the genetic background (IJPR: $\Delta phoPR$). Promoters are bent arrow and the red stars indicate modifications in YycG.

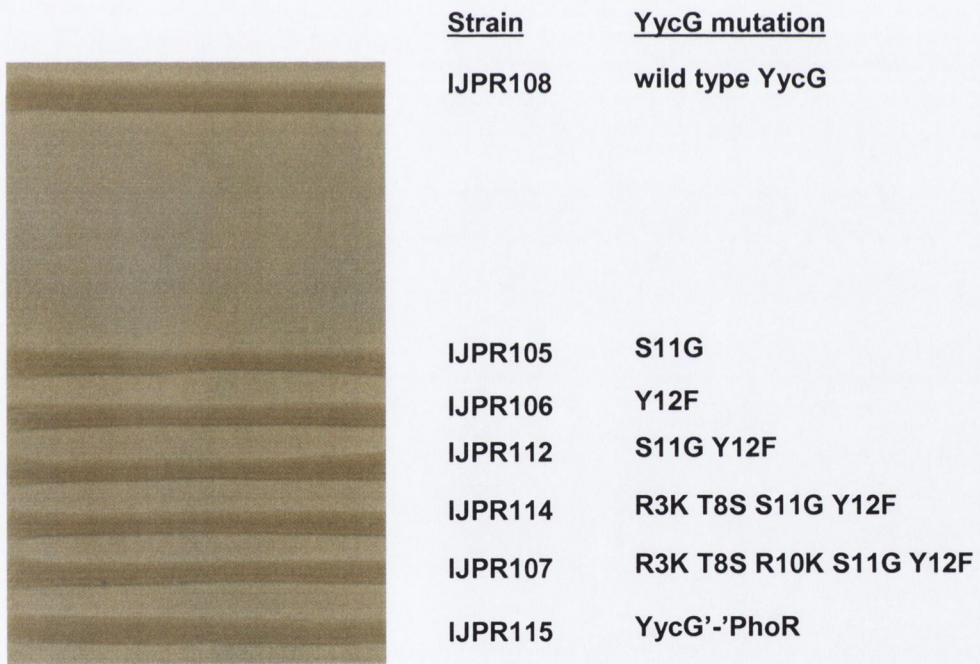


Figure 3.13 β -galactosidase activity of strains carrying YycG mutant proteins is Pho~P dependent. Strains carrying mutated YycG* in $\Delta phoPR$ background (IJPR strains) grown on LB agar supplemented with X-gal. The strain names and amino acid changes (outlined in Table 3.1) in YycG are indicated on the right. Strains IJPR101-IJPR104 were not constructed but a space is left to facilitate direct comparison with strains IJW and IJR (shown in Figure 3.9 and 3.10).

B. subtilis 168 chromosome

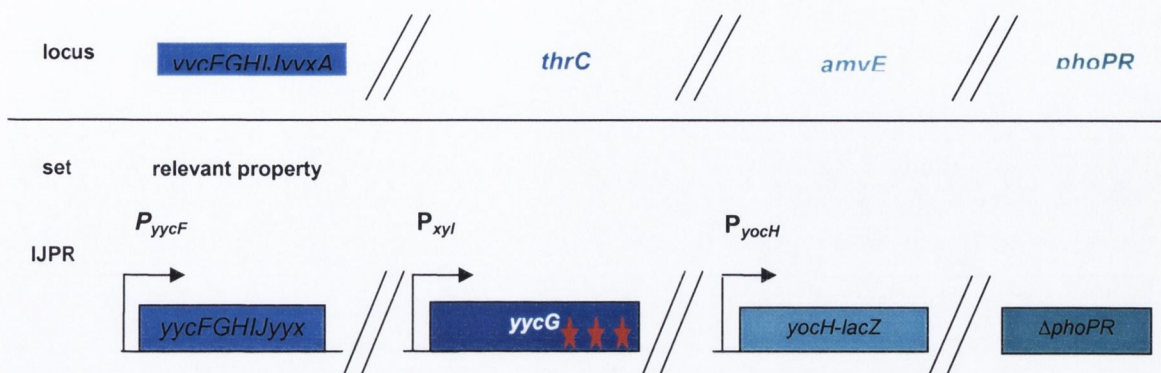


Figure 3.14 Genetic structure of strain set IJPR121-131. The relevant loci are indicated at the top and are separated by //. The set name indicates the genetic background (IJPR: $\Delta\rho PR$). The bent arrow indicates a promoter and the red stars indicated amino acid changes in YycG (outlined in Table 3.2).

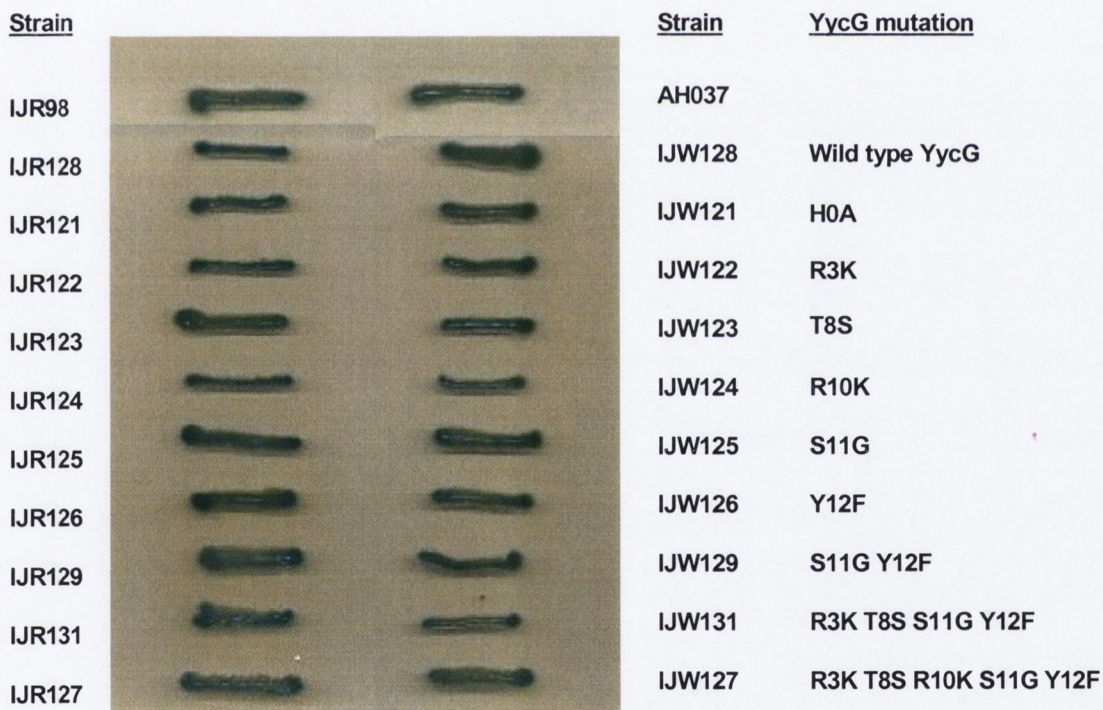


Figure 3.15 Expression of P_{yocH} -lacZ fusion. Strains expressing YycG* mutant proteins in $\Delta\rho R$ (IJR) and wild-type (IJW) background grown on solid LB medium supplemented with X-gal. The strain names are indicated to the left and right in bold. The relevant amino acid changes in YycG (as outlined in Table 3.1) are indicated to the right.

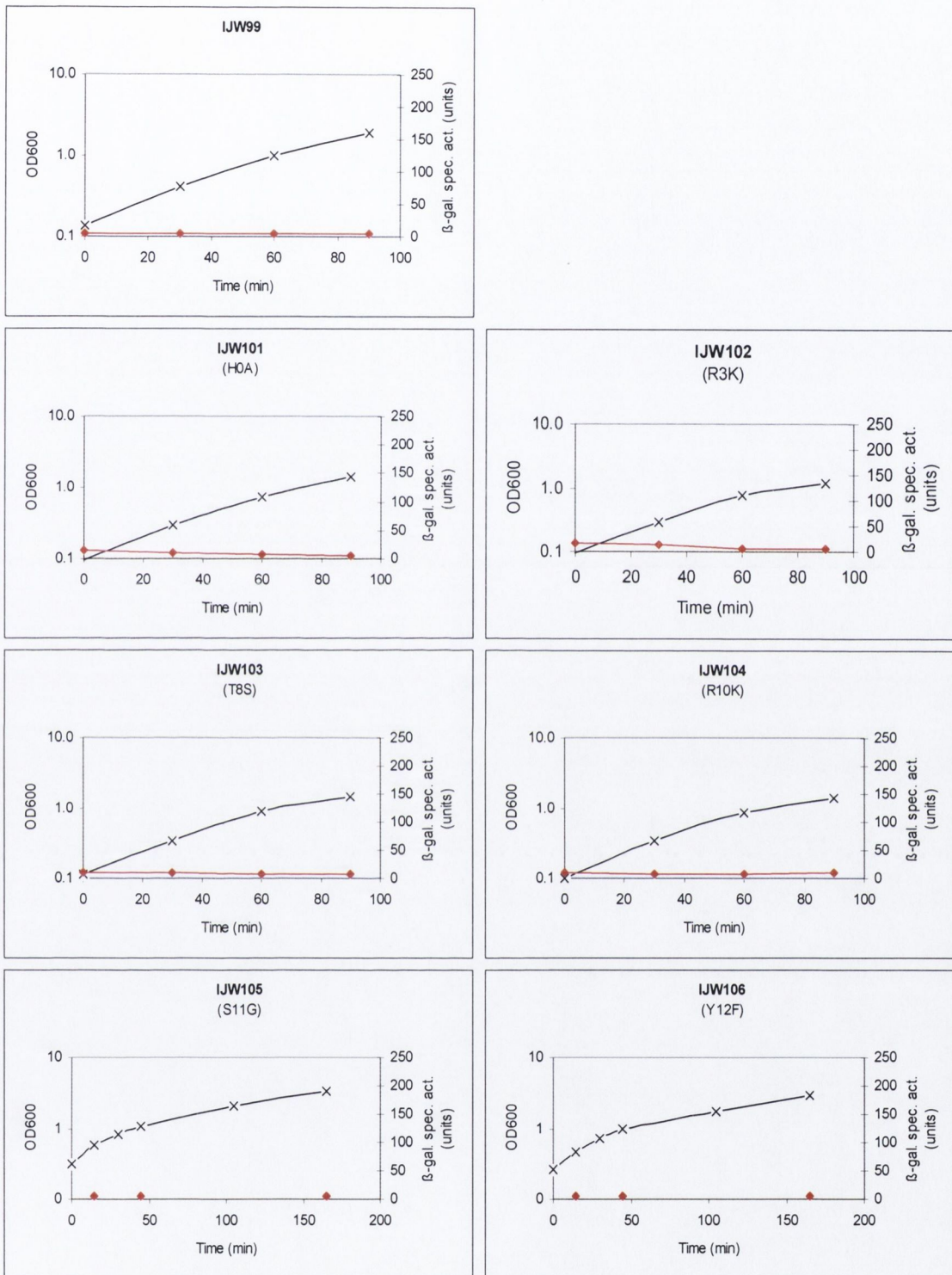


Figure 3.16 Growth and β -galactosidase profiles of IJW99 to IJW106. Strain names and the amino acid changes in YycG are indicated. Growth is shown with black crosses (OD₆₀₀ units) and the β -galactosidase specific activity (as defines in Material and Methods) is shown in red diamonds.

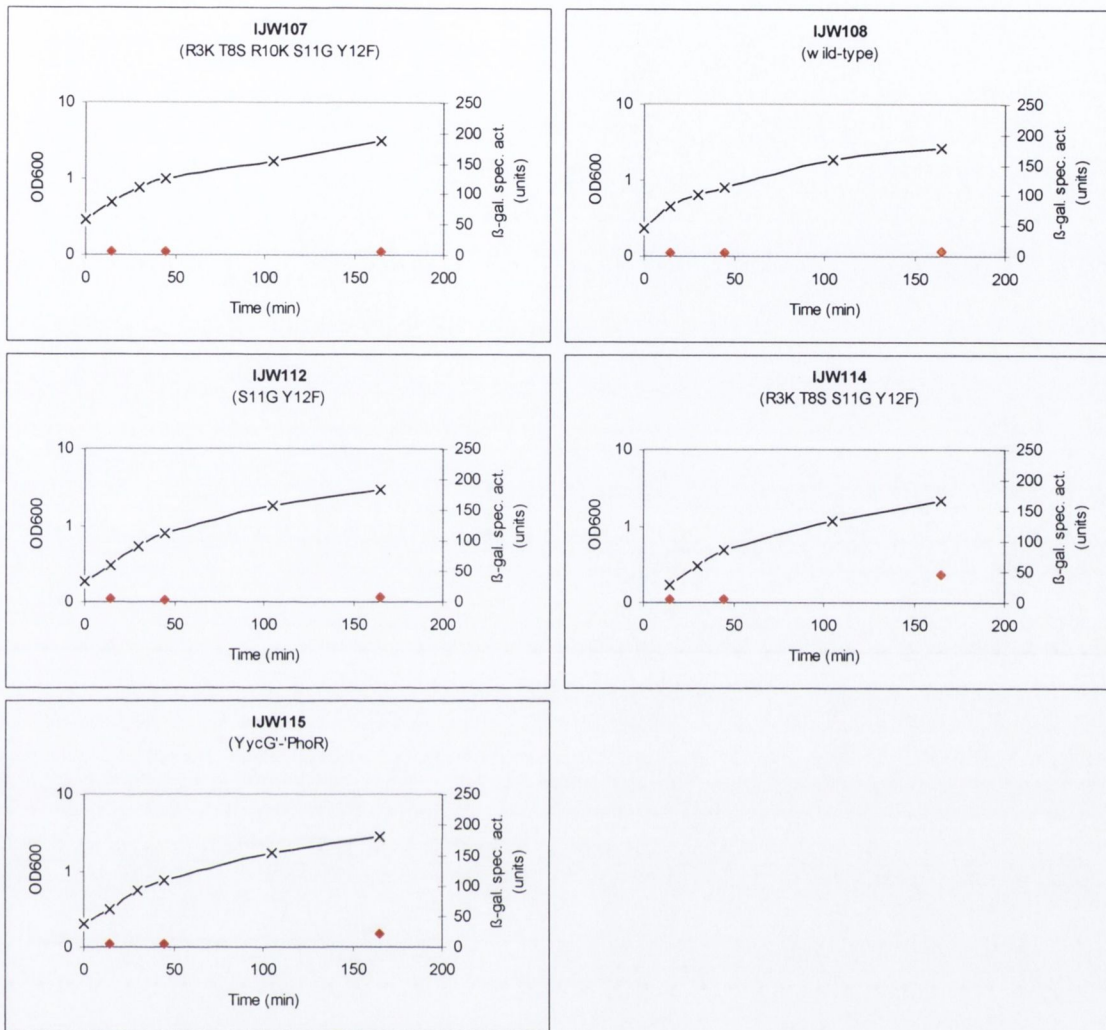


Figure 3.17 Growth and β -galactosidase profiles of IJW107, IJW108, IJW112, IJW114 and IJW115. Strain names and the amino acid changes in YycG are indicated. Growth is shown with black crosses (OD600 units) and the β -galactosidase specific activity (as defines in Material and Methods) is shown in red diamonds.

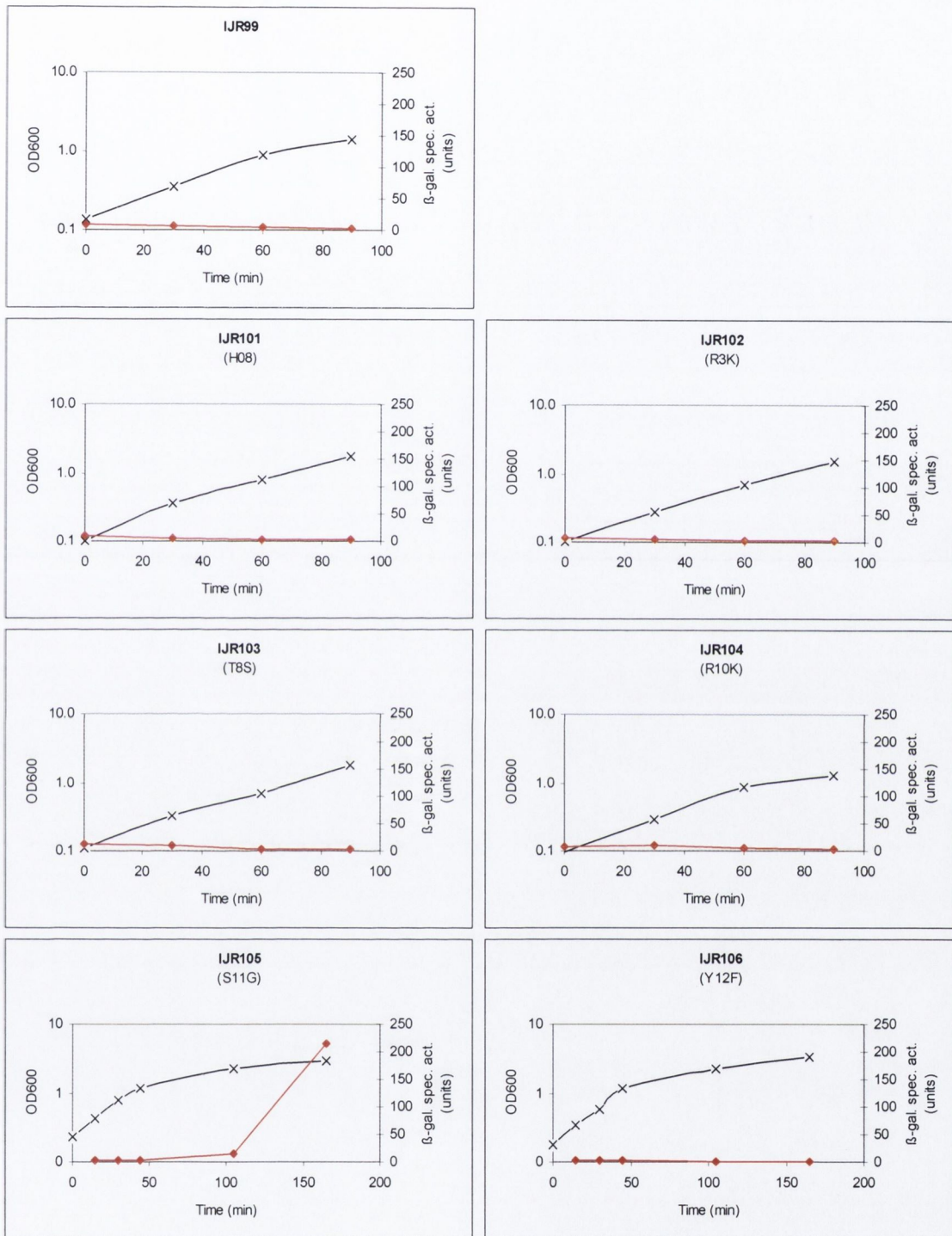


Figure 3.18 Growth and β -galactosidase profiles of IJR99 to IJR106. Strain names and the amino acid changes in YycG are indicated. Growth is shown with black crosses (OD₆₀₀ units) and the β -galactosidase specific activity (as defines in Material and Methods) is shown in red diamonds.

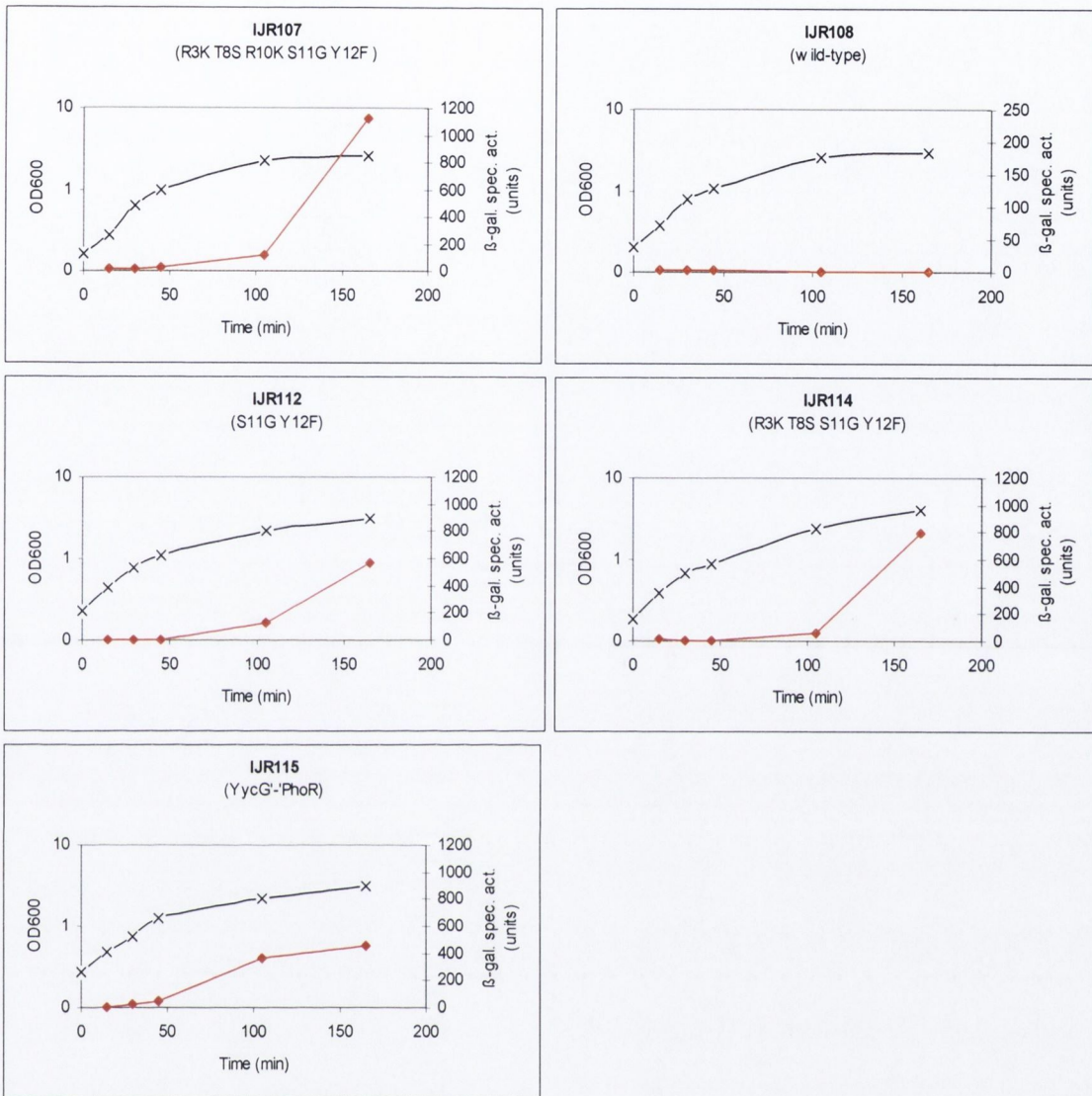


Figure 3.19 Growth and β -galactosidase profiles of IJR107, IJR108, IJR112, IJR114 and IJR115. Strain names and the amino acid changes in YycG are indicated. Growth is shown with black crosses (OD_{600} units) and the β -galactosidase specific activity (as defines in Material and Methods) is shown in red diamonds.

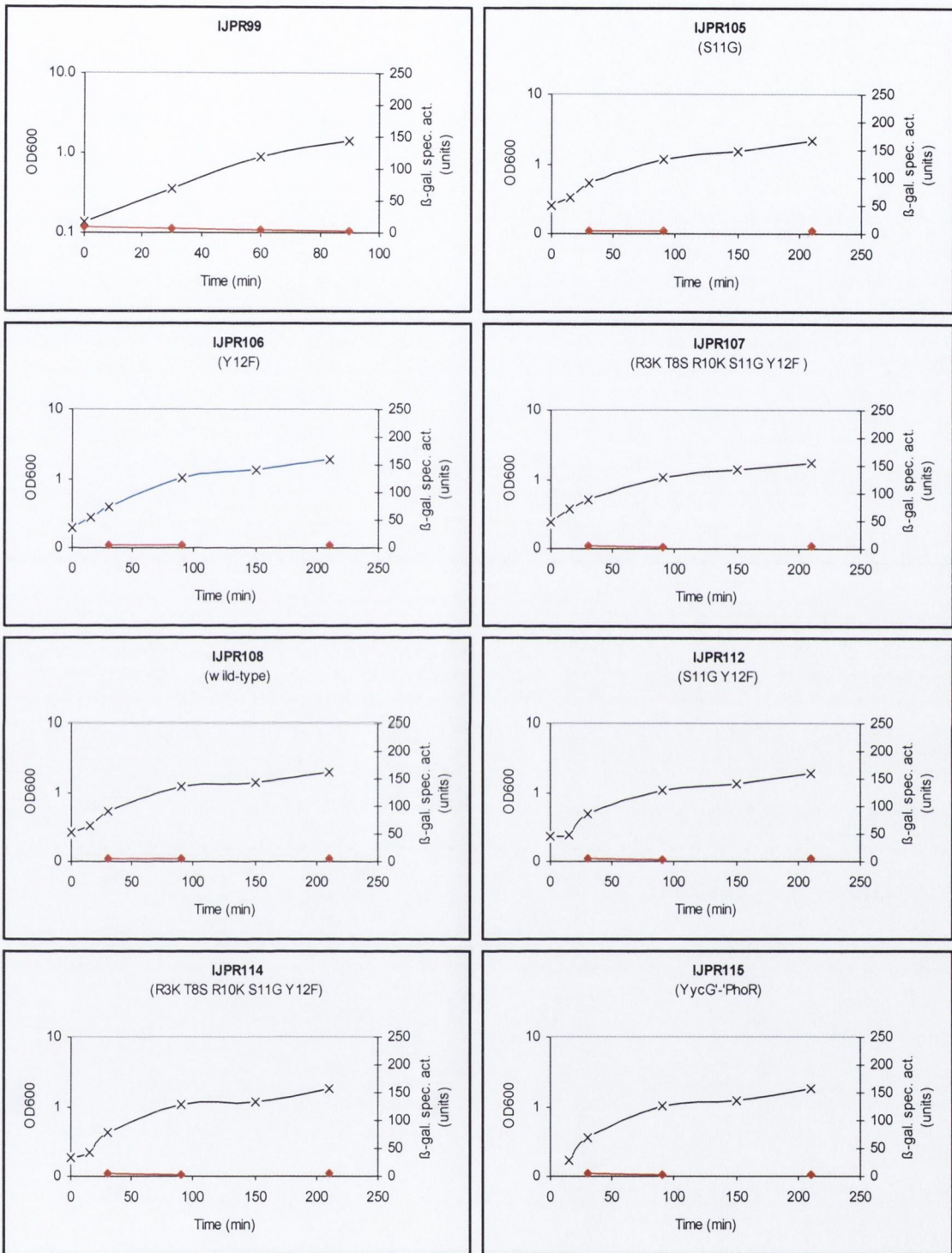


Figure 3.20 Growth and β -galactosidase profiles of IJPR strains.

Strain names and the amino acid changes in YycG are indicated. Growth is shown with black crosses (OD600 units) and the β -galactosidase specific activity (as defines in Material and Methods) is shown in red diamonds.

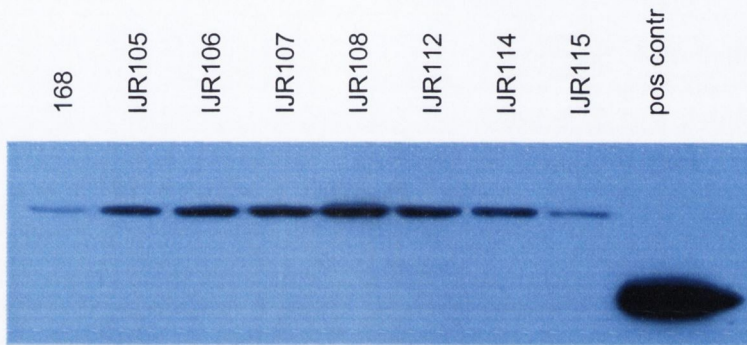
Table 3.2 YycG*:PhoP interaction and PhoP~P-mediated regulation of *phoA* expression in exponential growth.

Strain	Relevant YycG mutant	β -galactosidase activity ^a
IJR108	Reconstituted <i>yycG</i> wild type	4.89 \pm 0.79
IJR101	H0A	
IJR102	R3K	
IJR103	T8S	
IJR104	R10K	
IJR105	S11G	5.26 \pm 1.09
IJR106	Y12F	5.15 \pm 0.79
IJR112	S11G Y12F	5.32 \pm 0.98
IJR114	R3K T8S S11G Y12F	8.47 \pm 1.55
IJR107	R3K T8S R10K S11G Y12F	12.98 \pm 1.50
IJRHK	<i>yycG</i> '-' <i>phoR</i>	8.30 \pm 2.14

^a β -Galactosidase activities are given in β -gal units. Values are averages of at least three independent experiments in exponentially growing cells.

A

Exponential phase of growth $OD_{600} \sim 0.5$



B

Stationary phase of growth $OD_{600} \sim 2.0$

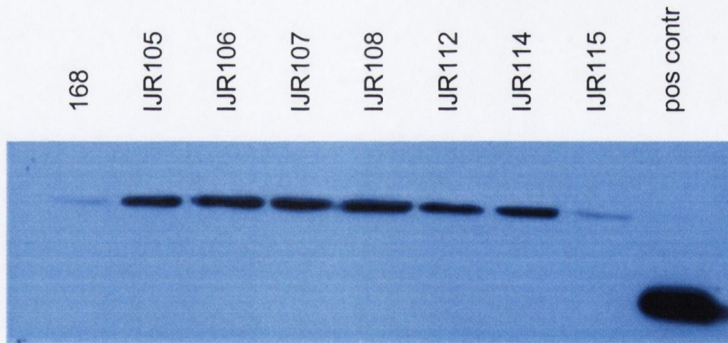


Figure 3.21 Western Blot analysis of YycG protein levels in wild-type strain 168 and selected IJR strains.

A) Western blot of samples taken during the exponential phase of growth. Strain names are indicated at the top of the gel. 10 μ g of total cell protein were loaded in each lane. Purified truncated YycG protein was loaded as positive control (pos contr.).

B) Western blot of samples taken during the stationary phase of growth. Strain names are indicated at the top of the gel. 10 μ g of total cell protein were loaded in each lane. Purified truncated YycG protein was loaded as positive control (pos contr.).

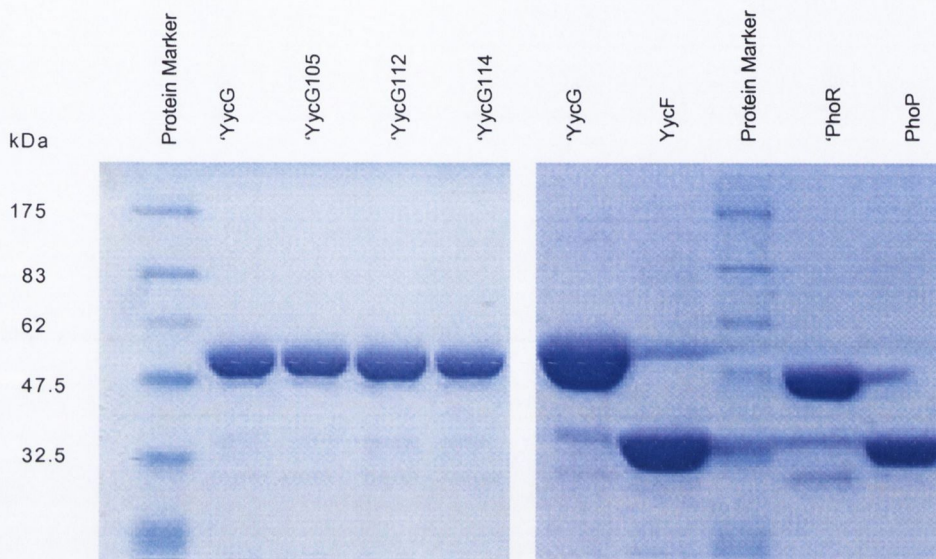


Figure 3.22 Analysis of purified 'YycG and 'PhoR kinases and the response regulators YycF and PhoP by SDS-PAGE. The molecular weight of the protein marker is indicated on the left. The proteins loaded are name above each lane ('YycG [wild-type], 'YycG105 [S11G], 'YycG112 [S11G Y12F], 'YycG114 [R8K T8S S11G Y12F], 'PhoR [wild-type], PhoP and YycF [wild-type RRs]). Each lane was loaded with 2 μ l dialyses protein prior to quantification.

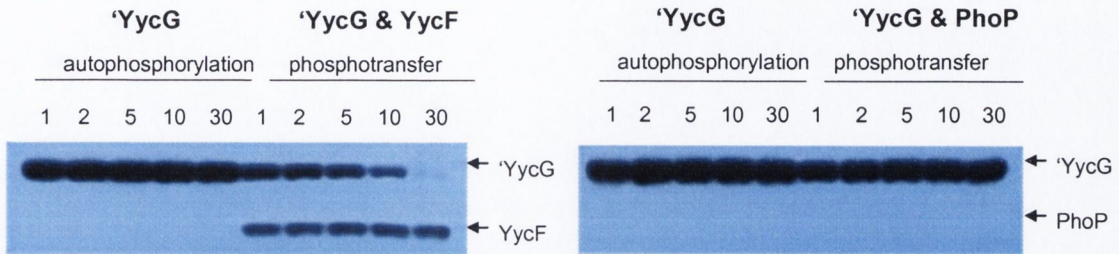
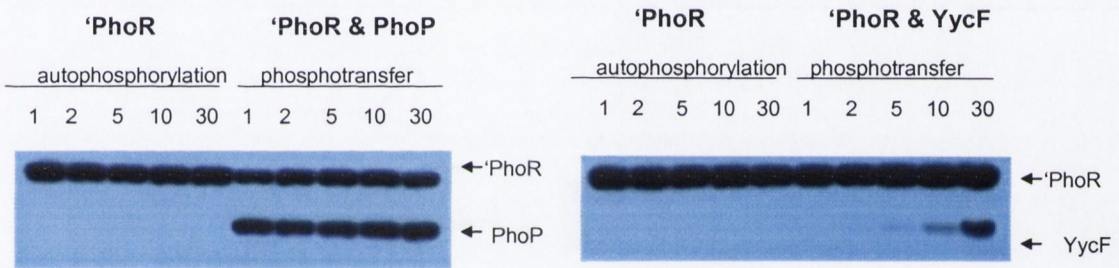
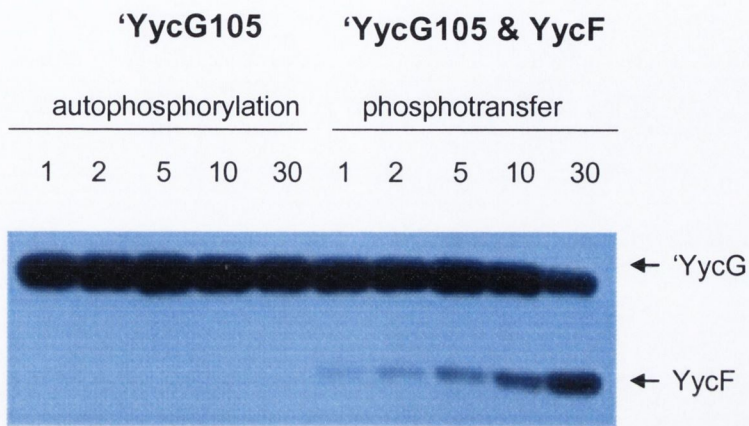
A**B**

Figure 3.23 Autophosphorylation and phosphotransfer *in vitro* of TCS pairs YycGF and PhoPR.

The 'YycG and 'PhoR histidine kinases were incubated at 37°C for the indicated time (1-30 min) either on its own or with the purified RRs YycF and PhoP as indicated above. Each lane contains 2 µg of each protein. The phosphorylation reactions were started by the addition of γ [32 P] ATP as described in Methods and Materials.

Panel A shows the autophosphorylation of YycG and the transphosphorylation to YycF (left) or PhoP (right). Panel B shows the autophosphorylation of PhoR and the transphosphorylation to PhoP (left) or YycF (right).

A



B

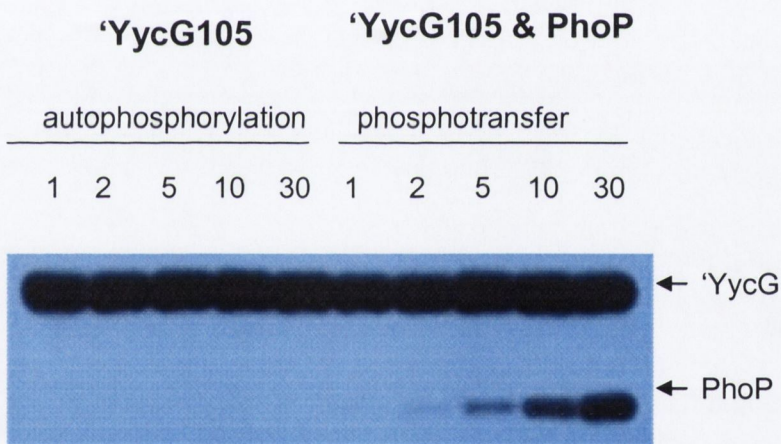
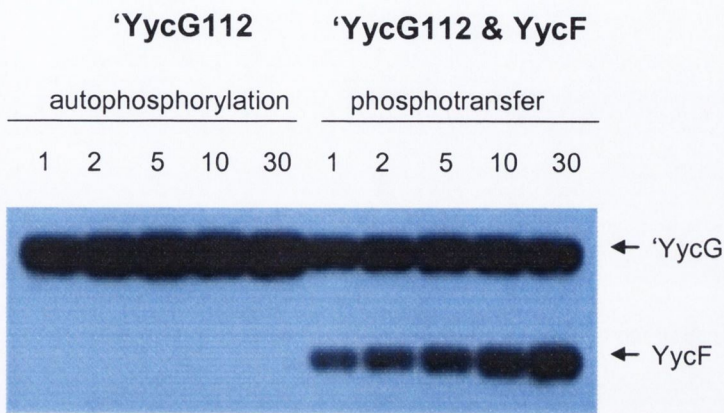


Figure 3.24 Phosphorylation YycF and PhoP by 'YycG105 *in vitro*. 'YycG105 (S11G) was incubated either on its own, or with purified YycF or PhoP for times indicated after the addition of γ [^{-32}P] ATP. Each lane contains 2 μg of each protein. The left hand side of both panels shows the autophosphorylation of YycG105. Panel A on the right shows the phosphotransfer between 'YycG105 and its cognate response regulator. Panel B on the right shows 'YycG105 incubated with the non-cognate RR PhoP. Time is indicated in minutes.

A



B

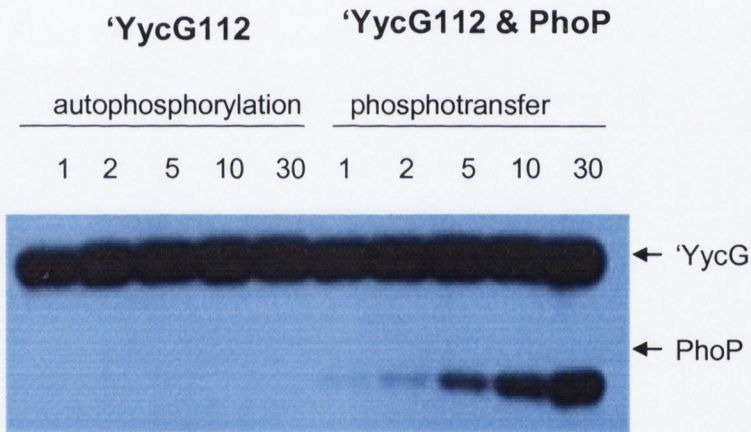
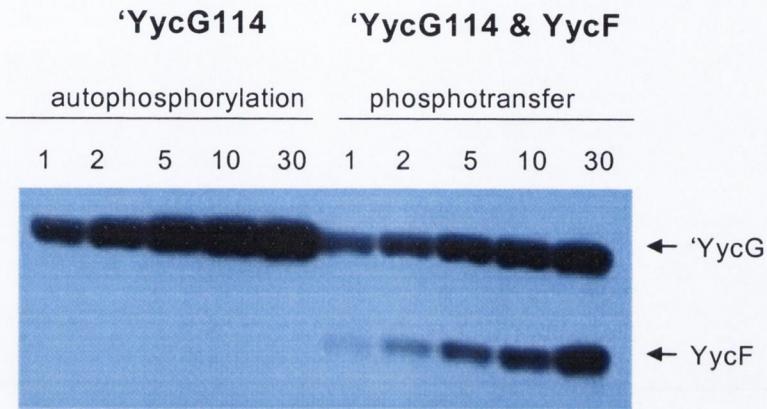


Figure 3.25 Phosphorylation of YycF and PhoP by 'YycG112 *in vitro*. 'YycG112 (S11G Y12F) was incubated either on its own, or with purified YycF or PhoP for times indicated after the addition of γ [32 P] ATP. Each lane contains 2 μ g of each protein. The left hand side of both panels shows the autophosphorylation of YycG112. Panel A on the right shows the phosphotransfer between 'YycG112 and its cognate response regulator. Panel B on the right shows 'YycG112 incubated with the non-cognate RR PhoP. Time is indicated in minutes.

A



B

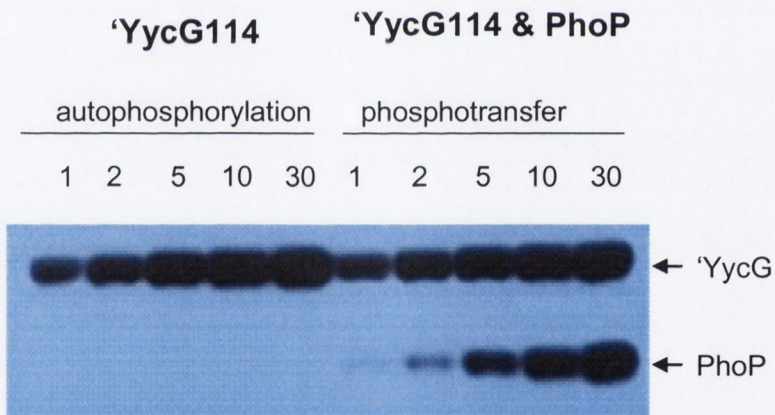
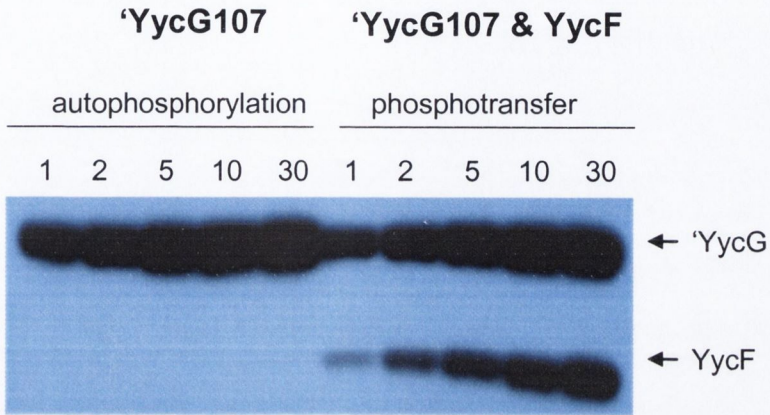


Figure 3.26 Phosphorylation of YycF and PhoP by 'YycG114 in vitro. 'YycG114 (R3K T8S S11G Y12F) was incubated either on its own, or with purified YycF or PhoP for times indicated after the addition of γ [32 P] ATP. Each lane contains 2 μ g of each protein. The left hand side of both panels shows the autophosphorylation of 'YycG114. Panel A on the right shows the phosphotransfer between 'YycG114 and its cognate response regulator. Panel B on the right shows 'YycG114 incubated with the non-cognate RR PhoP. Time is indicated in minutes.

A



B

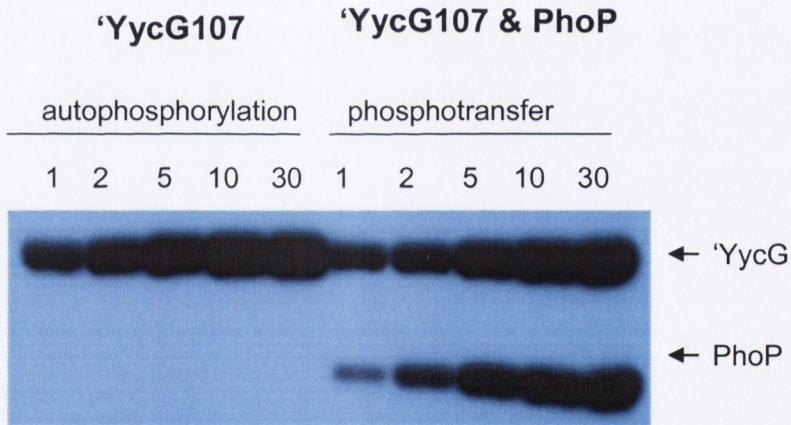


Figure 3.27 Phosphorylation of YycF and PhoP by 'YycG107 in vitro. 'YycG107 (R3K T8S R10K S11G Y12F) was incubated either on its own, or with purified YycF or PhoP for times indicated after the addition of γ [32] ATP. Each lane contains 2 μ g of each protein. The left hand side of both panels shows the autophosphorylation of YycG107. Panel A on the right shows the phosphotransfer between 'YycG107 and its cognate response regulator. Panel B on the right shows 'YycG107 incubated with the non-cognate RR PhoP. Time is indicated in minutes.

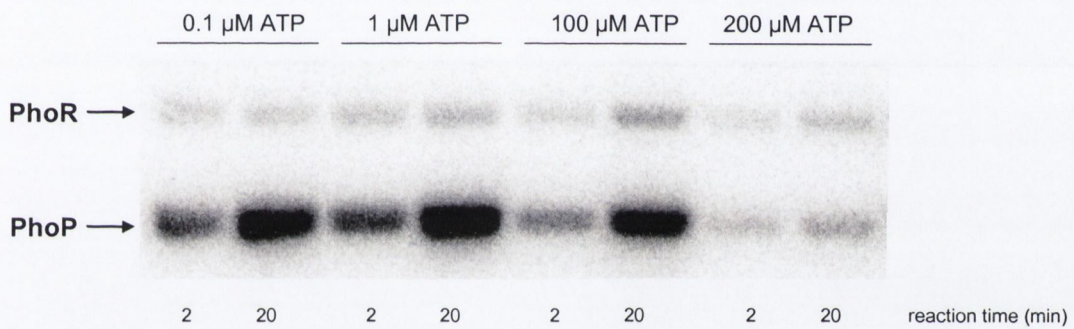
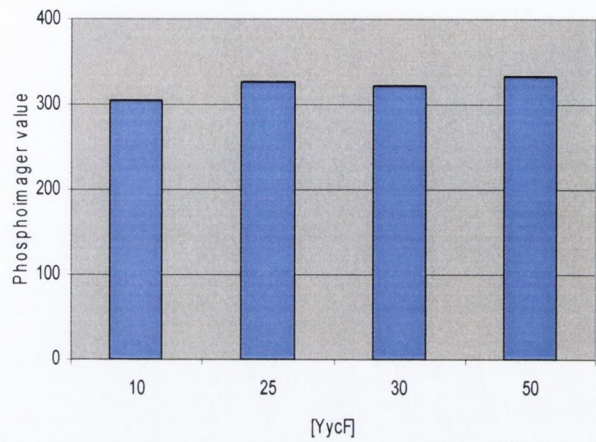
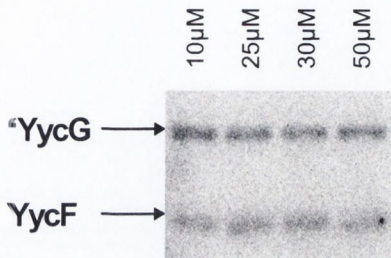


Figure 3.28 Determination of optimal ATP levels for *in vitro* phosphorylation reactions. Phosphotransfer reactions were set up as in Materials and Methods. Reactions contain different amounts of ATP as indicated above the phosphoimage. 2.5 μM of each , 'PhoR and PhoP , was used in each reaction. Reactions were continued for 2 and 20 minutes (indicated at the bottom of phosphoimage). Gel was exposed to a phosphoimager plate for 1 minute.

A



B

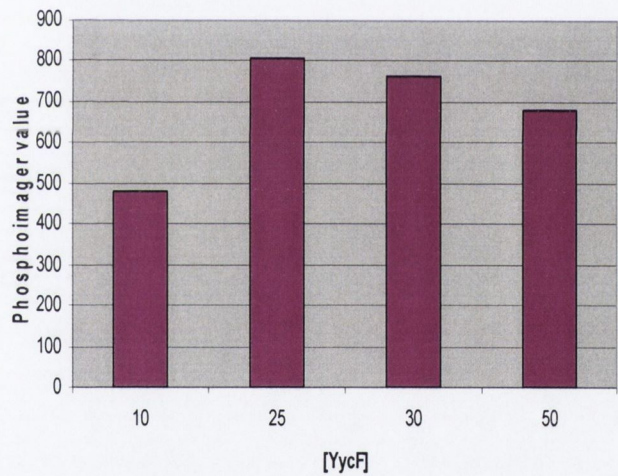
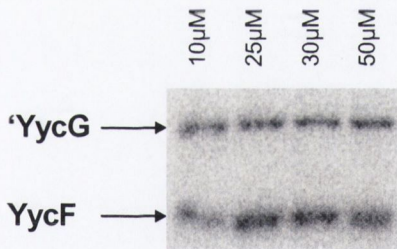
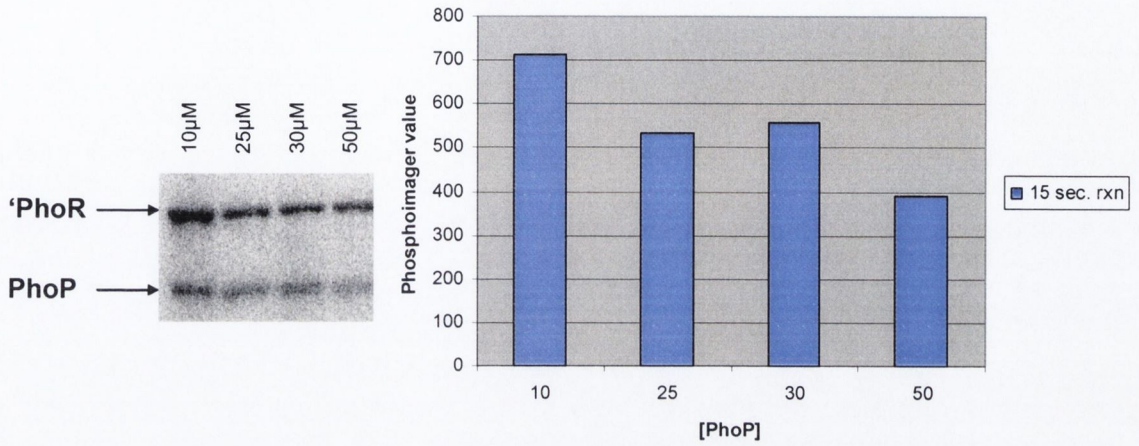


Figure 3.29 Test of different YycF concentrations for *in vitro* phosphorylation.

A) Phosphoimage and quantification of the phosphoimage of 2.5 μM YycG phosphorylating different amounts of YycF as indicated. The reactions continued for 15 seconds.

B) Phosphoimage and quantification of the phosphoimage of 2.5 μM YycG phosphorylating different amounts of YycF as indicated above. The reactions continued for 30 seconds.

A



B

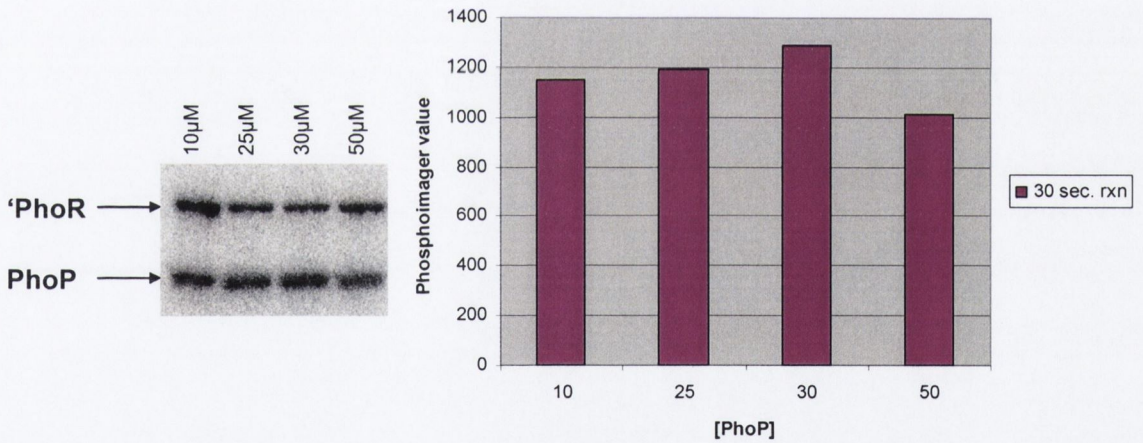


Figure 3.30 Test of different PhoP concentrations for *in vitro* phosphorylation.

A) Phosphoimage and quantification of the phosphoimage of 2.5 μM PhoR phosphorylating different amounts of PhoP as indicated. The reactions continued for 15 seconds.

B) Phosphoimage and quantification of phosphoimage of 2.5 μM PhoR phosphorylating different amounts of PhoP as indicated above. The reactions continued for 30 seconds.

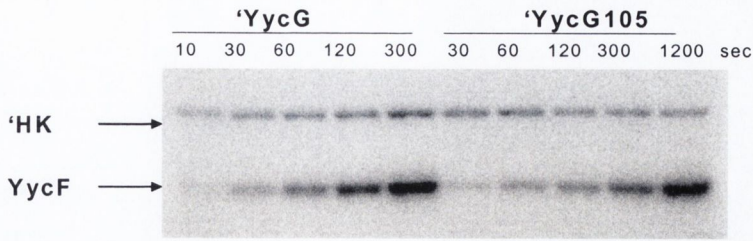
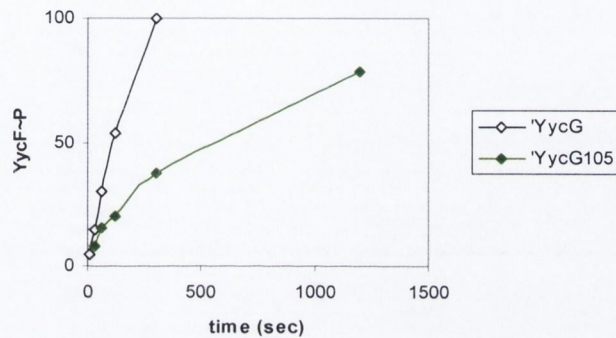
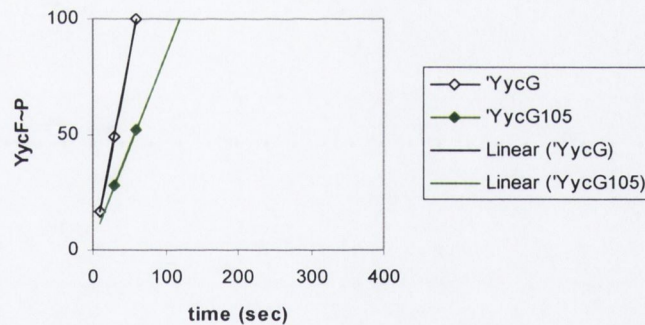
A**B****C**

Figure 3.31 Phosphorylation of the response regulator YycF by 'YycG and 'YycG105 *in vitro*.

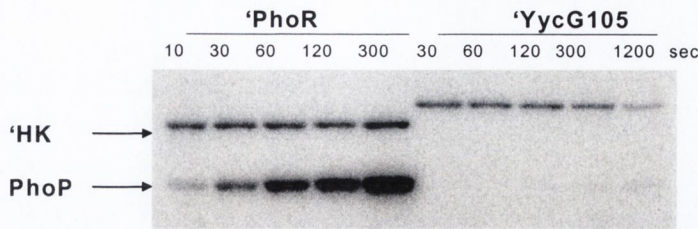
A kinetic analysis of YycF phosphorylation by 'YycG and 'YycG105 (S11G) *in vitro*.

A) Phosphoimage of YycF phosphorylation by 'YycG and 'YycG105 *in vitro*. Reaction continued for 300 sec ('YycG) and 1200 sec ('YycG105) with samples taken at the indicated time intervals (sec). The image was exposed for 90 min.

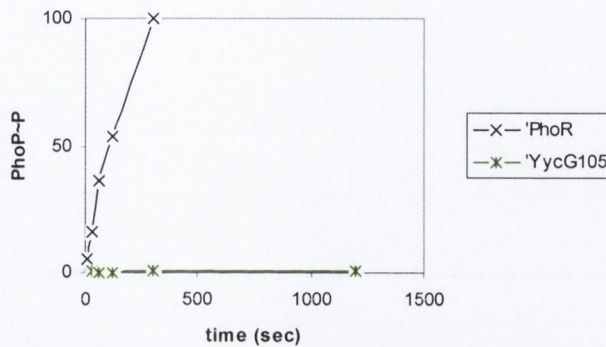
B) The phosphoimage (A) was quantified as described in materials and methods using MultiGauge2 software. Values were normalized to the amount of YycF~P present at the 300 sec timepoint for the 'YycG protein which was assigned a value of 100%. (Y black diamonds = phosphorylation of YycF by 'YycG; green diamonds = YycF phosphorylation by 'YycG105).

C) A trend line (Linear) was fitted to the initial time points of the reaction to estimate the relative initial rate of YycF phosphorylation. The slope for the trend line for phosphorylation of YycF by 'YycG is 1.67 while that for phosphorylation of YycF by 'YycG105 is 0.807.

A



B



C

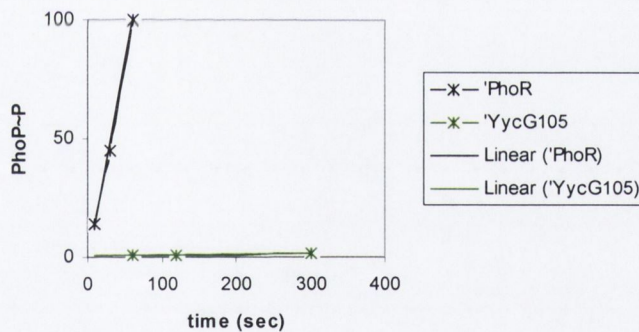


Figure 3.32 Phosphorylation of the response regulator PhoP by 'PhoR and 'YycG105 *in vitro*.

A kinetic analysis of PhoP phosphorylation by 'PhoR and 'YycG105 (S11G) *in vitro*.

A) Phosphoimage of PhoP phosphorylation by 'PhoR and 'YycG105 *in vitro*. Reaction continued for 300 sec ('PhoR) and 1200 sec ('YycG105) with samples taken at the indicated time intervals (sec). The image was exposed for 90 min.

B) The phosphoimage (A) was quantified as described in materials and methods using MultiGauge2 software. Values were normalized to the amount of PhoP~P present at the 300 sec timepoint for the 'PhoR protein which was assigned a value of 100%. (black crosses = phosphorylation of PhoP by 'PhoR; green crosses = PhoP phosphorylation by 'YycG105).

C) A trend line (Linear) was fitted to the initial time points of the reaction to estimate the relative initial rate of YycF phosphorylation. The slope for the trend line for phosphorylation of PhoP by 'PhoR is 1.73 while that for phosphorylation of PhoP by 'YycG105 is 0.004.

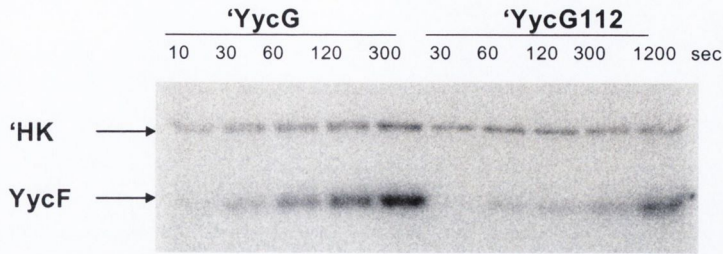
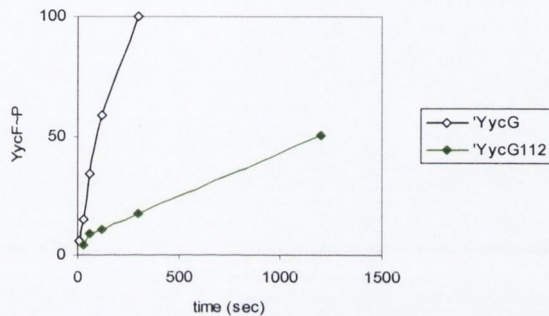
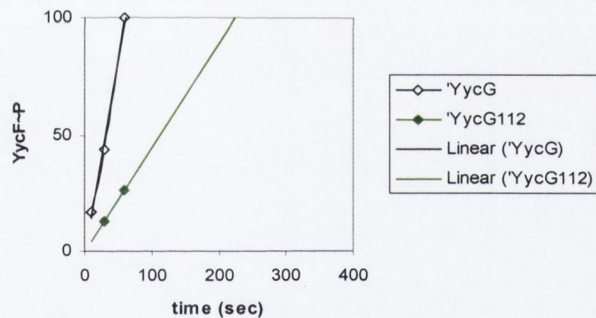
A**B****C**

Figure 3.33 Phosphorylation of YycF by histidine kinases 'YycG and 'YycG112 in vitro.

A kinetic analysis of YycF phosphorylation by 'YycG and 'YycG112 (S11G Y12F) *in vitro*.

A) Phosphoimage of YycF phosphorylation by 'YycG and 'YycG112 *in vitro*. Reaction continued for 300 sec ('YycG) and 1200 sec ('YycG112) with samples taken at the indicated time intervals (sec). The image was exposed for 90 min.

B) The phosphoimage (A) was quantified as described in materials and methods using MultiGauge2 software. Values were normalized to the amount of YycF~P present at the 300 sec timepoint for the 'YycG protein which was assigned a value of 100%. (black diamonds = phosphorylation of YycF by 'YycG; green diamonds = YycF phosphorylation by 'YycG112).

C) A trend line (Linear) was fitted to the initial time points of the reaction to estimate the relative initial rate of YycF phosphorylation. The slope for the trend line for phosphorylation of YycF by 'YycG is 1.68 while that for phosphorylation of YycF by 'YycG112 is 0.446.

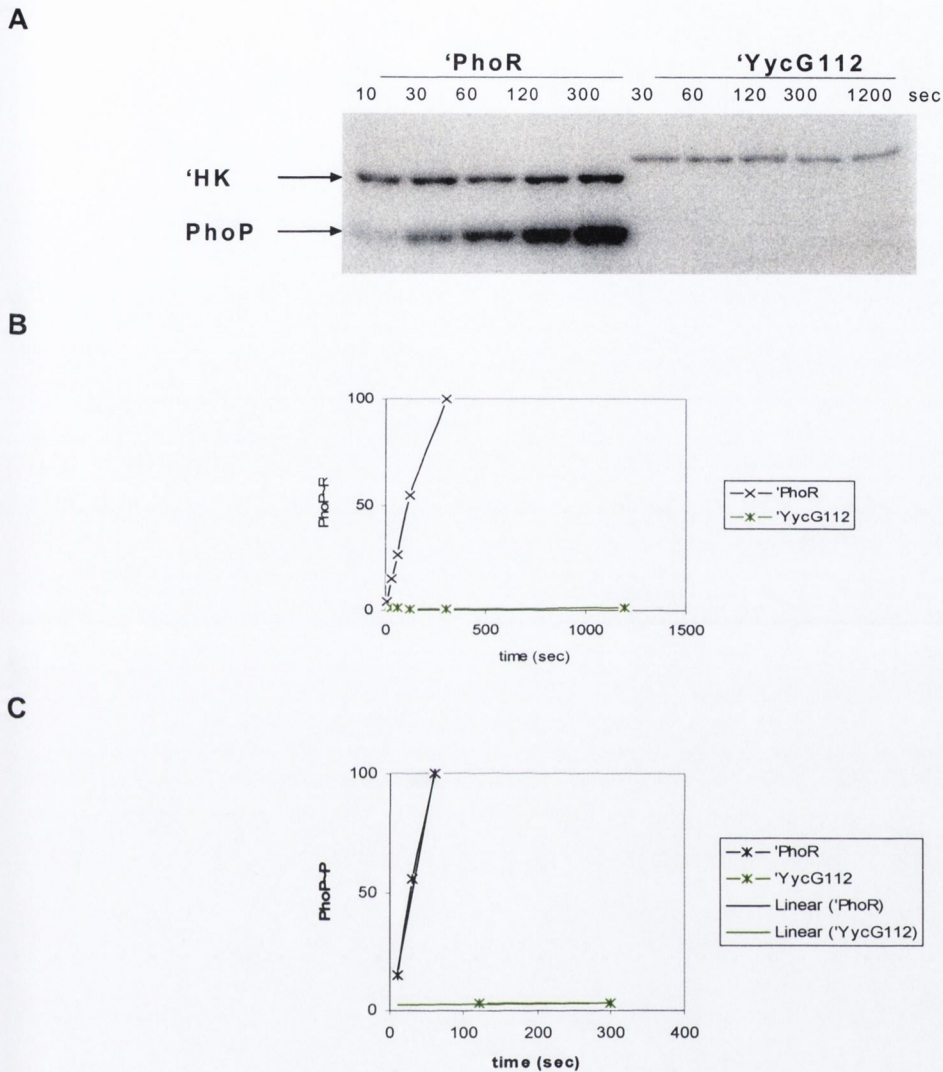


Figure 3.34 Phosphorylation of PhoP by histidine kinases 'PhoR and 'YycG112 in vitro.

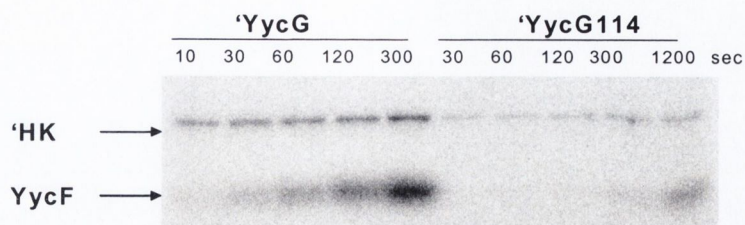
A kinetic analysis of PhoP phosphorylation by 'PhoR and 'YycG112 (S11G Y12T) *in vitro*.

A) Phosphoimage of PhoP phosphorylation by 'PhoR and 'YycG112 *in vitro*. Reaction conditions were as described in materials and methods. Reaction continued for 300 sec ('PhoR) and 1200 sec ('YycG112) with samples taken at the indicated time intervals (sec). The image was exposed for 90 min.

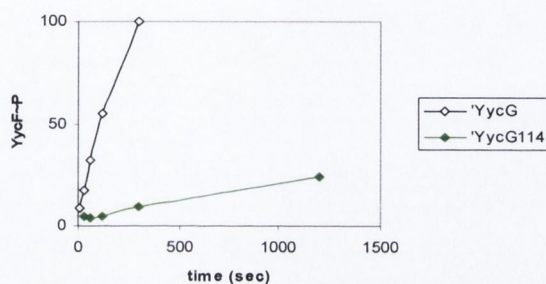
B) The phosphoimage (A) was quantified as described in materials and methods using MultiGauge2 software. Values were normalized to the amount of PhoP~P present at the 300 sec timepoint for the 'PhoR protein which was assigned a value of 100%. (black crosses = phosphorylation of PhoP by 'PhoR; green crosses = PhoP phosphorylation by 'YycG112).

C) A trend line (Linear) was fitted to the initial time points of the reaction to estimate the relative initial rate of YycF phosphorylation. The slope for the trend line for phosphorylation of PhoP by 'PhoR is 1.68 while that for phosphorylation of PhoP by 'YycG112 is 0.003.

A



B



C

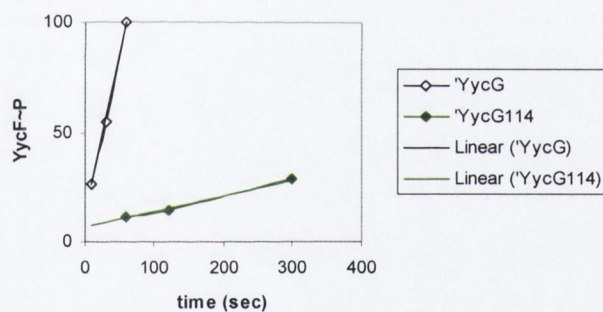


Figure 3.35 Phosphorylation of YycF by histidine kinases 'YycG and 'YycG114 in vitro.

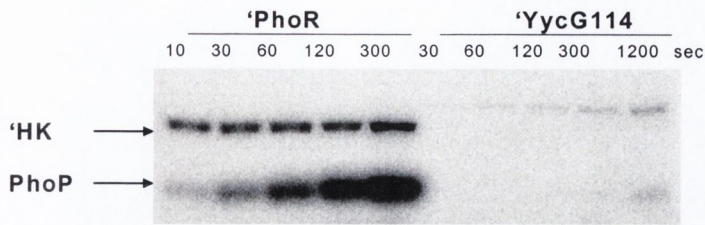
A kinetic analysis of YycF phosphorylation by 'YycG and 'YycG114 (R3K T8S S11G Y12F) *in vitro*.

A) Phosphoimage of YycF phosphorylation by 'YycG and 'YycG114 *in vitro*. Reaction continued for 300 sec ('YycG) and 1200 sec ('YycG114) with samples taken at the indicated time intervals (sec). The image was exposed for 90 min.

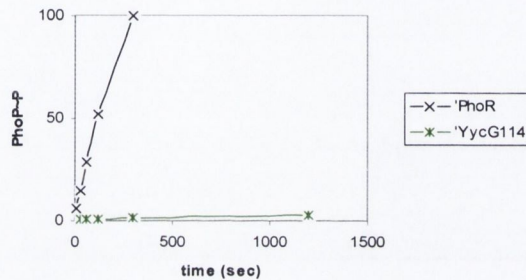
B) The phosphoimage (A) was quantified as described in materials and methods using MultiGauge2 software. Values were normalized to the amount of YycF~P present at the 300 sec timepoint for the 'YycG protein which was assigned a value of 100%. (black diamonds = phosphorylation of YycF by 'YycG; green diamonds = YycF phosphorylation by 'YycG114).

C) A trend line (Linear) was fitted to the initial time points of the reaction to estimate the relative initial rate of YycF phosphorylation. The slope for the trend line for phosphorylation of YycF by 'YycG is 1.77 while that for phosphorylation of YycF by 'YycG114 is 0.009.

A



B



C

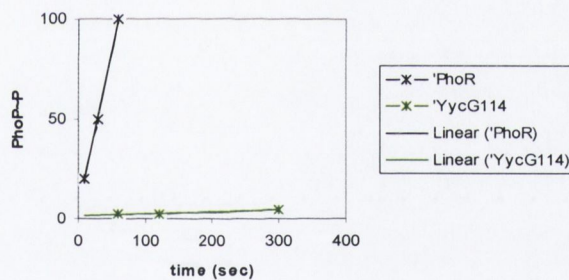


Figure 3.36 Phosphorylation of PhoP by histidine kinases 'PhoR and 'YycG114 in vitro.

A kinetic analysis of PhoP phosphorylation by 'PhoR and 'YycG114 (R3K T8S S11G Y12F) *in vitro*.

A) Phosphoimage of PhoP phosphorylation by 'PhoR and 'YycG114 *in vitro*. Reaction conditions were as described in materials and methods. Reaction continued for 300 sec ('PhoR) and 1200 sec ('YycG114) with samples taken at the indicated time intervals (sec). The image was exposed for 90 min.

B) The phosphoimage (A) was quantified as described in materials and methods using MultiGauge2 software. Values were normalized to the amount of PhoP~P present at the 300 sec timepoint for the 'PhoR protein which was assigned a value of 100%. (black crosses = phosphorylation of PhoP by 'PhoR; green crosses = PhoP phosphorylation by 'YycG114).

C) A trend line (Linear) was fitted to the initial time points of the reaction to estimate the relative initial rate of YycF phosphorylation. The slope for the trend line for phosphorylation of PhoP by 'PhoR is 1.60 while that for phosphorylation of PhoP by 'YycG114 is 0.01.

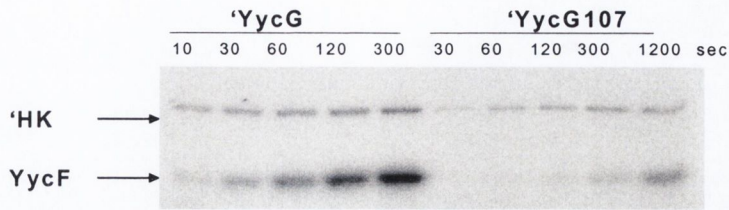
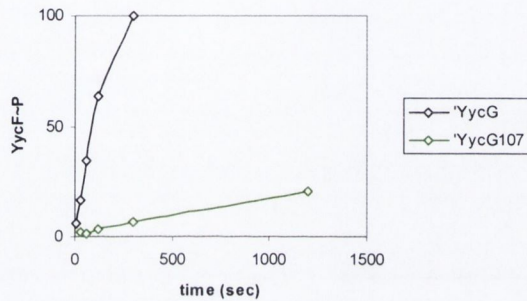
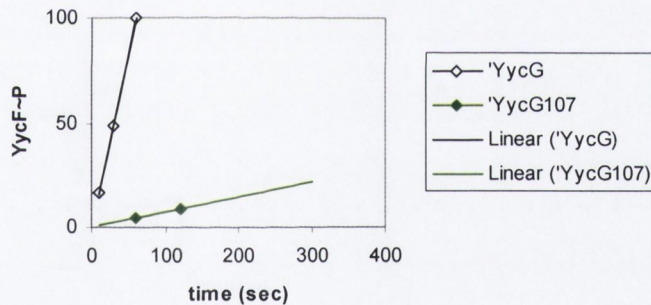
A**B****C**

Figure 3.37 Phosphorylation of YycF by histidine kinases 'YycG and 'YycG107 in vitro.

A kinetic analysis of YycF phosphorylation by 'YycG and 'YycG107 (R3K T8S R10K S11G Y12F) *in vitro*.

A) Phosphoimage of YycF phosphorylation by 'YycG and 'YycG107 *in vitro*. Reaction continued for 300 sec ('YycG) and 1200 sec ('YycG107) with samples taken at the indicated time intervals (sec). The image was exposed for 90 min.

B) The phosphoimage (A) was quantified as described in materials and methods using MultiGauge2 software. Values were normalized to the amount of YycF~P present at the 300 sec timepoint for the 'YycG protein which was assigned a value of 100%. (black diamonds = phosphorylation of YycF by 'YycG; green diamonds = YycF phosphorylation by 'YycG107).

C) A trend line (Linear) was fitted to the initial time points of the reaction to estimate the relative initial rate of YycF phosphorylation. The slope for the trend line for phosphorylation of YycF by 'YycG is 1.67 while that for phosphorylation of YycF by 'YycG107 is 0.070.

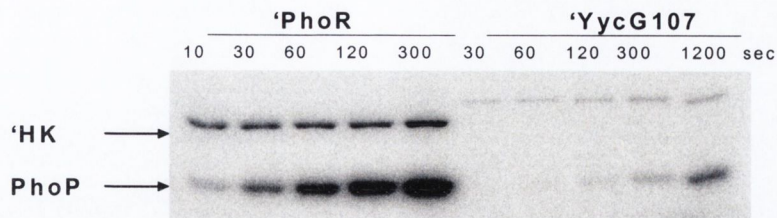
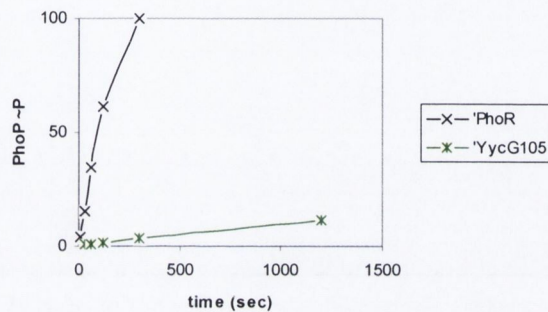
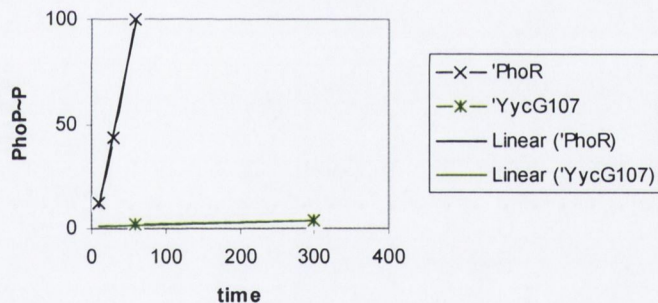
A**B****C**

Figure 3.38 Phosphorylation of PhoP by histidine kinase 'PhoR and 'YycG107 in vitro.

A kinetic analysis of PhoP phosphorylation by 'PhoR and 'YycG107 (R3K T8S R10K S11G Y12F) *in vitro*.

A) Phosphoimage of PhoP phosphorylation by 'PhoR and 'YycG107 *in vitro*. Reaction conditions were as described in materials and methods. Reaction continued for 300 sec ('PhoR) and 1200 sec ('YycG107) with samples taken at the indicated time intervals (sec). The image was exposed for 90 min.

B) The phosphoimage (A) was quantified as described in materials and methods using MultiGauge2 software. Values were normalized to the amount of PhoP~P present at the 300 sec timepoint for the 'PhoR protein which was assigned a value of 100%. (black crosses = phosphorylation of PhoP by 'PhoR; green crosses = PhoP phosphorylation by 'YycG107).

C) A trend line (Linear) was fitted to the initial time points of the reaction to estimate the relative initial rate of YycF phosphorylation. The slope for the trend line for phosphorylation of PhoP by 'PhoR is 1.77 while that for phosphorylation of PhoP by 'YycG107 is 0.009.

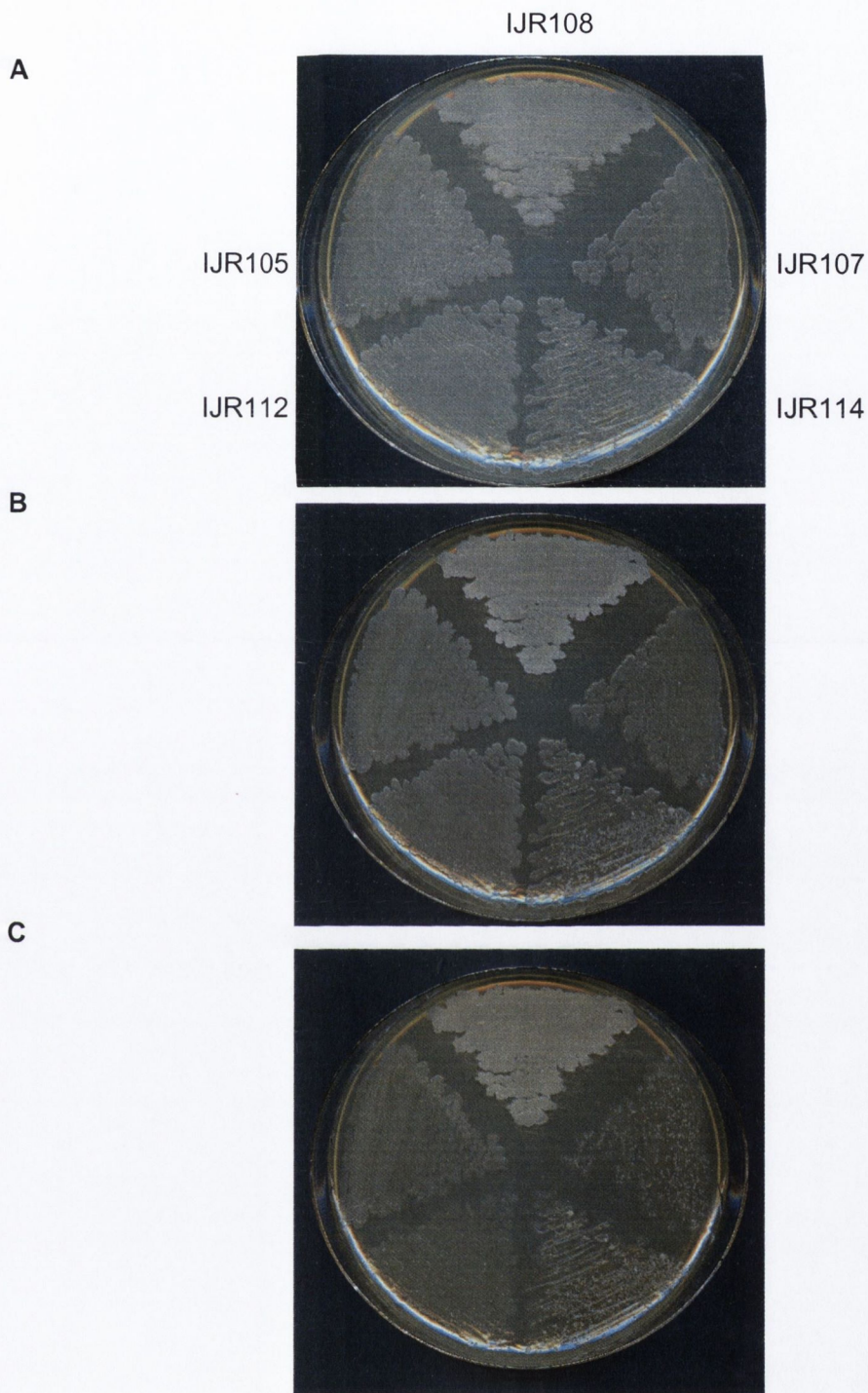


Figure 3.39 Growth of strains IJR108, IJR105, IJR112, IJR114 and IJR107 on LB agar. The strains IJR108 (wild-type), IJR105 (S11G), IJR112 (S11G Y12F), IJR114 (R3K T8S S11G Y12F) and IJR107 (R3K T8S R10K S11G Y12F) were grown of strains on LB supplemented with the appropriate antibiotics and monitored over a week. A) Growth after 24 hours, B) Growth after two days and C) after a week.

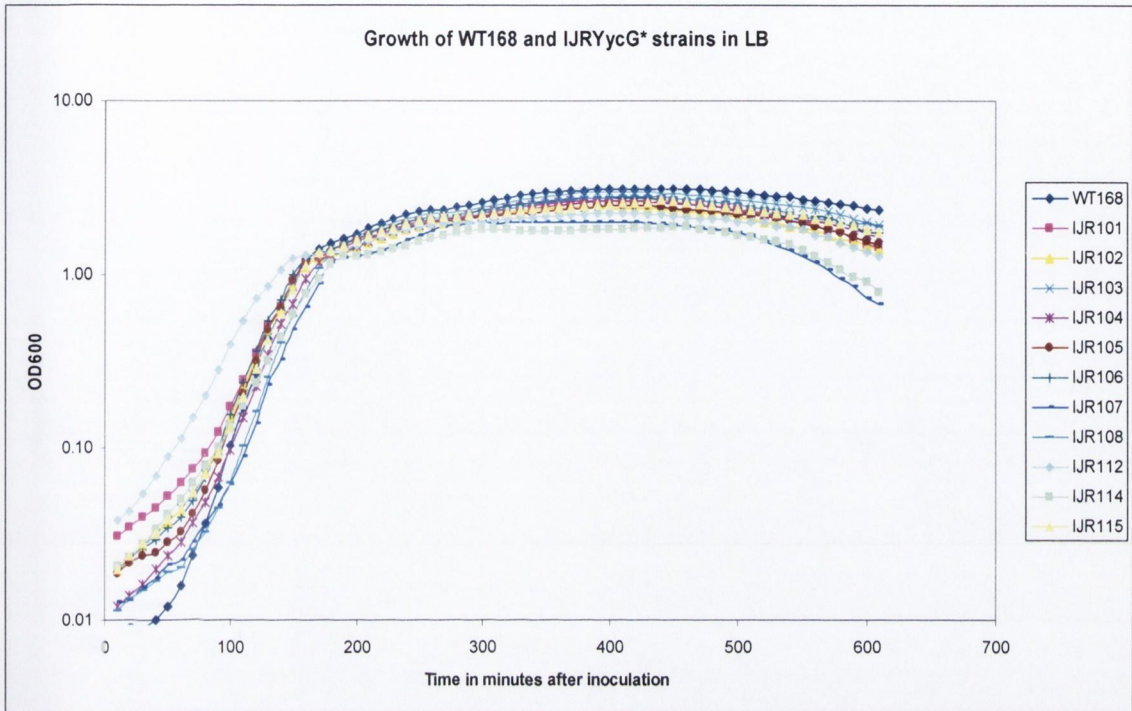


Figure 3.40 Growth of IJR strains in LB broth. Shown here are the growth curves of strain 168 and IJR101-115 in LB. The y-axis represents OD₆₀₀ on a log scale and the x-axis displays the time. Readings were taken every 10 min over a time course of 10 hours. The symbol and color designation of strains is shown in the legend on the right hand side. See text for details.

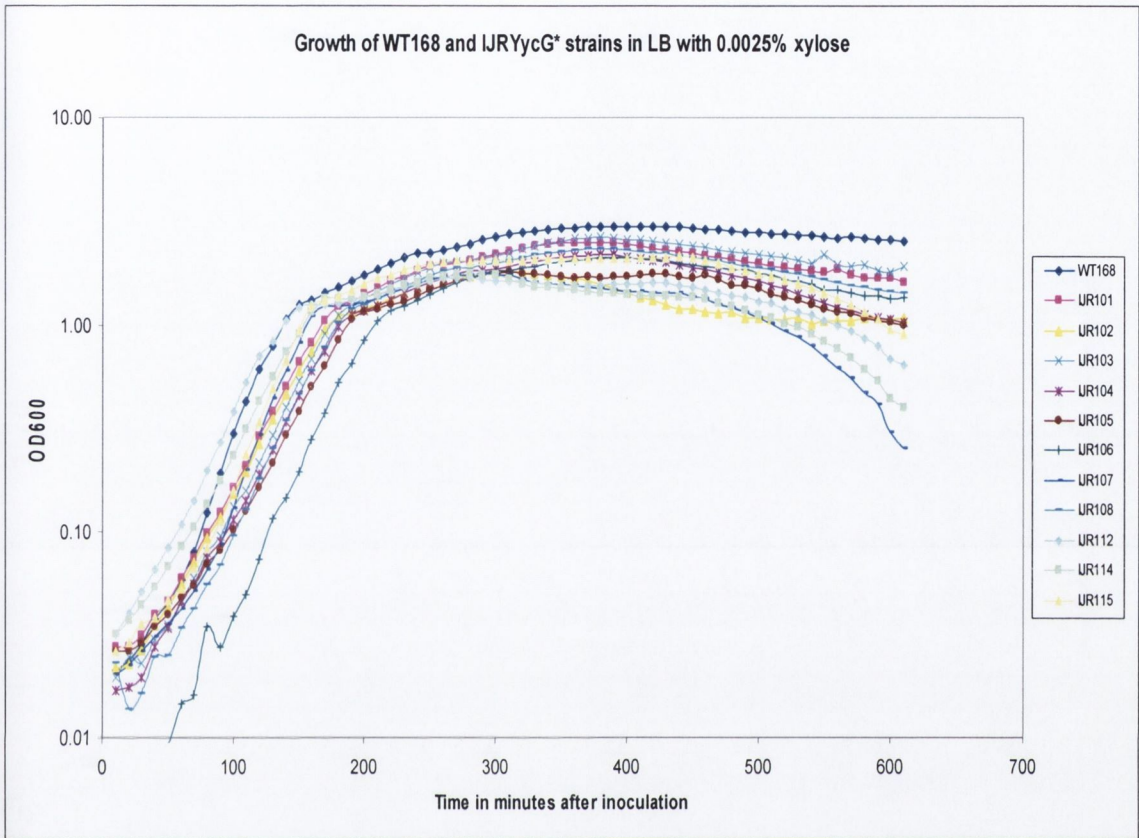


Figure 3.41 Growth of IJR strains in LB supplemented with 0.0025% xylose. Shown here are growth curves of strain 168 and IJR101-115 grown in LB supplemented with 0.0025% xylose. The y-axis represents OD_{600} in a log scale and the x-axis displays the time. Readings were taken every 10 min over a time course of 10 hours. The symbol and color designation of strains is shown in the legend on the right hand side. See text for details.

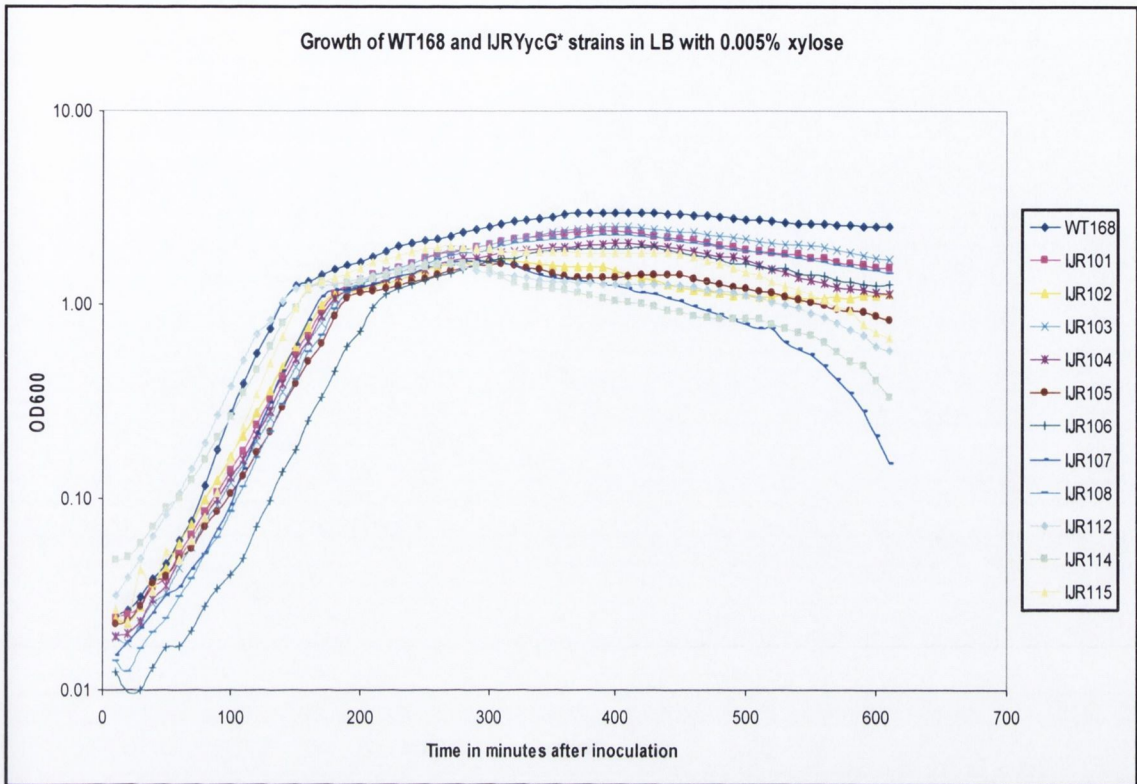


Figure 3.42 Growth of IJR strains in LB broth supplemented with 0.005% xylose. Shown here are the growth curves of strain 168 and IJR101-115 grown in LB supplemented with 0.005% xylose. The y-axis represents OD₆₀₀ in a log scale and the x-axis displays the time. Readings were taken every 10 min over a time course of 10 hours. The symbol and color designation of strains is shown in the legend on the right hand side. See text for detail.

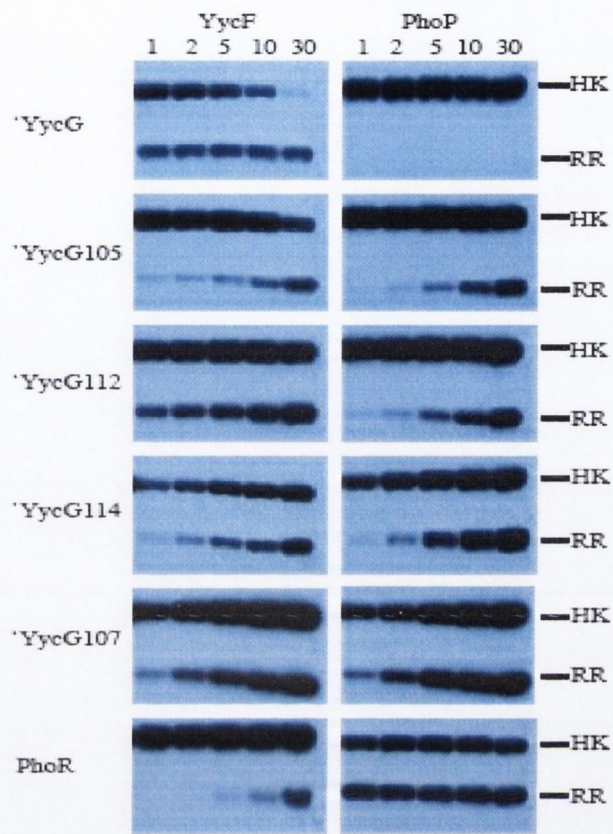


Figure 3.43 Summary of qualitative phosphorylation of YycF and PhoP RRs by the 'YycG, 'YycG* and 'PhoR kinases. The HK contained in the reaction is indicated on the left and the RR on top. The reactions were carried out as described continued for the indicated times measured in minutes. The mobility of the HK and RR in each reaction is indicated on the right.

Table 3.3 Summary of *in vivo* and *in vitro* assay results

amino acid change		<i>in vivo</i>	Qualitative <i>in vitro</i>		Quantitative <i>in vitro</i>	
		β -gal. spec.	phosphorylation		phosphorylation	
		act.	YycF	PhoP	YycF	PhoP
YycG	wild-type	3	++	-	ND	ND-
PhoR	wild-type	ND	+	++	ND	ND
YycG105	S11G	215	+	+	48%	0.2%
YycG112	S11G Y12F	570	++	+	27%	0.2%
YycG114	R3K T8S S11G Y12F	800	+	+	0.5%	0.6%
YycG107	R3K T8S R10K S11G Y12F	450	+	+	4%	0.5%

+ = phosphotransfer occurs
 ++ = strong phosphotransfer
 ND = not determined

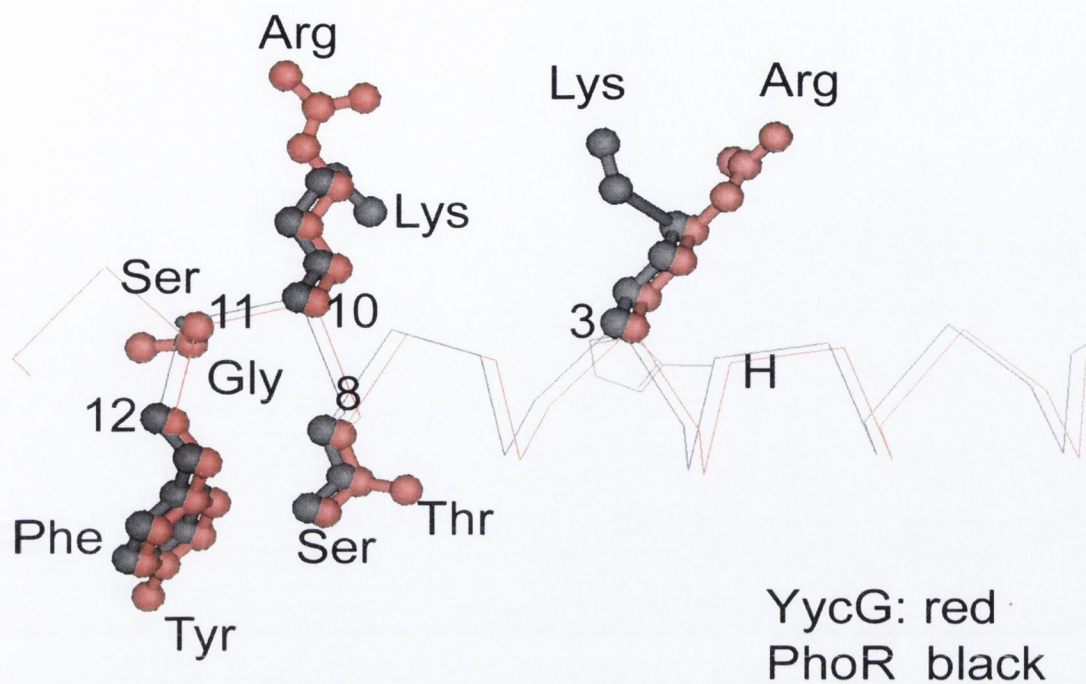


Figure 3.44 Alignment of the interacting residues of the YycG and PhoR α 1 helices. The five residues at positions +3, +8, +10, +11 and +12 of YycG (red) and PhoR (black). Comparing the size of the amino acid side of both HKs show that the side chains of those found in YycG are substantially larger than those at similar position in PhoR (K.I. Varughese, unpublished).

Anchor amino acids

Position	Spo0F	PhoP	YycF		
12	Q	E	E	α 1	
15	I	I	I	α 1	
18	L	L	I	α 1	L17I
56	K	M	M	loop3	
83	A	A	A	loop4	
84	Y	K	K	loop4	
105	P	P	P	loop5	
106	F	F	F	loop5	

Catalytic amino acids

10	D	D	D
11	D	D	D
54	D	D	D
82	T	T	T
104	K	K	K

Variable amino acids

14	G	S	P	α 1	S13P
21	E	Y	F	α 1	Y20F
85	G	D	D	loop4	
107	D	S	S	loop5	
108	I	P	T	loop5	P107T

Figure 4.2 Anchor, catalytic and variable amino acids of Spo0F, PhoP and YycF. The positions of the amino acids are designated according to Spo0F. The residues that differ between PhoP and YycF within these regions are shown in black according to their positions in PhoP. The catalytic amino acids are indicated in red, the anchor amino acids in blue and the variable amino acids in green.

Table 4.1 Amino acids changes introduced into PhoP.

Strain	Amino acid change	Mutation Number	Positions on the RR surface
IJ140		wild type	
IJ141	Pro->Thr	Single	107
IJ142	Ser->Pro	Single	13
IJ143	Leu->Ile	Single	17
IJ144	Tyr->Phe	Single	20
IJ145	Ser->Pro / Leu->Ile	Double	13/17
IJ146	Ser->Pro / Tyr->Phe	Double	13/20
IJ147	Leu->Ile / Tyr->Phe	Double	17/20
IJ148	Ser->Phe / Leu->Ile / Tyr->Phe	Triple	13/17/20
IJ149	Ser->Pro / Pro->Thr	Double	13/107
IJ150	Leu->Ile / Pro->Thr	Double	17/107
IJ151	Tyr->Phe / Pro->Thr	Double	20/107
IJ152	Ser->Pro / Leu->Ile / Pro->Thr	Triple	13/17/107
IJ153	Ser->Pro / Tyr->Phe / Pro->Thr	Triple	13/20/107
IJ154	Leu->Ile / Tyr->Phe / Pro->Thr	Triple	17/20/107
IJ155	Ser->Pro / Leu->Ile / Tyr->Phe / Pro->Thr	Quadruple	13/17/20/107

***B.subtilis* 168 chromosome**

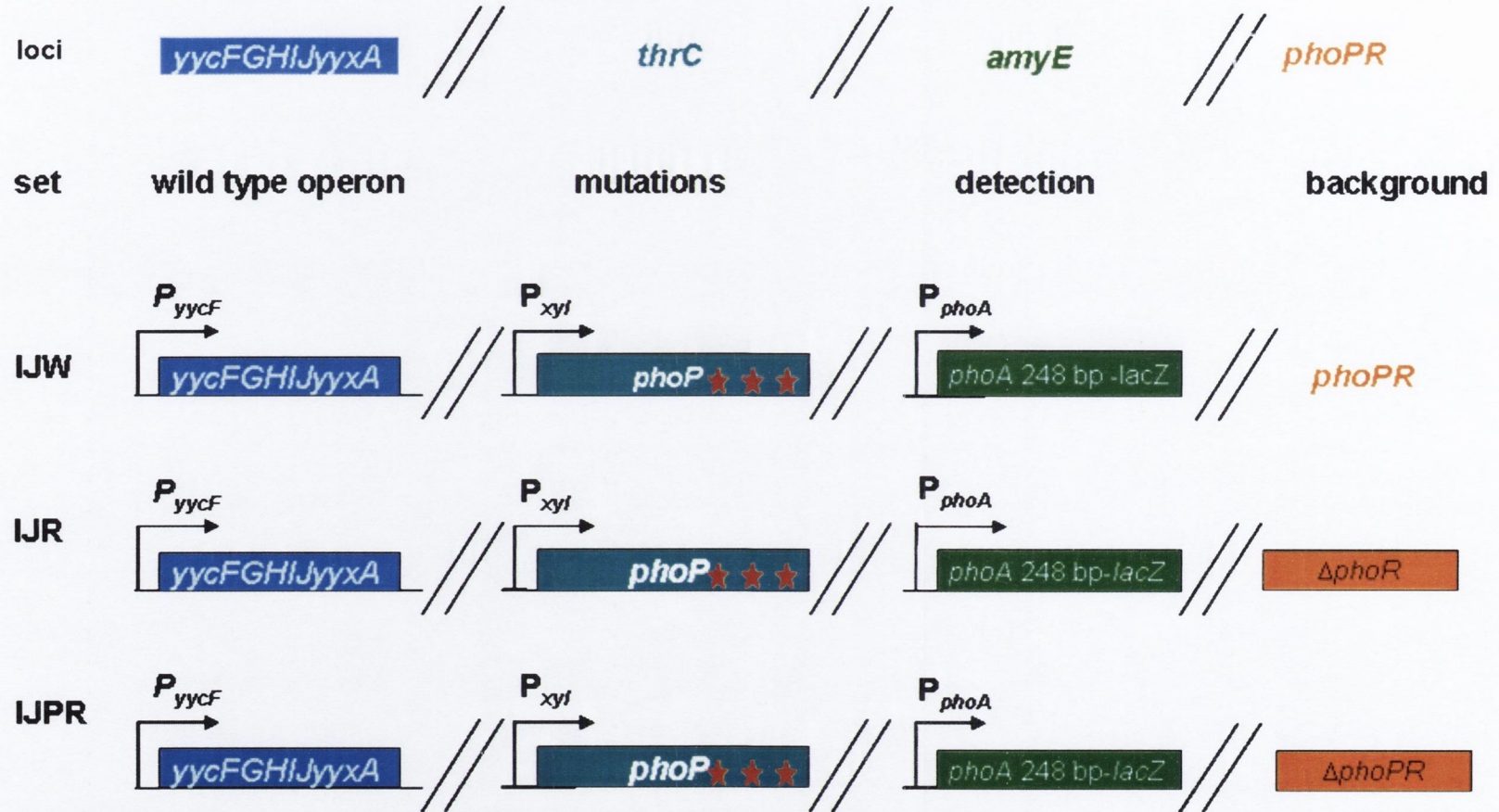


Figure 4.3 Genetic structure of strain sets IJW140-155, IJR140-155 and IJPR140-155. The relevant chromosomal loci of the *B.subtilis* chromosome are indicated at the top and are separated by //. The set name indicates the genetic background (IJW: wild-type, IJR: $\Delta phoR$ and IJPR: $\Delta phoPR$). The bent arrow stands for a promoter and the red star indicates mutations in PhoP as outlined in table 4.2.



Figure 4.4 Evaluation of PhoP* protein phosphorylation by YycG *in vivo*. β -galactosidase activity of strains carrying PhoP* mutant proteins in a $\Delta phoR$ background with single (left), double (middle) and triple (right) amino acid changes were plated on LB agar containing X-gal. Strain IJR140 (carrying wild-type PhoP) and IJR155 (four amino acid changes) were plated on each plate for reference.

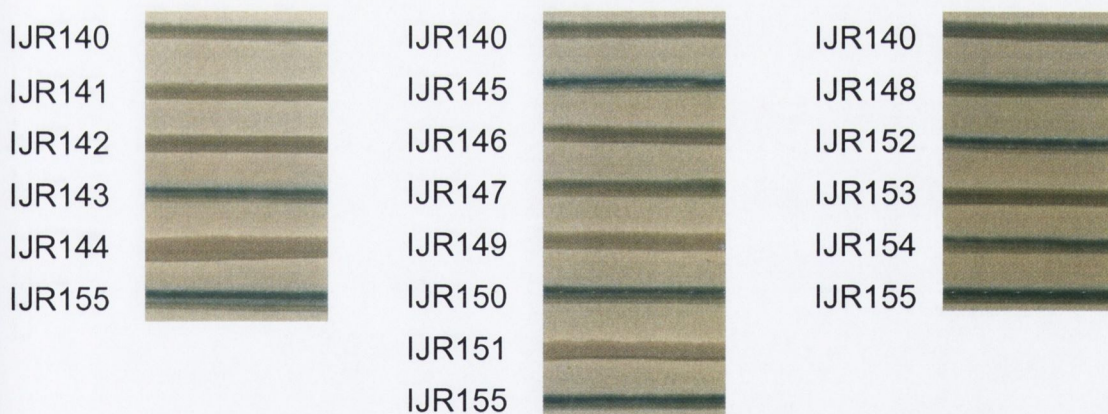


Figure 4.5 Evaluation of β -galactosidase activity in strains IJR140-155 in the presence of 0.005% xylose *in vivo*. β -galactosidase activity of strains carrying PhoP* mutant proteins in a $\Delta phoR$ background with single (left), double (middle) and triple (right) were plated on LB agar containing X-gal and 0.005% xylose. Strain IJR140 (carrying wild-type PhoP) and IJR155 (four amino acid changes) were plated on each plate for reference.



Figure 4.6 Evaluation of β -galactosidase activity of strains IJPR140-155 *in vivo*. β -galactosidase activity of strains carrying PhoP* mutant proteins in a $\Delta phoPR$ background with single (left), double (middle) and triple (right) amino acid changes were plated on LB agar supplemented with X-gal. Strain IJPR140 (carrying wild-type PhoP) and IJPR155 (four amino acids changes) were plated on each plate for reference.



Figure 4.7 *In vivo* β -galactosidase activity of strains IJPR140-155 in the presence of 0.0025% xylose. β -galactosidase activity of strains carrying PhoP* mutant proteins in a $\Delta phoPR$ background with single (left), double (middle) and triple (right) amino acid changes were plated on solid LB supplemented with 0.0025% xylose and X-gal. Strain IJPR140 (carrying wild-type PhoP) and IJPR155 (four amino acid changes) were plated on each plate for reference.



Figure 4.8 Evaluation of strains IJPR140-155 *in vivo* in the presence of 0.005% xylose supplementation. β -galactosidase activity of strains carrying PhoP* mutant proteins in a $\Delta phoPR$ background with single (left), double (middle) and triple (right) amino acid changes were plated on LB agar supplemented with 0.0025% xylose and X-gal. Strain IJPR140 (carrying wild-type PhoP) and IJPR155 (four amino acid changes) were plated on each plate for reference.

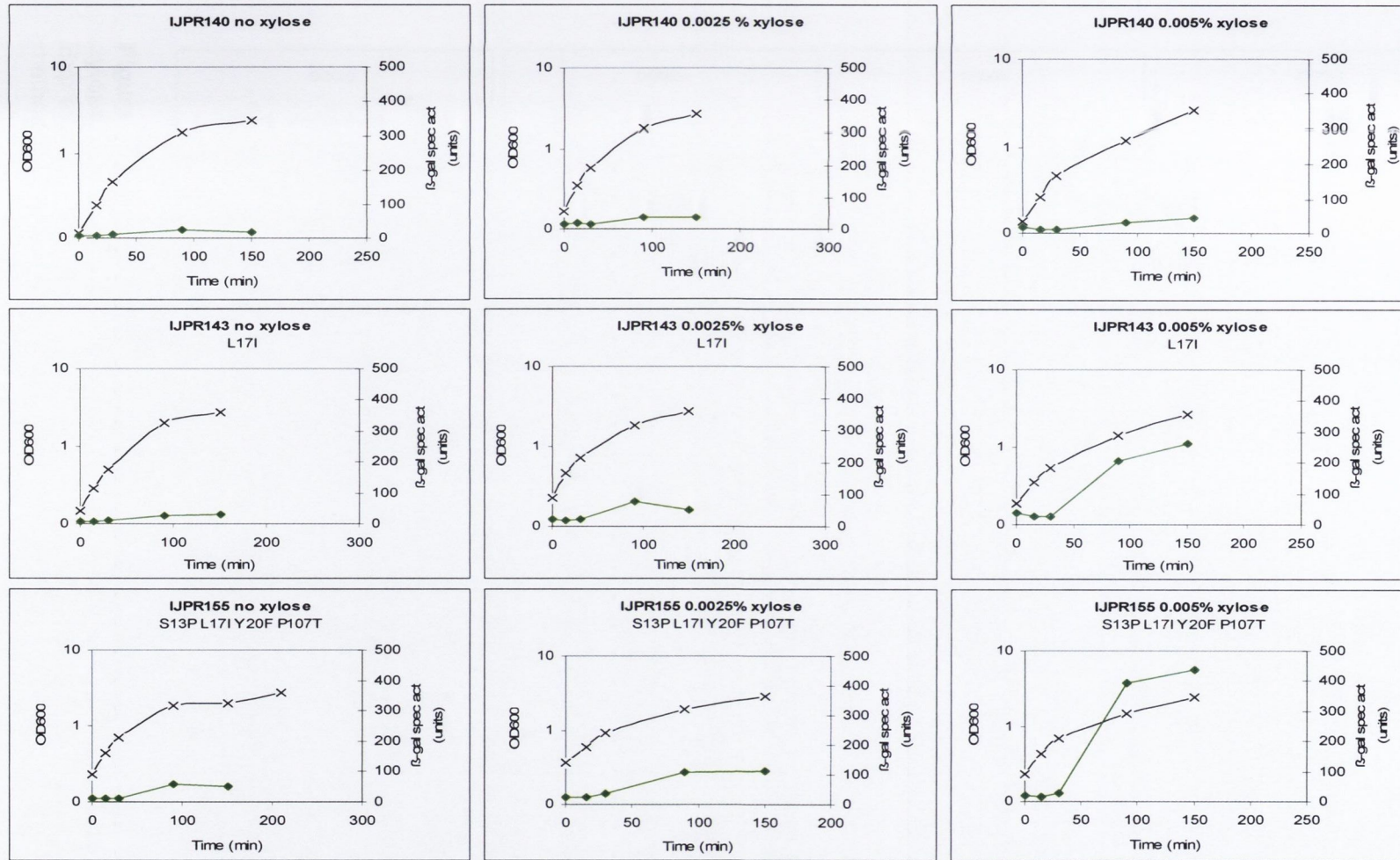


Figure 4.9 Growth and β -galactosidase profiles of IJPR140, IJPR143 and IJPR155. Strain names and the level of xylose in LB broth are indicated. Growth is shown in black crosses and the β -galactosidase specific activity (spec. act.) is shown in green diamonds.

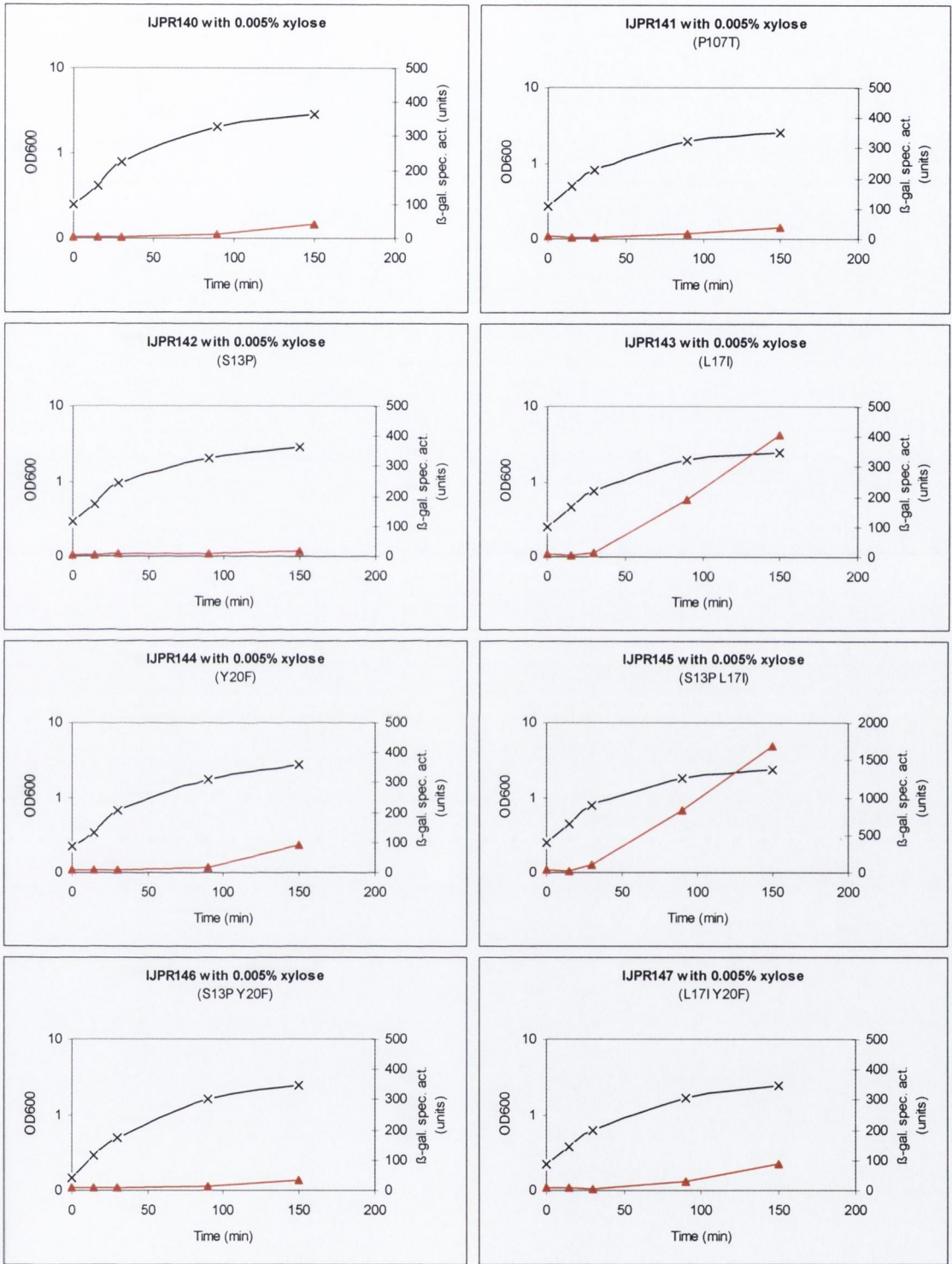


Figure 4.10 Growth of IJPR P_{xyl} - $phoP^*$ strains in LB broth supplemented with 0.005% xylose. Growth is measured by optical density (OD₆₀₀) and is indicated by crosses (X). Expression of β -galactosidase is measured in specific activity units (sec. act.) defined in methods and material) and indicated by red triangles (\blacktriangle). Time is measured in minutes.

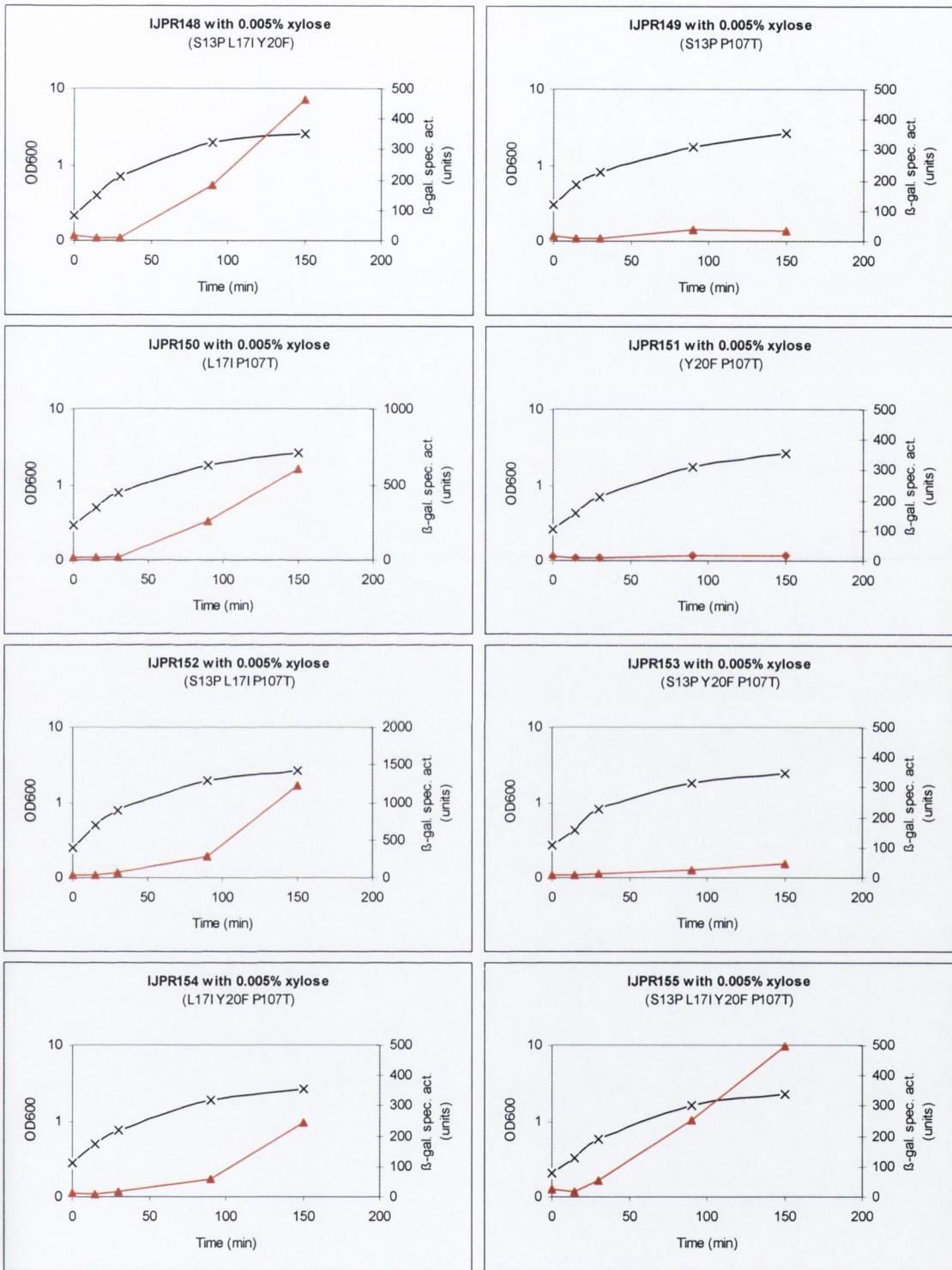


Figure 4.11 Growth of IJPR $P_{xyl}phoP^*$ strains in LB broth supplemented with 0.005% xylose. Growth is measured by optical density (OD_{600}) and is indicated by crosses (X). Expression of β -galactosidase is measured in specific activity units (sec. act.) defined in methods and material) and indicated by red triangles (\blacktriangle). Time is measured in minutes.

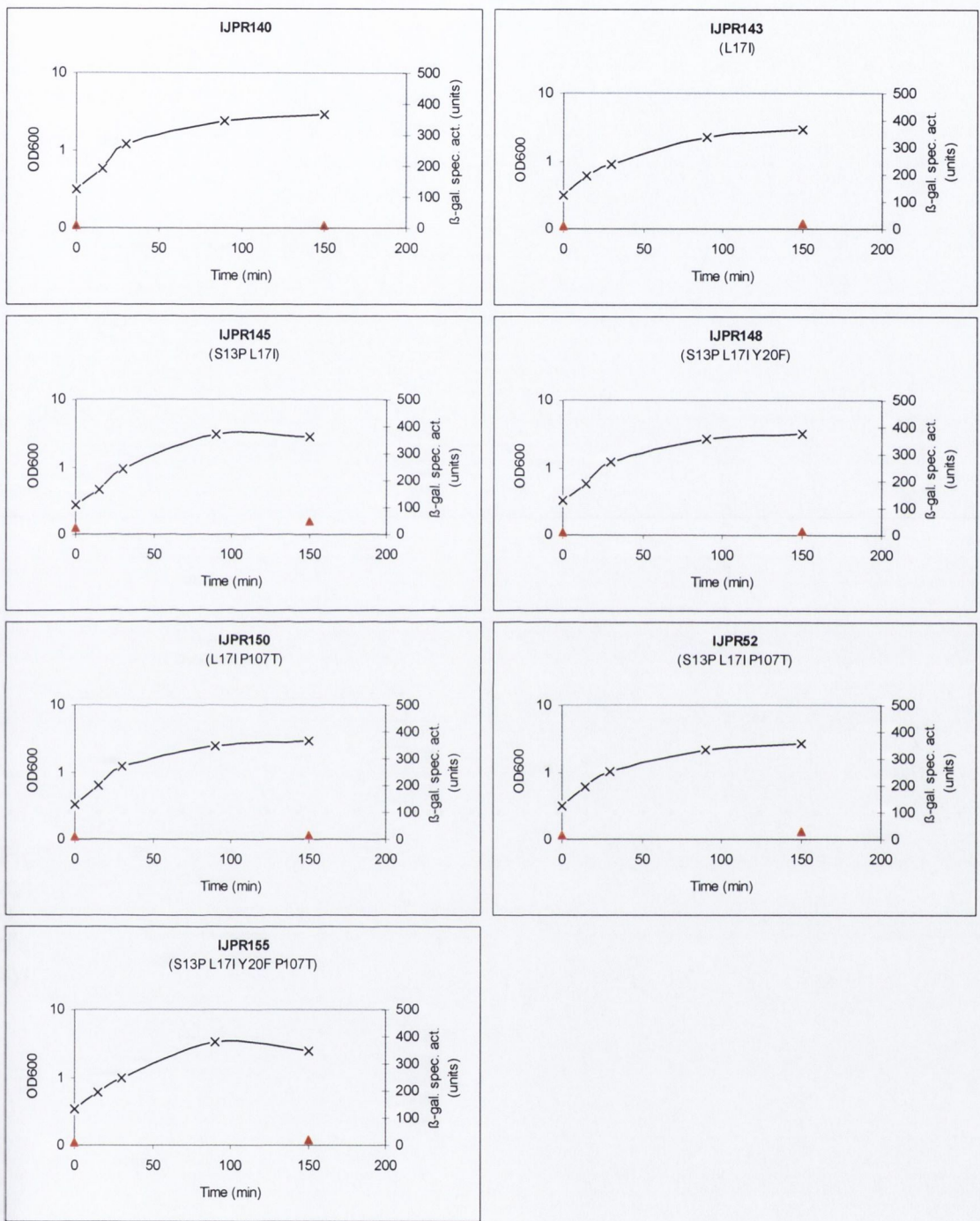


Figure 4.12 Growth of IJPR $P_{xyl}phoP^*$ strains in LB broth without addition of xylose. Growth is measured by optical density (OD₆₀₀) and is indicated by crosses (X). Expression of β -galactosidase is measured in specific activity units (sec. act.) defined in methods and material) and indicated by red triangles (▲). Time is measured in minutes.

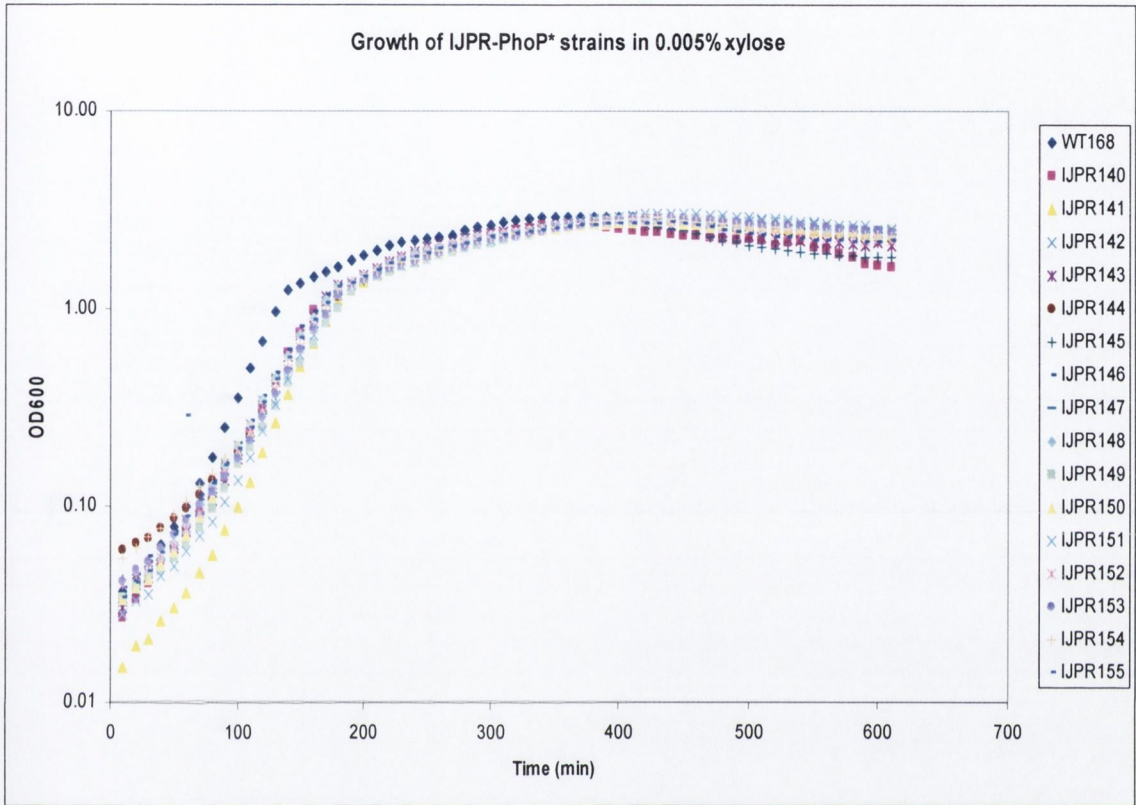


Figure 4.13 Growth of IJPR mutant strains in LB broth supplemented with 0.005% xylose. The growth curves of strains 168 and IJPR140-155 in LB broth supplemented with 0.005% xylose. The y-axis shows growth measured at OD₆₀₀ on a log scale and the x-axis displays the time. Readings were taken every 10 min over a time course of 10 hours. The symbol and color designation of strains is shown in the legend on the right hand side.

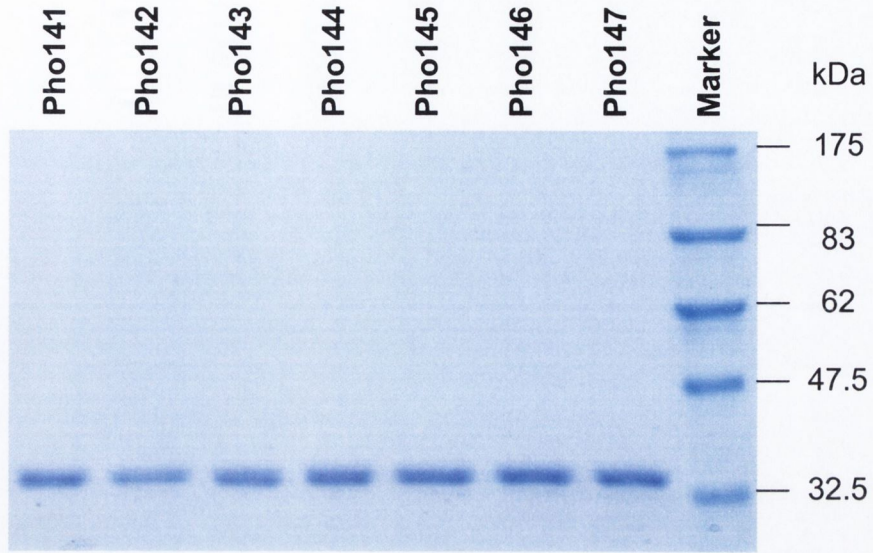
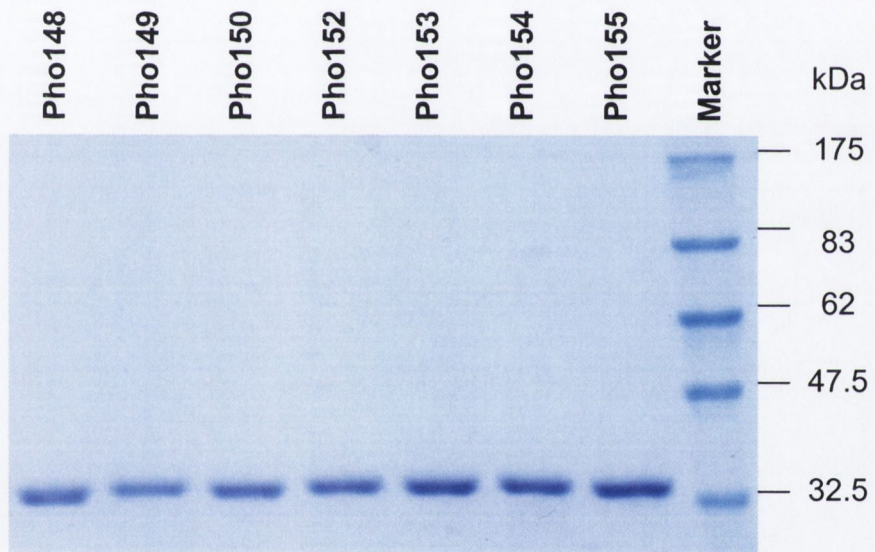
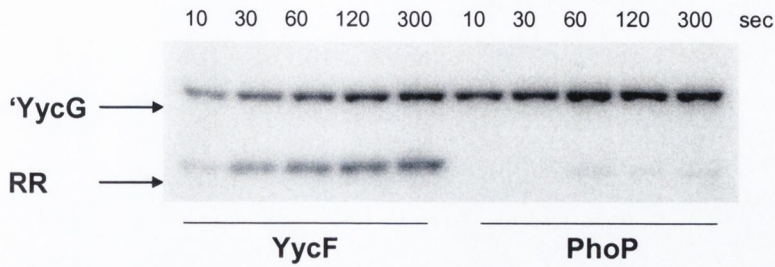
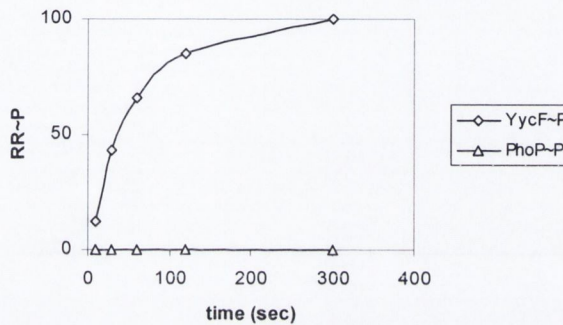
A**B**

Figure 4.14 Analysis of purified mutated PhoP* protein by SDS PAGE. A) Shown are the purified proteins PhoP141-PhoP147 as indicated above. The molecular weight marker is shown on the right in kDa. B) Shown are the purified proteins Pho148-Pho155. The molecular weight marker is shown on the right in kDa. 4.3 μg of each protein was loaded onto each lane.

A



B



C

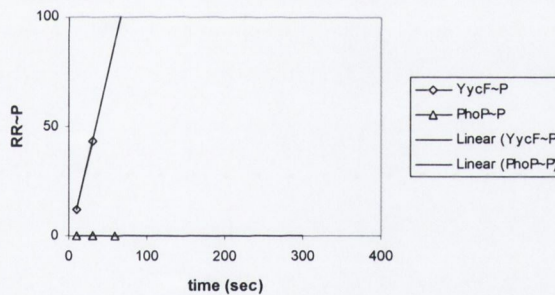


Figure 4.15 Phosphorylation of response regulators YycF and PhoP by 'YycG *in vitro*.

A kinetic analysis of YycF and PhoP phosphorylation by 'YycG *in vitro*.

A) Phosphoimage of YycF and PhoP phosphorylation by 'YycG *in vitro*. Reactions continued for 300 (YycF) and 300 (PhoP) sec with samples taken at the indicated time intervals (sec). This image was exposed for 90 min.

B) The phosphoimage (A) was quantified as described in Materials and Methods using MultiGauge2 software. Values were normalized to the amount of YycF~P present at the 300 sec timepoint for the 'YycG protein which was assigned a value of 100% (black diamonds = phosphorylation of YycF by 'YycG; black triangles = phosphorylation of PhoP by 'YycG).

C) A linear trend line was fitted to the initial time points of the reaction to estimate the relative initial rate of PhoP phosphorylation. The slope for the trend line for phosphorylation of YycF by 'YycG is 1.567 while that for phosphorylation of PhoP by 'YycG is 0.000.

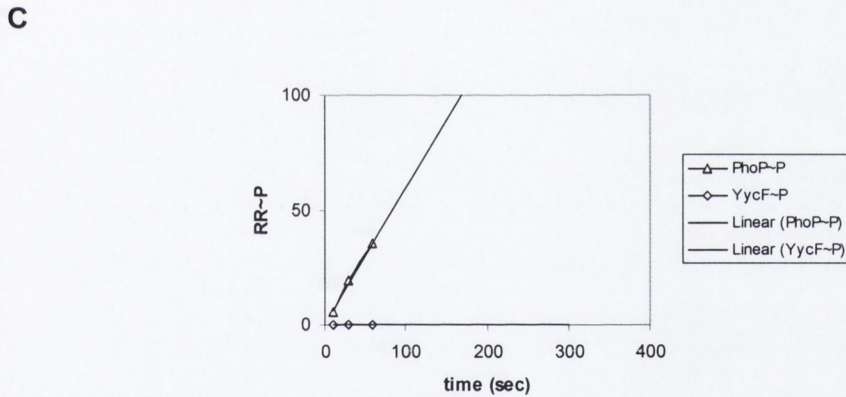
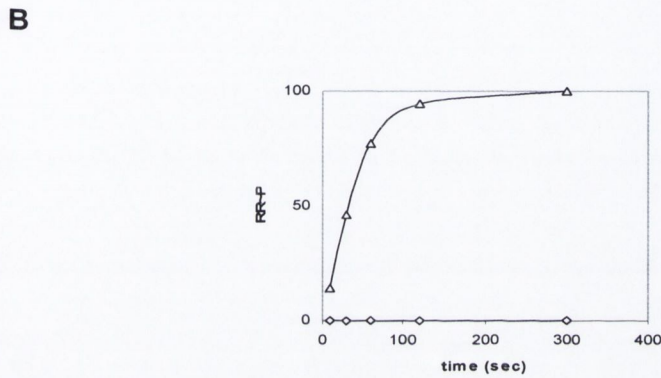
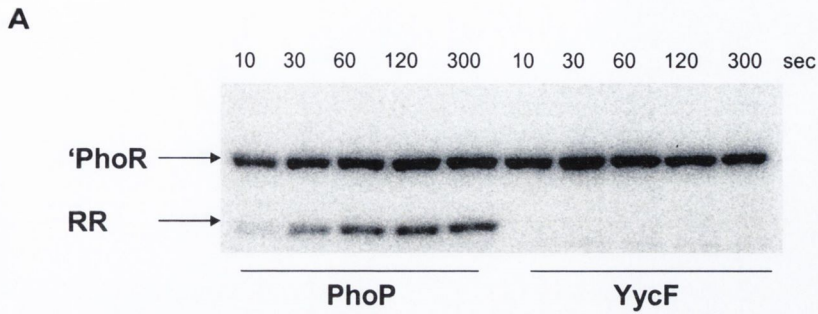


Figure 4.16 Phosphorylation of response regulators PhoP and YycF by 'PhoR *in vitro*. A kinetic analysis of PhoP and YycF phosphorylation by 'PhoR *in vitro*.

A) Phosphoimage of PhoP and YycF phosphorylation by 'PhoR *in vitro*. Reactions continued for 300 (PhoP) and 300 (YycF) sec with samples taken at the indicated time intervals (sec). This image was exposed for 90 min.

B) The phosphoimage (A) was quantified as described in Materials and Methods using MultiGauge2 software. Values were normalized to the amount of PhoP~P present at the 300 sec timepoint for the 'PhoR protein which was assigned a value of 100% (black triangles = phosphorylation of PhoP by 'PhoR; black diamonds = phosphorylation of YycG by 'PhoR).

C) A linear trend line was fitted to the initial time points of the reaction to estimate the relative initial rate of PhoP phosphorylation. The slope for the trendline for phosphorylation of PhoP by 'PhoR is 0.592 while that for phosphorylation of YycF by 'PhoR is 0.000.

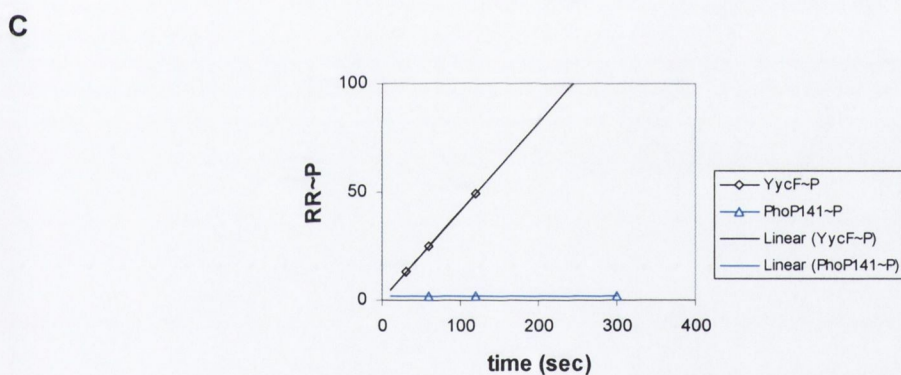
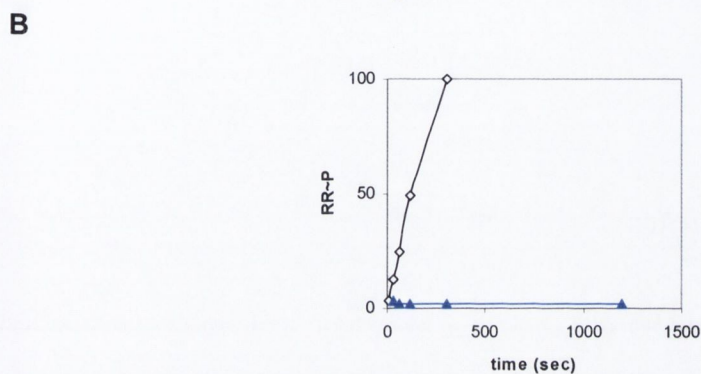
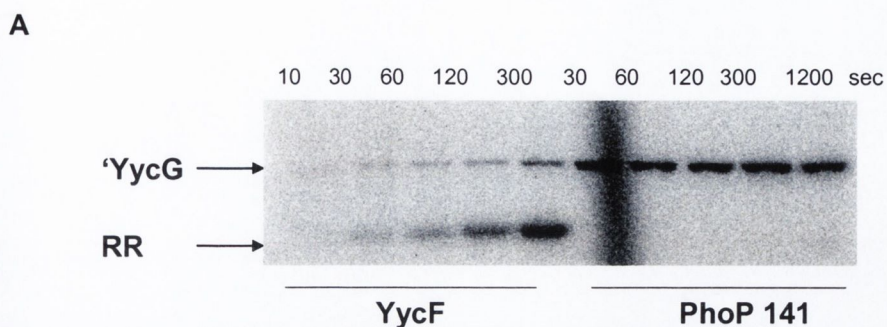


Figure 4.17 Phosphorylation of response regulators YycF and PhoP141 by 'YycG *in vitro*. A kinetic analysis of YycF and PhoP141 (P107T) phosphorylation by 'YycG *in vitro*.

A) Phosphoimage of YycF and PhoP141 phosphorylation by YycG *in vitro*. Reactions continued for 300 (YycF) and 1200 (PhoP141) sec with samples taken at the indicated time intervals (sec). This image was exposed for 90 min.

B) The phosphoimage (A) was quantified as described in Materials and Methods using MultiGauge2 software. Values were normalized to the amount of YycF~P present at the 300 sec timepoint for the 'YycG protein which was assigned a value of 100% (black diamonds = phosphorylation of YycF by 'YycG; blue closed triangles = phosphorylation of PhoP142 by 'YycG).

C) A linear trend line was fitted to the initial time points of the reaction to estimate the relative initial rate of PhoP phosphorylation. The slope for the trend line for phosphorylation of YycF by 'YycG is 0.408 while that for phosphorylation of PhoP141 by 'YycG is 0.000.

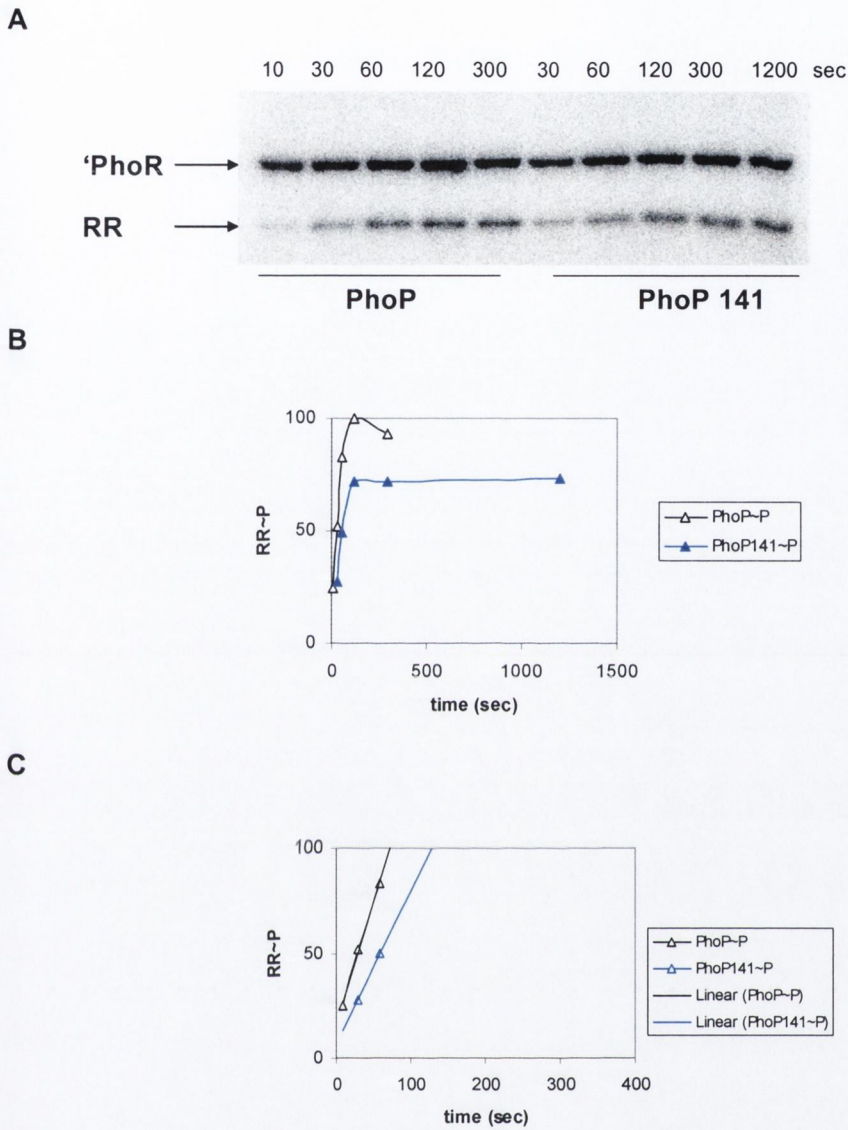


Figure 4.18 Phosphorylation of response regulators PhoP and PhoP141 by 'PhoR *in vitro*. A kinetic analysis of PhoP and PhoP141 (P107T) phosphorylation by 'PhoR *in vitro*. A) Phosphoimage of PhoP and PhoP141 phosphorylation by 'PhoR *in vitro*. Reactions continued for 300 (PhoP) and 1200 (PhoP141) sec with samples taken at the indicated time intervals (sec). This image was exposed for 90 min. B) The phosphoimage (A) was quantified as described in Materials and Methods using MultiGauge2 software. Values were normalized to the amount of PhoP~P present at the 300 sec timepoint for the 'PhoR protein which was assigned a value of 100% (black triangles = phosphorylation of PhoP by 'PhoR; blue open triangles = phosphorylation of PhoP141G by 'PhoR). C) A linear trend line was fitted to the initial time points of the reaction to estimate the relative initial rate of PhoP phosphorylation. The slope for the trendline for phosphorylation of PhoP by 'PhoR is 1.161 while that for phosphorylation of PhoP141 by 'PhoR is 0.731.

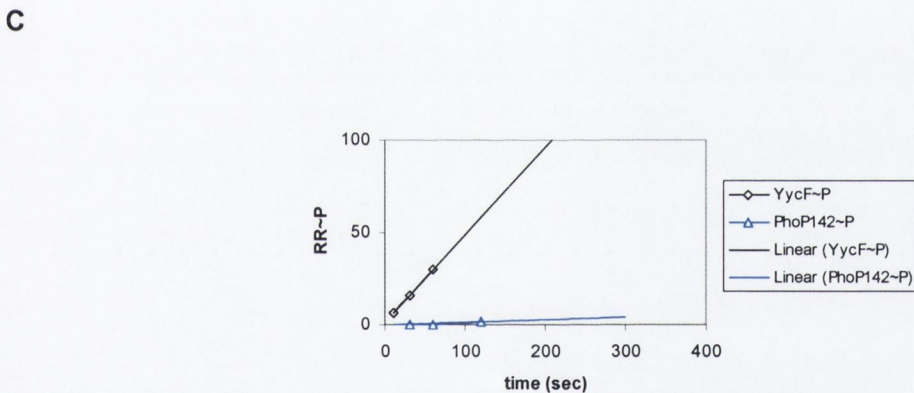
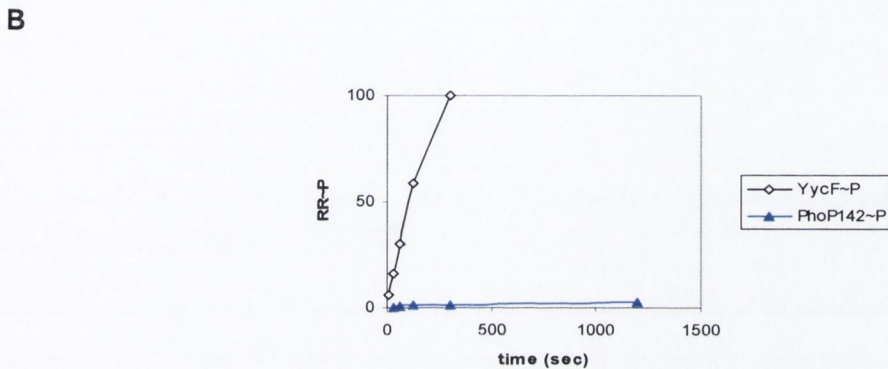
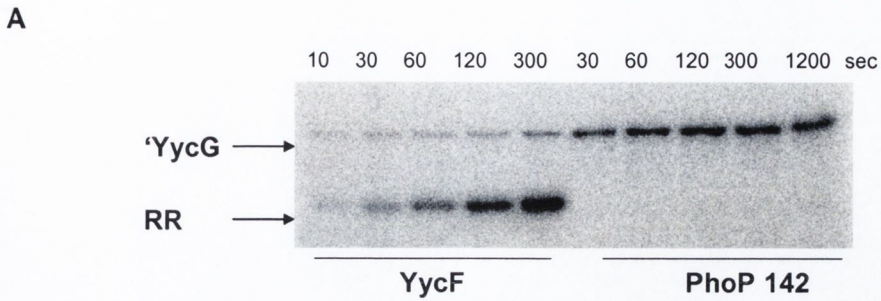


Figure 4.19 Phosphorylation of response regulators YycF and PhoP142 by 'YycG *in vitro*. A kinetic analysis of YycF and PhoP142 (S13P) phosphorylation by 'YycG *in vitro*.

A) Phosphoimage of YycF and PhoP141 phosphorylation by YycG *in vitro*. Reactions continued for 300 (YycF) and 1200 (PhoP142) sec with samples taken at the indicated time intervals (sec). This image was exposed for 90 min.

B) The phosphoimage (A) was quantified as described in Materials and Methods using MultiGauge2 software. Values were normalized to the amount of YycF~P present at the 300 sec timepoint for the 'YycG protein which was assigned a value of 100% (black diamonds = phosphorylation of YycF by 'YycG; blue closed triangles = phosphorylation of PhoP142 by 'YycG).

C) A linear trend line was fitted to the initial time points of the reaction to estimate the relative initial rate of PhoP phosphorylation. The slope for the trend line for phosphorylation of YycF by 'YycG is 0.472 while that for phosphorylation of PhoP142 by 'YycG is 0.014.

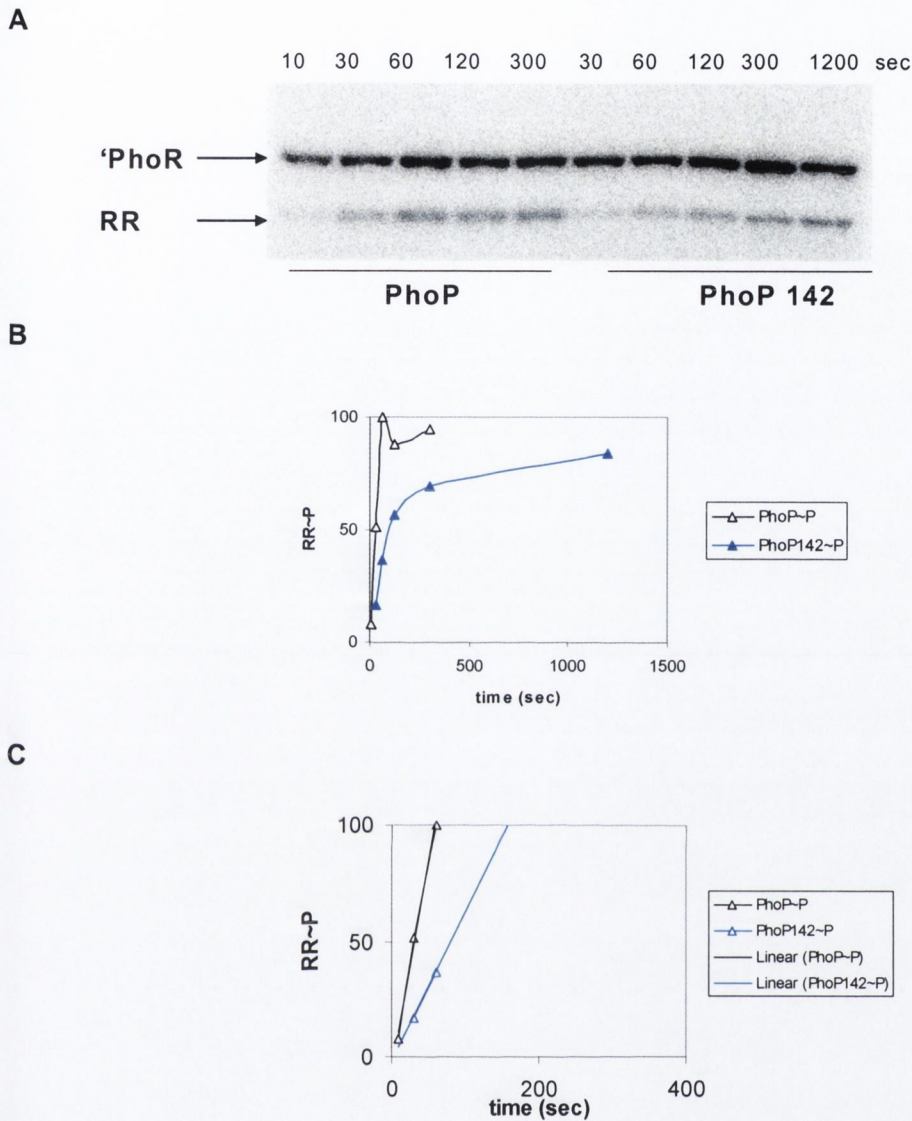
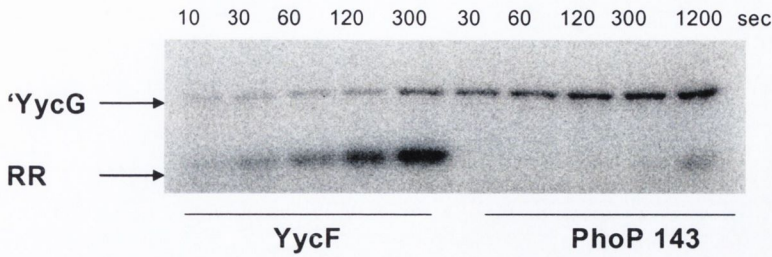
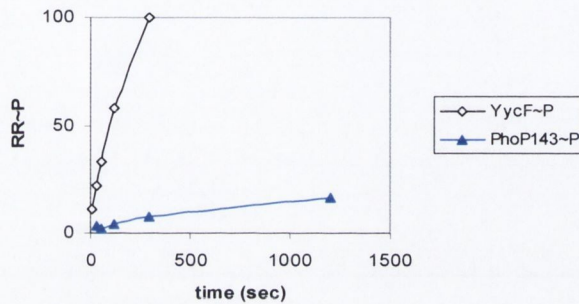


Figure 4.20 Phosphorylation of response regulators PhoP and PhoP142 by 'PhoR *in vitro*. A kinetic analysis of PhoP and PhoP142 (S13P) phosphorylation by 'PhoR *in vitro*. A) Phosphoimage of PhoP and PhoP142 phosphorylation by 'PhoR *in vitro*. Reactions continued for 300 (PhoP) and 1200 (PhoP142) sec with samples taken at the indicated time intervals (sec). This image was exposed for 90 min. B) The phosphoimage (A) was quantified as described in Materials and Methods using MultiGauge2 software. Values were normalized to the amount of PhoP~P present at the 300 sec timepoint for the 'PhoR protein which was assigned a value of 100% (black triangles = phosphorylation of PhoP by 'PhoR; blue open triangles = phosphorylation of PhoP142 by 'PhoR). C) A linear trend line was fitted to the initial time points of the reaction to estimate the relative initial rate of PhoP phosphorylation. The slope for the trendline for phosphorylation of PhoP by 'PhoR is 1.82 while that for phosphorylation of PhoP141 by 'PhoR is 0.650.

A



B



C

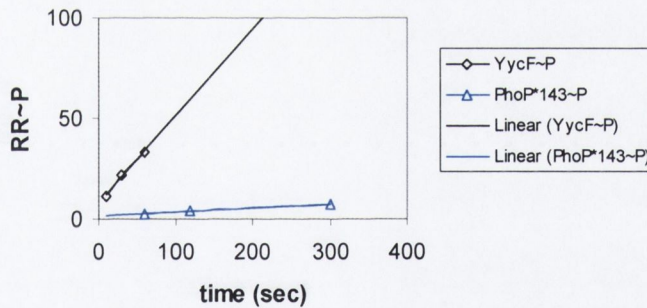
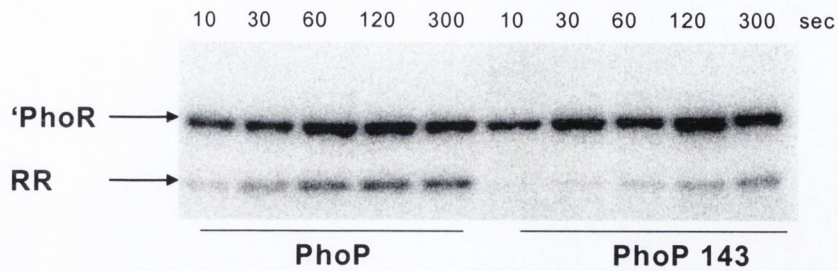
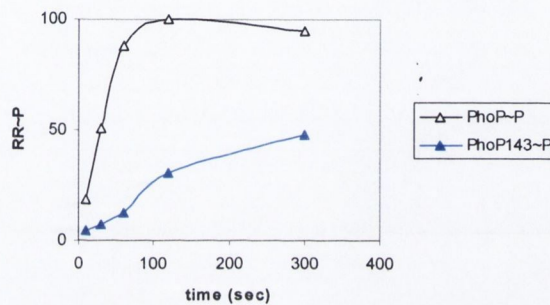


Figure 4.21 Phosphorylation of response regulators YycF and PhoP143 by 'YycG *in vitro*. A kinetic analysis of YycF and PhoP143 (L171) phosphorylation by 'YycG *in vitro*. A) Phosphoimage of YycF and PhoP143 phosphorylation by YycG *in vitro*. Reactions continued for 300 (YycF) and 1200 (PhoP143) sec with samples taken at the indicated time intervals (sec). This image was exposed for 90 min. B) The phosphoimage (A) was quantified as described in Materials and Methods using MultiGauge2 software. Values were normalized to the amount of YycF~P present at the 300 sec timepoint for the 'YycG protein which was assigned a value of 100% (black diamonds = phosphorylation of YycF by 'YycG; blue closed triangles = phosphorylation of PhoP143 by 'YycG). C) A linear trend line was fitted to the initial time points of the reaction to estimate the relative initial rate of PhoP phosphorylation. The slope for the trend line for phosphorylation of YycF by 'YycG is 0.434 while that for phosphorylation of PhoP143 by 'YycG is 0.021.

A



B



C

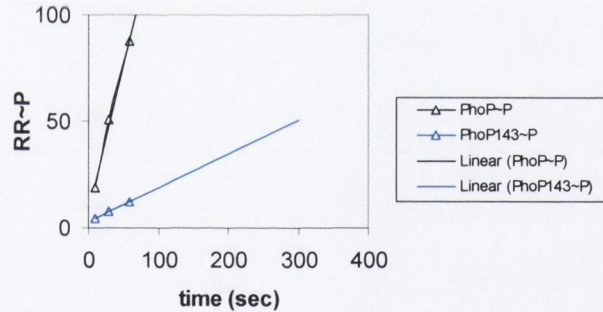
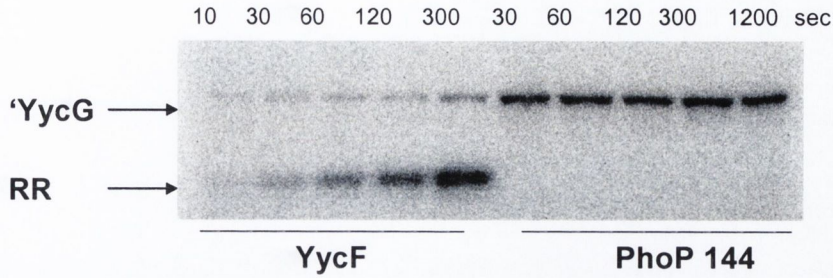
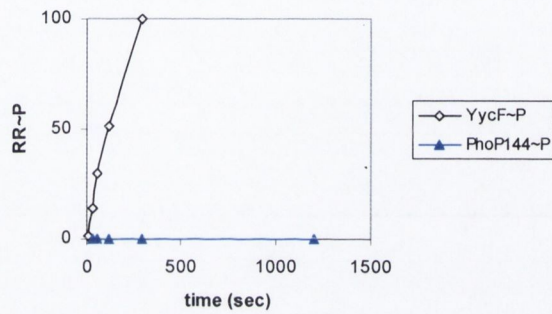


Figure 4.22 Phosphorylation of response regulators PhoP and PhoP143 by 'PhoR *in vitro*. A kinetic analysis of PhoP and PhoP143 (L171) phosphorylation by 'PhoR *in vitro*. A) Phosphoimage of PhoP and PhoP143 phosphorylation by 'PhoR *in vitro*. Reactions continued for 300 (PhoP) and 300 (PhoP143) sec with samples taken at the indicated time intervals (sec). This image was exposed for 90 min. B) The phosphoimage (A) was quantified as described in Materials and Methods using MultiGauge2 software. Values were normalized to the amount of PhoP~P present at the 300 sec timepoint for the 'PhoR protein which was assigned a value of 100% (black triangles = phosphorylation of PhoP by 'PhoR; blue open triangles = phosphorylation of PhoP143 by 'PhoR). C) A linear trend line was fitted to the initial time points of the reaction to estimate the relative initial rate of PhoP phosphorylation. The slope for the trendline for phosphorylation of PhoP by 'PhoR is 1.375 while that for phosphorylation of PhoP143 by 'PhoR is 0.159.

A



B



C

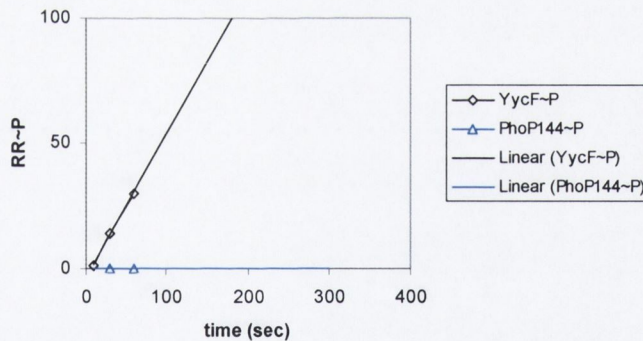


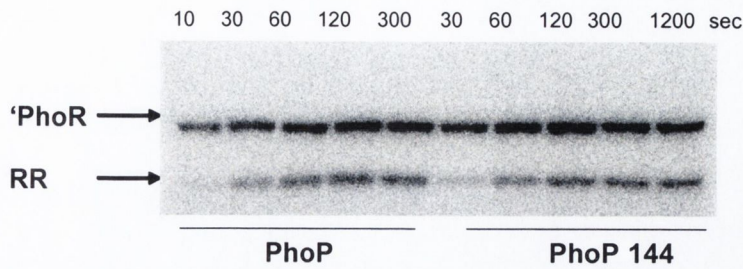
Figure 4.23 Phosphorylation of response regulators YycF and PhoP144 by YycG *in vitro*. A kinetic analysis of YycF and PhoP144 (Y20F) phosphorylation by YycG *in vitro*.

A) Phosphoimage of YycF and PhoP144 phosphorylation by YycG *in vitro*. Reactions continued for 300 (YycF) and 1200 (PhoP144) sec with samples taken at the indicated time intervals (sec). This image was exposed for 90 min.

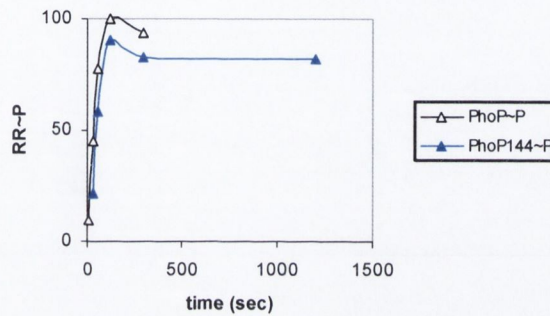
B) The phosphoimage (A) was quantified as described in Materials and Methods using MultiGauge2 software. Values were normalized to the amount of YycF~P present at the 300 sec timepoint for the YycG protein which was assigned a value of 100% (black diamonds = phosphorylation of YycF by YycG; blue closed triangles = phosphorylation of PhoP144 by YycG).

C) A linear trend line was fitted to the initial time points of the reaction to estimate the relative initial rate of PhoP phosphorylation. The slope for the trend line for phosphorylation of YycF by YycG is 0.574 while that for phosphorylation of PhoP144 by YycG is 0.000.

A



B



C

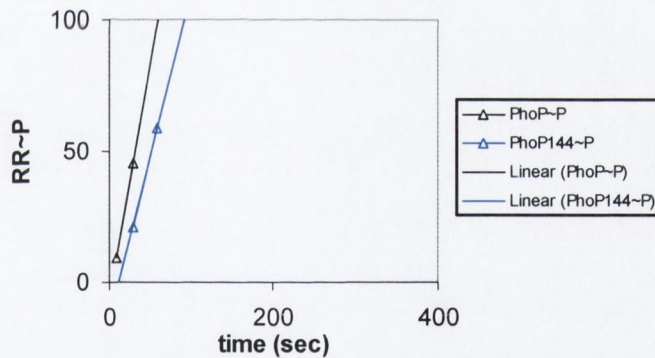


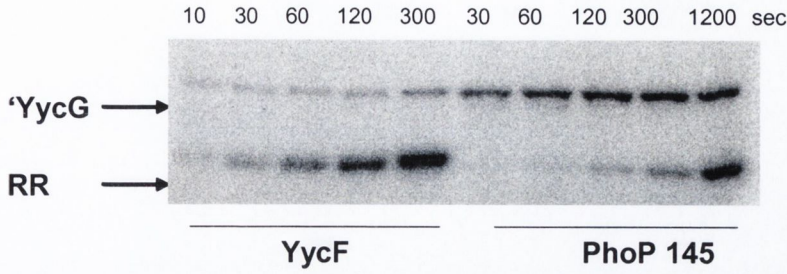
Figure 4.24 Phosphorylation of response regulators PhoP and PhoP144 by 'PhoR *in vitro*. A kinetic analysis of PhoP and PhoP144 (Y20F) phosphorylation by 'PhoR *in vitro*.

A) Phosphoimage of PhoP and PhoP144 phosphorylation by 'PhoR *in vitro*. Reactions continued for 300 (PhoP) and 1200 (PhoP144) sec with samples taken at the indicated time intervals (sec). This image was exposed for 90 min.

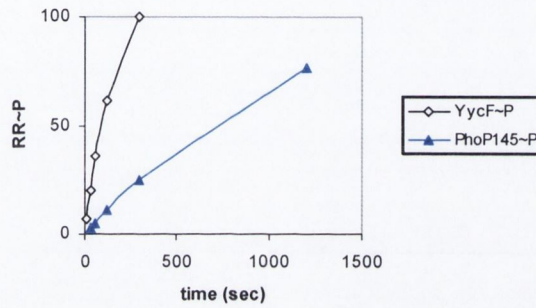
B) The phosphoimage (A) was quantified as described in Materials and Methods using MultiGauge2 software. Values were normalized to the amount of PhoP~P present at the 300 sec timepoint for the 'PhoR protein which was assigned a value of 100% (black triangles = phosphorylation of PhoP by 'PhoR; blue open triangles = phosphorylation of PhoP144 by 'PhoR).

C) A linear trend line was fitted to the initial time points of the reaction to estimate the relative initial rate of PhoP phosphorylation. The slope for the trendline for phosphorylation of PhoP by 'PhoR is 1.788 while that for phosphorylation of PhoP144 by 'PhoR is 1.243.

A



B



C

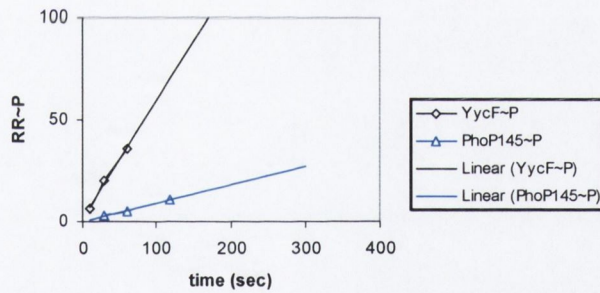


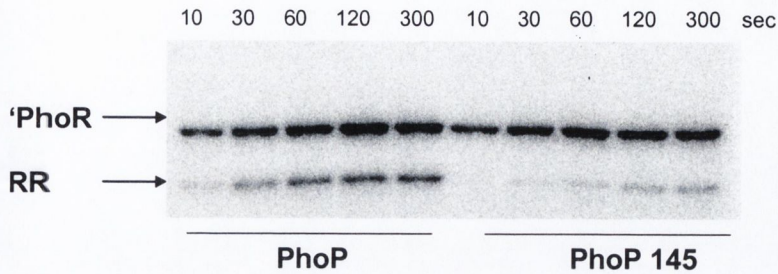
Figure 4.25 Phosphorylation of response regulators YycF and PhoP145 by 'YycG *in vitro*. A kinetic analysis of YycF and PhoP145 (S13 P L171) phosphorylation by 'YycG *in vitro*.

A) Phosphoimage of YycF and PhoP phosphorylation by YycG *in vitro*. Reactions continued for 300 (YycF) and 1200 (PhoP145) sec with samples taken at the indicated time intervals (sec). This image was exposed for 90 min.

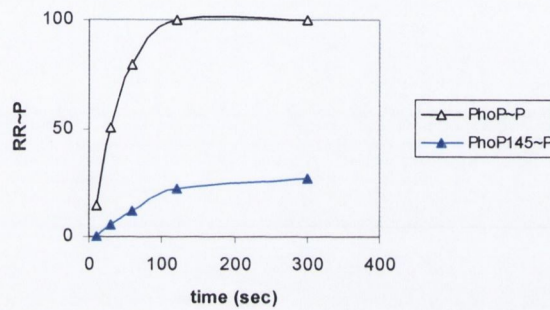
B) The phosphoimage (A) was quantified as described in Materials and Methods using MultiGauge2 software. Values were normalized to the amount of YycF~P present at the 300 sec timepoint for the 'YycG protein which was assigned a value of 100% (black diamonds = phosphorylation of YycF by 'YycG; blue closed triangles = phosphorylation of PhoP145 by 'YycG).

C) A linear trend line was fitted to the initial time points of the reaction to estimate the relative initial rate of PhoP phosphorylation. The slope for the trend line for phosphorylation of YycF by 'YycG is 0.577 while that for phosphorylation of PhoP145 by 'YycG is 0.091.

A



B



C

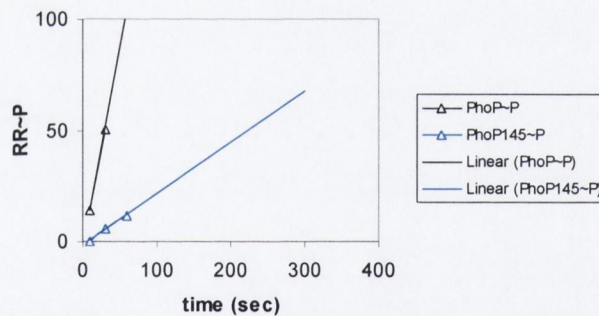


Figure 4.26 Phosphorylation of response regulators PhoP and PhoP145 by 'PhoR *in vitro*. A kinetic analysis of PhoP and PhoP145 (S13 P L17I) phosphorylation by 'PhoR *in vitro*.

A) Phosphoimage of PhoP and PhoP145 phosphorylation by 'PhoR *in vitro*. Reactions continued for 300 (PhoP) and 300 (PhoP145) sec with samples taken at the indicated time intervals (sec). This image was exposed for 90 min.

B) The phosphoimage (A) was quantified as described in Materials and Methods using MultiGauge2 software. Values were normalized to the amount of PhoP~P present at the 300 sec timepoint for the 'PhoR protein which was assigned a value of 100% (black triangles = phosphorylation of PhoP by 'PhoR; blue open triangles = phosphorylation of PhoP145 by 'PhoR).

C) A linear trend line was fitted to the initial time points of the reaction to estimate the relative initial rate of PhoP phosphorylation. The slope for the trendline for phosphorylation of PhoP by 'PhoR is 1.808 while that for phosphorylation of PhoP145 by 'PhoR is 0.231.

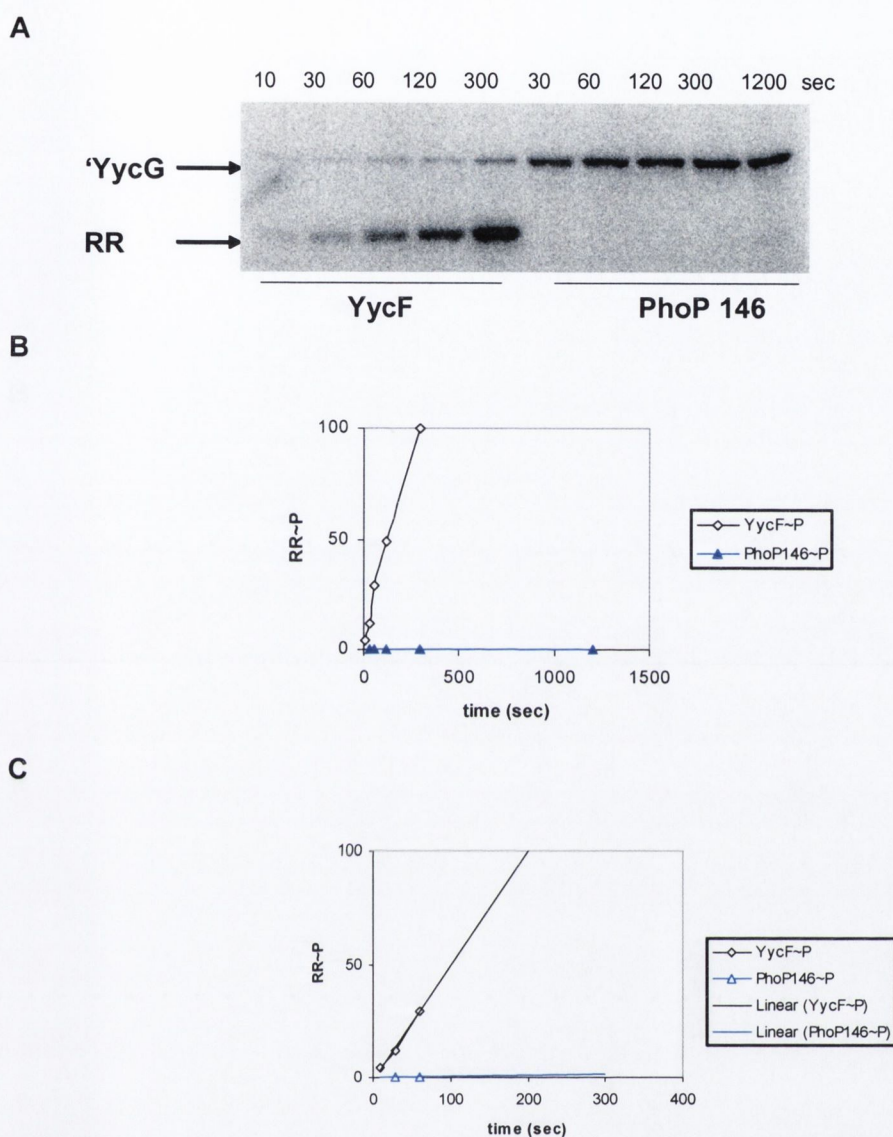


Figure 4.27 Phosphorylation of response regulators YycF and PhoP146 by 'YycG *in vitro*. A kinetic analysis of YycF and PhoP146 (S13P Y20F) phosphorylation by 'YycG *in vitro*.

A) Phosphoimage of YycF and PhoP146 phosphorylation by YycG *in vitro*. Reaction conditions were as described in Materials and Methods. Reactions continued for 300 (YycF) and 1200 (PhoP146) sec with samples taken at the indicated time intervals (sec). This image was exposed for 90 min.

B) The phosphoimage (A) was quantified as described in Materials and Methods using MultiGauge2 software. Values were normalized to the amount of YycF~P present at the 300 sec timepoint for the 'YycG protein which was assigned a value of 100% (black diamonds = phosphorylation of YycF by 'YycG; blue closed triangles = phosphorylation of PhoP146 by 'YycG).

C) A linear trend line was fitted to the initial time points of the reaction to estimate the relative initial rate of PhoP phosphorylation. The slope for the trend line for phosphorylation of YycF by 'YycG is 0.506 while that for phosphorylation of PhoP146 by 'YycG is 0.0005.

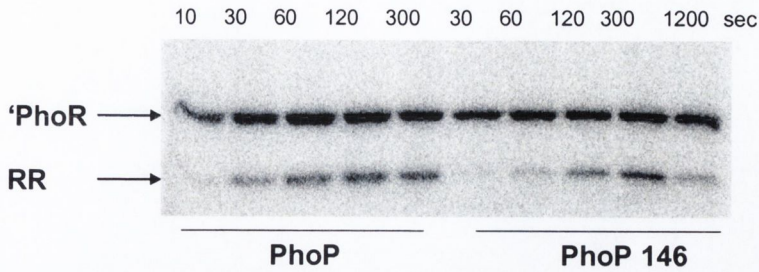
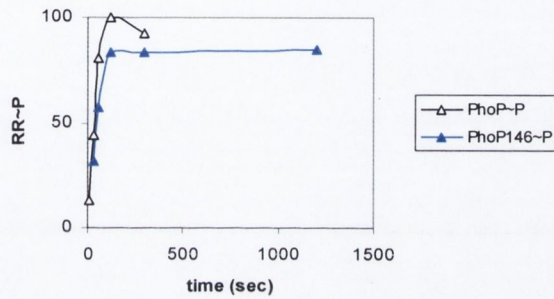
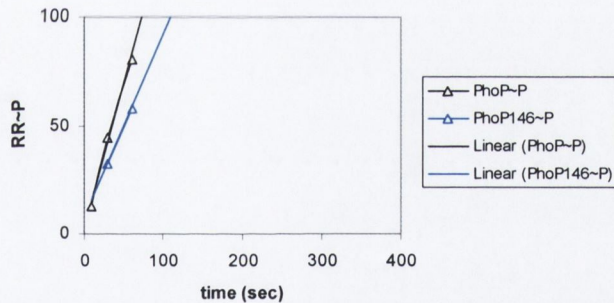
A**B****C**

Figure 4.28 Phosphorylation of response regulators PhoP and PhoP146 by 'PhoR *in vitro*. A kinetic analysis of PhoP and PhoP146 (S13P Y20F) phosphorylation by 'PhoR *in vitro*.

A) Phosphoimage of PhoP and PhoP146 phosphorylation by 'PhoR *in vitro*. Reactions continued for 300 (PhoP) and 1200 (PhoP146) sec with samples taken at the indicated time intervals (sec). This image was exposed for 90 min.

B) The phosphoimage (A) was quantified as described in Materials and Methods using MultiGauge2 software. Values were normalized to the amount of PhoP~P present at the 300 sec timepoint for the 'PhoR protein which was assigned a value of 100% (black triangles = phosphorylation of PhoP by 'PhoR; blue open triangles = phosphorylation of PhoP146 by 'PhoR).

C) A linear trend line was fitted to the initial time points of the reaction to estimate the relative initial rate of PhoP phosphorylation. The slope for the trendline for phosphorylation of PhoP by 'PhoR is 1.343 while that for phosphorylation of PhoP146 by 'PhoR is 0.846.

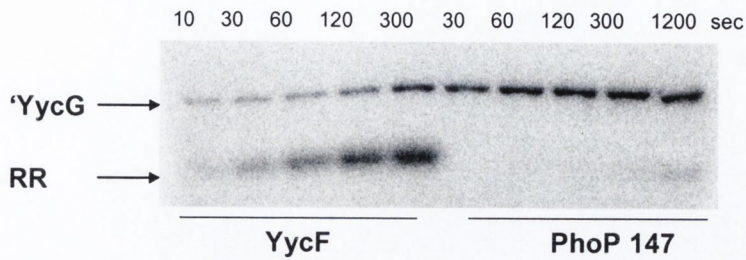
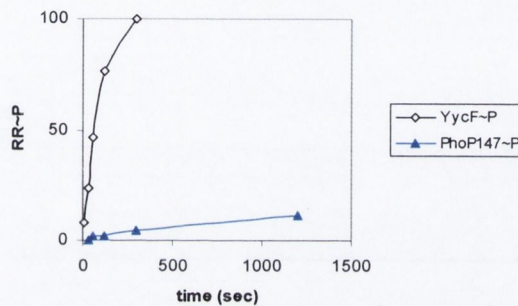
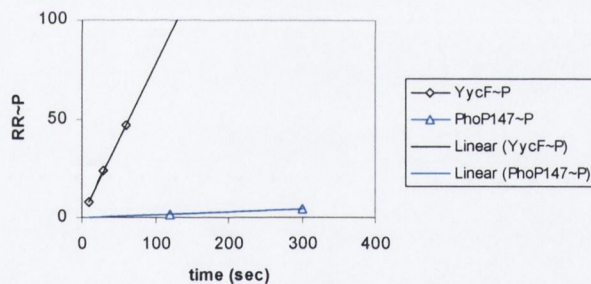
A**B****C**

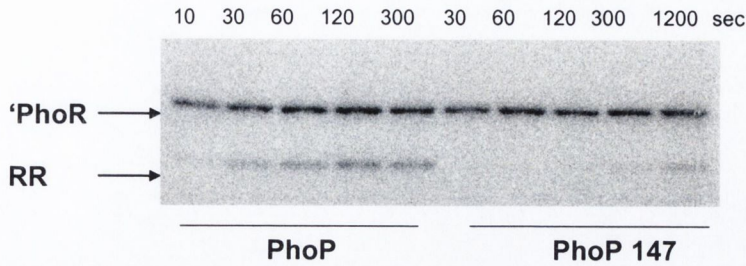
Figure 4.29 Phosphorylation of response regulators YycF and PhoP147 by 'YycG *in vitro*. A kinetic analysis of YycF and PhoP147 (L17I Y20F) phosphorylation by 'YycG *in vitro*.

A) Phosphoimage of YycF and PhoP147 phosphorylation by YycG *in vitro*. Reaction conditions were as described in Materials and Methods. Reactions continued for 300 (YycF) and 1200 (PhoP147) sec with samples taken at the indicated time intervals (sec). This image was exposed for 90 min.

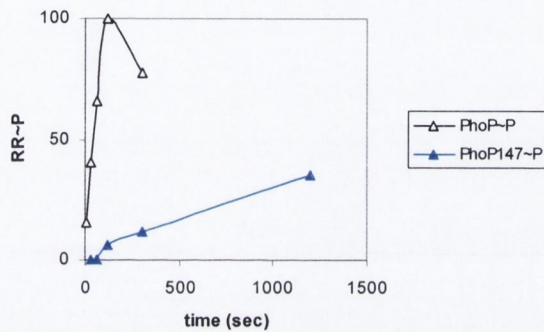
B) The phosphoimage (A) was quantified as described in Materials and Methods using MultiGauge2 software. Values were normalized to the amount of YycF~P present at the 300 sec timepoint for the 'YycG protein which was assigned a value of 100% (black diamonds = phosphorylation of YycF by 'YycG; blue closed triangles = phosphorylation of PhoP147 by 'YycG).

C) A linear trend line was fitted to the initial time points of the reaction to estimate the relative initial rate of PhoP phosphorylation. The slope for the trend line for phosphorylation of YycF by 'YycG is 0.772 while that for phosphorylation of PhoP147 by 'YycG is 0.015.

A



B



C

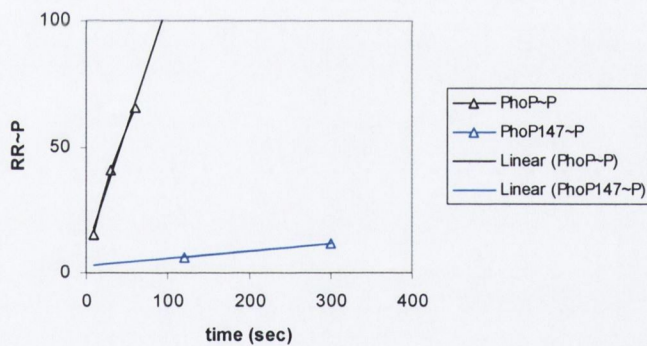


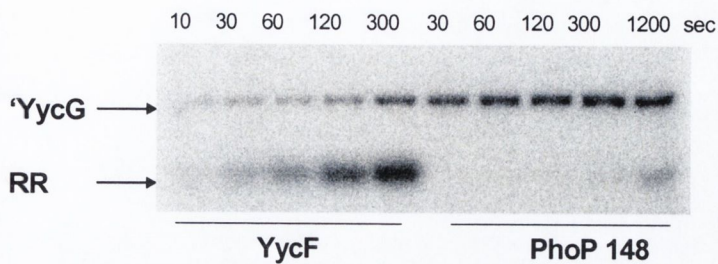
Figure 4.30 Phosphorylation of response regulators PhoP and PhoP147 by 'PhoR *in vitro*. A kinetic analysis of PhoP and PhoP147 (L17I Y20F) phosphorylation by 'PhoR *in vitro*.

A) Phosphoimage of PhoP and PhoP147 phosphorylation by 'PhoR *in vitro*. Reactions continued for 300 (PhoP) and 1200 (PhoP147) sec with samples taken at the time intervals (sec). This image was exposed for 90 min.

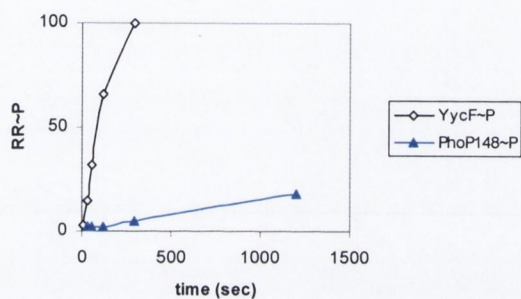
B) The phosphoimage (A) was quantified as described in Materials and Methods using MultiGauge2 software. Values were normalized to the amount of PhoP~P present at the 300 sec timepoint for the 'PhoR protein which was assigned a value of 100% (black triangles = phosphorylation of PhoP by 'PhoR; blue open triangles = phosphorylation of PhoP147 by 'PhoR).

C) A linear trend line was fitted to the initial time points of the reaction to estimate the relative initial rate of PhoP phosphorylation. The slope for the trendline for phosphorylation of PhoP by 'PhoR is 0.991 while that for phosphorylation of PhoP147 by 'PhoR is 0.031.

A



B



C

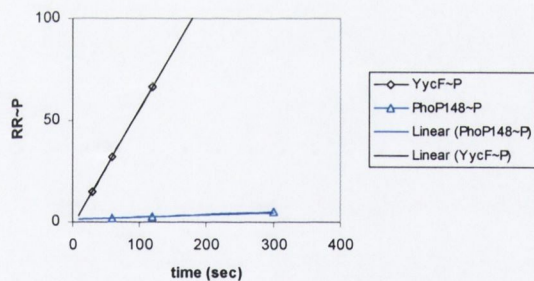


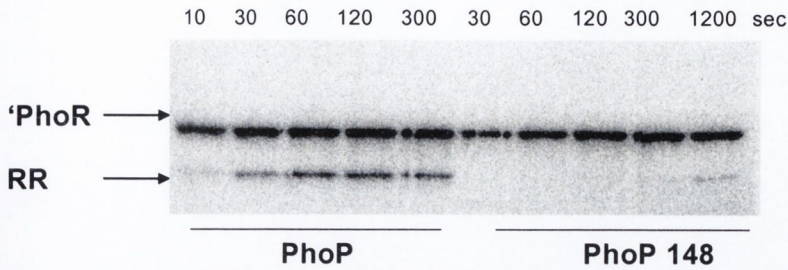
Figure 4.31 Phosphorylation of response regulators YycF and PhoP148 by 'YycG *in vitro*. A kinetic analysis of YycF and PhoP148 (S13P L17I Y20F) phosphorylation by 'YycG *in vitro*.

A) Phosphoimage of YycF and PhoP148 phosphorylation by YycG *in vitro*. Reactions continued for 300 (YycF) and 1200 (PhoP148) sec with samples taken at the indicated time intervals (sec). This image was exposed for 90 min.

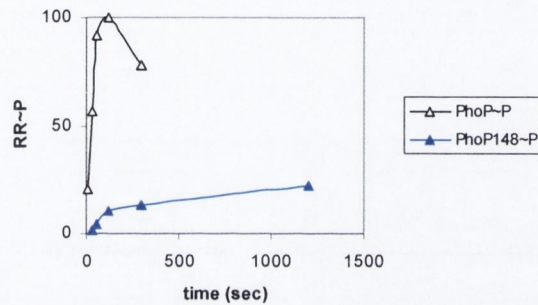
B) The phosphoimage (A) was quantified as described in Materials and Methods using MultiGauge2 software. Values were normalized to the amount of YycF~P present at the 300 sec timepoint for the 'YycG protein which was assigned a value of 100% (black diamonds = phosphorylation of YycF by 'YycG; blue closed triangles = phosphorylation of PhoP148 by 'YycG).

C) A linear trend line was fitted to the initial time points of the reaction to estimate the relative initial rate of PhoP phosphorylation. The slope for the trend line for phosphorylation of YycF by 'YycG is 0.574 while that for phosphorylation of PhoP148 by 'YycG is 0.012.

A



B



C

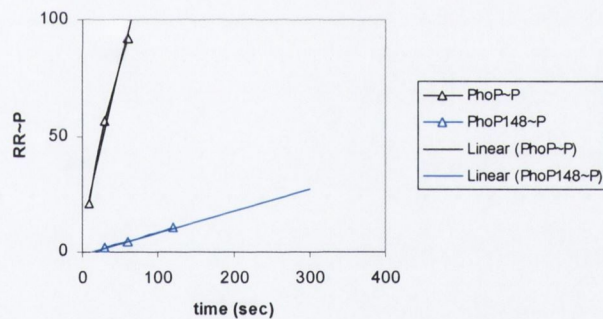


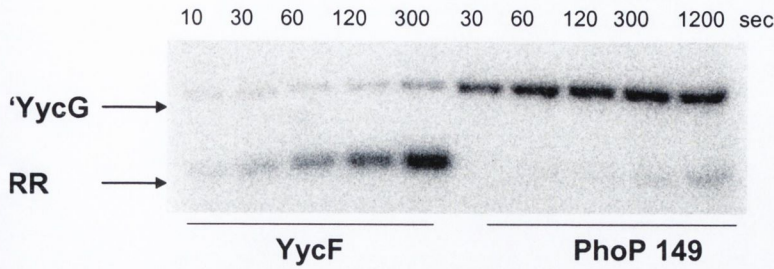
Figure 4.32 Phosphorylation of response regulators PhoP and PhoP148 by 'PhoR *in vitro*. A kinetic analysis of PhoP and PhoP148 (S13P L17I Y20F) phosphorylation by 'PhoR *in vitro*.

A) Phosphoimage of PhoP and PhoP148 phosphorylation by 'PhoR *in vitro*. Reactions were for 300 (PhoP) and 1200 (PhoP148) sec with samples taken at the time intervals (sec). This image was exposed for 90 min.

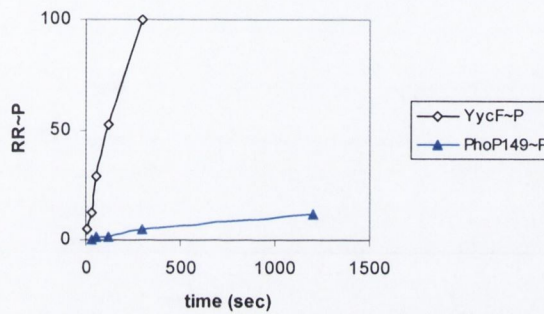
B) The phosphoimage (A) was quantified as described in Materials and Methods using MultiGauge2 software. Values were normalized to the amount of PhoP~P present at the 300 sec timepoint for the 'PhoR protein which was assigned a value of 100% (black triangles = phosphorylation of PhoP by 'PhoR; blue open triangles = phosphorylation of PhoP148 by 'PhoR).

C) A linear trend line was fitted to the initial time points of the reaction to estimate the relative initial rate of PhoP phosphorylation. The slope for the trendline for phosphorylation of PhoP by 'PhoR is 1.408 while that for phosphorylation of PhoP148 by 'PhoR is 0.095.

A



B



C

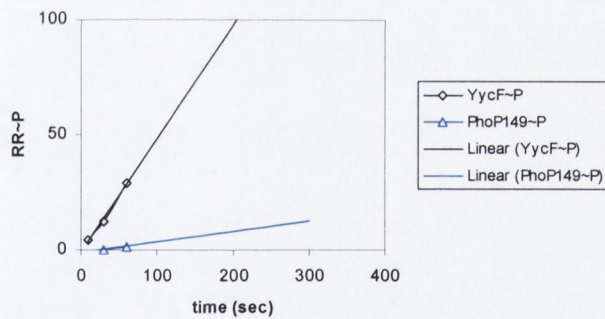


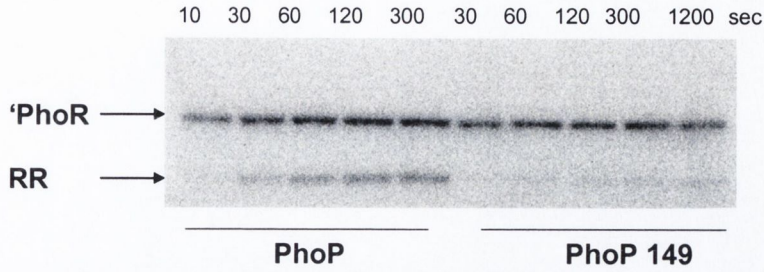
Figure 4.33 Phosphorylation of response regulators YycF and PhoP149 by 'YycG *in vitro*. A kinetic analysis of YycF and PhoP149 (S13P P107T) phosphorylation by 'YycG *in vitro*.

A) Phosphoimage of YycF and PhoP149 phosphorylation by YycG *in vitro*. Reactions continued for 300 (YycF) and 1200 (PhoP149) sec with samples taken at the indicated time intervals (sec). This image was exposed for 90 min.

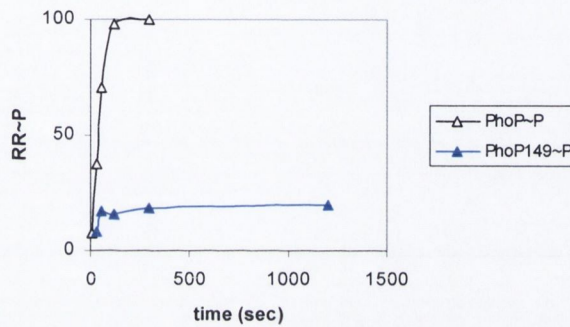
B) The phosphoimage (A) was quantified as described in Materials and Methods using MultiGauge2 software. Values were normalized to the amount of YycF~P present at the 300 sec timepoint for the 'YycG protein which was assigned a value of 100% (black diamonds = phosphorylation of YycF by 'YycG; blue closed triangles = phosphorylation of PhoP149 by 'YycG).

C) A linear trend line was fitted to the initial time points of the reaction to estimate the relative initial rate of PhoP phosphorylation. The slope for the trend line for phosphorylation of YycF by 'YycG is 0.495 while that for phosphorylation of PhoP149 by 'YycG is 0.046.

A



B



C

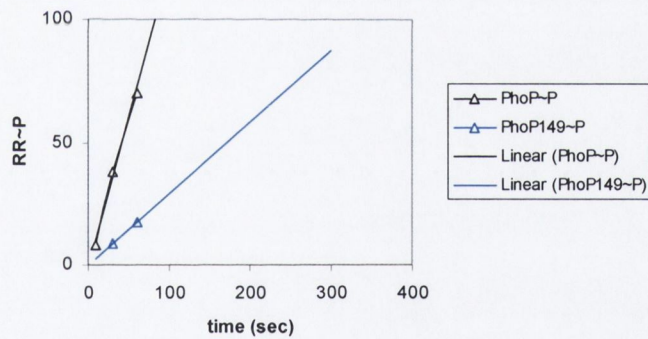


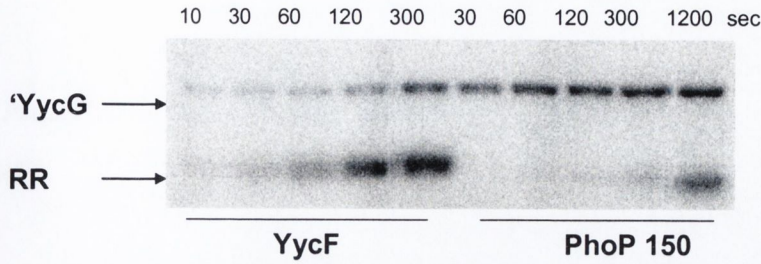
Figure 4.34 Phosphorylation of response regulators PhoP and PhoP149 by 'PhoR *in vitro*. A kinetic analysis of PhoP and PhoP149 (S13P P107T) phosphorylation by 'PhoR *in vitro*.

A) Phosphoimage of PhoP and PhoP149 phosphorylation by 'PhoR *in vitro*. Reactions continued for 300 (PhoP) and 1200 (PhoP149) sec with samples taken at the time intervals (sec). This image was exposed for 90 min.

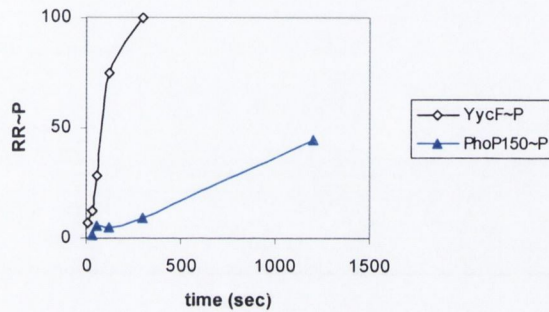
B) The phosphoimage (A) was quantified as described in Materials and Methods using MultiGauge2 software. Values were normalized to the amount of PhoP~P present at the 300 sec timepoint for the 'PhoR protein which was assigned a value of 100% (black triangles = phosphorylation of PhoP by 'PhoR; blue open triangles = phosphorylation of PhoP149 by 'PhoR).

C) A linear trend line was fitted to the initial time points of the reaction to estimate the relative initial rate of PhoP phosphorylation. The slope for the trendline for phosphorylation of PhoP by 'PhoR is 1.238 while that for phosphorylation of PhoP149 by 'PhoR is 0.293.

A



B



C

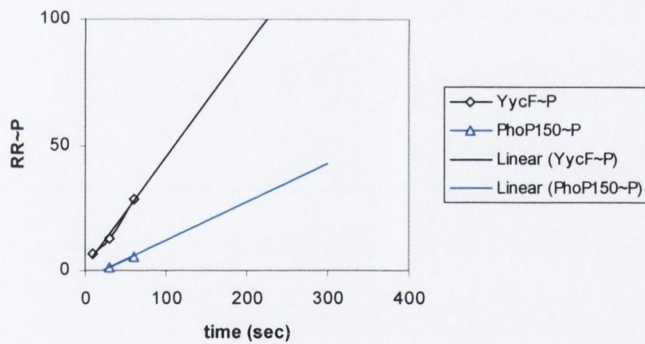


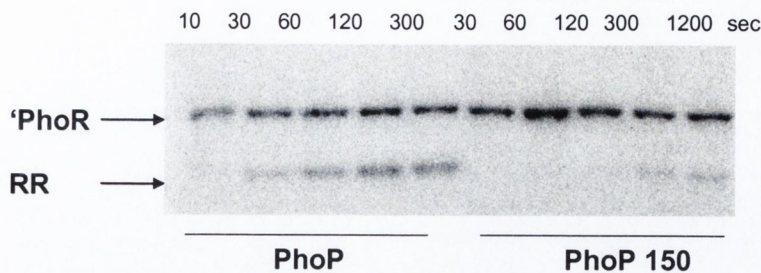
Figure 4.35 Phosphorylation of response regulators YycF and PhoP150 by 'YycG *in vitro*. A kinetic analysis of YycF and PhoP150 (L17I P107T) phosphorylation by 'YycG *in vitro*.

A) Phosphoimage of YycF and PhoP150 phosphorylation by YycG *in vitro*. Reactions continued for 300 (YycF) and 1200 (PhoP150) sec with samples taken at the indicated time intervals (sec). This image was exposed for 90 min.

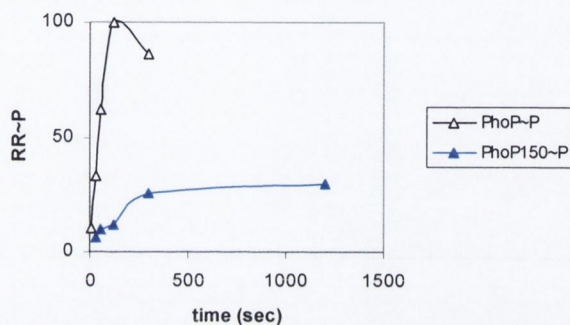
B) The phosphoimage (A) was quantified as described in Materials and Methods using MultiGauge2 software. Values were normalized to the amount of YycF~P present at the 300 sec timepoint for the 'YycG protein which was assigned a value of 100% (black diamonds = phosphorylation of YycF by 'YycG; blue closed triangles = phosphorylation of PhoP150 by 'YycG).

C) A linear trend line was fitted to the initial time points of the reaction to estimate the relative initial rate of PhoP phosphorylation. The slope for the trend line for phosphorylation of YycF by 'YycG is 0.440 while that for phosphorylation of PhoP150 by 'YycG is 0.153.

A



B



C

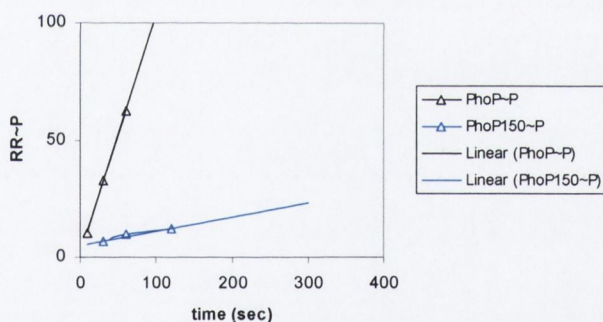


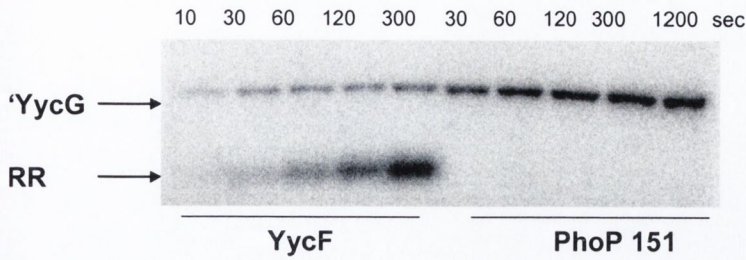
Figure 4.36 Phosphorylation of response regulators PhoP and PhoP150 by 'PhoR *in vitro*. A kinetic analysis of PhoP and PhoP150 (L17I P107T) phosphorylation by 'PhoR *in vitro*.

A) Phosphoimage of PhoP and PhoP150 phosphorylation by 'PhoR *in vitro*. Reactions continued for 300 (PhoP) and 1200 (PhoP150) sec with samples taken at the time intervals (sec). This image was exposed for 90 min.

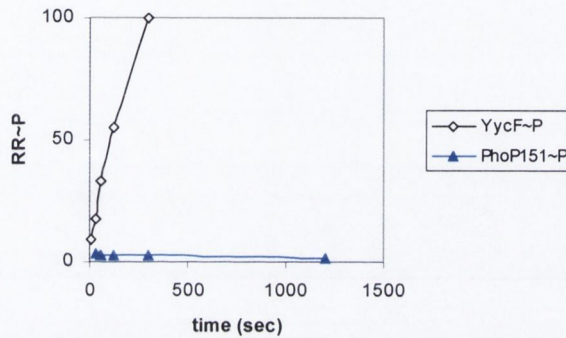
B) The phosphoimage (A) was quantified as described in Materials and Methods using MultiGauge2 software. Values were normalized to the amount of PhoP~P present at the 300 sec timepoint for the 'PhoR protein which was assigned a value of 100% (black triangles = phosphorylation of PhoP by 'PhoR; blue open triangles = phosphorylation of PhoP150 by 'PhoR).

C) A linear trend line was fitted to the initial time points of the reaction to estimate the relative initial rate of PhoP phosphorylation. The slope for the trendline for phosphorylation of PhoP by 'PhoR is 1.032 while that for phosphorylation of PhoP150 by 'PhoR is 0.059.

A



B



C

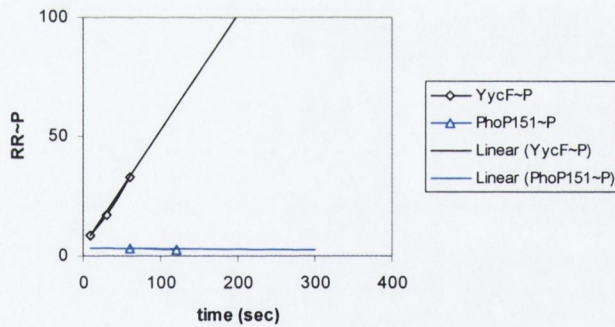


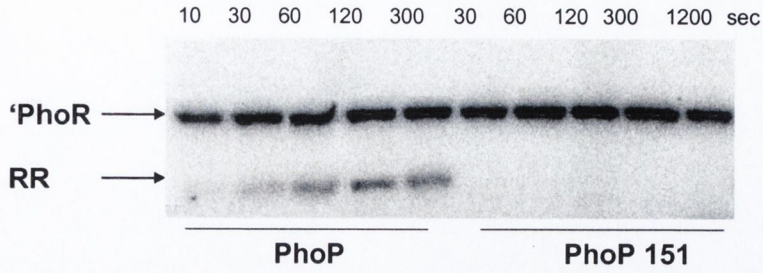
Figure 4.37 Phosphorylation of response regulators YycF and PhoP151 by 'YycG *in vitro*. A kinetic analysis of YycF and PhoP151 (Y20F P107T) phosphorylation by 'YycG *in vitro*.

A) Phosphoimage of YycF and PhoP151 phosphorylation by YycG *in vitro*. Reactions continues for 300 (YycF) and 1200 (PhoP151) sec with samples taken at the indicated time intervals (sec). This image was exposed for 90 min.

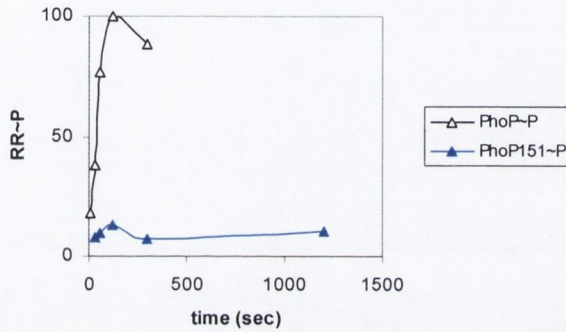
B) The phosphoimage (A) was quantified as described in Materials and Methods using MultiGauge2 software. Values were normalized to the amount of YycF~P present at the 300 sec timepoint for the 'YycG protein with was assigned a value of 100% (black diamonds = phosphorylation of YycF by 'YycG; blue closed triangles = phosphorylation of PhoP151 by 'YycG).

C) A linear trend line was fitted to the initial time points of the reaction to estimate the relative initial rate of PhoP phosphorylation. The slope for the trend line for phosphorylation of YycF by 'YycG is 0.486 while that for phosphorylation of PhoP151 by 'YycG is 0.00.

A



B



C

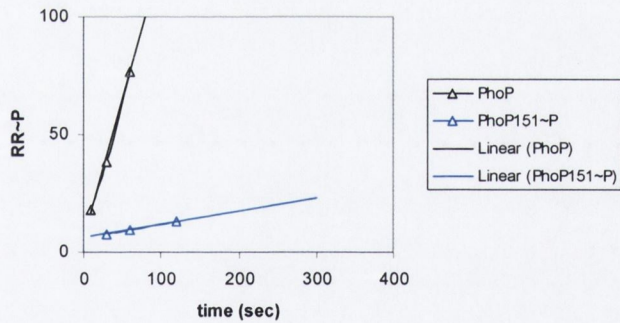


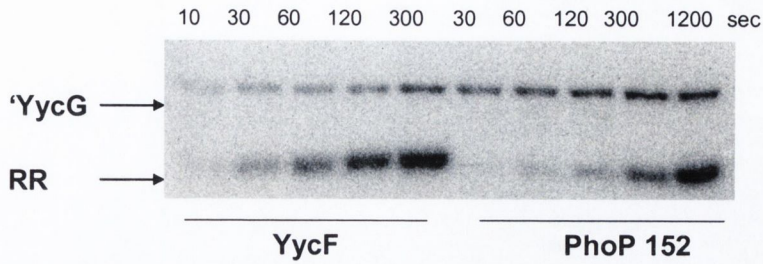
Figure 4.38 Phosphorylation of response regulators PhoP and PhoP151 by 'PhoR *in vitro*. A kinetic analysis of PhoP and PhoP151 (Y20F P107T) phosphorylation by 'PhoR *in vitro*.

A) Phosphoimage of PhoP and PhoP151 phosphorylation by 'PhoR *in vitro*. Reactions continued for 300 (PhoP) and 1200 (PhoP151) sec with samples taken at the time intervals (sec). This image was exposed for 90 min.

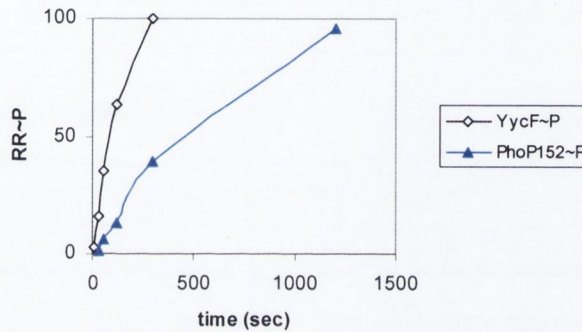
B) The phosphoimage (A) was quantified as described in Materials and Methods using MultiGauge2 software. Values were normalized to the amount of PhoP~P present at the 300 sec timepoint for the 'PhoR protein which was assigned a value of 100% (black triangles = phosphorylation of PhoP by 'PhoR; blue open triangles = phosphorylation of PhoP151 by 'PhoR).

C) A linear trend line was fitted to the initial time points of the reaction to estimate the relative initial rate of PhoP phosphorylation. The slope for the trendline for phosphorylation of PhoP by 'PhoR is 1.186 while that for phosphorylation of PhoP151 by 'PhoR is 0.057.

A



B



C

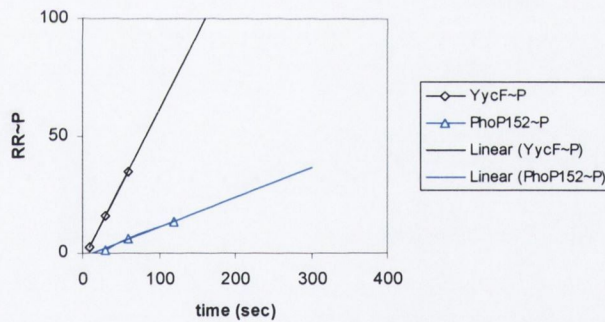


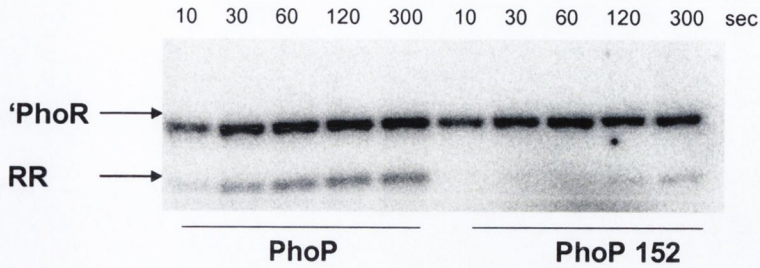
Figure 4.39 Phosphorylation of response regulators YycF and PhoP152 by 'YycG *in vitro*. A kinetic analysis of YycF and PhoP152 (S13P L17I P107T) phosphorylation by 'YycG *in vitro*.

A) Phosphoimage of YycF and PhoP152 phosphorylation by YycG *in vitro*. Reactions continued for 300 (YycF) and 1200 (PhoP152) sec with samples taken at the indicated time intervals (sec). This image was exposed for 90 min.

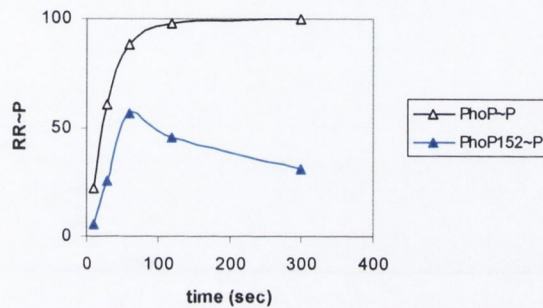
B) The phosphoimage (A) was quantified as described in Materials and Methods using MultiGauge2 software. Values were normalized to the amount of YycF~P present at the 300 sec timepoint for the 'YycG protein which was assigned a value of 100% (black diamonds = phosphorylation of YycF by 'YycG; blue closed triangles = phosphorylation of PhoP152 by 'YycG).

C) A linear trend line was fitted to the initial time points of the reaction to estimate the relative initial rate of PhoP phosphorylation. The slope for the trend line for phosphorylation of YycF by 'YycG is 0.647 while that for phosphorylation of PhoP152 by 'YycG is 0.128.

A



B



C

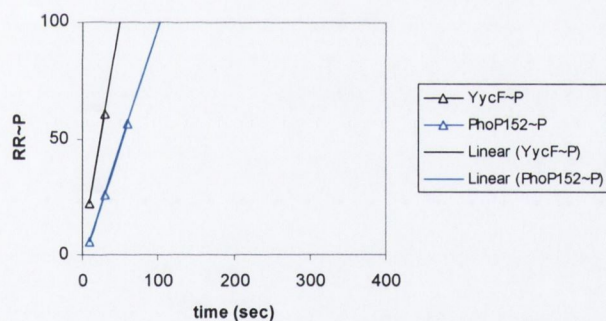


Figure 4.40 Phosphorylation of response regulators PhoP and PhoP152 by 'PhoR *in vitro*. A kinetic analysis of PhoP and PhoP152 (S13P L17I P107T) phosphorylation by 'PhoR *in vitro*.

A) Phosphoimage of PhoP and PhoP152 phosphorylation by 'PhoR *in vitro*. Reactions continued for 300 (PhoP) and 300 (PhoP152) sec with samples taken at the time intervals (sec). This image was exposed for 90 min.

B) The phosphoimage (A) was quantified as described in Materials and Methods using MultiGauge2 software. Values were normalized to the amount of PhoP~P present at the 300 sec timepoint for the 'PhoR protein which was assigned a value of 100% (black triangles = phosphorylation of PhoP by 'PhoR; blue open triangles = phosphorylation of PhoP152 by 'PhoR).

C) A linear trend line was fitted to the initial time points of the reaction to estimate the relative initial rate of PhoP phosphorylation. The slope for the trendline for phosphorylation of PhoP by 'PhoR is 1.944 while that for phosphorylation of PhoP152 by 'PhoR is 1.021.

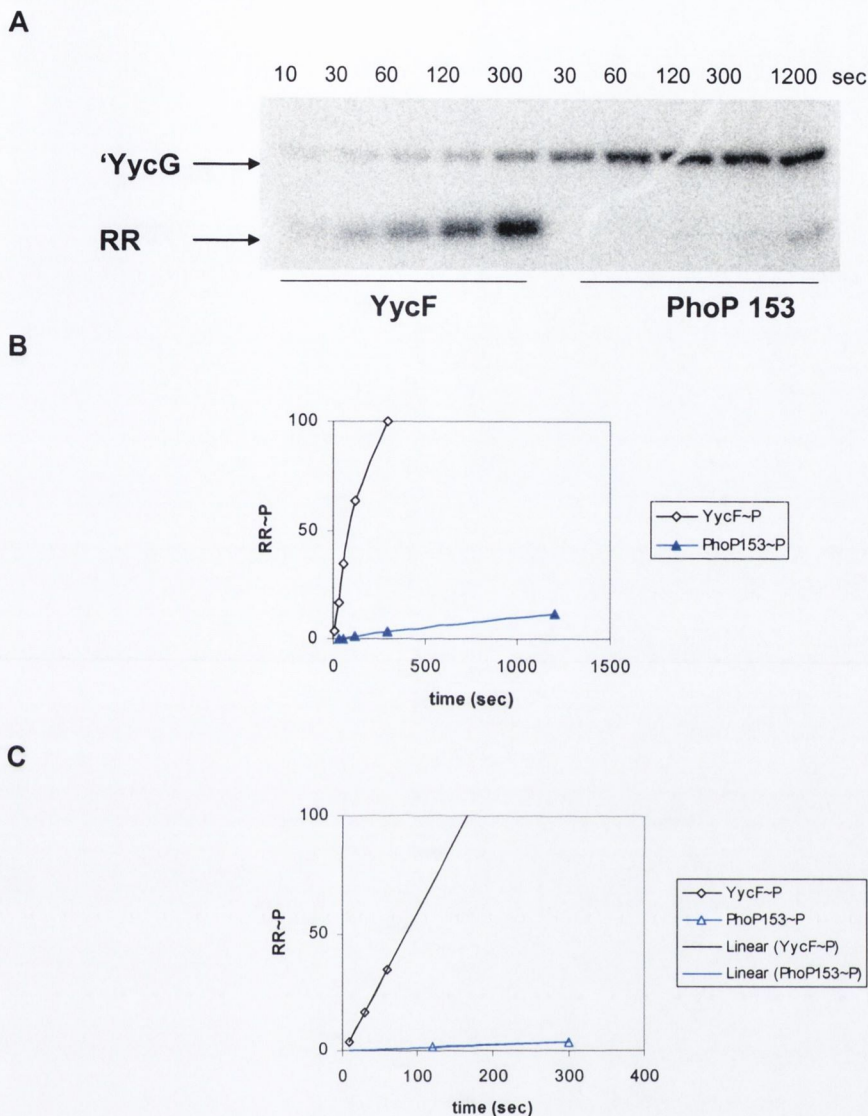


Figure 4.41 Phosphorylation of response regulators YycF and PhoP153 by 'YycG *in vitro*. A kinetic analysis of YycF and PhoP153 (L17I Y20F P107T) phosphorylation by 'YycG *in vitro*.

A) Phosphoimage of YycF and PhoP153 phosphorylation by YycG *in vitro*. Reactions continued for 300 (YycF) and 1200 (PhoP153) sec with samples taken at the indicated time intervals (sec). This image was exposed for 90 min.

B) The phosphoimage (A) was quantified as described in Materials and Methods using MultiGauge2 software. Values were normalized to the amount of YycF~P present at the 300 sec timepoint for the 'YycG protein which was assigned a value of 100% (black diamonds = phosphorylation of YycF by 'YycG; blue closed triangles = phosphorylation of PhoP153 by 'YycG).

C) A linear trend line was fitted to the initial time points of the reaction to estimate the relative initial rate of PhoP phosphorylation. The slope for the trend line for phosphorylation of YycF by 'YycG is 0.612 while that for phosphorylation of PhoP153~P by 'YycG is 0.012.

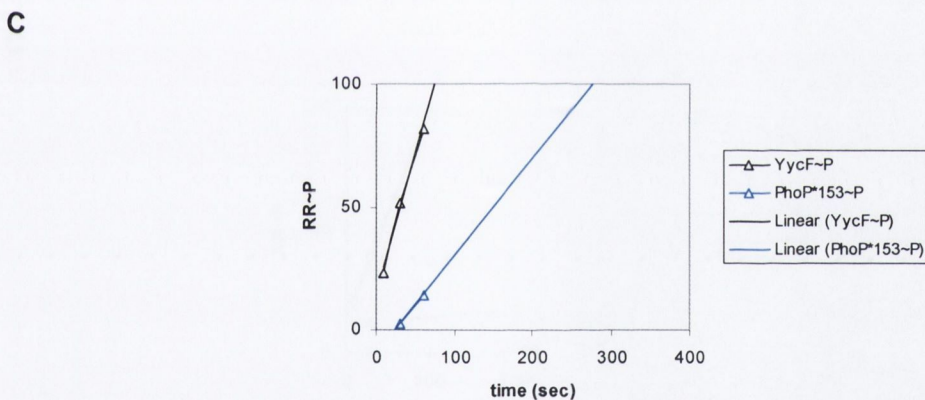
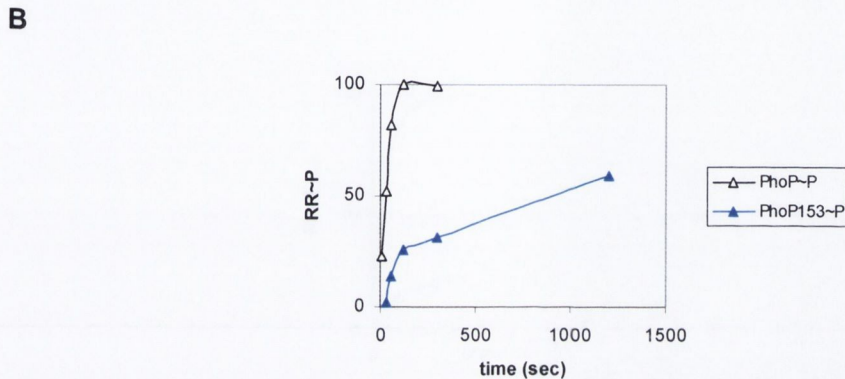
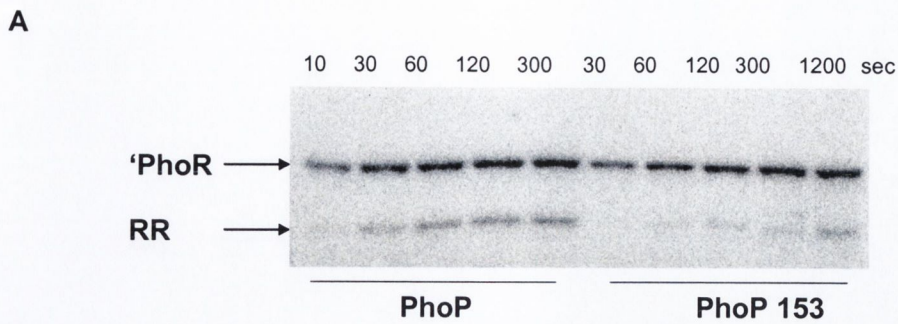


Figure 4.42 Phosphorylation of response regulators PhoP and PhoP153 by 'PhoR *in vitro*. A kinetic analysis of PhoP and PhoP153 (L17I Y20F P107T) phosphorylation by 'PhoR *in vitro*.

A) Phosphoimage of PhoP and PhoP153 phosphorylation by 'PhoR *in vitro*. Reactions continued for 300 (PhoP) and 1200 (PhoP153) sec with samples taken at the time intervals (sec). This image was exposed for 90 min.

B) The phosphoimage (A) was quantified as described in Materials and Methods using MultiGauge2 software. Values were normalized to the amount of PhoP~P present at the 300 sec timepoint for the 'PhoR protein which was assigned a value of 100% (black triangles = phosphorylation of PhoP by 'PhoR; blue open triangles = phosphorylation of PhoP153 by 'PhoR).

C) A linear trend line was fitted to the initial time points of the reaction to estimate the relative initial rate of PhoP phosphorylation. The slope for the trendline for phosphorylation of PhoP~P by 'PhoR is 1.163 while that of phosphorylation of PhoP153~P by 'PhoR is 0.397.

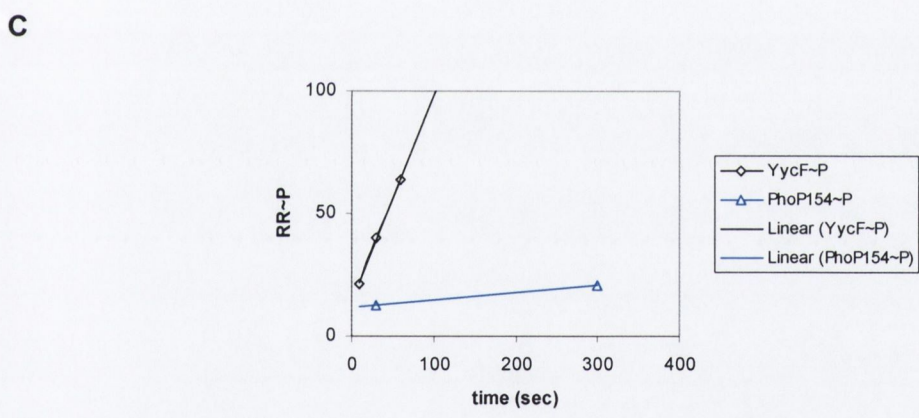
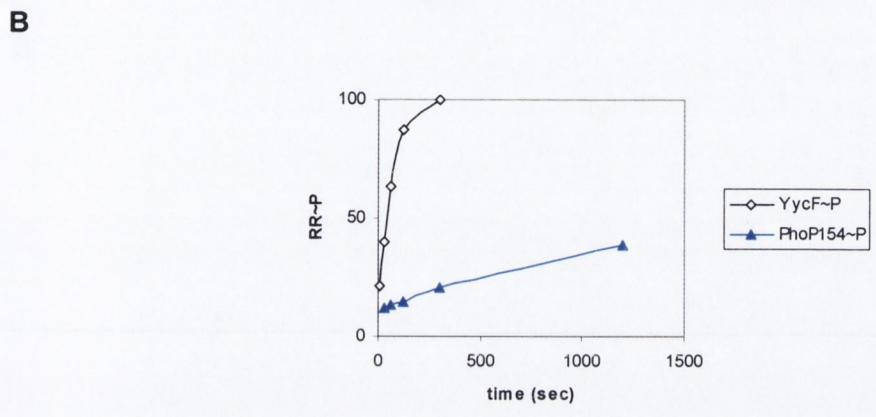
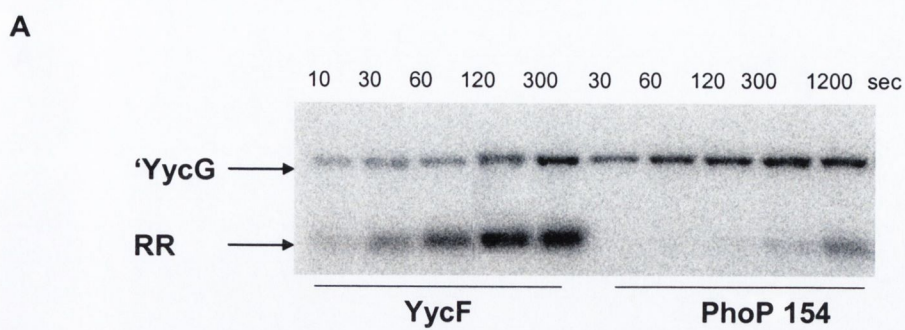


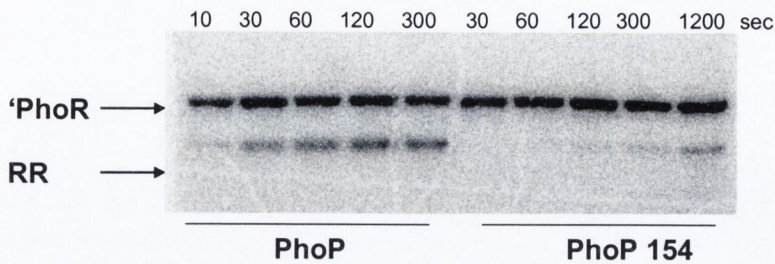
Figure 4.43 Phosphorylation of response regulators YycF and PhoP154 by 'YycG *in vitro*. A kinetic analysis of YycF and PhoP154 (L17I Y20F P107T) phosphorylation by 'YycG *in vitro*.

A) Phosphoimage of YycF and PhoP154 phosphorylation by YycG *in vitro*. Reactions continued for 300 (YycF) and 1200 (PhoP154) sec with samples taken at the indicated time intervals (sec). This image was exposed for 90 min.

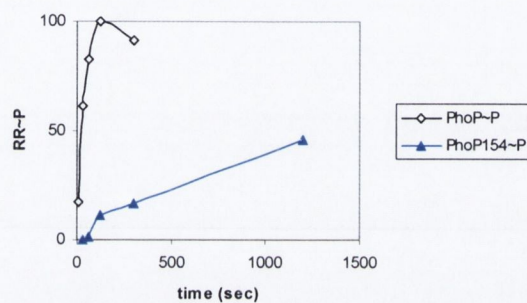
B) The phosphoimage (A) was quantified as described in Materials and Methods using MultiGauge2 software. Values were normalized to the amount of YycF~P present at the 300 sec timepoint for the 'YycG protein which was assigned a value of 100% (black diamonds = phosphorylation of YycF by 'YycG; blue closed triangles = phosphorylation of PhoP154 by 'YycG).

C) A linear trend line was fitted to the initial time points of the reaction to estimate the relative initial rate of PhoP phosphorylation. The slope for the trend line for phosphorylation of YycF by 'YycG is 0.844 while that for phosphorylation of PhoP154~P by 'YycG is 0.032.

A



B



C

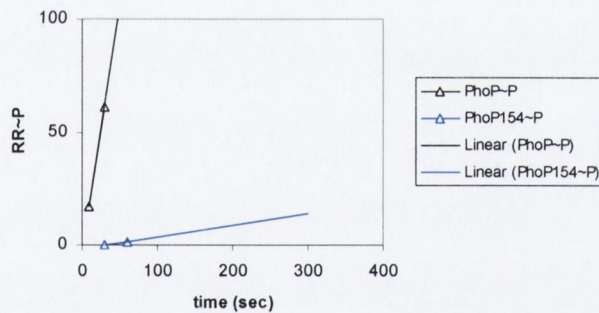


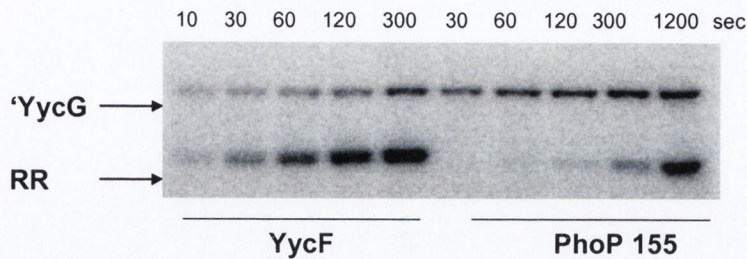
Figure 4.44 Phosphorylation of response regulators PhoP and PhoP154 by 'PhoR *in vitro*. A kinetic analysis of PhoP and PhoP154 (L17I Y20F P107T) phosphorylation by 'PhoR *in vitro*.

A) Phosphoimage of PhoP and PhoP154 phosphorylation by 'PhoR *in vitro*. Reactions continued for 300 (PhoP) and 1200 (PhoP154) sec with samples taken at the time intervals (sec). This image was exposed for 90 min.

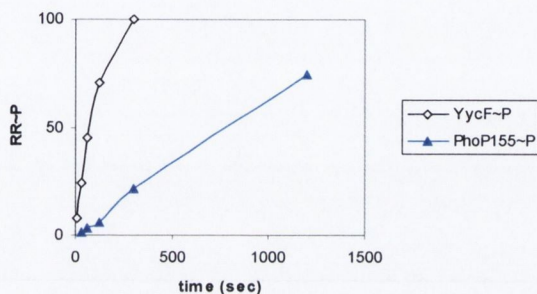
B) The phosphoimage (A) was quantified as described in Materials and Methods using MultiGauge2 software. Values were normalized to the amount of PhoP~P present at the 300 sec timepoint for the 'PhoR protein which was assigned a value of 100% (black triangles = phosphorylation of PhoP by 'PhoR; blue open triangles = phosphorylation of PhoP154 by 'PhoR).

C) A linear trend line was fitted to the initial time points of the reaction to estimate the relative initial rate of PhoP phosphorylation. The slope for the trendline for phosphorylation of PhoP~P by 'PhoR is 2.195 while that of phosphorylation of PhoP154~P by 'PhoR is 0.051.

A



B



C

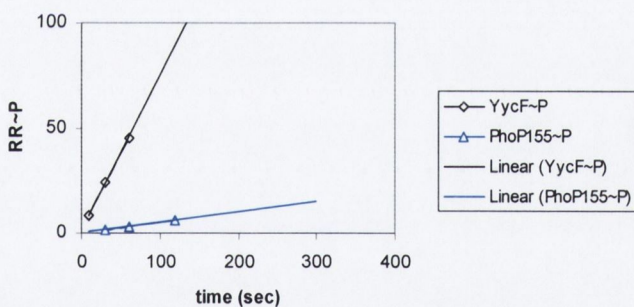


Figure 4.45 Phosphorylation of response regulators YycF and PhoP155 by 'YycG *in vitro*. A kinetic analysis of YycF and PhoP155 (S13P L17I Y20F P107T) phosphorylation by 'YycG *in vitro*.

A) Phosphoimage of YycF and PhoP155 phosphorylation by YycG *in vitro*. Reactions continued for 300 (YycF) and 1200 (PhoP155) sec with samples taken at the indicated time intervals (sec). This image was exposed for 90 min.

B) The phosphoimage (A) was quantified as described in Materials and Methods using MultiGauge2 software. Values were normalized to the amount of YycF~P present at the 300 sec timepoint for the 'YycG protein which was assigned a value of 100% (black diamonds = phosphorylation of YycF by 'YycG; blue closed triangles = phosphorylation of PhoP155 by 'YycG).

C) A linear trend line was fitted to the initial time points of the reaction to estimate the relative initial rate of PhoP phosphorylation. The slope for the trend line for phosphorylation of YycF by 'YycG is 0.738 while that for phosphorylation of PhoP154~P by 'YycG is 0.048.

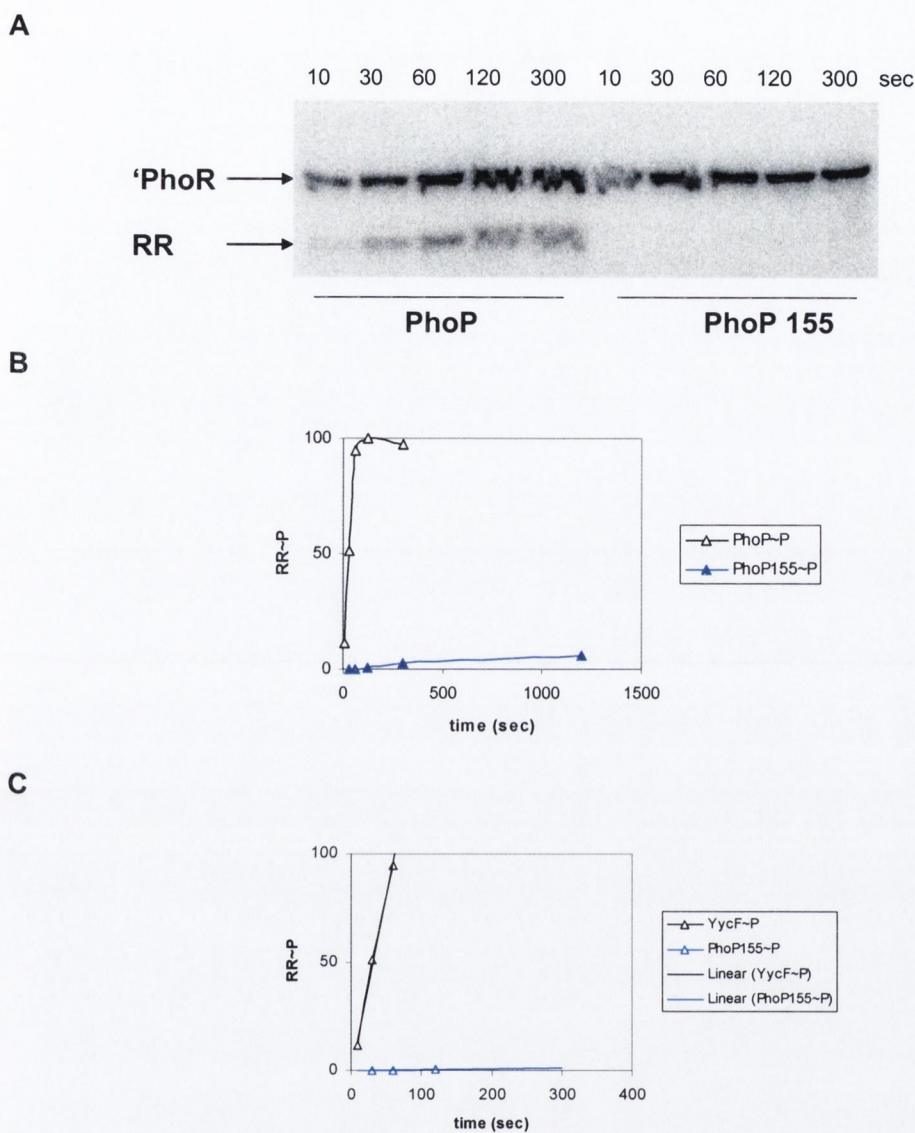


Figure 4.46 Phosphorylation of response regulators PhoP and PhoP155 by 'PhoR *in vitro*. A kinetic analysis of PhoP and PhoP155 (S13P L17I Y20F P107T) phosphorylation by 'PhoR *in vitro*.

A) Phosphoimage of PhoP and PhoP155 phosphorylation by 'PhoR *in vitro*. Reactions continued for 300 (PhoP) and 300 (PhoP155) sec with samples taken at the time intervals (sec). This image was exposed for 90 min.

B) The phosphoimage (A) was quantified as described in Materials and Methods using MultiGauge2 software. Values were normalized to the amount of PhoP~P present at the 300 sec timepoint for the 'PhoR protein which was assigned a value of 100% (black triangles = phosphorylation of PhoP by 'PhoR; blue open triangles = phosphorylation of PhoP155 by 'PhoR).

C) A linear trend line was fitted to the initial time points of the reaction to estimate the relative initial rate of PhoP phosphorylation. The slope for the trendline for phosphorylation of PhoP~P by 'PhoR is 1.639 while that of phosphorylation of PhoP155~P by 'PhoR is 0.005.

Table 4.5 Summary of *in vivo* and *in vitro* assay results.

	amino acid change in PhoP	<i>in vivo</i>		<i>in vitro</i> phosphorylation by the HKs (%)	
		β -gal. spec. act.	(units)	by YycG	by PhoR
PhoP140		+	40	0	100
YycF		-	-	100	0
PhoP141	P107T	+	40	0.07	45.24
PhoP142	S13P	+	20	2.88	35.62
PhoP143	L17I	+++	400	4.84	11.55
PhoP144	Y20F	++	90	0	69.5
PhoP145	S13P L17I	+++	1700	15.79	12.75
PhoP146	S13P Y20F	+	30	0.79	62.96
PhoP147	L17I Y20F	++	90	1.95	3.12
PhoP149	S13P P107T	+	30	9.38	23.67
PhoP150	L17I P107T	+++	600	34.82	5.72
PhoP151	Y20F P107T	+	15	0	4.77
PhoP148	S13P L17I Y20F	++	460	2.1	6.71
PhoP152	S13P L17I P107T	+++	1200	19.74	52.52
PhoP153	S13P Y20F P107T	+	45	3.79	34.13
PhoP154	L17I Y20F P107T	++	245	3.83	2.31
PhoP155	S13P L17I Y20F P107T	++	500	6.55	0.29

- = not determined

+ = low β -galactosidase activity

++ = high β -galactosidase activity

+++ = very high β -galactosidase activity

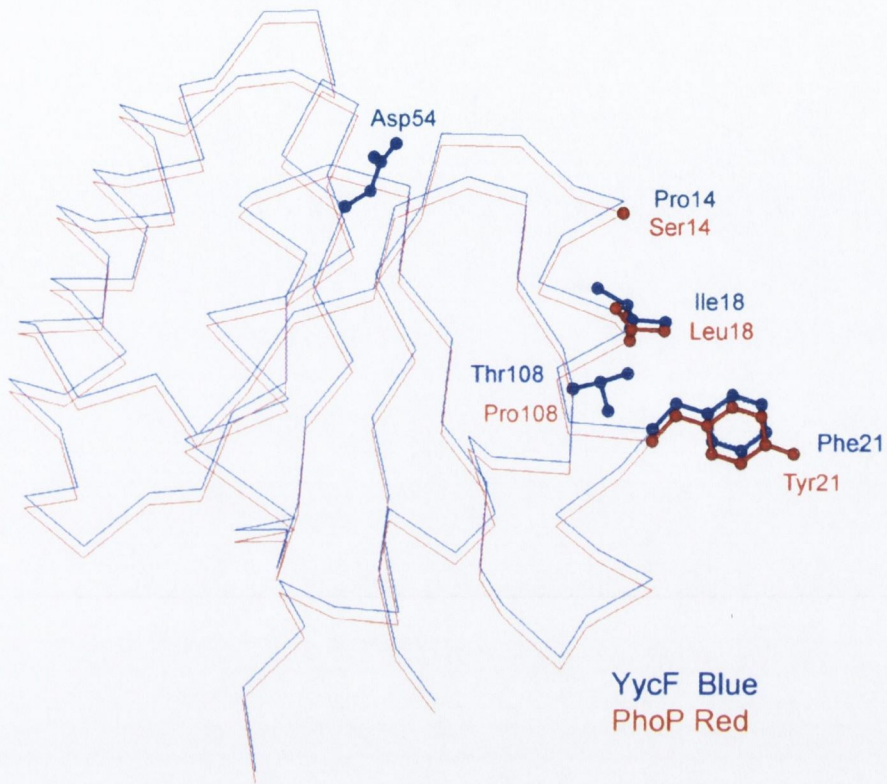
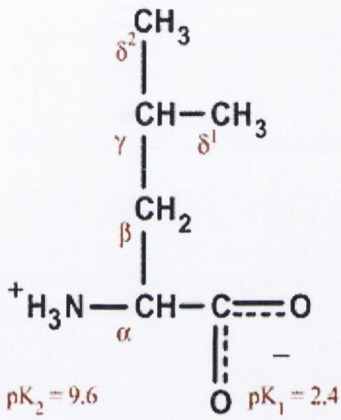


Figure 4.47 Superimposed receiver domains of PhoP and YycF. The residues of the receiver domain of YycF (blue) and PhoP (red) thought to be involved in specificity of interaction that have been investigated in this study are shown. In YycF and PhoP the amino acids changes were at positions S13P, L17I, Y20F and P107T, the numbering of positions is according to Spo0F that is off by +1. (K.I. Varughese, personal correspondence)

A



B

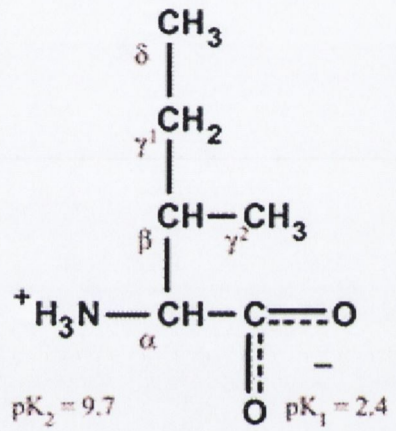


Figure 4.48 Structures of Leucine and Isoleucine.

Structure of the amino acid leucine (A) and isoleucine (B), when compared it is noticeable that the difference is that a -CH_3 group moved from position δ^1 in leucine to position γ^2 in isoleucine (from www.biology.arizona.edu/biochemistry/problem-sets/aa/aa.html).